EVALUATION OF THE FUNCTIONAL ROLE(S) OF TIMP-3 IN PROSTATE CANCER PROGRESSION

A thesis submitted to fulfill the requirements for the degree of PhD with Integrated Studies

by

Olajumoke O. Popoola

(formerly Adeniji)

Department of Infection and Immunity

School of Medicine and Biomedical Sciences

University of Sheffield

February 2013

THESIS SUMMARY

Prostate cancer is the second highest cause of cancer death in men and its transformation to an untreatable state depends on the loss of the cells' requirement for androgen. Metalloproteinases such as matrix metalloproteinases (MMPs), a disintegrin and metalloproteinases (ADAMs) and a disintegrin and metalloproteinase with thrombospondin motifs (ADAMTSs) are implicated in prostate cancer. Tissue inhibitor of metalloproteinase (TIMP) is a family of 4 inhibitors whose major functions are to regulate the activity of metalloproteinases. TIMP-3 inhibits ADAMTSs, MMPs and ADAMs, and independently inhibits angiogenesis.

The aims of this research were to investigate the expression and modulation of TIMP-3 in prostate stromal and cancer cells in order to better understand its role(s) in prostate cancer. The effects of androgen, growth factors and cytokines on TIMP-3 expression in prostate stromal and cancer cells were analysed. Co-culture analyses were employed to investigate the effect of cell-cell contact on TIMP-3 expression. RNAi experiments were carried out to study the effects of TIMP-3 inhibition on biological functions. Tissue microarray analyses were carried out in order to investigate correlation of TIMP-3 expression with prostate cancer malignancy.

TIMP-3 expression was higher in prostate stromal cells than cancer cells. Co-culture analyses showed up-regulation of TIMP-3 in stromal cells and down-regulation in cancer cells. Immuno-staining in prostate tissues demonstrated higher TIMP-3 staining normal and benign tissues compared to malignant tissue. The modulation of TIMP-3 expression observed by androgen was cancer-cell-specific and by growth factors/cytokines was stromal-cell-specific. RNAi-mediated down-regulation of TIMP-3 in cancer-associated stromal cells resulted in increased migration and invasion. ECM lysates from transfected stromal cells demonstrated reduced MMP-2 inhibition.

Overall, these results show the interplay of the stromal and tumour compartments in modifying the activity of prostate tumour, and suggest that TIMP-3 is important in modulating the migration and invasive potential.

TABLE OF CONTENTS

LIST OF TABLES AND FIGURES

Chapter 1

Chapter 2

Chapter 3

Chapter 4

Chapter 5

Appendix

ACKNOWLEDGEMENTS

Funding from my parents, Revd. and Mrs Abiade Adeniji, as well as the New Route PhD Students' Bursary, supported this project. I am entirely grateful to my parents for the faith in me, which made them invest a fortune in my education. I am also indebted to the University of Sheffield for selecting me as one of the recipients of their bursary – without this rebate; my parents may have struggled to pay my tuition.

I would like to take this opportunity to thank all the people without which this project would not have been completed; Dr. Dave Buttle for his invaluable supervision, academic and personal advice, his listening ear, chastisement when I was not living up to his expectations, constructive criticisms of my errors, constant mentoring, devotion and patience during the 6 years I have spent with him as a researcher. Not forgetting Dr. Mike Barker and Dr. Chidi Molokwu for all the help with 'learning the ropes' of molecular medicine experiments and assays in my first year, Dr. Elizabeth Waterman, Dr. Neil Cross and Dr. Yung-Yi Chen for the useful information on the pathology of prostate cancer and all the training and assistance they gave me during my project, Dr. Colby Eaton and his research group for all the kind donations of cells and tissues for this research, Dr. Ingunn Holen and her research group for their scientific advice and assistance as well, and my dear friends and colleagues Lucksy Kottam, Yi-Ping Hsu, for their continued friendship throughout the years, and all the members of former D-Floor laboratory – a big thank you to you all.

My most sincere gratitude goes to my husband and best friend, Olayiwola Popoola, for being there for me all through the 11 years I have known him and especially for putting up with all the 'scientific jargon' I bombarded him with for the last 6 years and for his listening ear even when he was too tired to make sense of what I was saying. Without you, I would not have had any motivation to keep going all those days I felt like giving up – you are simply the best and I love you very much. Finally, the biggest thanks go to the Lord Almighty who led me through from start to finish and never left my side.

PUBLICATIONS AND PRESENTATIONS

Publication (Second Author):

Molokwu CN, **Adeniji OO**, Chandrasekharan S, Hamdy FC and Buttle DJ. Androgen regulates ADAMTS-15 gene expression in prostate cancer cells. *Cancer Investigations 2010, Aug. 28 (7); 698 – 710*

Presentations:

AMERICAN ASSOCIATION FOR CANCER RESEARCH (AACR) 100th ANNUAL MEETING: "SCIENCE, SYNERGY AND SUCCESS", April 2009. Molokwu CN, Adeniji OO, Hamdy FC and Buttle DJ. Regulation of ADAMTS-15 and TIMP-3 gene expression by androgen in prostate cancer cells and identification of putative androgen response elements. *AACR Conference Proceedings 2009*

AMERICAN ASSOCIATION FOR CANCER RESEARCH (AACR) SPECIAL CONFERENCE: "CYTOSKELETAL SIGNALLING IN CANCER", February 2008. Adeniji OO, Molokwu CN, Eaton CL, Hamdy FC and Buttle DJ. TIMP-3 modulation in prostate stromal and cancer cells. *AACR Conference Proceedings 2008*

BIOCHEMICAL SOCIETY/BRITISH SOCIETY FOR MATRIX BIOLOGY (BSMB) CONFERENCE: "SHAPING AND SENSING OF THE EXTRACELLULAR MATRIX", April 2007. Adeniji OO, Molokwu CN, Waterman EA, Cross N, Eaton CL, Hamdy FC and Buttle DJ. TIMP-3 mRNA is differentially regulated by TNF in prostate stromal and cancer cells.

AMERICAN ASSOCIATION FOR CANCER RESEARCH (AACR) SPECIAL CONFERENCE: "INNOVATIONS IN PROSTATE CANCER RESEARCH", December 2006. Adeniji OO, Molokwu CN, Waterman EA, Cross N, Eaton CL, Hamdy FC and Buttle DJ. Functional role(s) of ADAMTSs and TIMP-3 in prostate cancer progression. *AACR Conference Proceedings 2006*

NATIONAL CANCER RESEARCH INSTITUTE (NCRI) ANNUAL CONFERENCE, October 2006. Adeniji OO, Molokwu CN, Waterman EA, Cross N, Eaton CL, Hamdy FC and Buttle DJ. Regulation of ADAMTS-1 and TIMP-3 expression by androgen, growth factors and cytokines, and their role(s) in prostate cancer progression. *NCRI Conference Proceedings 2006*

BRITISH SOCIETY FOR MATRIX BIOLOGY (BSMB) CONFERENCE: THE MULTI-DIMENSIONAL MATRIX, September 2006. Adeniji OO, Molokwu CN, Waterman EA, Cross N, Eaton CL, Hamdy FC and Buttle DJ. Evaluating the role of ADAMTSs and TIMP-3 in prostate cancer progression. *BSMB Conference Proceedings 2006*

LIST OF ABBREVIATIONS

AR	Androgen Receptor
ADAM	A Disintegrin and Metalloproteinase
ADAMTS	ADAM with Thrombospondin Spanning Domain
APMA	p-Aminophenylmercuric Acetate
ARE	Androgen Response Element
BPH	Benign Prostatic Hyperplasia
BSA	Bovine Serum Albumin
cDNA	Complementary deoxyribonucleic acid
dATP	Deoxy-adenosine Triphosphate
dCTP	Deoxy-cytosine Triphosphate
DEPC	Diethyl Pyrocarbonate
dGTP	Deoxy-guanosine Triphosphate
DHT	Dihydrotestosterone
DEPC	Diethyl Pyrocarbonate
DMEM	Dulbecco's Modification of Eagles' Medium
dNTP	Deoxy-nucleoside Triphosphates
DRE	Digital rectal examination
DTT	Dithiothreitol
dTTP	Deoxy-tyrosine Triphosphate
ECM	Extracellular Matrix
EDTA	Ethylene Diamine Tetra-acetic acid
FACS	Fluorescence activated cell sorting
FCS	Foetal calf serum
GAPDH	Glyceraldehyde Phosphate Dehydrogenase
GFP	Green fluorescence protein
GG	Gleason Grade
GS	Gleason Score
HBS	Hepes Buffered Saline
H&E	Haematoxylin and Eosin
hK3	Human Kallikrein 3
HRP	Horse Radish Peroxidase

HSPG	Heparan Sulphate Proteoglycans
ICC	Immunocytochemistry
IHC	Immunohistochemistry
kD	Kilo Daltons
MMP	Matrix Metalloproteinase
mRNA	Messenger Ribonucleic Acid
PNGASE-F	Peptide-N-Glycosidase F
PBS	Phosphate Buffered Saline
PCR	Polymerase Chain Reaction
PIN	Prostate Intra-epithelial Neoplasia
PSA	Prostate Specific Antigen
SDS-PAGE	Sodium dodecyl sulphate polyacrylamide gel electrophoresis
siRNA	Short interfering Ribonucleic Acid
TACE	Tumour necrosis factor alpha converting enzyme
TBS	Tris Buffered Saline
TBST	Tris Buffered Saline with Tween-20
TEMED	Tetramethylethylenediamine
TGF-β1	Transforming Growth Factor Beta 1
TIMP	Tissue inhibitor of Metalloproteinases
TNF	Tumour Necrosis Factor
TURP	Transurethral Prostatectomy
VEGF	Vascular Endothelial Growth Factor
VEGFR	Vascular Endothelial Growth Factor Receptor
WT	Wild-type

CHAPTER 1: INTRODUCTION AND LITERATURE REVIEW

1.1. THE PROSTATE GLAND

In humans, the male reproductive system comprises internal and external organs, all of which work together for reproduction. The external organs are the penis and the scrotum and the internal organs are the testes, vas deferens, epididymis, seminal vesicle, Cowper glands and the prostate gland (Benoit et al., 1993). The prostate gland surrounds the urethra and is located behind the bladder and in front of the rectum (Figure 1.1). It participates in the production of semen, in conjunction with the testes, seminal vesicles and Cowper glands and also plays an important role in the transportation of sperm out of the penis (Kumar and Majumder, 1995). The prostate is small, walnut-shaped and measures about 3 cm in diameter and weighs about 20 – 25 g. The prostate secretes prostatic fluid which makes up about 35% of the total semen (Aumuller and Seitz, 1990). The seminal vesicle also secretes viscous fluid into the prostate and mixes with the prostatic fluid to form seminal fluid. The testicles are based within the scrotum and they secrete the male hormone – testosterone that facilitates the production of sperm – this is further transported by the vas deferens into the prostate and this mixes with the seminal fluid to form semen. The prostate is responsible for contracting and expelling the semen into the penis by the action of the smooth muscle cells contained in the prostate gland (Aumuller and Seitz, 1990).

The prostate is divided into three zones (Figure 1.1):

- Peripheral zone
- Transitional zone
- Central zone

The peripheral zone is located at the posterior of the prostate and is the largest zone in the gland while the transitional zone is located at the anterior of the prostate. The central zone can be found between the anterior and the posterior of the prostate and this is the zone connected to the seminal vesicle (McNeal, 1997).

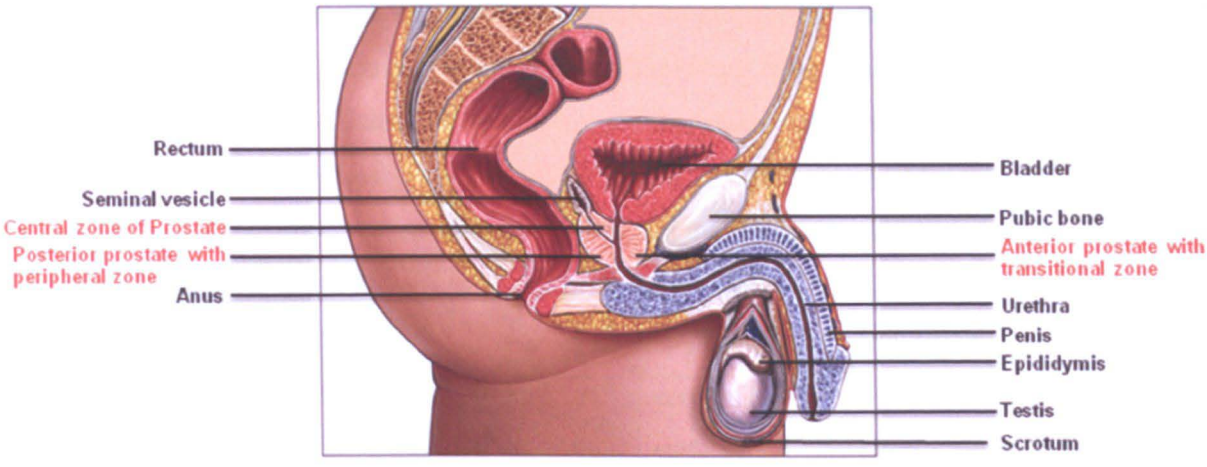

Figure 1.1: The Anatomy of the Male Reproductive System.
This diagram shows both the external and internal organs that are in the male reproductive system. The three zones of the prostate gland are highlighted in red. This image is used and modified with the permission of the copyright owner: Nucleus Medical Images (see Appendix for more information).

Alterations in the rate of growth of epithelial cells within the peripheral region results in majority of tumours of the prostate, while overgrowth of predominantly stromal and fibroblast cells within the transitional zone and, to a lesser extent, the overgrowth of epithelial cells in the transitional zone, results in the majority of benign prostatic hyperplasia (BPH) (McNeal, 1978).

1.2 BENIGN PROSTATIC HYPERPLASIA (BPH)

BPH is a disorder which occurs as a result of overgrowth of the stromal fibroblast and smooth muscle cells within the transitional zone of the prostate (Figure 1.2) (McNeal, 1978). This is an occurrence that increases with age (Altwein and Orestano, 1975). In BPH, there is an altered balance in the homoeostasis of ECM turnover, in favour of increased accumulation of ECM. This is mediated my several growth factors, including fibroblast growth factors (FGF), insulin-like growth factors (IGF) and transforming growth factor beta (TGF-β) (Eaton, 2003). The overgrowth is benign and, if sufficiently large, results in constriction of the prostatic urethra. The outcome of this constriction is blockage of the passage of urine from the bladder to the penis, leading to symptoms of urinary retention and the need for frequent urination, otherwise known as lower urinary tract symptoms (LUTS) (Roberts, 1994). If unchecked, these symptoms could develop into infection of the

urinary tract, formation of bladder stones in the bladder as a result of accumulation of salts from urine inside the bladder, and, more serious, failure of the kidneys (Reynard and Abrams, 1994).

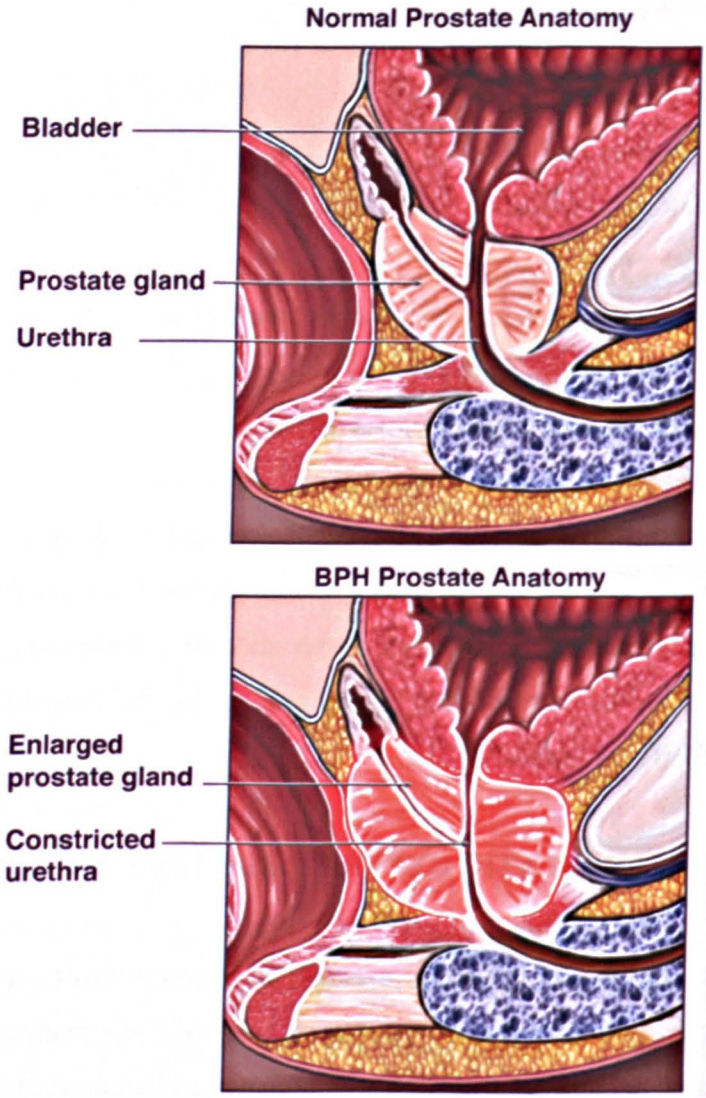

Figure 1.2: The Normal and BPH Prostate Anatomy.
This diagram illustrates the conformation of the prostatic urethra in normal prostate and its constriction in an enlarged prostate in BPH. This image is used with the permission of the copyright owner: Nucleus Medical Images (see Appendix for more information).

The occurrence of clinical BPH is most common in men above the age of 50 and as much as one third of men have BPH by the age of 50. This percentage increases to about 85% by the age of 90 (McVary, 2006). As at 2010, about 30 million cases of BPH had been

recorded worldwide, with the highest percentage of cases recorded within the U.S.A. (Gabuev and Oelke, 2011).

The role of androgen in the form of dihydrotestosterone in the manifestation of BPH cannot be overlooked. The main androgen produced in the prostate is testosterone and this is converted to an active dihydrotestosterone by the enzyme 5-α-reductase (Silver et al., 1994, Russell and Wilson, 1994). Up regulation of both circulating DHT and 5-α-reductase levels have been reported in BPH cases (Silver et al., 1994) and this led to the use of 5-α-reductase inhibitors such as finasteride for management of BPH (Seftel, 2005). These inhibitors are used either for monotherapy or alongside alpha-adrenergic blockers such as Tamsulosin as combinatorial therapy for patients that do not respond to 5-α-reductase inhibitors only and require alpha blockers to relax the smooth muscle cells in the prostate and relieve the pressure on the urethra (Shakir et al., 2001). The presence of elevated levels of growth factors other than DHT in the prostate has also been implicated in the progression of BPH. The accumulation and formation of stromal fibroblasts in the benign growth in the prostate has been shown to result in an increase in the secretion of cytokines such as TGF-β which can then trigger several signalling pathways such as the MAPK pathway and activate transcription factors that drive continuous growth of the fibroblasts and ECM synthesis within the prostate (Macoska, 2011). TGF-β transforms fibroblasts to myofibroblasts, which make smooth muscle actin, ECM matrix and proteinases (Border and Noble, 1994, Border et al., 1994) and is pivotal to many cancers where the progression is enhanced as a result of stromal fibroblasts producing more matrix and proteinases (Kohrmann et al., 2009, Duffy and McCarthy, 1998). Stromal fibroblasts can also regulate the growth of epithelial cells by the secretion of growth factors such as IGF-1 (McLaren et al., 2011, Crescioli et al., 2002), which plays a cellular proliferative role and can lead to an increase in both the stromal compartment and glandular epithelial compartment of the prostate and subsequent enlargement of the size of the prostate and LUTS. Thus, the epithelial and stromal interaction within the prostate is very important in the progression of BPH.

Diagnosis of BPH is initially by digital rectum evaluation (DRE) of the size of the prostate via the rectum and blood test to measure the levels of prostate-specific antigen (PSA; kallikrein-related peptidase 3; hK3;) (Uno, 1995). PSA is a serine proteinase secreted by epithelial cells in the prostate into the lumen of the prostatic ducts and forms part of the seminal fluid (Wang et al., 1979).These tests are also used for the diagnosis of prostate

cancer (as well as BPH) and a high level of PSA in serum is indicative of elevated seminal fluid levels and subsequent escape into the blood. Histological examination of prostate tissue will confirm the presence or absence of malignancy and will differentiate whether the increase in prostate size is as a result of development of prostate cancer or BPH. It will also show a larger stromal compartment relative to normal prostate tumour (see Figure 1.3).

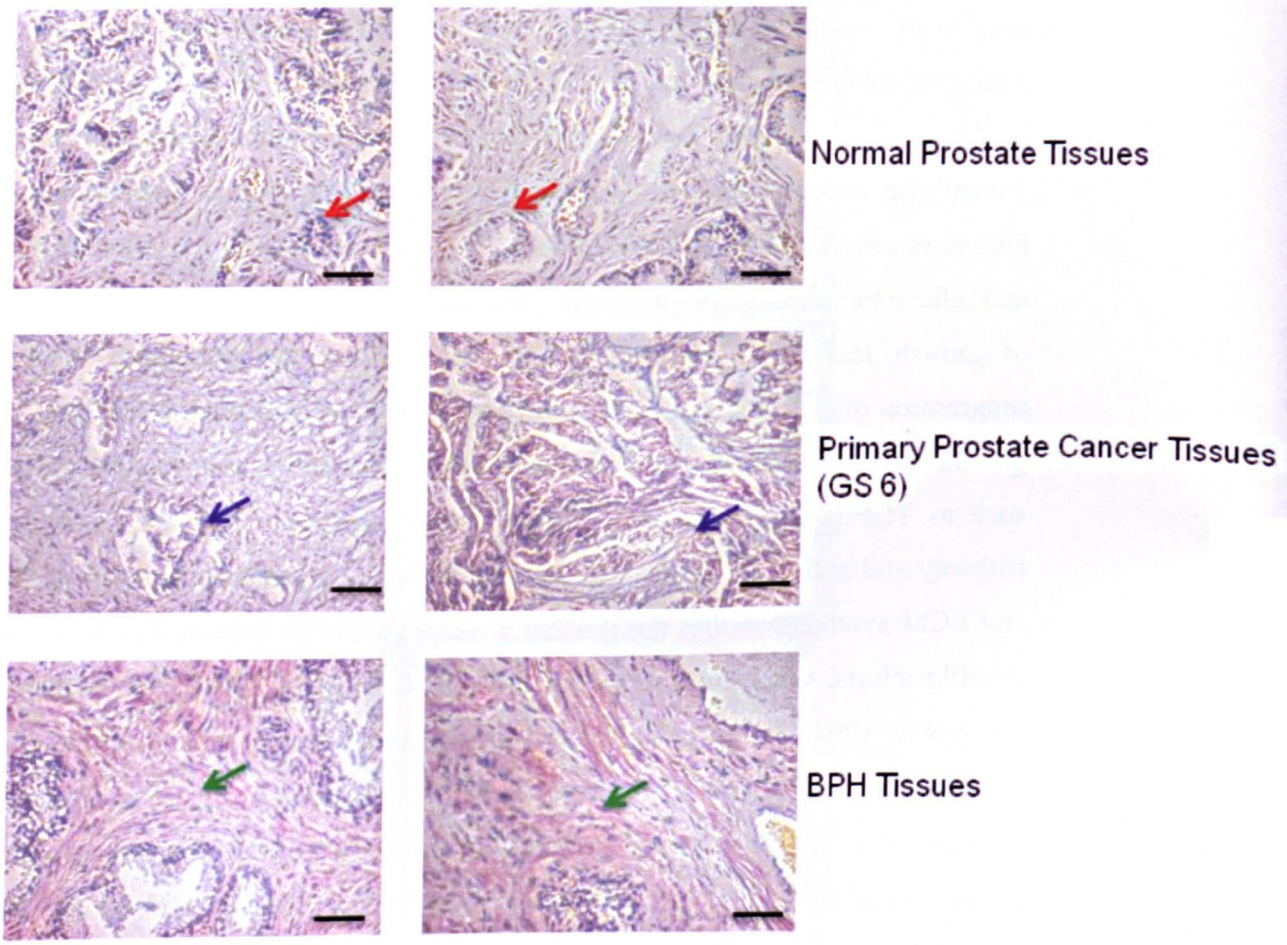

Figure 1.3: Immuno-histochemical Analyses of Prostate Tissues.
Normal, primary prostate cancer and BPH tissues were donated by Dr Colby Eaton's group at the University of Sheffield, U.K. Haematoxylin and Eosin Staining was carried out according to methods described in Section 2.17. Normal prostate tissues are characterised by the presence of intact glandular structures (red arrows) while erosion of basement membrane and disruption of glandular structures are present in primary prostate cancer tissue (blue arrows). In BPH, there is an increase in the surrounding stroma (green arrows) and this distinguishes the BPH tissue from prostate cancer tissues. The images were obtained using an inverted microscope and black bar represents size of 100 μM.

1.3 PROSTATE CANCER

1.3.1 Pathophysiology of Prostate Cancer

Prostate cancer is a malignant tumour that occurs predominantly in the peripheral region of the prostate gland and has metastatic potential i.e. it can spread to surrounding tissues and organs. It begins as a form that is treatable particularly among the elderly (Hemminki et al., 2005) but often progresses to become untreatable. Prostate cancer is a multifactorial disease and the aetiology is not completely understood. The most prominent phenotype is the loss of androgen-dependence on cell growth and survival within the prostate. Androgen is the main growth hormone in the prostate and normal prostate epithelial cells require constant levels of DHT to survive and this survival mechanism is regulated by the presence of the androgen receptor (Veldscholte et al., 1990). In prostate cancer, the tumour cells bypass this androgen signalling pathway via alternative means, the most common of which is androgen receptor mutation, and therefore are able to multiply unchecked (Trapman and Brinkmann, 1996, Craft et al., 1999, D'Antonio et al., 2010). Several mutations in the AR have been identified – replacement, addition or deletion of amino acids can lead to alteration of the protein function (Rajender et al., 2010, Rajender et al., 2007, Zhao et al., 1999) and therefore render the AR unable to regulate the levels of DHT. The increase in circulating DHT levels results in the increase in epithelial cell growth and is an initiating factor for growth of malignant tumours. The intricacies of androgen receptor signalling are discussed at length in Chapter 4: Section 4.1 of this report.

1.3.2 Epidemiology of Prostate Cancer

Prostate cancer is the most common cancer in men and accounts for 24 out of every 100 cases of male cancers in the U.K (Ferlay et al., 2010). It is the most common cancer in males and is the second highest cause of cancer death in males in the U.K. and the U.S.A, exceeded only by lung cancer (Hsing and Chokkalingam, 2006) (Ferlay et al., 2010). Its occurrence is usually linked to age and ethnic background (Parker et al., 2011), genetic pre-disposition, environmental factors (Wu et al., 2009b, Ekman et al., 1999) and even diet (Kenfield et al., 2007, Wolk, 2005, Mills et al., 1989). As with BPH, prostate cancer is prevalent in men over 50 (Ferlay et al., 2010) and can remain non-progressive, undetected

and undiagnosed for several years. Prostate cancer is prevalent in Europe and Africa, and not so much in Asia (Ferlay et al., 2010). There is a greater prevalence in black-Africans compared to Caucasians, and the least number of cases have been reported in Asians. In the U.K. alone, the number of prostate cancer cases in men over 50 years of age is 155 out of 100,000 men – this rate increases with age and the incidence increases to 510 out of 100,000 in men over the age of 60 and 750 per 100,000 in men over the age of 70. The rate of diagnosis is higher in developed regions of the world such as Europe, Australia and North America, with the lowest rate in Asia (Ferlay et al., 2010). Although black Africans have a higher risk of prostate cancer, under-diagnosis and late presentation are quite common (Heyns et al., 2003) as a result of almost non-existent PSA screening and reluctance of patients to seek medical advice when presenting with symptoms (Kehinde, 1995) reviewed in (Olapade-Olaopa et al., 2008). Therefore the data collated from regions such as West Africa are already biased as a result of these factors (Chu et al., 2011). The mortality rate is usually lower than the incidence rate (as shown in Figure 1.4) in developed countries as a result of better screening regimes and availability of resources for disease management. Developing and under-developed regions, on the contrary, have a higher proportion of mortality in cases presented and almost 1:1 ratio of incidence to mortality ratios. This is not surprising, given the lack of management resources available in these regions.

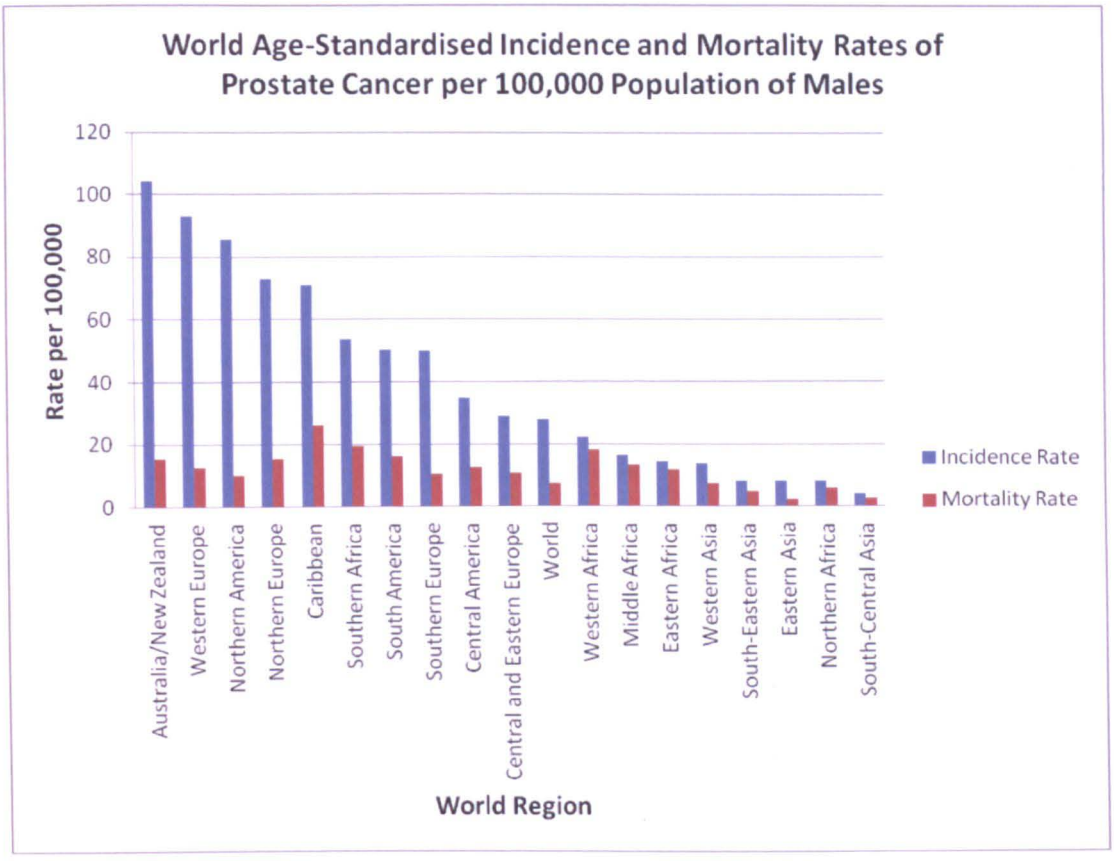

Figure 1.4: Rates of Incidence and Mortality of Prostate Cancer Worldwide.
These data were culled from the GLOBOCAN database, as compiled by the International Agency for Research on Cancer (2010) (Ferlay, Shin et al, 2008). The raw data are also available from http://globocan.iarc.fr

1.3.3 Staging of Prostate Cancer

The size of a tumour and the extent of its migration and invasion can be described using the TNM system of classification of cancer. This system was first described in 1942 and has since been adapted by the Union for International Cancer Control (UICC) as a standard method of classification of the severity of several cancers, including prostate cancer (Wallace et al., 1975). The acronym stands for:

- T = size of the Tumour
- N = degree of spread of tumour to proximal lymph Nodes
- M = degree of distal tumour Metastasis

Usually, a letter X denotes the absence of any of the above occurrences and numbers denote the size of the tumour (T) or the extent of local spread (N) or distal metastasis of the tumour (M). The different stages are described below:

- **T**
  - Tx: primary tumour cannot be evaluated
  - T0: no apparent sign of tumour
  - T1, T2, T3 or T4: size and extension of the primary tumour
- **N**
  - Nx: lymph nodes cannot be evaluated
  - N0: primary tumour cells absent from regional lymph nodes
  - N1: regional lymph node tumour metastasis present in small number of lymph nodes or lymph nodes closest to primary site of tumour
  - N2: tumor spread to an extent between N1 and N3
  - N3: regional and distal lymph node tumour metastasis or tumour present in numerous lymph nodes
- **M**
  - Mx: distant metastasis of primary tumour cannot be evaluated
  - M0: no distant metastasis
  - M1: metastasis to distant organs (beyond regional lymph nodes)

The stage of prostate cancer is usually assessed by a combination of DRE, imaging and surgical evaluation. DRE identifies the palpable size of the tumour and imaging techniques

such as x-rays, computed tomography scan (CT scan) and magnetic resonance imaging (MRI) can inform the physician about the location of the tumour both in the primary and any secondary sites (Quintens et al., 1990, Khoo et al., 1999). In instances whereby surgery has been utilized as a management regime, the surgeon is able to report any proximal or distant metastasis of the tumour away from the primary site. All of the information collected enables the patient to be assigned a stage e.g. prostate cancer T1N0M0 is cancer with small palpable tumour and no lymph node or distal metastasis away from the primary site (see Figure 1.5).

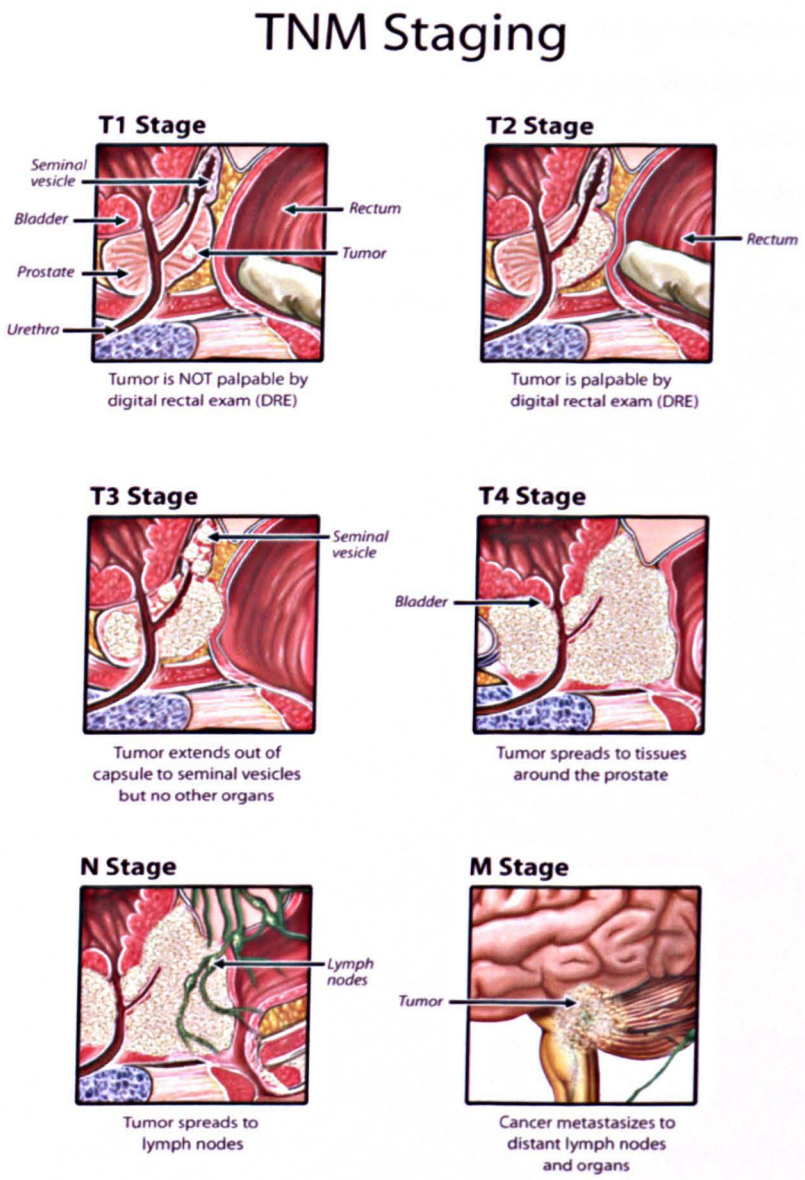

Figure 1.5: The TNM Staging in Prostate Cancer.
The T stages T1 – T4 are represented, with T1 being the small prostate confined tumour, T2 is the enlarged prostate confined tumour that is palpable by DRE and restricted only to the peripheral zone of the prostate, T3 is showing tumour extending to the central and transitional zones of the prostate and neighbouring seminal vesicles while T4 is showing the tumour enlarged, filling the three prostate zones and spreading to tissues around the prostate, constricting the neighbouring bladder and rectal muscles. N stage depicts the spread of the tumour into neighbouring lymph nodes and M stage depicts the distant metastasis of the tumour to secondary sites such as the brain. Copyright permission granted for the use of the image (see Appendix).

1.3.4 Grading of Prostate Cancer

The Gleason system was developed in 1977 and has been widely accepted as a standard for grading of prostate tumours (Gleason, 1977). This system is based solely on morphology and histochemical analyses of the tumour. Prostate tissue biopsy samples are sent to the lab for analysis by a pathologist. Microscopic examination of the biopsy specimens reveal tumour patterns ranging from well-differentiated, small glands to poorly differentiated sheets or cords of malignant cells. Five distinct glandular patterns are graded progressively from most to least differentiated. This is referred to as the Gleason Grade (GG) of the tumour and range from GG of 1 (well differentiated) to GG of 5 (poorly differentiated). The GG of the two predominant patterns present in a biopsy specimen are added to yield the final Gleason Score (GS) (see Figure 1.6). GS correlates well with other known prognostic factors, such as tumour size, presence of pelvic lymph-node metastasis, and PSA level (Baker AH et al., 2002) The lower the GS, the better the patient's prognosis and *vice versa.* Together with the TNM staging, the degree of malignancy of a tumour can be reported.

The occurrence of prostatic intra-epithelial neoplasia (PIN) is characteristic of pre-malignant tumours and is commonly detected in prostate tissue biopsies collected for examination to diagnose prostate cancer (Bostwick et al., 1995, Gaudin et al., 1997). PIN is characterised by the presence of abnormally formed epithelial cells contained within the glandular ducts. The cells form abnormally shaped glands that appear enlarged and sheet-like and erode into the surrounding stroma (Egevad et al., 2006, Algaba Arrea et al., 1997). PIN is a precursor to prostate cancer and many patients with detectable PIN in their tissue biopsy specimen go on to develop prostate cancer (Zlotta and Schulman, 1999) (Dickinson, 2010) (see Figure 1.7).

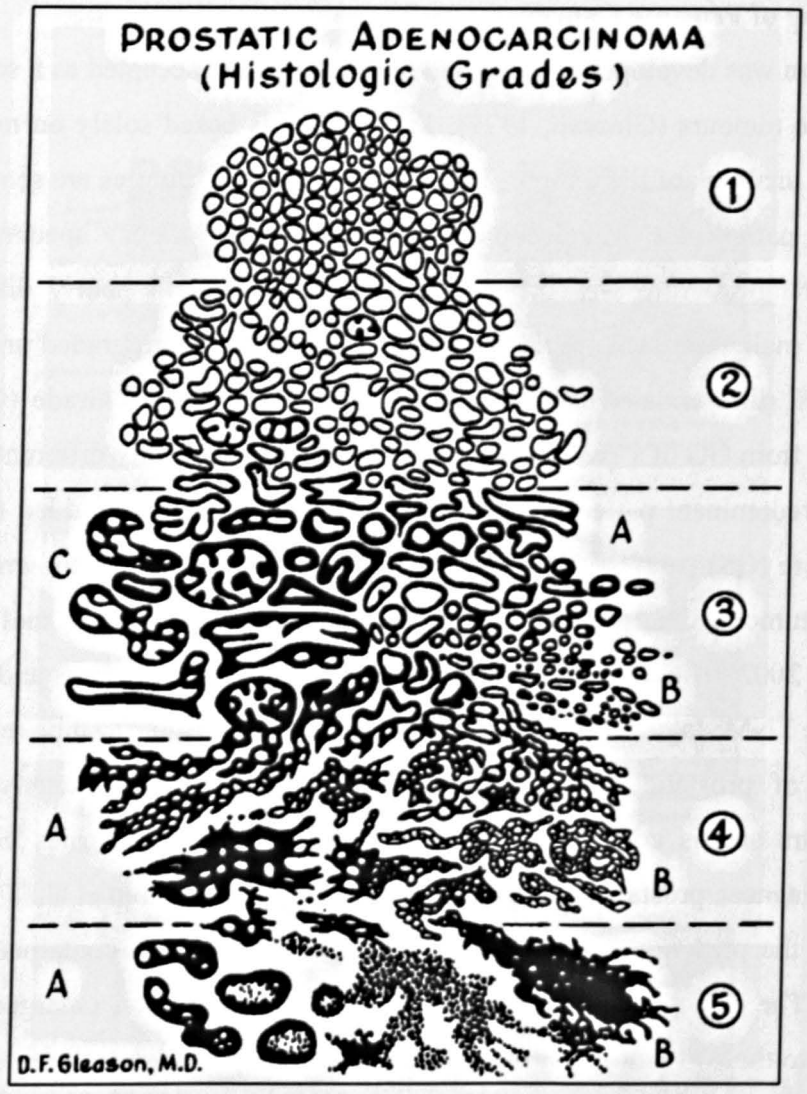

Figure 1.6: The Gleason Grading of Prostate Cancer.
The Copyright permission granted by Elsevier/RightsLink for the use of the image (see Appendix). Gleason grade (GG) of 1 is assigned to tissue that is well differentiated and retains the glandular structures and is very similar to the glandular conformation observed in normal tissue. GG of 2 is assigned to tissue that is still differentiated but less so, in comparison to GG 1 tissue. GG of 3 is assigned to tissue with signs of glandular disintegration and can be mild to moderate (A), moderate (B) or prominent (C) glandular disaggregation within the tissue. GG of 4 is assigned to tissue with poor differentiation and invasion of surrounding stroma, with the formation of non-distinct shaped cell masses and can range from tissues with minimal glandularity (A) to no glandularity (B). GG of 5 is assigned to tissues with no existing glands and the formation of infiltrating sheets of cells that can range from moderately flat sheets (A) to flat sheets (B).

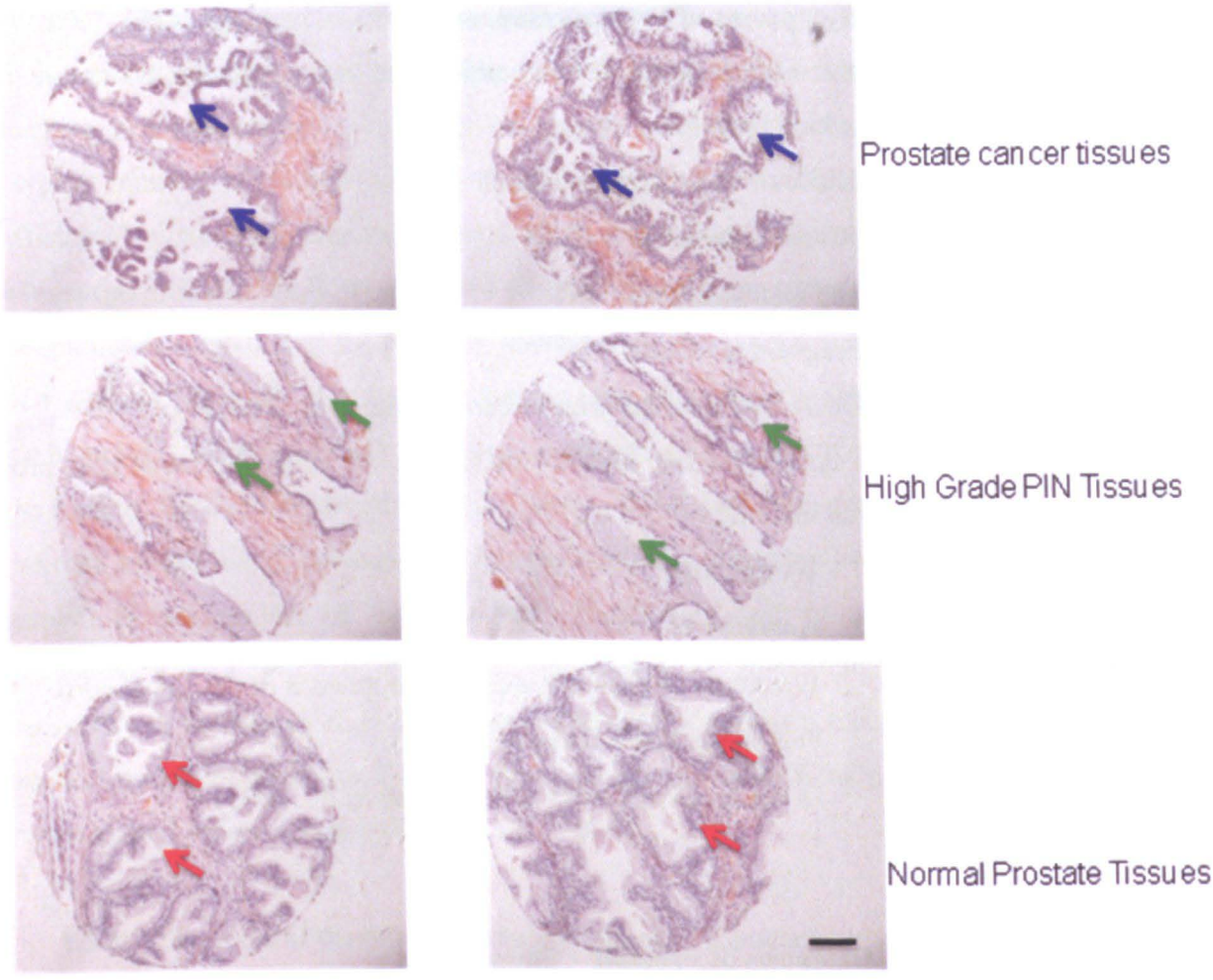

Figure 1.7: Immuno-histochemical Analyses of Prostate Tissues.
Prostate cancer, high-grade PIN and normal prostate tissues were donated by Dr Colby Eaton's group at the University of Sheffield, U.K. Haematoxylin and Eosin Staining was carried out according to methods described in Section 2.17. Normal prostate tissues are characterised by the presence of intact glandular structures (red arrows) while erosion of basement membrane and disruption of glandular structures are present in primary prostate cancer tissue (blue arrows). In high-grade PIN tissues, there is formation of abnormally shaped glands and glandular infiltration of surrounding stroma (green arrows). The images were obtained using an inverted microscope and black bar represents size of 100 μM.

1.3.5 Symptoms of Prostate Cancer

Many people with prostate cancer experience no symptoms but some patients have symptoms, which include:

- Difficult and painful urination
- Blood in the urine
- Hip and back pain
- Frequent urination
- Decreased force of urine stream (Miller et al., 2003)

The above symptoms are also characteristic of BPH. In metastatic prostate cancer, symptoms can include:

- Weight loss
- Anaemia
- Weakness or paralysis due to compression of the spinal cord
- Pain in the bones and joints
- In some cases, kidney failure (Kufe et al., 2003)

1.3.6 Diagnosis of Prostate Cancer

Prostate cancer progression is usually monitored by carrying out a prostate specific antigen (PSA) test. This involves measuring the serum levels of PSA, which is originally produced in the semen. PSA is a glycoprotein and a member of the kallikrein family of serine proteases (MEROPS ID: S01.162, http://merops.sanger.ac.uk). PSA is an androgen dependent marker for prostate cancer progression and can also be used during screening to identify those at risk of prostate cancer (Heinlein and Chang, 2004). However, this test is not a very good diagnostic marker as some patients with benign prostate enlargement also produce elevated levels of PSA (Baker AH et al., 2002) Therefore, tissue biopsy specimen has to be collected and histologically analysed for a complete diagnosis of prostate cancer. In some cases, CT and MRI scans can also be carried out to detect any metastasis specific to malignancy only (Tzikas et al., 2011).

1.3.7 Management of Prostate Cancer

In patients at the early stage of the disease, where the tumour is still localised within the prostate and patients have low Gleason grades and PSA levels, patients may undergo surgical removal of the tumour and radiotherapy as curative measures, though not 100% efficient. However, the chances of eradicating the disease at this early stage are increased with surgery (Balk, 2002). In advanced stages of the disease where the cancer has spread to lymph nodes surrounding the prostate, androgen ablation therapy is employed as a method of treatment, whereby anti-androgen drugs such as flutamide (Higano et al., 1996) and bicalutamide (See et al., 2001) are given to patients with a view to controlling the growth of the tumour. By the time the disease advances to the distant metastatic stage, the majority of patients would have developed hormone-refractory prostate cancer, whereby tumour growth is independent of the presence of androgen and so anti-androgen drugs are ineffective (Balk, 2002). At this stage, the disease is untreatable. The loss of androgen sensitivity is thought to arise from a mutation in the androgen receptor a ligand-activated nuclear transcription factor that is important for the growth of prostate cancer and its response to hormone therapy (Taplin et al., 2003).

1.3.8 The Role of the Stromal compartment in Cancer

The stroma is an important component of the cellular microenvironment, providing support and nutrition for growing cells. In the tumour microenvironment, the role of the stroma is particularly important because there exists alterations in the conformation of the epithelial cells, leading to a concomitant change in the stromal compartment as well (De Wever and Mareel, 2003, Bishop, 1991). There are several components of the stroma – these include: inflammatory cells, endothelial cells, fibroblasts and matrix components, all of which play crucial roles in the development of the tumour (Mareel and Leroy, 2003).

The inflammatory cells comprise mast cells, macrophages and polymorphonuclear leukocytes (PMN), all of which work together to effect tissue response to injury or inflammation. The mast cells secrete soluble growth factors, proteinases and cytokines that mediate angiogenesis and proliferation of endothelial, fibroblast and tumour cells (Coussens et al., 1999). Macrophages also produce several cytokines and pro-angiogenic factors that support stromal cell proliferation (Ono et al., 1999). PMNs are immune-response mediators and act as first line of defense in tissue invasion and inflammation. They recruit immune cells and secrete a host of cytokines and chemokines in response to

inflammation (Di Carlo et al., 2001). In the hypoxic conditions associated with the tumour microenvironment, the inflammatory cells produce cytokines and proteases that effect alterations in the ECM and guide both cell proliferation and cell killing (Di Carlo et al., 2001).

The endothelial cells respond to the presence of a tumour by eliciting increased angiogenesis to supply blood to the growing tumour (Carmeliet and Jain, 2000). Also, the increase in tumour vasculature enables the tumour cells to metastasize out of the primary site – a phenomenon characteristic of several advanced cancers as reviewed previously (Folkman, 1995). Angiogenesis is mediated by secreted growth factors both from the tumour cells as well as the endothelial and inflammatory cells and these growth factors mediate endothelial cell growth and motility. One of the most important of these pro-angiogenic factors is vascular endothelial growth factor (VEGF) which is primarily secreted by the endothelial cells and macrophages, and to some extent by the cancer cell in the tumour environment (Carmeliet and Jain, 2000). Endothelial cells also secrete endothelin-1 (ET-1) which enables proliferation of endothelial cells (Unoki et al., 1999). With increase in tumour size come increases in pro-angiogenic factors such as transforming growth factor beta (TGF-β) and platelet-derived growth factor (PDGF), all of which modulate vascularisation and metastasis of the tumour (Lippman et al., 1987, Jechlinger et al., 2006).

The fibroblasts, also components of the stroma, play an important role in the tumour microenvironment. First there is a paracrine effect of the tumour cells on the fibroblasts – an increase in the secreted levels of TGFβ by tumour cells result in recruitment of fibroblasts to the tumour and subsequent activation of fibroblasts to myofibroblasts (Ronnov-Jessen and Petersen, 1993). ET-1 from endothelial cells and PDGF from tumour cells also nourish and facilitate proliferation of myofibroblasts in the tumour microenvironment. Myofibroblasts act as a major 'supplier' of proteinases and proteinase inhibitors in the ECM (Knowles et al., 2012, Ito et al., 1995) and help to regulate their homeostasis. Fibroblasts also secrete other major components of the stromal matrix such as proteoglycans (Hassell et al., 1992), collagen (Noel et al., 1992), fibronectin (Clark et al., 1997) all of which contribute to the structural framework of the supporting ECM. They are also major secretors of matrix-degrading proteinases such as members of the MMPs (Stuelten et al., 2005, Wandel et al., 2000) as well as proteinase inhibitors such as TIMPs (Fernandez-Gomez et al., 2011), both of which play regulatory roles in tissue homeostasis.

The importance of stromal cells to the growth and progression of tumours is clear and the ever-increasing evidence suggests that the cancer cells are not independent of their stromal compartments and that stromal cells even drive tumour progression via expression of matrix-degrading proteases.

The summary of interactions of tumour and stromal cells is schematically represented in Figure 1.8. In light of these findings, it is important to better understand the proteases and their inhibitors and these will be discussed below.

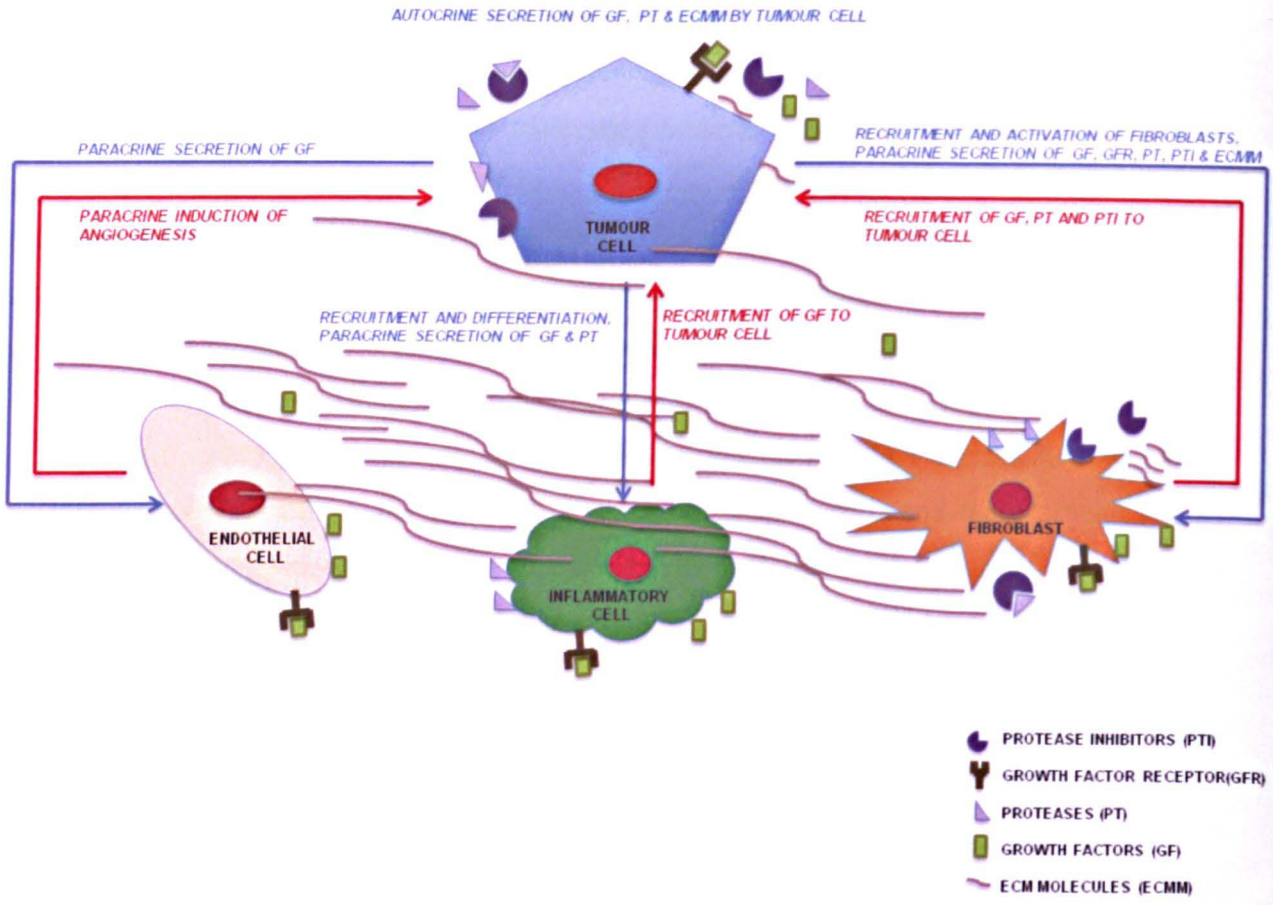

Figure 1.8: The Interactions between Tumour and Stromal Cells.
The stromal compartment comprises endothelial cells, inflammatory cells, fibroblast cells and ECM components. The autocrine secretion of growth factors by the tumour cells induces the proliferation of stromal cells and vice versa. Also, angiogenesis is mediated in the tumour microenvironment via paracrine signalling between the endothelial and tumour cells. The production of cytokines and growth factors by inflammatory cells also modulate tumour cell growth. Proximity of the tumour cells to fibroblasts also results in activation of fibroblasts to myofibroblasts and concomitant secretion of growth factors, proteinases, proteinase inhibitors into the microenvironment – these are all recruited to the tumour cells and mediate their growth, migration and invasion.

1.4 PROTEASES

Proteases or peptidases, as they are sometimes called, are a group of enzymes that function by cleaving peptide bonds formed by amino acids in proteins (Simpson, 2007). They are ubiquitously expressed in nature and function mainly by cleaving peptide bonds within a protein (endopeptidase), at the N- or C- terminal regions of a protein (exo-peptidases) and thus are generally classed on these characteristics. In humans, proteases are key players in biological processes such as digestion of food (e.g. pepsin), blood clotting (e.g. thrombin), growth and development of cells (e.g. PSA) and signalling pathways (e.g. the proteasome and caspases). The classification of proteases based on the type of peptide bonds they cleave (Bairoch, 1994), is described in Figure 1.9.

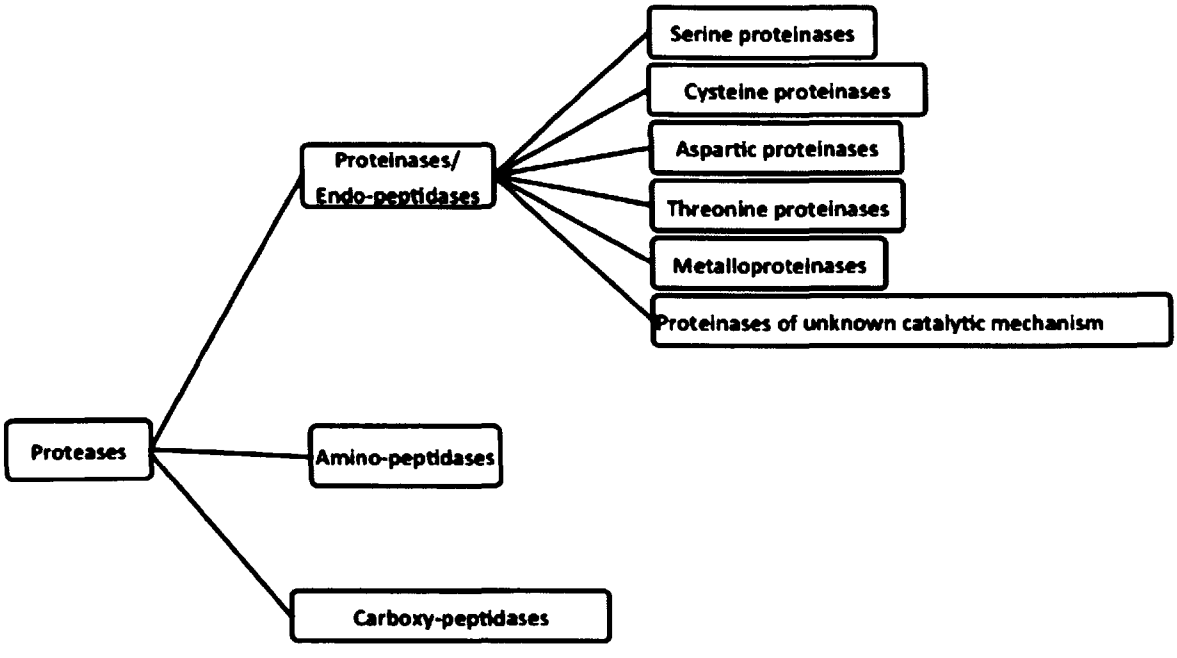

Figure 1.9: Schematic Representation of the Super-family and Family of Proteinases According to the MEROPS Database of Proteinases and their Inhibitors.
Also see MEROPS database available on http://merops.sanger.ac.uk (Rawlings et al., 2010)

For the purpose of this report, only the endopeptidases will be discussed, with emphasis on metalloproteinases, as relevant to the research project.

1.4.1 Serine Proteinases

This is the most widely studied and largest class of proteinases and belongs to the E.C. 3.4.21 class of enzymes according to the international union of biochemistry and molecular biology (IUBMB) (Bairoch, 1994). They act primarily by cleavage of peptide bonds within the core of the protein and this is mediated by a triad of amino acids (Ser 195, His 57, and Asp 102) located in the catalytic site of the proteinase. This triad of amino acids is collectively called the catalytic triad and is widely conserved amongst members of this family of enzymes, and is important in their mechanism of action (Hartley, 1970, Hedstrom, 2002, Kraut, 1977). Serine proteinases are broadly divided into 12 clans and 79 families – only 8 of these families are found in humans. Mammalian serine proteinases participate in diverse biological functions such as digestion (e.g. trypsin); blood clotting (e.g. thrombin, plasmin), signal pathway processing (e.g. signal peptidase I, furin, the proteasome) and reproduction (e.g. kallikrein 3). According to the MEROPS database of proteinases, members of the serine proteinases are denoted by a prefix "S" followed by a specific number, which defines the family.

1.4.2 Cysteine Proteinases

This is a class of proteinases that is ubiquitously expressed in plants and animals and play diverse roles in physiology and pathophysiology in mammals (Leung-Toung et al., 2002). They are widely grouped into 8 clans and 96 families – only 11 of the families are found in humans. Their enzymatic activity is mediated by a catalytic triad in their active site comprising a cysteine, aspartate and histidine residue, located close to each other (Nishihira and Tachikawa, 1999). In mammals, cysteine proteinases comprise some cathepsins, calpains and caspases, all of which play important roles in biological processes e.g. cathepsin K plays a major role in bone resorption and skeletal muscle integrity (Inaoka et al., 1995), caspase 8 plays a major role in programmed cell death alongside caspase 3 (Denault and Salvesen, 2002, Salvesen, 2002) and calpain 1 has been shown to be involved in cell cycle progression (Janossy et al., 2004). They belong to the E.C. 3.4.22 class of enzymes according to IUBMB and are denoted by "C" followed by the family number.

1.4.3 Aspartic Proteinases

This class of proteinases belong to the E.C. 3.4.23 class of enzymes according to IUBMB and members are denoted by "A" followed by a number, according to MEROPS. They are widely grouped into 5 clans and 16 families – only 2 of the families are found in humans. Their enzymatic activity is largely dependent on two conserved aspartate residues in their catalytic domain (Pearl, 1987). In mammals, their main function is digestion, with pepsin A found predominantly in gastric secretions (Baxter et al., 1990) and cathepsin E in endosomes where it is implicated in antigen processing (Maric et al., 1994, Chain et al., 2005)

1.4.4 Threonine Proteinases

This is a relatively small class of proteinases, in comparison to serine proteinases and belongs to the E.C. 3.4.25 class of enzymes according to IUBMB and is denoted by "T" followed by a number, according to MEROPS. They are widely grouped into 6 families, 2 of which are found in humans. The catalytic site of this family contains a threonine residue necessary for its enzymatic activity (Seemuller et al., 1995). Members of this family include polycystin-1 that plays an important role in renal tube formation in kidneys (Scheffers et al., 2000) and are also found in the proteasome. The N-terminal threonine residues of some of the beta subunits are the nucleophiles in catalysis (Seemuller et al., 1995).

1.4.5 Metalloproteinases

This class of proteinases belongs to the E.C.3.4.24 according to IUBMB and are denoted by 'M' followed by the family member, according to the MEROPS database. They constitute a family of metal ion-dependent enzymes, with a zinc-binding site in their catalytic domain (Stocker and Bode, 1995, Stocker et al., 1995). The zinc-binding domain is well conserved in this family, with the sequence x-x-x-H-E-x-x-H-x-x. They are also commonly called the "metzincins" because of their conserved zinc-binding domain (Rawlings and Barrett, 1995, Hege and Baumann, 2001). They are widely grouped into 16 clans and 86 families – only 11 of these families are found in humans.

1.4.5.1 Matrix Metalloproteinases (MMPs)

In many biological processes such as development, wound healing and in many pathological processes, there is extracellular matrix (ECM) breakdown resulting from an increase in proteinase activity. Some of the proteinases implicated include the matrix metalloproteinases (MMPs) otherwise known as the matrixins. The MMPs belong to the family M10 subfamily M10A of proteinases, according to the MEROPS database. These enzymes are secreted by cells as inactive pro-enzymes or zymogens that become activated via initial cleavage of the signal peptide post-translationally in the endoplasmic reticulum, followed by furin cleavage of the pro-peptide giving rise to an active neutral metalloproteinase that depends on water molecules bound to the Zn^{2+} binding site for its activity (Visse and Nagase, 2003). There are 24 known MMPs in mammals, majority of which are responsible for the degradation of components of the ECM (Nagase and Woessner, 1999b, Bode et al., 1999). They have been implicated in several degenerative disorders, including arthritis and cancer, with correlation between MMP activity and invasion and metastatic potential observed in various cancers as previously reviewed (Folgueras et al., 2004).

The basic structure of MMPs consists of a preceding signal peptide at the N-terminal domain followed by a pro-peptide, a furin cleavage site and then a catalytic domain. The catalytic domain contains a Zinc binding region that is mandatory for the maintenance of the catalytic function of the metalloproteinase (Bode et al., 1999). The zinc ion is bound to the catalytic domain via three histidine residues in the conserved zinc-binding motif: H-E-x-x-H-x-x-G-x-x-H of the metallo-enzyme. The pro-peptide maintains the enzyme in its latent state via the cysteine residue in a conserved motif P-R-C-G-x-P-D. The cysteine residue is able to associate with the zinc binding domain to prevent its catalytic function (Nagase and Woessner, 1999a). In some MMPs, the catalytic domain also contains fibronectin type II inserts, which play a role in the substrate specificity of the MMP e.g. gelatinase/MMP-2 (Murphy et al., 1985). In the C-terminal region, the haemopexin-like domain is a tetrad structure, which is essential for the interaction of MMP with other proteins and is a determinant of most MMPs specificity for their substrate (Murphy et al., 1985) (see Figure 1.10).

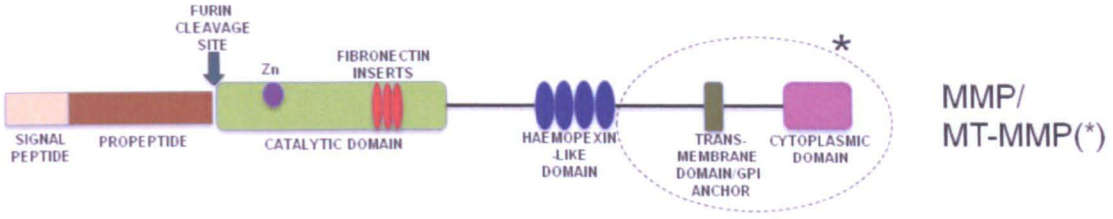

Figure 1.10: Schematic Diagram Representing the MMPs and MT-MMPs.
The signal peptide, furin cleavage site, pro-peptide, catalytic domain and haemopexin-like domains are characteristic of most MMPs, with the exception of MMP-7 and MMP-26 that have no haemopexin domain. The trans-membrane/GPI anchor and cytoplasmic domains in dotted circle is only present in MT-MMP.

MMPs are further divided into subsets based on the organization of their domains. These subsets are: membrane-bound MMPs, collagenases, stromelysins, matrilysins, gelatinases and other MMPs (Visse and Nagase, 2003).

The MT-MMP is a subset of the MMPs whose members are characteristically anchored to the cell membrane via a C-terminal trans-membrane or GPI-anchored domain, with an additional C-terminal cytoplasmic domain at the tail end of the enzyme (Zucker et al., 2003). Members include: MT1-MMP (MMP-14), MT2-MMP (MMP-15), MT3-MMP (MMP-16), MT4-MMP (MMP17), MT5-MMP (MMP-24) and MT6-MMP (MMP-25) (Zucker et al., 2003).

The collagenases subset comprises MMPs that cleave interstitial collagen molecules in the ECM. Their C-terminal region contains the tetrad haemopexin-like domain that enables them to carry out their collagenolytic function (Tam et al., 2004). Members include: collagenase-1 (MMP-1), collagenase-2 (MMP-8), collagenase-3 (MMP-13) and non-mammalian collagenase-4 (MMP-18) (Visse and Nagase, 2003). MMP-14 is also a very efficient collagenase (Tchetina et al., 2005, Schneider et al., 2008).

The stromelysins subset comprises MMPs that share structural similarity to the collagenases in general, but lack the collagenolytic activity. Their members include stromelysin-1 (MMP3) and stromelysin-2 (MMP-10) both of which are able to cleave several non-collagen ECM molecules and are players in the activation of pro-MMPs (Visse and Nagase, 2003). Stromelysin-3 (MMP-11) is the third member of this subset but is structurally different from the other stromelysins because it contains a furin recognition site

at the C-terminal of its pro-peptide, enabling intracellular cleavage and activation of the enzyme. Stromelysin-3 also has a weak affinity for ECM molecules but strong affinity for serpins (Gall et al., 2001).

The Matrilysins subset comprises MMPs that lack a haemopexin-like domain (Windsor et al., 1997). The members include matrilysin-1 (MMP-7) and matrilysin-2 (MMP-26). Matrilysin-1 is characteristically secreted by epithelial cells and is able to degrade ECM molecules as well as some cell surface molecules like E-cadherin (Noe et al., 2001). Matrilysin-2 is an intra-cellular enzyme that is capable of digesting ECM molecules like fibronectin and vitronectin (Noe et al., 2001, Marchenko et al., 2001).

The gelatinases subset comprises MMPs that have the haemopexin-like domain in their C-terminal region as well as fibronectin inserts in the N-terminal catalytic domain. This enables them to bind to ECM components like gelatin, elastin and collagen to effect digestion of these molecules (Allan et al., 1995, Patterson et al., 2001). Members include gelatinase-A (MMP-2) and gelatinase-B (MMP-9).

In addition to the above subsets, there are also other MMPs that have diverse functions. Members include macrophage elastase (MMP-12) which is expressed in human alveolar macrophages and is capable of cleaving elastin (Shapiro et al., 1993) and has been implicated in the development of emphysema (Haq et al., 2011), rheumatoid arthritis synovial inflammation (MMP-19) which cleaves molecules of the basement membrane and is found in lymphocytes of rheumatoid arthritis patients (Sedlacek et al., 1998, Kolb et al., 1997) and has also been identified as an anti-angiogenic tumour suppressor, (Chan et al., 2010). Enamelysin (MMP-20) possesses amelogeninolytic properties and is primarily found in the enamel of newly formed teeth (Sulkala et al., 2002). MMP-21 has gelatinolytic properties and is largely expressed in melanomas (Skoog et al., 2006, Kuivanen et al., 2005) and squamous cell carcinomas (Boyd et al., 2009).

MMP-23 is a unique member of this subset of MMPs as a result of the different arrangement of its domains in comparison to other MMPs – it has no haemopexin-like domain but instead, contains a cysteine-rich domain. It also has a trans-membrane domain in its pro-peptide at the N-terminal region (Pei, 1999). Next to the pro-peptide is a furin cleavage site, which enables the enzyme to be activated intracellularly or during secretion (Pei et al., 2000). MMP-27 is the same enzyme as chicken MMP-22 (Yang and Kurkinen, 1998) but the function remains unclear. MMP-28 is found in keratinocytes (Lohi et al.,

2001) and may also play a role in the epithelial to mesenchymal transition of lung cancer epithelial cells (Illman et al., 2008).

MMPs have been implicated in several developmental and pathological roles over the years. They are particularly implicated in cancers such as breast, colon, and prostate cancer as previously reviewed (Folgueras et al., 2004) where their expression has been shown to positively correlate with disease progression. Several drugs have been manufactured as synthetic MMP inhibitors e.g. Prinomastat and Marismastat, but poor efficacies and tolerability has been reported due largely to the cytotoxic effect of the drug and its inability to improve survival rates of cancer patients has led to its discontinuation as therapy for cancer (Bissett et al., 2005, Sparano et al., 2004).

1.4.5.2 A Disintegrin and metalloproteinase (ADAM)

This is a subset of the adamalysin subfamily of metzincins and belongs to the M12B subfamily according to MEROPS. They share N-terminal sequence similarity to the MMPs in that they are synthesized as pro-enzymes and possess a signal peptide domain, pro-peptide domain and a catalytic domain within their N-terminal region (Seals and Courtneidge, 2003). Also the H-E-x-x-H-x-x-G-x-x-H zinc-binding motif in the catalytic domain and the R-C-G-x-P-D conserved cysteine motif in the pro-peptide in MMPs are also conserved in ADAMs (Seals and Courtneidge, 2003). However, the difference lies in the C-terminal region of these proteinases, which contains a characteristic cysteine-rich domain, a disintegrin-like domain, an epidermal growth factor (EGF)-like domain, a trans-membrane domain and a cytoplasmic domain, hence their alias of MDC (metallo-proteinase-like, disintegrin-like, cysteine-rich proteins (Takeda et al., 2006). The presence of the trans-membrane domain enables the enzyme to be membrane-anchored and therefore localized on the cell surface. The cysteine-rich domain and the disintegrin-like domain present in the extra-cellular region of the proteinase enable its interaction with ECM proteins in order to enforce its proteolytic function. The presence of an integrin-binding motif R-x-x-x-x-x-x-D-E-V-F in the disintegrin-like domain of the ADAMs enable them to bind to integrins in the ECM while the cysteine-rich domain has high affinity for ECM molecules like heparan sulphate proteoglycans (Seals and Courtneidge, 2003) (see Figure 1.11). The role of the EGF-like domain is unclear.

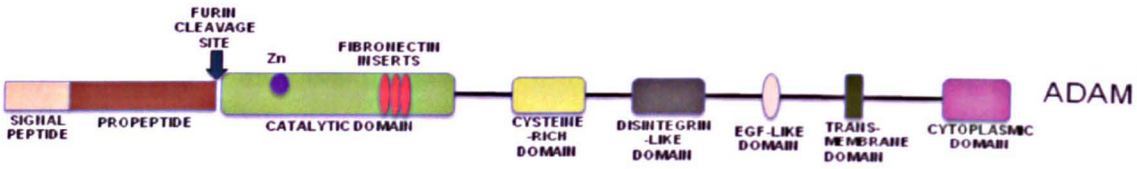

Figure 1.11: Schematic Diagram Representing the ADAMs.
The signal peptide, pro-peptide, furin cleavage site, catalytic domain, cysteine-rich domain, disintegrin-like domain, EGF-like domain, trans-membrane and cytoplasmic domains are characteristic of members of the ADAM family, with the exception of ADAM-8, ADAM-20, ADAM-28 and ADAM-30 that lack the furin cleavage site.

ADAM metalloproteinases function as "Sheddases" with characteristic ability to cleave proteins from their membrane-bound form, and release them from the cell membrane with diverse biological consequences (Zhang et al., 2000).

There are 24 known human ADAMs (Klein and Bischoff, 2011). In humans, the ADAM family is broadly divided into two subsets: ADAMs with no known proteolytic activity and ADAMs with known proteolytic activity.

ADAMs with no known proteolytic activity include: ADAM-2, -3, -6, -7, -11, -16, -18, -21/-31, -22, -23, -27 and -29.

ADAMs with known proteolytic activity includes: ADAM-1, -8, -9, -10, -12, -15, -17, -19, -20, -28, -30 and -33. ADAM10 and ADAM17 are the most relevant to this research and will be discussed further.

ADAM-10 is also known as CD156c and its pro-enzyme is also cleaved by proteolytic cleavage to release its active form which plays multifunctional roles; it sheds chemokines and their receptors e.g. CXCL16 (Abel et al., 2004) as well as the membrane-bound form of FAS ligand, releasing soluble FAS which plays a major role in the regulation of cellular apoptosis (Kirkin et al., 2007, Liu and Chang, 2011). It was first identified due to its myelin basic protein-cleaving activity (Amour et al., 2000). It promotes tumour migration and metastasis via its ability to shed CD44 (pro-migratory molecule) (Murai et al., 2004). ADAM-10 also plays a role in shedding of HER2 in the HER2 signalling pathway required in breast cancer (Liu et al., 2006).

ADAM-17 is the most widely studied member of the ADAMs and is also known as TNF-alpha converting enzyme (TACE). It is produced as a pro-enzyme and activated by proteolytic cleavage (Moss et al., 1997a). Its major role is in the conversion of membrane-

bound pro-TNF to soluble TNF (Moss et al., 1997a). It also plays roles as a sheddase of L-selectin which is important in cellular adhesion (Condon et al., 2001), TGF-α, an important pro-inflammatory cytokine (Liu et al., 2009), and epigen (Sahin and Blobel, 2007). It is also an important mediator of tumour formation and metastasis as evident in studies showing cells that had lost ADAM-17 were unable to form tumours and also unable to invade the surrounding environment (Franovic et al., 2006).

1.4.5.3 A Disintegrin and metalloproteinase with Thrombospondin Motif (ADAMTSs)

This is a subset of the adamalysin subfamily of metzincins and belongs to the M12B subfamily according to the MEROPS database. They possess a signal peptide domain, pro-peptide domain and a catalytic domain within their N-terminal region (Kaushal and Shah, 2000). The H-E-x-x-H-x-x-G-x-x-H zinc-binding motif in the catalytic domain and the R-C-G-x-P-D conserved cysteine motif in the pro-peptide in MMPs are also conserved in ADAMTSs. However, the differences lie in the C-terminal region of these proteinases, which contains a characteristic cysteine-rich domain, a thrombospindin type-1 domain, spacer region and several thrombospondin type-1 repeats (Kuno and Matsushima, 1998), with the exception of ADAMTS-4 which has no thrombospondin repeats (Kashiwagi et al., 2004). The ADAMTSs also bear structural similarity to the ADAMs in their N-terminal region, with the presence of the furin cleavage site between the signal peptide and the pro-peptide (Apte, 2004) (see Figure 1.12). Another unique characteristic that distinguishes them from the ADAMs is that although they are secreted proteins, they are localized predominantly in the ECM (Tang, 2001).

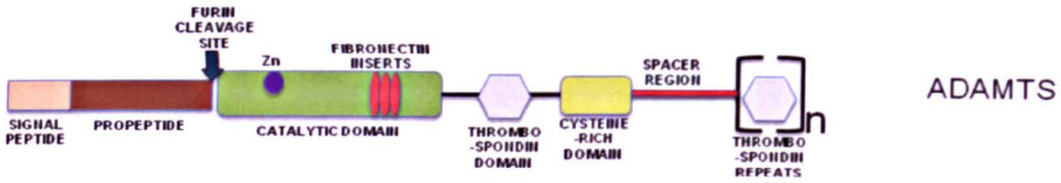

Figure 1.12: Schematic Diagram Representing the ADAMTSs.
The signal peptide, pro-peptide, furin cleavage site, catalytic domain, thrombospondin repeats and cysteine-rich domain are characteristic of members of the ADAM family,

Figure 1.12 shows the conserved domains present in all ADAMTS members. They undergo signal peptidase processing to remove the signal peptide co-translationally and proteolytic cleavage to activate the enzymes. There are 19 known ADAMTSs in the human genome, which are classified based on their proteolytic properties: the 'orphan' ADAMTSs, whose functions remain more-or-less obscure, and the known proteolytic ADAMTSs. The 'orphan' ADAMTSs include: ADAMTS -6, -7, -10, -17, -18, -19 and -20 and the known proteolytic ADAMTSs include: ADAMTS -1, -2, -3, -4, -5 (-11), -8, -9, -12, -13, -14, -15 and -16 (Porter et al., 2005).

The aggrecanases include ADAMTS -1, -4, -5, -9 and -15 and have been shown to break down predominantly aggrecan and homologous large aggregating proteoglycans (Nagase and Kashiwagi, 2003). ADAMTS-1 is also known as METH-1 and has also been shown to break down versican (Nakamura et al., 2005b). ADAMTS-4 is also known as aggrecanase 1 and ADAMTS-5 is also known as aggrecanase-2 - both cleave brevican, (proteoglycan that is expressed in the CNS) and versican (Matthews et al., 2000, Kuno et al., 2000). ADAMTS -1, -4 and -8 possess anti-angiogenic properties (Dunn et al., 2006, Hsu et al., 2012), and ADAMTS-8 is expressed at low levels in breast carcinoma (Porter et al., 2004). ADAMTS-9 has been reported to also cleave versican (Kern et al., 2010) while the role of ADAMTS-15 is not very clear and recent studies may indicate that it is protective against prostate cancer progression (Molokwu et al., 2010).

The pro-collagen-N-proteinases include ADAMTS -2, -3 and -14 and their role is in the conversion of pro-collagens to collagens via removal of the pro-peptide in the N-terminus of the proteins. ADAMTS-2 has the widest catalytic profile, with reported activity on pro-collagens I, II and III (Colige et al., 1997). ADAMTS-3 has been reported to cleave pro-collagen II (Fernandes et al., 2001) while ADAMTS-14 cleaves pro-collagen-I (Colige et

al., 2002). ADAMTS-2 has also been reported to inhibit angiogenesis via mechanisms that are independent of its collagenolytic functions (Dubail et al., 2010)

The GON-ADAMTSs include ADAMTS -9 and -20. They are so named because of the sequence similarity they bear to the ADAMTS gene *gon-1* found in *C elegans* (gon-1 is responsible for gonadal development). They both have an additional gon domain in their C-terminal region as well as 14 thrombospondin repeats adjacent to their cysteine-rich domain (Somerville et al., 2003). The role of these ADAMTSs in human gonadal development has not been shown, despite the similarity of their C-terminal region with the well-characterized *C elegans gon-1* gene. ADAMTS-9 mRNA has been shown to be elevated in metastatic head and neck cancer (Demircan et al., 2009) and in a rat model of stroke (Reid et al., 2009).

The von-Willebrand factor cleaving and activating enzyme is ADAMTS-13 and is so named because its main substrate is von-Willebrand factor – a protein that plays an important role in haemostasis through interactions with Factor VIII and platelets (Sadler, 1998). Mutations in the *ADAMTS-13* gene have been shown to result in thrombotic thrombocytopenic purpura, which results in renal failure, neurological dysfunction and anaemia (Fontana et al., 2004).

Some of the orphan ADAMTSs have variable expression patterns in pathological processes e.g. *ADAMTS-16* gene expression is up regulated in osteoarthritis (Kevorkian et al., 2004) and ADAMTS-12 expression in breast cancer (Porter et al., 2004).

1.5 PROTEINASE INHIBITORS

Proteinase inhibitors are proteins that inhibit proteinases and are ubiquitously expressed in nature. They are mainly classified into super families according to the type of proteinase they inhibit. These are:

- Serine proteinase inhibitors
- Cysteine proteinase inhibitors
- α-2-Macroglobulin
- Metallo-proteinase inhibitors

There are 415 known proteinase inhibitors in the human genome, compared to 698 proteinases (MEROPS). To date, there are 91 families of proteinase inhibitors.

1.5.1 Serine Proteinase Inhibitors

Whilst this is not the best name for this group of inhibitors, their characteristic ability to inhibit S1 and S8 families of serine proteinases (Dufour et al., 1998) have earned them this nickname. There are over 500 members of this inhibitor family identified to date. They also inhibit family C1 (Irving et al., 2002) and family C14 (Komiyama et al., 1994) of cysteine proteinases. They exert their inhibitory property by irreversibly binding to the active catalytic region on the proteinase thereby causing conformational distortion of and subsequent inactivation of the enzyme (Silverman et al., 2001). They are also commonly known as Serpins although this term rightly refers to the I4 family of serine and cysteine proteinase inhibitors. Serpins are sub-divided into 36 clades, 29 of which are inhibitory and 7 of which are non-inhibitory (Silverman et al., 2001).

The non-inhibitory clades of serpins include: Serpin A2, A11, A12, A13, B10, B11 and B12 while the inhibitory clades include: Serpin A1, A3, A4, A5, A6, A7, A8, A9, A10, B1, B2, B3, B4, B5, B6, B7, B8, B9, B13, C1, D1, E1, E2, F1, F2, G1, H1, N1 and N2.

1.5.2 Cysteine Proteinase Inhibitors

This super-family of inhibitors comprises inhibitors from the I4, I25, I27 and I32 of inhibitors according to MEROPS. They inhibit C1, C2 and C14 families of proteinases and include the stefins, cystatins, calpastatins, survivin and kininogens (Muller-Esterl et al., 1985a)

The stefins are largely intracellular and include cystatin A and cystatin B; cystatin A is expressed by neutrophilic granulocytes and epithelial cells (Jarvinen et al., 1987) while cystatin B is expressed during embryonic development (Afonso et al., 1997).

The cystatin family is largely extracellular and includes cystatin C, cystatin D and cystatin S. Cystatin C has a wide distribution (Nagai et al., 2008). Cystatin D is expressed in saliva (Freije et al., 1991) while cystatin S is expressed in tears, urine, saliva, pancreas, bronchi and gall bladder.

Calpastatins inhibit calpains 1 and 2 of the C2 family of proteinases (Todd et al., 2003) and to a lesser degree, calpain 3.

Survivin is an inhibitor of the caspases in C14 family of proteases and plays a major role in cellular survival and homeostasis (Guzman et al., 2009, Chandele et al., 2004, Shankar et al., 2001).

The kininogen family comprises H-kininogen and L-kininogen, both of which are expressed as extracellular proteins in plasma. Their roles include inhibition of C1 proteases including cathepsin L and are also involved in blood clotting processes (Muller-Esterl et al., 1985b).

1.5.3 α-2-Macroglobulin

This is an inhibitor of most proteinases that was first discovered in 1973 (Barrett and Starkey, 1973). It has a unique mode of action (Salvesen & Barrett, 1980) and is produced in the liver and is abundant in the blood. It is also expressed by fibroblasts (Boel et al., 1990) and macrophages (Hussaini et al., 1990).

1.5.4 Metalloproteinase Inhibitors

In humans, there are several metalloproteinase inhibitors, including: α-2-macroglobulin (see Section 1.5.3), β-amyloid precursor protein (inhibition of MMP-2) (Hashimoto et al., 2011) and reversion-inducing cysteine-rich protein RECK (inhibition of several MMPs including MMP-9, MMP-2) (Oh et al., 2001, Takeuchi et al., 2004). However, the most widely studied metalloproteinase inhibitors are members of the TIMP family and these will be discussed further.

1.6 TISSUE INHIBITOR OF METALLOPROTEINASES

The tissue inhibitor of metalloproteinases are a family of metalloproteinase inhibitors that are ubiquitously expressed in a variety of tissues and biological systems (Fata JE et al., 2001). They belong to the I35 family of inhibitors according to the MEROPS database. In humans, this family consists of four family members TIMP-1, -2, -3 and –4, and these TIMPs are all secreted proteins (Apte et al., 1994). By virtue of their MMP-inhibitory activity, the TIMPs have a major role in regulation of matrix composition and therefore affect a wide range of physiological processes such as growth, invasion, migration, angiogenesis, transformation and apoptosis (Lambert et al., 2004). The human TIMPs possess sequence identity of about 40% and contain 12 cysteine residues that are conserved in all members that form 6 disulphide bonds (Apte SS et al., 1995) (see Figures. 1.14 and 1.15). The N-terminal region of all TIMPs is highly conserved across all members and takes up about 2/3 of the entire protein (Murphy et al., 1991). As well as inhibiting the

MMPs (Visse and Nagase, 2003), TIMPs also inhibit most of the proteolytic ADAMs (Klein and Bischoff, 2011) and the ADAMTS aggrecanases (Porter et al., 2004). The TIMP: proteinase binding consists of a unique 1:1 stoichiometry thus maintaining homeostasis and proteolytic regulation in tissue physiology. Alteration in the balance in favour of the proteinases often results in pathological conditions (Nagase and Woessner, 1999a).

1.6.1 TIMP-1

TIMP-1 comprises 207 amino acids, with 23 amino acids in its signal peptide and 184 amino acid residues in its mature protein structure. Its relative molecular mass in its unglycosylated form is about 21kDa and has 2 known N-glycosylation sites (Okada et al., 1994). Its X-ray crystal structure has been solved and demonstrates binding of the N-terminal domain of TIMP-1 to the catalytic domain of MMP-1 thus eliciting an inhibitory function (Iyer et al., 2007). TIMP-1 has also been reported to inhibit ADAM-10 (Schelter et al., 2011, Amour et al., 2000). TIMP-1 is mainly expressed as a soluble protein and has been reported to confer proliferative advantages to cells such as fibroblasts (Welgus et al., 1979).

1.6.2 TIMP-2

TIMP-2 comprises 220 amino acids, with 26 amino acids in its signal peptide and 194 amino acid residues in its mature protein structure and has a relative molecular mass of 22kDa (Fridman et al., 1992). There are no known glycosylation sites in the protein (Wingfield et al., 1999) and it is constitutively expressed as a soluble protein known to inhibit MMPs and ADAMs as previously reviewed (Brew and Nagase, 2010). It has proliferative functions as shown in its enhancement of the growth of fibroblasts and erythroid precursors as well as pro-apoptotic effects as shown in its inhibition of the growth of human T-lymphocytes and colorectal cells (reviewed in (Brew and Nagase, 2010)

1.6.3 TIMP-4

TIMP-4 comprises 224 amino acids, with 29 amino acids in its signal peptide and 196 amino acids in its mature protein structure. It has no known glycosylation sites and is

synthesized as a soluble protein with a relative molecular mass of about 22kDa (Bigg et al., 1997).

1.6.4 TIMP-3

TIMP-3 is the main focus of the project. It comprises 211 amino acids, with 23 amino acids in its signal peptide and 188 amino acids in its mature protein (Apte SS et al., 1995).

1.6.4.1 Structure of TIMP-3

The TIMP-3 gene is large, compared to other members. It is about 30kbp in size and contains large introns and a long 3' untranslated region. Exon 1 of the gene contains the 5' untranslated region and also encodes the signal peptide as well as the N-terminal region of the mature protein. The translation termination codon and the 3' untranslated region are in exon 5 (Figure1.13) (Apte SS et al., 1995).

Figure 1.13: Schematic structure of the timp-3 gene.
The solid line represents the full length of the gene, both the translated and untranslated regions (UTR). The translated region comprises 5 exons labelled E1 – E5 and 4 introns labelled I1 – I4. The size of exon 5 is variable, depending on polyadenylation signal (grey box) and has been denoted E5 +/- (A)n.

TIMP-3 is also unique in that unlike other members of the family that become freely diffusible within the cellular microenvironment after secretion, TIMP-3 becomes tightly bound to the ECM via its C-terminus, although the basicity of the N-terminus with Lysine residues at Lys 26, 27, 30 and 76 (see Figure 1.6.4.1.2) may also be a contributing factor to the molecule's affinity to the ECM (Langton et al., 1998).

The stability of TIMP-3 in the ECM is a feature that is specified by the 3 loops comprising its C-terminus, and studies showed that recombinant TIMP-3 lacking the COOH region was obtained from the medium used, and did not bind to the ECM (Baker AH et al.). The six disulphide bonds arise from the 12 conserved cysteine residues and these form the basis of

the 6-loop protein structure (see Figure 1.14); three of which make up the N-terminal domain and the other three make up the C-terminal domain (Apte SS et al., 1995).

The x-ray crystal structure of TIMP-3 is yet unknown. However, there is a postulated model based on its similarity to TIMP-1. The structure of N-TIMP-3 in complex with TACE is shown in Figure 1.14 and the sequence similarity between TIMP-3 and other TIMPs is represented as a PRALINE multiple alignment format (Simossis and Heringa, 2005) in Figure 1.15. The beta sheets and helices of N-TIMP-3 are super-imposed on the sequence alignment:

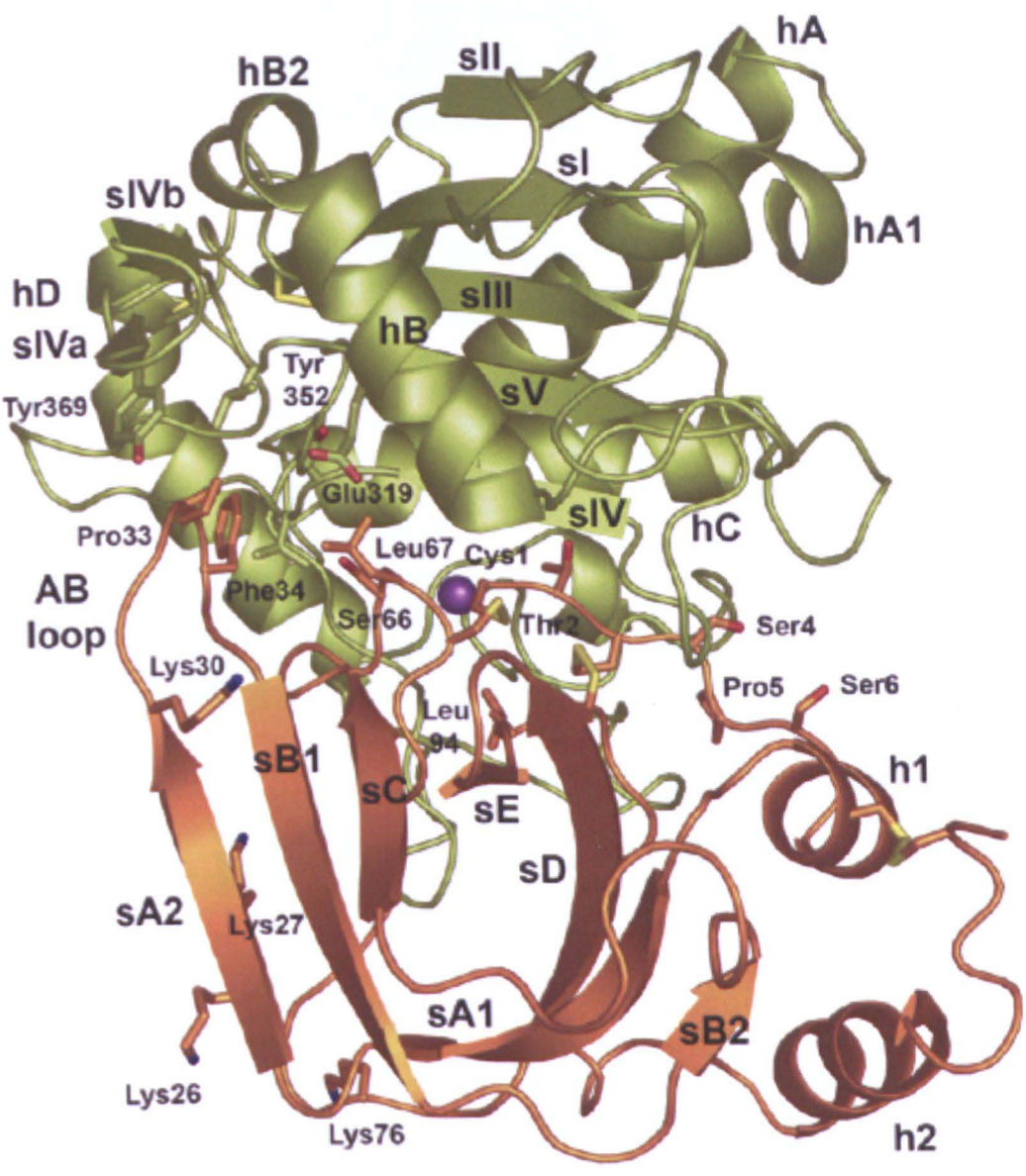

Figure 1.14: 3D Ribbon Structure of TACE-N-TIMP-3 Interaction

The 3D structure of the complex formed by binding of the catalytic domain of TACE (green) to the N-terminal domain of TIMP-3 (orange). The TIMP-3 structure is based on the similarity of TIMP-3 to TIMP-1, whose structure is well characterised and x-ray structure available. The 5 interrupted beta-sheets (sA – sE) and the 2 helices (h1 – h2) of the N-terminal TIMP-3 are shown. The Lysine residues (Lys26, 27, 30 and 76) that are important for ECM binding are shown as protruding orange and blue sticks. Copyright permission to reproduce image is detailed in Appendix.

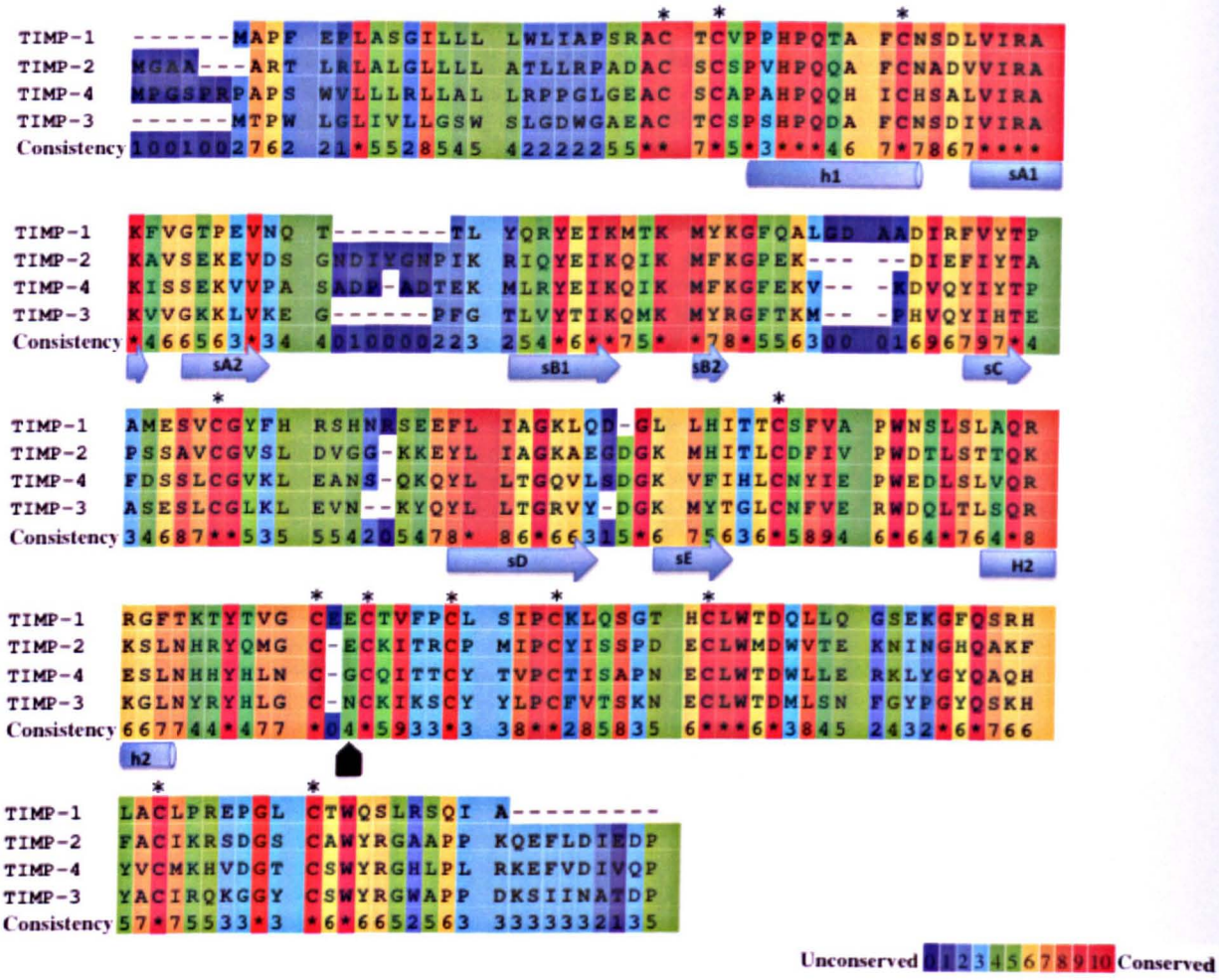

Figure 1.15: PRALINE Sequence Alignment of the TIMPs Showing Similarity. *The sequences of TIMPs 1-4 were imput into PRALINE online software for generation of colour-coded alignment and conserved motif identification. The key on the lower right side of the image shows colour coding for unconserved and conserved amino acids in the sequences, with blue representing least conserved amno acids and red representing most conserved amino acids ad scored from 1-10 likewise. "*" represents the alignment of the 12 cysteine residues that make up the 6 disulfide bonds characteristic of TIMPs. The beta sheets sA - sE (blue arrows) and helices h1 and h2 (blue cylinders) depicted in Figure 1.6.4.1.2 are superimposed on the sequences. The black arrow indicates the end of the N-terminal and the start of the C-terminal region of TIMP-3.*

1.6.4.2 Expression Profile of TIMP-3

TIMP-3 is widely expressed in different tissue types and to different degrees. It is highly expressed in placenta, lung and retina of the eye (see Figure 1.16). The expression and relative amounts of TIMP-3 transcripts in different tissues are represented below:

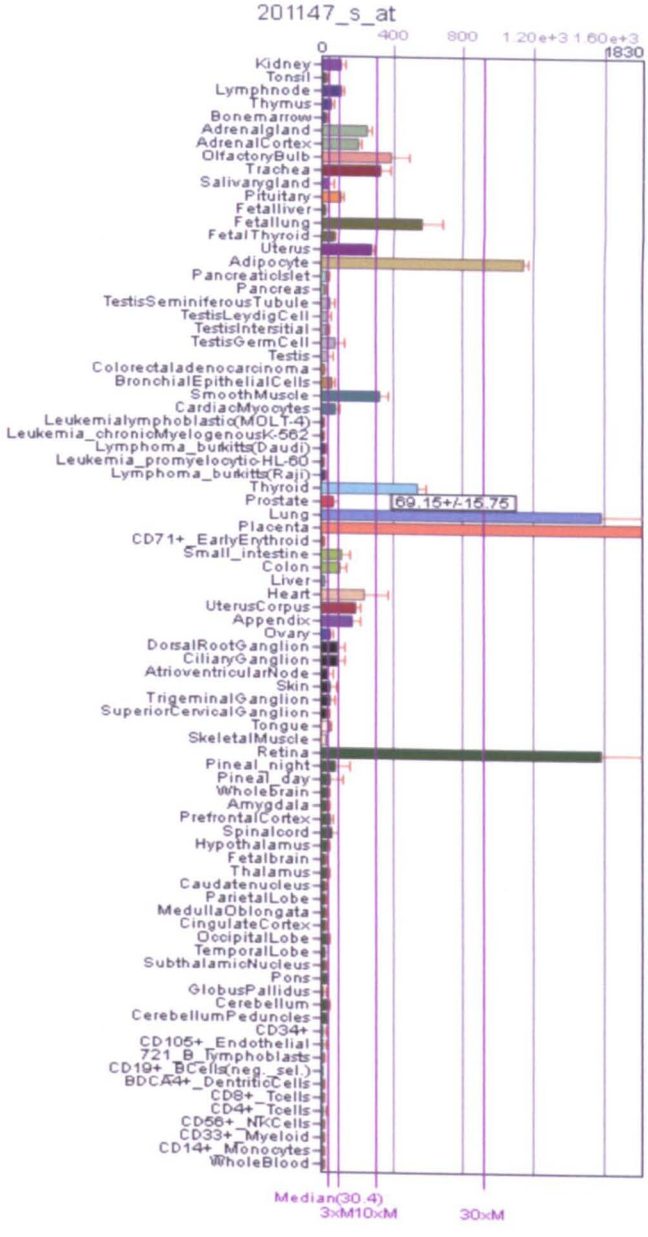

Figure 1.16: Expression Profile of TIMP-3 Transcripts in Different Tissues.
These data were obtained using the free BIOGPS software available at http://biogps.com (Wu et al., 2009a). Units represent relative quantification of TIMP-3 mRNA in tissue samples. Expression levels of TIMP-3 mRNA in the prostate is highlighted in the black box.

1.6.4.3 Functions of TIMP-3

1.6.4.3.1 Growth and Development

TIMP-3 expression in foetal hair follicle and foetal kidney has highlighted its role in foetal development. This is mediated by the balance of homeostasis of proteinases and TIMP-3, thereby regulating tissue turnover and normal development of the foetus (Airola et al., 1998).

1.6.3.4.2 Inhibition of Metalloproteinases

TIMP-3 inhibits several metalloproteinases and this is summarised in tabular format below:

Proteinase	TIMP-3 K*i* Value (nM)	Literature References
MMP-1	0.16	(Zhao et al., 2004)
MMP-2	N/R	(Zhao et al., 2004)
MMP-3	N/R	(Wetzel et al., 2003)
MMP-7	N/R	(Woessner, 1996)
MMP-8	N/R	(Pavloff et al., 1992)
MMP-9	N/R	(Negro et al., 1997)
MMP-13	N/R	(Knauper et al., 1996)
MMP-14 (MT1-MMP)	0.16	(Zhao et al., 2004)
MMP-15 (MT2-MMP)	N/R	(Butler et al., 1997)
MMP-16 (MT3-MMP)	0.008	(Zhao et al., 2004)
MMP-17 (MT4-MMP)	10	(Amour et al., 2002)
MMP-19	0.005	(Stracke et al., 2000)
ADAM-10	10	(Amour et al., 2002)
ADAM-12	100	(Amour et al., 2002)
ADAM-15	N/R	(Maretzky et al., 2009)
ADAM-17 (TACE)	10	(Amour et al., 2002)
ADAM28	N/R	(Mochizuki et al., 2004)
ADAMTS-1	N/R	(Rodriguez-Manzaneque et al., 2002)
ADAMTS-2	106	(Wang et al., 2006)
ADAMTS-4	7.9	(Hashimoto et al., 2001)
ADAMTS-5	N/R	(Kashiwagi M et al., 2001)

Table 1.1: Proteinases Inhibited by TIMP-3 and the Inhibitory Constants (Ki).
NR = not reported.

ADAM-17/TACE (TNF Alpha Convertase Enzyme) is responsible for processing membrane bound TNF to its soluble form. TIMP-3 controls TNF shedding by inhibiting TACE, and thus regulating the levels of TNF both in tissue homeostasis and tissue response to injury. Mohammed *et al* (Mohammed et al., 2004) demonstrated that TACE activity was up regulated in the livers of *timp-3*$^{-/-}$ mice, and that partial hepatectomy resulted in uncontrolled production of TNF (Wang et al., 2006) by the recruited macrophages, which, in the absence of TIMP-3, resulted in hepatic necrosis and eventual morbidity in these mice. TIMP-3 can also inhibit ADAMTSs, some of which, like TIMP-3, are located in the ECM via interactions with sulphated glycosaminoglycans (GAG). Wang et al (Wang et al., 2006) demonstrated the inhibition of the pro-collagen N-proteinase ADAMTS-2 by TIMP-3 and studies carried out by Kashiwagi *et al* (Kashiwagi M et al., 2001) have shown that the ADAMTSs -4 and -5 are inhibited by TIMP-3. In both studies, none of the other TIMP family members inhibited these ADAMTSs to the magnitude with which TIMP-3 did.

1.6.4.3.3 Inhibition of Angiogenesis

Qi *et al* (Qi et al., 2003) demonstrated that TIMP-3 inhibited angiogenesis by binding to VEGFR2, thus competing with binding of the bioactive ligand, VEGF. Consequently, there is inhibition of the downstream signalling pathways imperative for endothelial cell differentiation. TIMP-1 and TIMP-2 did not block VEGF binding in the above experiment, demonstrating that the interaction with VEGFR2 was TIMP-3-specific. Thus, TIMP-3 over-expression suppressed primary tumour growth and metastasis by suppressing cell growth and survival, necessary for tumour progression. This feature is independent of its MMP-inhibitory activity, as demonstrated by this group. However, MMP inhibition would be expected to also inhibit angiogenesis, as some of the MMPs are pro-angiogenic (Basile et al., 2007, Huang et al., 2007). The mechanism of TIMP-3 inhibition of angiogenesis is illustrated in Figure 1.17:

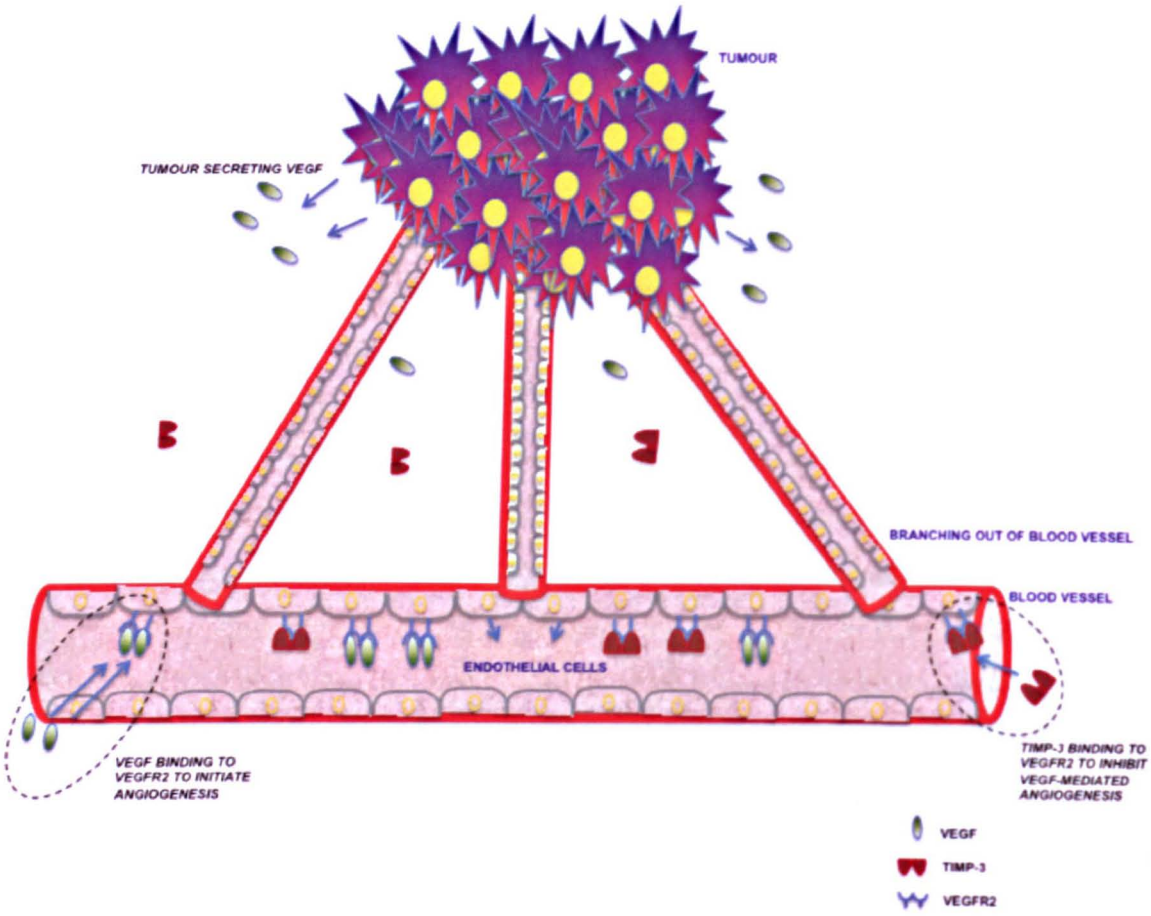

Figure 1.17: Schematic Representation of Tumour Angiogenesis and TIMP-3-specific Inhibition of Angiogenesis.

It is known that there is an increase in the blood supply in established tumours and the process of angiogenesis is mediated by VEGF binding to its receptor, VEGFR2. It has been demonstrated that TIMP-3 is able to competitively bind to VEGFR2 to inhibit the mediation of angiogenesis by VEGF, and this anti-angiogenic property is independent of its MMP-inhibitory activity (Qi et al., 2003).

1.6.4.3.4 Regulation of Apoptosis

Fata et al (Fata JE et al., 2001) demonstrated that TIMP-3 is a critical epithelial survival factor during mammary gland involution. According to their results, deficiencies in TIMP-3 function led to excessive and unscheduled physiological apoptosis in the mammary epithelium. They demonstrated that TIMP-3 influenced mammary epithelial apoptosis during involution through its ability to inhibit ecto-domain shedding of apoptotic regulatory factors such as TACE, which processes cell-bound TNF to its soluble, pro-apoptotic form Although their findings demonstrated an anti-apoptotic characteristic of TIMP-3, they concluded that the several effects of TIMP-3 on cell survival are largely dependent on the cell type, the cell microenvironment and the amount of TIMP-3 in the microenvironment. Also, recent studies by Mylona et al (Mylona et al., 2006), showed a positive correlation between the anti-apoptotic Bcl-2, and TIMP-3, suggesting that this inhibitor may play a role in suppressing cell death. One study showed an increase in the levels of secreted TACE and TIMP-3 in head and neck cancer, with expression positively correlating with lower survival rate in patients. As TACE is required for initiation of cellular apoptosis and inhibited by TIMP-3, the inhibitor is functioning in an anti-apoptotic manner, and may be contributing to the progression of head and neck cancer (Kornfeld et al., 2011). TIMP-3 also plays pro-apoptotic functions in cells as demonstrated by studies which show increase in cellular death in cancer cells over-expressing TIMP-3 or a decrease in apoptosis in neuronal cells from *timp-3* -/- mice following oxygen and glucose deprivation (Wetzel et al., 2008, Finan et al., 2006). Thus, TIMP-3 could be a risk factor for cancer as well as a "tumour suppressor", depending on which of its various activities predominates. A schematic diagram showing the TIMP-3 mediated inhibition apoptosis via TACE inhibition is illustrated in Figure 1.18.

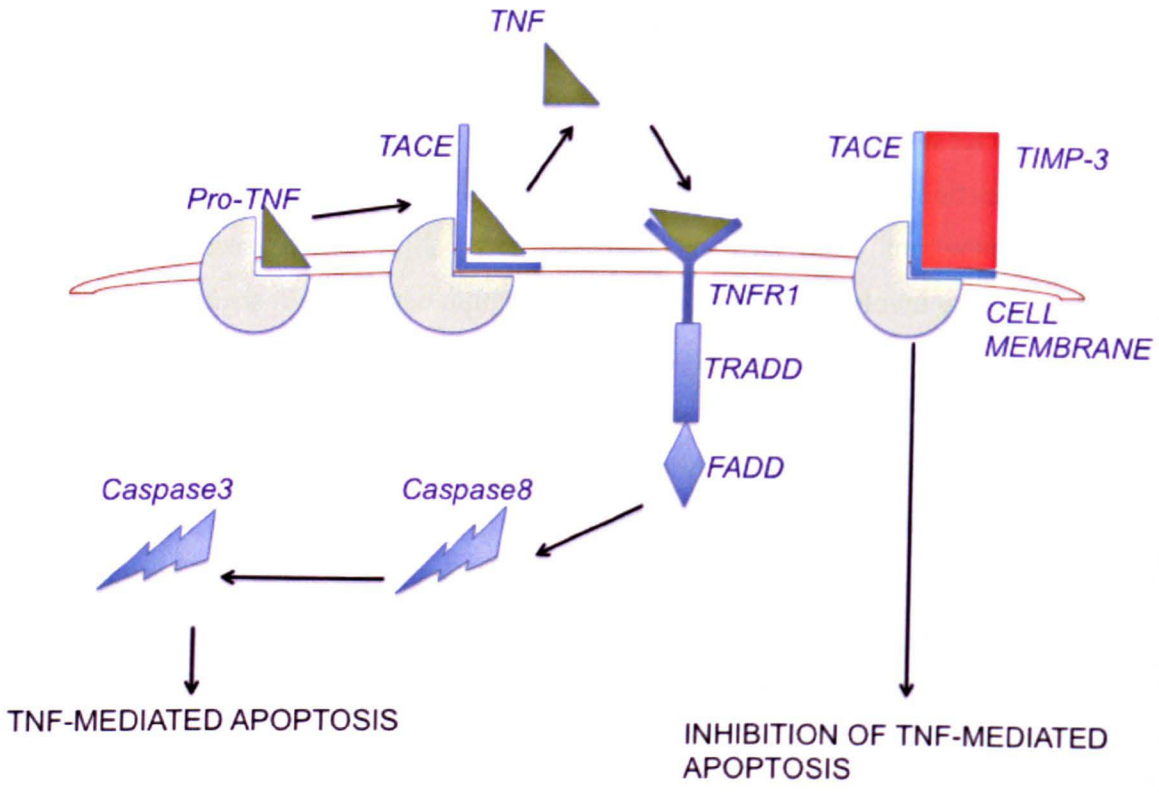

Figure 1.18: Schematic Representation of TIMP-3-specific Inhibition of Apoptosis.

TNF is a multi-functional cytokine that is synthesized by cells as a pro-TNF that requires the TNF-α-converting enzyme TACE/ADAM-17 to cleave its pro-peptide and release soluble TNF. Soluble TNF can then bind to its receptor, TNFR1, a trans-membrane receptor, to initiate the Fas-associated protein with death domain (FADD)-mediated apoptotic pathway. TIMP-3 is a known and potent inhibitor of TACE and can prevent its sheddase activity; thereby preventing the solubilisation of TNF and so plays an anti-apoptotic role.

1.6.4.3.5 Inhibition of Tumour Growth

Tumours frequently show an increase in MMP expression and/or a decrease in TIMP expression leading to a net increase in proteolytic activity, which may be necessary for tissue remodelling during tumour growth, angiogenesis, invasion, and metastasis. TIMP expression can suppress primary tumour growth, angiogenesis, invasion (in vitro and in vivo), and metastasis, whereas depletion of TIMPs can increase primary tumour growth, invasion, and metastasis, as demonstrated by Bachman et al (Bachman KE et al., 1999). They speculated that TIMP-3 expression may be critical for the normal growth of the kidney and brain, and that cancers, particularly from the kidney, have the highest frequency of timp-3 gene methylation – this methylation corresponds to the loss of TIMP-3 expression, and is prevalent in many primary solid tumours. It is thought that loss of TIMP-3 may inhibit normal apoptotic programs, enhance primary tumour growth and angiogenesis, invasiveness, and metastasis and possibly, therefore, contribute to all stages of malignant progression (Airola et al., 1998, Baker AH et al., 2002, Cruz-Munoz et al., 2006).

1.6.4.4 Non-malignant Pathological Conditions

Apart from the role(s) TIMP-3 plays in the development of several cancers via its proteinase-inhibitory properties, there are some disorders that have been associated with the over-expression or reduced expression of TIMP-3 in tissues and these include:

1.6.4.4.1 Age-related Macular Degeneration

Age-related macular degeneration is also known as AMD. Single nucleotide polymorphisms (SNPs) have been identified upstream of the TIMP-3 gene and about 24 of these occur in up to 90 % of AMD cases. The alteration of the *TIMP-3* gene in the retinal pigment epithelium and Bruch's membrane in the eye result in abnormal matrix turnover and increase in muscular degeneration and subsequent dystrophy of the macula (Kamei and Hollyfield, 1999).

1.6.4.4.2 Myocardial Infarction

The process of cardiac re-modelling is crucial to the repair of the heart following myocardial infarction. The existence of abnormal accelerated cardiac re-modelling in TIMP-3 knockout mice and an increase in the expression of matrix metalloproteinases and inflammatory cytokines has been demonstrated (Ikonomidis et al., 2005). This suggests that TIMP-3 may be important for minimizing cases of myocardial infarction in heart attack patients if the levels of TIMP-3 expressed in the myocardium could be up regulated.

1.6.4.4.3 Sorsby's Fundus Dystrophy

In Sorsby's fundus dystrophy, a mutation in the C-terminal region of TIMP-3 causes its accumulation in the Bruch's membrane of the eye, leading to blindness (Langton et al., 2005). The increased expression of TIMP-3 in the Bruch's membrane of SFD patients has been described and this has shed light on the aetiology of the disease whilst suggesting that therapeutic interventions that favour the reduction of TIMP-3 accumulation may prove beneficial for treating SFD patient (Chong et al., 2000, Fariss et al., 1998)

1.7 HYPOTHESIS AND AIMS OF THIS RESEARCH

Hypothesis: DHT, TNF and TGF-β regulate the amount of TIMP-3 present in prostate cancer and stromal cells, and that a loss of this inhibitor could enable the cancer cells to behave more aggressively and to grow and metastasize more efficiently.

The aims of this research are to:

- Investigate the expression of TIMP-3 in prostate stromal and cancer cells
- Study the factors that regulate the expression of TIMP-3, with a view to understanding the role of this inhibitor in prostate cancer progression.

Some of the factors controlling cell behaviour include dihydrotestosterone (DHT), tumour necrosis factor (TNF) and transforming growth factor beta (TGF-β) – these will be further discussed in Chapter 3, Section 3.1. DHT is a growth factor for prostate cancer cells (Burnstein, 2005) and elevated levels of the proinflammatory cytokine TNF have been observed in the serum of prostate cancer patients (Nakashima et al., 1998). Also, the

expression levels of ECM proteins and TIMP-3 mRNA are up regulated in peri-tumoural stroma of the breast (Bryne et al, 1995) and in prostatic stromal cells (Cross et al, 2005) *in vitro*. In order to elucidate in vitro the possible role of this inhibitor in prostate cancer, I will also analyse the role of TIMP-3 in biological processes such as growth, migration, invasion, angiogenesis and apoptosis, as well as proteinase inhibitory functional assays. In addition, the expression pattern of TIMP-3 will also be analysed in available histological samples, with a view to identifying if localization and expression pattern correlate positively or negatively with prostate cancer staging. Together, all of these experiments will help us to understand the importance of TIMP-3 in the initiation and/or progression of prostate cancer.

CHAPTER 2: MATERIALS AND METHODS

2.1 TISSUES AND CELL LINES

2.1.1 Prostate Tissues

All the prostate tissues and tissue micro-arrays were obtained as formalin-fixed paraffin-embedded slides from Dr. Colby Eaton, The Mellanby Centre; University of Sheffield Medical School. All tissues and primary cells obtained from patients were done in line with the Trent Multi Centre Research Ethics Committee approval, (REC reference 01/4/061 and STH reference SS02/196). The ethical approval was granted for the study titled: "Molecular mechanisms and the development of novel treatment strategies in progressing prostate cancer (ProMPT) with validity from January 2001 to January 2016.

The prostate tissues used in this project include:

- Normal Prostate Tissue
- Benign Prostatic Hyperplasia (BPH) tissue
- Primary Prostate Cancer Tissue

2.1.2 Stromal Cells (Non-Malignant)

2.1.2.1 Benign Prostatic Hyperplasia Stromal Cells:

BPH stromal cells were obtained from patients undergoing routine trans-urethral resectioning of the prostate (TURP) for bladder outlet obstruction (Cross et al., 2005). All tissues had been previously independently identified as BPH by histopathology, and in all cases, no signs of cancer were present. Our collaborator, Dr. Colby Eaton, provided all BPH cell types used for the experiments. Their markers of stromal cell origin have been previously described in BPH cells (Cardoso et al., 2004, True et al., 2009).

2.1.2.2 Prostate cancer associated fibroblasts (PCAF):

PCAF cells are carcinoma-associated fibroblasts originally obtained from patients undergoing re-sectioning of the prostate and were kind gifts from Dr. Colby Eaton's team. They had been previously characterised prior collection for this project.

2.1.2.3 Non-cancer associated prostate fibroblasts

WPMY-1 cells are prostate fibroblasts obtained from ATCC (Webber et al., 1999). They express the fibroblast-specific markers vimentin and fibronectin), do not express PSA and have also been shown by the depositors to have no cancer cell phenotype.

2.1.3 Cancer Cells

2.1.3.1 Poorly Metastatic Prostate Cancer Cells

LNCaP cells were obtained from cultures that were initially isolated from a needle aspiration biopsy of a lymph node metastatic lesion from a male caucasian prostate cancer patient (Sobel and Sadar, 2005a). The cell line was previously confirmed to be androgen-sensitive as a result of its expression of the androgen receptor (AR) and androgen-mediated up-regulation of prostate-specific antigen (PSA).

2.1.3.1 Highly Metastatic Prostate Cancer Cells:

The PC3 cell line was obtained from cultures that were initially isolated from a lumbar vertebral metastasis in a male Caucasian prostate cancer patient (Sobel and Sadar, 2005b). This cell line is known to be androgen-independent in its growth and does not express AR.

2.1.4 Cell Culture and Media Preparation

2.1.4.1 Serum-containing Media

All cells were routinely cultured in Dulbecco's modified eagle's medium (DMEM) (Invitrogen, 41965) supplemented with 10% (v/v) foetal calf serum, 100units/mL penicillin, 100μg/mL streptomycin and 0.25μg/mL amphotericin-B. This will be described as complete medium. The cells were incubated in a humidified incubator at 37°C with 5% CO_2 atmosphere.

2.1.4.2 Serum-free Media

For the purpose of cell treatment experiments, all cell lines were first cultured in complete medium, as described above, and after they had reached 90% confluence, were cultured in

serum-free DMEM, supplemented with antibiotics but without phenol red (Invitrogen, 21063). The cell cultures were maintained in serum-free media for at least 48hours prior to cell treatments.

2.1.5 Co-culturing of Cells

Lentivirally-transfected green fluorescent protein(GFP)-expressing LNCaP cells were kind gifts from Dr. Colby Eaton's lab, for use in this project. They were confirmed as GFP-positive by fluorescence microscopy and fluorescence-activated cell sorting (FACS) analysis. The stromal fibroblast cells were tagged with a cell membrane label; PKH26 (Sigma, MINI26), making them fluoresce red. For the labelling, 4μM final concentration of PKH26 was introduced to 100,000 cells suspended in serum-free media and incubated at ambient temperature for 4 minutes. Addition of an equal volume of complete medium to the cell-dye suspension for another 1 minute stopped the reaction by greatly reducing the binding effect of the dye to the cell membrane. The mixture was centrifuged for 5 minutes at 400 x *g*. The supernatant was aspirated and fresh complete medium was added to the cell pellet and centrifuged for 5 minutes at 400 x *g*. This wash step was repeated 3 times in order to remove unbound dye. 100,000 red fluorescing stromal cells PCAF or 100,000 WPMY-1 were plated along with an equal number of LNCaP-GFP cells for 24 or 48 hours in wells of a 6-well plate. This gave a mixed cell layer of cells in physical contact with one another.

2.2 COLLECTION OF CONDITIONED MEDIA FOR ASSAYS

Complete medium was used to culture cells until they were 80% confluent. The medium was then removed; the cell monolayer washed twice with PBS and then serum-free medium was added to the cells. This was left for 24, 48 or 72 hours and collected. The medium was centrifuged at 400 x *g* for 5 minutes and the supernatant media collected and stored at -70°C until further use, to prevent microbial contamination.

2.3 CELL TREATMENTS

Cells were subject to treatment with androgens and cytokines in order to investigate modulation of gene expression post-treatment. The treatments used for this project included:

2.3.1 DHT

Cells were seeded at 50,000/well, into 12-well plates with 1 mL of complete medium. When the cells reached 60 – 70% confluence, the medium was changed to serum-free medium. The cells were allowed to adjust to the serum-free condition for 48 hours after which the medium was again changed to serum-free medium with 0 nM, 0.1 nM, 1 nM and 10 nM DHT (Sigma, A8380), 1 μM flutamide – an androgen receptor antagonist, (Sigma, F9397), as well as a combination of 1 μM flutamide + 10 nM DHT. The physiological serum concentration of DHT in humans is 1 – 5 nM (Raivio et al., 2002). The inhibitory constant of flutamide is 175nM (Kemppainen et al., 1999) so an excess of this concentration, up to 1000nM was used in order to investigate the reversal of any androgenic effects that DHT might show. 100% ethanol was used as diluent and maintained in all the culture media at a final concentration of 0.1% (v/v). The treated cell cultures were incubated for 24 hours at 37°C, prior to RNA extraction.

2.3.2 TNF

The cells were cultured as described in 2.3.1 except for the cell treatment where the serum-free media contained 0 pg/mL, 10 pg/mL (0.57pM), 100 pg/mL (5.71pM) and 10 ng/mL (571 pM) of recombinant human TNF (Biosource, PHC3015) in a 0.1% (w/v) BSA in PBS to give a final concentration of 0.001% BSA. This acts as a carrier molecule and prevents the loss of TNF onto the plastic surfaces of the culture plates. Treated cell cultures were again incubated for 24 hours at 37°C, prior to RNA extraction. As an experimental constant 0.001% BSA was maintained in control and test experiments.

2.3.3 TGF-β

Stromal cells were seeded at 10,000 cells/well with 1 mL of complete medium in12-well tissue culture plates. The cells were incubated at 37°C and 5% CO_2 for 48 hours in order to

allow the cells to form monolayers at the base of each well. The medium was then changed to serum-free DMEM supplemented with 100 units/mL penicillin, 100 μg/mL streptomycin and 0.25 μg/mL amphotericin-B. The cells were allowed to adjust to the serum-free condition for 48 hours after which the medium was again changed to serum-free medium containing 0.05 nM, 0.5 nM or 50 nM of TGF-β1 (Gibco, PHG9204) diluted in PBS containing 0.1% (v/v) BSA. Treated cell cultures were incubated at 37°C and 5% CO_2 for 24 hours prior to RNA extraction and 72 hours for protein extraction. 0.001% BSA was maintained in control and test experiments.

2.4 RNA EXTRACTION

Cells were lysed directly in the culture flasks using 1 mL of Tri Reagent (Sigma, T9424) per $10cm^2$ of culture flask surface area. The culture medium was removed and Tri Reagent was added and cell lysates were homogenised by repeated pipetting. 0.2 mL Chloroform was then added to homogenates, vortexed for 15 seconds and allowed to stand for 10 minutes at ambient temperature. Resulting mixtures were then centrifuged at 2400 x *g* for 15 minutes at 4°C in order to separate the various phases, the top aqueous phase being the one that contained RNA. Once the aqueous phase had been obtained, 0.5mL isopropanol per 1mL Tri Reagent was used to precipitate the pellet by centrifuging at 2400 x *g* for 10 minutes at 4°C. The resulting supernatant was then removed and the RNA gel-like pellet was washed with 1mL 75% v/v ethanol per 1 mL Tri Reagent used. The mixtures were centrifuged at 1500 x *g* for 5 minutes at 4°C after which ethanol was removed and samples were dried at ambient temperature. Then 50 μL of diethyl pyrocarbonate (DEPC)-treated water (RNAse-free water) was added to dried RNA pellets and repeated pipetting at 50°C for 10 minutes facilitated dissociation. The resulting RNA solutions were stored at -80°C.
RNA thus obtained was assayed using the Bio-Rad Spectrophotometer; this was carried out to estimate the degree of RNA purity and quantity of RNA obtained. The absorbance of 40 μg/mL of RNA at UV wavelength of 260 nm is 1. The RNA concentration of samples was measured by reading the absorbance of the diluted total RNA at wavelength of 260 nm. The values obtained were then multiplied by the dilution factor. The equation below was used for the derivation of RNA concentration:

RNA (μg/mL) = Absorbance at 260 nm x dilution factor x 40 μg RNA/mL

Measuring the absorbance of the diluted samples at A_{280} and comparing the A_{260}:A_{280} ratios also identified any protein contamination. The ratio should approach 2.0 if the RNA sample is free of protein contamination and generally a ratio of about 2.0 indicates good RNA (Glasel, 1995).

2.5 REVERSE TRANSCRIPTION

After RNA extraction, cDNA was prepared by reverse transcription using Superscript II Reverse Transcriptase kit (Applied Biosystems, 18064-014), which contains a modified version of Moloney Murine Leukemia Virus Reverse Transcriptase (M-MLV RT) designed for good thermal stability and low RNase H activity. The kit also contained deoxynucleotide triphosphates (dNTP) mixture. This was primed with random primers (Applied Biosystems, 48190-011). Reverse transcription was carried out using 20 μl reaction mixture per tube, consisting of:

- 4 μL of 5 X first strand Buffer, 2 μL of 0.1M dithiothreitol (DTT),
- 0.5 μL of 10 nM each of deoxynucleotide triphosphates (dNTP) mixture of dATP, dCTP, dTTP and dGTP
- 1 μL of 100 ng random primers (these are hexamers that can simultaneously act as primers to reverse-transcribe all mRNAs)
- 0.5 μL of 40 units/μL of RNAseOUT RNAse inhibitor (Applied Biosystems, 10777-019)
- 10.5 μL of DEPC-treated water
- 1 μL of a 1 μg/μl RNA sample
- 1 μL of 200 units/μL of Superscript II reverse transcriptase

Each tube represented different treated and untreated samples. Control reactions were also set up with no Superscript reverse transcriptase. The tubes were placed in the GeneAmp® PCR System 9700 and set at the following temperatures:

25°C for 2 minutes, for activation of the enzyme

42°C for 50 minutes for annealing of the random primers and cDNA synthesis

70°C for 15 minutes, for inactivation of the enzyme.
These parameters facilitated the reverse transcription process, after which the tubes were stored at -20°C prior to use.

2.6 REAL-TIME POLYMERASE CHAIN REACTION

Real-time PCR (qPCR) allows the monitoring of the PCR as it occurs, and so data are collected throughout the PCR process, rather than at the end of the PCR. Here, the relative quantification method of qPCR was used, whereby differences in the expression of a target gene between different samples were quantified, relative to another reference sample. In addition to the target sequence (TIMP-3, Versican or PSA), endogenous controls, glyceraldehyde phosphate dehydrogenase (GAPDH) and RNA polymerase 2 (RNAPII) were quantified as a means of correcting results that may be skewed due to differences in the cDNA quantities loaded into the reactions. GAPDH and RNAPII are constitutively expressed genes that remain fairly unaltered upon treatment of the cells with external stimuli or factors (Radonic et al., 2004) and in these project experiments acted as references for the normalisation of the test results. With androgen-sensitive cell lines the expression levels of PSA were also analysed, as a positive control to confirm the activity of DHT used in the experiments, as previously reported (Lilja, 1993).

First, the cDNA samples were diluted by a factor of 0.5 with DEPC-treated water, after which 10 µL of reaction mixture was set up in wells of 384-well plates, each comprising of the following:

- 5 µL of Taqman® Universal PCR Mastermix, no AmpErase® UNG (Applied Biosystems, 4324018) – this contains DNA polymerase capable of instant hot-start PCR and does not require activation
- 4.5 µL of the diluted cDNA
- 0.5 µL of 20X Assay-on-Demand™ Gene Expression Assay mix (this contains pre-formulated primers and Taqman probes with a reporter dye, FAM, labelled to the 5' end of the probe and a non-fluorescent quencher at the 3' end of the probe). The pre-formulated primers targeted timp-3, PSA/hK-3, Versican, GAPDH or RNA Polymerase II.

Table 2.1 below shows the sequence information for all assay used:

Gene Name	Assay ID	Accession #	Primer-Probe Seq. (5'-3')
TIMP-3	Hs00165949_m1	NM_000362	CCGACATCGTGATCCGGGCCAAGGT
hK-3/PSA	Hs00426859_g1	NM_001030047	GCCCACTGCATCAGGAACAAAAGCG
Versican	Hs00171642_m1	NM_004385	GACTGTGGATGGGGTTGTGTTTCAC
GAPDH	Hs99999905_m1	NM_002046	GGCGCCTGGTCACCAGGGCTGCTTT
RNA Pol. II	Hs00992801_m1	NM_021974	TCAGACAACGAGGACAATTTTGATG

Table 2.1: Sequence information of the assays ordered from Applied Biosystems. *Assay ID, accession number and probe sequences for timp-3, hK-3/PSA, versican, GAPDH and RNA Polymerase II.*

The PCR reaction exploited the 5' nuclease activity of the DNA polymerase to cleave a Taqman primer-probe during PCR. When the probe was intact, the proximity of the fluorescent reporter dye (FAM™) to the non-fluorescent quencher resulted in repression of the reporter fluorescence. During the reaction, if the target sequence was present, the probe specifically annealed between the forward and reverse primer sites. If the probe hybridised to the target, the DNA polymerase cleaved off the probe and separated the reporter dye and the quencher dye, resulting in increased fluorescence of the reporter dye. The probe fragments were then displaced from the target, and strand polymerisation continued.

The different treated and control samples were set up in triplicate wells and then wells were sealed tightly to prevent spillage. The ABI Prism 7900 HT Sequence Detector Platform was then set up for the real time PCR reactions by first connecting it to the computer. Then the probes containing FAM™ dye were added to all the well plates. The wells were labelled accordingly and the ABI system set at:

(i) 95°C for 5 minutes for cDNA strand separation

Then 40 cycles of:

(ii) 95°C for 15 seconds for primer-probe annealing

(iii) 60°C for 1 minute for polymerisation of DNA strands

2.7 PCR DATA ANALYSES

qPCR data were analysed using SDS 2.0 Software (Applied Biosystems, U.K) and using the comparative delta Ct method as previously described (Livak and Schmittgen, 2001). Baseline gene expression was first expressed as ΔCt, namely cycle threshold at which fluorescence was detectable above background for TIMP-3, minus Ct of endogenous control gene, e.g. GAPDH. The data obtained were then expressed as fold increase. Here, all ΔCt values for treated samples were standardised to the control for each experiment by subtracting them from the control/untreated sample. Fold increases were determined by applying the formula $2^{-\Delta\Delta Ct}$ where

ΔCt = Ct of endogenous gene – Ct of test gene

and

ΔΔCt = ΔCt of test gene (treated) – ΔCt of test gene (untreated)

2.8 PROTEIN EXTRACTION

Total protein (i.e. cells plus ECM) was extracted from the cells using the Mammalian Cell Lysis Kit containing protease inhibitor cocktail (Sigma, MCL1) or 0.1% Triton-X-100 containing protease inhibitor cocktail (Sigma, P8340), and following the manufacturer's protocol. The cell lysis buffer (CLB) made up from the kit contained 50 mL each of 250 mM Tris-HCl, pH 7.5, 5 mM EDTA, 750 mM NaCl, 0.5% SDS in water, 2.5% deoxycholic acid sodium salt in water, 5% Igepal CA-630 detergent in deionised water and 2.5 mL of protease inhibitor cocktail (Sigma) containing (4-(2-aminoethyl) benzenesulfonyl fluoride, pepstatin A, bestatin, leupeptin, aprotinin and L-*trans*-epoxysuccinyl-L-leucyl-amido (4-guanidino)-butane (E-64).

For the extraction of total lysates, the monolayer of cells was washed with PBS for 1 hour at 4°C and then 200 μL of CLB was added per 10^6 cells. The mixture was centrifuged at 2,500 x *g* for 10 minutes at 4°C. The supernatant was collected as the protein sample, and the pellet was discarded. The supernatant was stored at -20°C until needed.

For the extraction of cellular proteins only, the cells were trypsinised from the wells or plates prior to addition of the CLB. The same procedures as above were carried out.

For the extraction of extracellular matrix (ECM) proteins only, the cells were detached from the wells or plates using enzyme free Hanks Buffer (Invitrogen, 13150-016). This

contained EDTA that gently dissociated cells from each other and from their support substrates, leaving the ECM in the wells. The cells were counted for use in standardisation of amount of ECM loaded. Then loading buffer was made up and this consisted of:

- 5 parts of 4X lithium dodecyl sulphate (LDS) sample buffer containing 106 mM Tris HCl, 141 mM Tris base, 2% LDS, 10% Glycerol, 0.51 mM EDTA, 0.22 mM Coomassie blue G250 and 0.175 mM Phenol red (Invitrogen, U.K.) with a pH of 8.5
- 2 parts of 500 mM DTT at a 10X concentration (Invitrogen, U.K.)
- 7 parts of water

200 µL of the loading buffer was added directly to the ECM in the wells and left at 4°C for 1 hour, after which the solution was scraped off the base of the well or plate and pipetted into a tube. The solution, now containing the ECM proteins, was stored at -20°C prior to use.

2.9 PROTEIN CONCENTRATION ASSAY

Protein concentration was assayed using the BCA (Bichinconinic acid) assay (Pierce, 23225) and following the manufacturer's protocol. For this assay, a 96-well format was used. Serial dilutions of bovine serum albumin (Pierce, 23225) were diluted with CLB to give concentrations of BSA of 2000, 1500, 1000, 750, 500, 250, 125, 25 and 0 µg/mL. The working reagent (WR) was made up by diluting BCA by 1:50. Then 25 µL of either BSA or diluted total or cell only protein was added to each well of a clear 96 well plate after which 200 µL of WR was added to the samples, giving a sample to WR ratio of 1:8. The plate was covered and incubated at 37°C for 30 minutes then for 15 minutes at ambient temperature. The absorbance of the mixtures was read off at 562 nm wavelength using a spectrophotometer. Standard curves were plotted using the absorbance of the BSA dilutions versus the concentrations of the BSA samples. The concentrations of the protein extracts were calculated from the BSA standard curve.

2.10 SDS-PAGE

This was carried out in order to separate proteins from cell extracts, based on their molecular weight. This is in line with previously described protocols (Jovin, 1973a, Jovin, 1973b). The sulphate present in the anionic detergent (LDS) contained in the loading buffer (see Section 2.8) applies negative charges to proteins thereby linearising the protein. Loading them onto polyacrylamide gel and applying constant voltage to the gel separated the proteins. By using a combination of acrylamide and bis- acrylamide at a defined ratio, a gel matrix comprising of a network of pores was achieved. The negatively charged linearised proteins migrate through the gel matrix towards the positive electrode/anode. The speed of migration varies with the protein size; smaller proteins migrate faster than bigger ones, and appear as bands in the lower region of the gel. Bands in the upper region of the gel represent bigger proteins.

12% resolving polyacrylamide/bis acrylamide gels were prepared by combining the following reagents in the order below:

- 40% Acrylamide/Bis-acrylamide solution, 37.5:1 (Biorad, 161-0148) = 3.00 mL
- Resolving gel buffer, (1.5 M Tris-HCl, pH 8.8) (Biorad, 161-0798) = 2.50 mL
- Water = 4.35 mL
- 10% (w/v) SDS (Biorad, 161-0416) = 0.10 mL
- 100 mg/mL Ammonium Persulphate/APS (Biorad, 161-0700) = 0.05 mL
- TEMED (Biorad, 161-0801) = 0.01 mL

The first 4 components were mixed gently and both APS and TEMED were added just before the mixture was introduced into a gel cassette assembly (the gel cassette assembly is made up of a spacer plate, a short plate and a casting frame, all components of Biorad Mini-Protean 3 gel assembly system). APS and TEMED are cross-linkers that increase the spontaneous polymerisation of acrylamide in the absence of oxygen. Some butan-2-ol was added to the top of the gel to smoothen it and prevent the introduction of O_2 into the gel. The gel was left to polymerise at ambient temperature by placing it in the casting stand for 40 minutes. Once dried, the butan-2-ol on top of the resolving gel was discarded and the gel was rinsed with water. The top of the gel was air-dried and placed back on the casting stand.

Stacking gel was made up and introduced to the top of the resolving gel to enable the protein bands to migrate slowly until they reach the top of the resolving gel. 10 mL of stacking gel was made up in the order below:

- 40% Acrylamide/Bis-acrylamide solution, 37.5:1 (Biorad, 161-0148) = 1.00 mL
- Stacking gel buffer, (0.5 M Tris-HCl, pH 6.8) (Biorad, 161-0798) = 3.00 mL
- Water = 6.84 mL
- 10% v/v SDS (Biorad, 161-0416) = 0.10 mL
- 100 mg/mL Ammonium Persulphate/APS (Biorad, 161-0700) = 0.05 mL
- TEMED (Biorad, 161-0801) = 0.01 mL

Immediately after adding the stacking gel, moulded combs (also part of the mini-protean 3 system) were introduced into the gel before allowing polymerization at ambient temperature for 40 minutes. Once done, the combs were gently removed from the gel and the gel cassette sandwich was removed from the casting frame and inserted into the electrode assembly. When running only one gel, a buffer dam was placed in the other side of the electrode assembly clamped shut. The electrode assembly was placed into the clamping frame, making up the inner chamber assembly. This assembly was inserted into the mini tank.

For electrophoresis, running buffer was made up, which consisted of 25 mM Tris/192 mM Glycine/0.1% SDS, pH 8.3 (Biorad, 161-0732). The inner chamber assembly was filled with running buffer and care was taken to prevent overfilling and spillage. The protein samples were prepared as described in Section 2.8, and heated at 70 degrees for 10 minutes. The samples were left to cool at ambient temperature and loaded into individual wells. Protein dual colour molecular weight standards (Biorad, 161-0374) were loaded on to one lane to monitor band migration and determine approximate molecular weights. Also, recombinant human full length TIMP-3 (R & D Systems, 973-TM) was loaded alongside proteins as a positive loading control of known molecular weight. Running buffer was added to the lower buffer chamber. The mini tank was covered with the tank lid and the set up was connected to a power supply and constant current of 20 mA applied for 60 minutes for separation of proteins through the gel.

2.11 WESTERN BLOTTING

Before the electrophoresis was complete, transfer buffer was made up. This consisted of 60 mM Tris/40 mM CAPS buffer containing 15% methanol, pH 9.6 (Biorad, 161-0778)
Once proteins were separated, the gel was removed from the gel sandwich and equilibrated in transfer buffer for 15 minutes. Blotting pads were also soaked in transfer buffer for 15 minutes and blotting paper was lightly wet with transfer buffer. A PVDF membrane was soaked in methanol for 60 seconds and then equilibrated in transfer buffer for 15 minutes.
The blotting sandwich was set up using the above materials and in the order below:
Clear side down –> blotting pad –> blotting paper –> PVDF membrane –> gel –> blotting paper –> blotting pad –> Black side up.
The sandwich was clamped shut with the attached white clip and inserted into the mini-trans-blot module (Biorad) with the black side of the sandwich next to the black side of the module cassette. The inner part of the module was filled with transfer buffer, up to the white clip and outer chamber of the module was filled to the top. The module was closed with its lid and inserted into a container filled with ice (to prevent temperature increase) and connected to a power supply. The proteins were then transferred to the membrane by applying a constant voltage of 20 V for 2 hours.
After transfer, the protein-binding sites on the PVDF membrane were blocked in blocking buffer consisting of TBS containing 1% (w/v) casein (Bio-Rad, 161-0782) with 0.05% v/v Tween-20. This incubation was carried out for 60 minutes at ambient temperature whilst rocking the membrane gently on a rotor. Afterwards, the membrane was washed 3 times at 5 minutes each, with the prepared TBS-casein buffer (Biorad, 170-6435) and protein bands were detected with the following primary antibodies diluted in blocking buffer:

- 1 μg/ml (50 nM or 1:500 dilution of 500 μg/ml stock) of mouse monoclonal anti-TIMP-3 antibody, raised against residues 24 – 211 of recombinant human TIMP-3 (R&D Systems, MAB973)
- 1 μg/ml (50 nM or 1:200 dilution of 200 μg/ml stock) of rabbit polyclonal anti-TIMP-3 antibody raised against the C-terminal region of TIMP-3 (Sigma, T7812)

- 0.1 μg/ml (5 nM or 1:10,000 dilution of 1 mg/ml stock) of rabbit polyclonal anti-GAPDH antibody (Sigma, G9545). This was used for GAPDH detection, as a loading control when loading total cell lysates.

The primary antibody was incubated with the membrane overnight at 4°C. The membrane was then washed 3 times for 5 minutes each. The membrane was probed with HRP-conjugated secondary antibodies, depending on the primary antibody used for initial membrane probing:

- 1:1000 dilution of HRP-conjugated goat anti-mouse IgG (Dako, P0447)
- 1:1000 dilution of HRP-conjugated swine anti-rabbit IgG (Dako, P0399)

The membrane was incubated for 60 minutes at ambient temperature with gentle rocking and then washed 3 times for 5 minutes each.

The ECL plus western blotting detection reagent (GE Healthcare, RPN2132) was used for the detection of blotted proteins. This reagent is made up of lumigen PS-3 acridan substrate that produces highly luminescent acridinium ester intermediates upon reacting with peroxidase found in the HRP-conjugated secondary antibodies. The result of this reaction is the production of chemiluminescence that can be exposed to autoradiography films to be visualised as bands on the film. The ECL plus solution was applied onto the membranes for 5 minutes and removed from the membranes. The membranes were drained of any excess reagent and placed into a thin cling film to prevent adherence of contaminants, and then exposed to x-ray films (GE Healthcare, RPN2103) in a dark room.

2.12 DENSITOMETRIC ANALYSIS OF WESTERN BLOTS

Western blots were scanned and the blots were analysed using the Bio-Rad Quantity One software. This measures the pixels of the blot in comparison to the background pixels to generate a value for the blot with optical density x area as the unit (OD mm^2). It can also compare one blot to another, and correct the values using the same background so that there is unbiased quantification. The higher the value obtained, the higher the protein content of that particular blot, and *vice versa*. With this, semi-quantification of proteins can be achieved using the values obtained.

2.13 DOWN-REGULATION OF GENE EXPRESSION USING siRNA

Commercially available siRNA to TIMP-3 (Ambion, AM16708), GAPDH (Ambion, AM4655) and non-targetting control siRNA (Ambion, 4611) were obtained from Applied Biosciences/Ambion, U.K. This commercial TIMP-3 siRNA was designed to target exon 5 of timp-3 gene. The 5' --> 3' sequences of the siRNA are:

Sense: GGAACUACAAGAGAGUCGGtt

Anti-sense: CCGACUCUCUUGUAGUUCCtt

Several methods of transfection were employed in order to determine the optimal protocol for introducing siRNA into the cells. These included:

(i) Calcium Phosphate transfection

(ii) Lipid-based Dharmafect transfection and

(iii) Electroporation.

(iv)

For all protocols, silencer siRNA to TIMP-3 and a housekeeping gene GAPDH, and non-targeting siRNA were used. GAPDH knockdown served as a positive experimental control as all actively metabolising cells express GAPDH. The sequence of the GAPDH siRNA was not supplied by Ambion but is proprietary. Non-targeting siRNA acted as a negative control and did not target any known human gene sequence. Again, this sequence was not supplied but is proprietary. Mock-transfection controls were also set up, where no siRNA was added to the transfection complexes. Untransfected cells were also plated and analysed alongside transfected and mock-transfected cells so as to monitor any differences observed in expression levels due to the transfection reagent only.

2.13.1 Calcium Phosphate Transfection Method

This is based on the formation of a calcium phosphate-RNA precipitate as a by-product of the addition of calcium chloride to Hepes buffered saline (HBS), which contains $Na_2HPO_4;2H_2O$ as one of its components (Invitrogen, K2780-01).

Reaction:

$Na_2HPO_4 + CaCl_2 \rightarrow 2NaCl + CaHPO_4$

The calcium phosphate thus formed facilitates RNA binding to the surface of the cell and subsequent introduction into the cytoplasm via endocytosis. This method has previously been described (Graham and van der Eb, 1973). First, the cells were trypsinised, complete DMEM medium containing antibiotics and serum was then added to neutralise the trypsin, and the cell suspension centrifuged at 1500 X *g* for 5 minutes. The cell pellet was re-suspended in antibiotic-free DMEM and the cells were counted using a coulter counter (as described in Section 2.16). A total of $3X10^4$ cells were re-suspended per 80 µl of antibiotic-free medium.

1.5 µl of a 20 µM TIMP-3 silencer siRNA stock concentration (Ambion) was mixed with 1.5 µl of 2 M $CaCl_2$ and the volume made up to 10µl in a test tube labelled (a). To another tube labelled (b), 10 µl of 2 X HBS was added. Using a sterile pipette, the contents of (a), was slowly introduced into (b) whilst bubbling air into (b) using another pipette. At this point, there was formation of a calcium phosphate complex, which enables endocytosis to occur. The mixture of (a) and (b) was incubated at ambient temperature for 30 minutes. Then 400 µl of the antibiotic-free medium was introduced into 48-well plates and the 80 µl of cell suspension was also added to this. After the 30-minute incubation, the mixture of (a) and (b) was then introduced, drop-wise, into the wells containing the suspended cells. This is a process known as reverse-transfection or neo-transfection, and it allows more contact between the siRNA-$CaCl_2$-HBS mixture and the surface of the cells, resulting in more efficient transfection, relative to the traditional transfection protocol, where the cells are in monolayer and part of the surface area is unavailable for complete siRNA binding. The final siRNA concentration in the complex/culture was 60 nM. The plates were incubated at 37°C/5%CO_2 for 16 hours, after which the transfection complex-media was removed (to prevent cell toxicity) and replaced with fresh medium for another 32 hours prior to RNA extraction.

2.13.2 Lipid-Based Transfection Method

This method also employs the neo-transfection technique but instead, utilises a liposome complex that entraps the siRNA and transports it into the cell via endocytosis. The cells were trypsinised, counted and re-suspended in antibiotic-free medium, as above. $3X10^4$ cells/60 µl of antibiotic-free medium was prepared and added into 48-well plates already containing 100 µl of antibiotic-free medium per well. The transfection complex comprised 10 µl of a 2 µM siRNA concentration diluted in 10 µl of antibiotic- and serum-free medium

in one tube labelled (a) and 0.4 µl of Dharmafect-2 transfection reagent (Dharmacon/Thermo Fisher Scientific, T2002) diluted in 10 µl of antibiotic and serum-free medium in tube (b). The contents of both (a) and (b) were mixed together by careful pipetting and then incubated for 20 minutes at ambient temperature prior to careful pipetting of the complex into the cell suspension in the wells. The final siRNA concentration in culture was 100 nM. The plates were incubated for 16 hours at 37°C/5%CO_2 after which the transfection complex was removed because according to the manufacturer's protocol, Dharmafect-2 is toxic to cells if maintained for more than 16 hours in culture. The medium was replaced with fresh antibiotic-free medium and incubated for another 32 hours prior to RNA extraction for analysis.

2.13.3 Electroporation

This method entails subjecting the cells to electric shock, which temporarily opens up pores in the lipid bilayer and allows the entry of highly charged molecules such as polynucleotides (Neumann et al., 1982). Again, the cells were trypsinised, counted, and re-suspended, this time, into 100 µl of Nucleofector R reagent (Amaxa, VCA1001) at ambient temperature, at $1X10^6$ cells/100 µl of reagent. Then 2 µg of siRNA was introduced into the mixture and the entire mixture was transferred into an Amaxa-certified cuvette with a lid on. The cuvette was then inserted into the Amaxa nucleofector machine and the program set at T-09 for electroporation, according to manufacturer's recommended protocol. The cell mixture was immediately removed from the cuvette after electroporation and transferred into 37°C pre-warmed antibiotic-free DMEM containing 10% v/v serum, and pre-plated into 6-well plates. The final siRNA concentration in culture was 100nM. The plates were incubated at 37°C/5%CO_2 for 48 hours, prior to RNA extraction because according to the manufacturer's protocol, the nucleofector reagent is not toxic to cells and did not need to be removed post-transfection.

2.14 FACS SORTING OF CELLS

Cells to be sorted were trypsinized, harvested and counted (as described in Section 2.18.1). They were then suspended in DMEM media with 0.5% FCS and taken to the University's FACS (fluorescence activated cell sorting) facility (students were not allowed to operate the

FACS equipment and had to submit samples for analysis by trained technicians). FACS is a technique that employs the use of light to sort specific populations of cells from a mixed population based on the fluorescence emitting from cells.

Cells were sorted either by inherent fluorescence as in the case of stably-GFP-transfected LNCaP cells, or by membrane fluorescence as in the case of PKH26-labelled cells. The different cell populations were sorted and collected into different tubes. Non-transfected/non-labelled cells also had to be submitted for standardisation and optimisation of the FACS sorter. Data reported by the technicians include:

- Total cell number
- Percentage of fluorescent cells
- Percentage of non-fluorescent cells
- Percentage of cell debris or dead cells

The sorted cells were further analysed for timp-3 mRNA expression by qPCR or protein expression by western blotting (as described in Sections 2.6 and 2.11).

2.15 FUNCTIONAL ASSAYS

Several assays were carried out in order to assess whether there were any changes in biological functions of the cells after down-regulation of the TIMP-3 transcript. They include:

2.15.1 Proliferation Assays

2.15.1.1 Coulter Counter Method

This is based on cell counting using the Beckman Coulter Z2 particle count and size analyser. It allows a threshold particle diameter to be set, such that the counts obtained will exclude any dead cells and cell debris that will fall under this threshold. Different cell types have different sizes and so the coulter counter first analyses the particle size and gives an approximate diameter of the cells, then counts the cell number. The diameters of the cell lines used in this project were determined as follows:

- PC3: ~ 7 μm
- LNCaP: ~ 9 μm
- PCAF: ~ 12 μm
- WPMY-1: ~ 9 μm
- BPH45: ~ 12 μm

Cells were trypsinised and harvested as normal (see Section 2.2) and suspended in 10 mL of complete medium. The cell suspension was diluted by a factor of 20 in isotonic solution such as saline, by adding 0.5mL into 9.5 mL diluent, and placed in the counting chamber to be counted. Resulting counts were multiplied by the dilution factor of 20 and then by 2 to give the total number of cells per 1mL of cell suspension. This allowed for comparison of cell numbers between untreated and treated cells as an indication of the rate of proliferation of the cells. Any modulation of cell growth by treatment was indicated by cell number changes.

2.15.1.2 Haemocytometer Method

This method of counting uses a conventional haemocytometer. The cells were harvested and suspended in complete media such that they were sparsely diluted. Then the cells were further diluted 1:1 in trypan blue which stained the dead cells blue. When counting the cells under the microscope, any cells stained blue were excluded. Counts were obtained from 5 sections out of the nine sections of the haemocytometer: the four edges and the central section. The total count was divided by 5 and then multiplied by 2 and again by 10,000 in order to give the total number of cells per mL of cell suspension i.e.

Total cell count per mL = (haemocytometer count/5) x 2 (for trypan blue dilution) x 10^4

This gave a measure of changes in rates of cell proliferation pre- or post-treatment.

2.15.2 Migration Assays

This is based on the Boyden chamber construct placed into a well of a 24-well plate. The cells are able to migrate through a membrane from the outer into the inner part of the chamber. 5,000 cells were suspended in 100 μl media and introduced into the outer part of the chamber. Over 24 hours or 48 hours (depending on cell type), the cells migrated through the pores of the membrane via chemotaxis into the inner part of the membrane i.e.

to the membrane that is in contact with the media inside the well. The non-migrated cells on the outer part of the membrane were removed by swabbing with a clean cotton bud and the membrane was fix-stained with crystal violet in 70% v/v ethanol and migrated cells were counted. This assay required the presence of a chemo-attractant such as growth factors or nutrient-rich media in the lower chamber (see Figure 2.5). With this assay, comparison was made between migratory potential of un-transfected and TIMP-3-down-regulated cells.

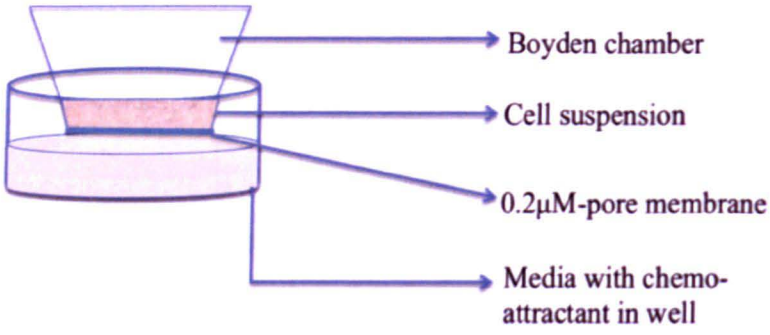

Figure 2.1: Transwell-migration assay.
The cells are seeded into the Boyden chamber and allowed to migrate towards the lower chamber over 48 hours. Number of cells on surface of membrane facing the lower chamber with the media and chemo-attractant are counted.

2.15.3 Invasion Assays

This is also based on a Boyden chamber set-up and is similar to the 3-D migration assay (Section 2.15.2). However, the membrane in the chamber was first coated with 50 μL of growth factor reduced matrigel (BD Biosciences, 354230), which was allowed to polymerise for about 30 minutes at ambient temperature. Matrigel is routinely used as a semi-solid medium for promoting adherence of cells to surfaces *in vitro*, mimicking the basement membrane naturally found *in vivo* (Oridate et al., 1996). This added layer therefore represents a basement membrane-like ECM as it also contains collagen IV, laminin and heparan sulphate proteoglycans that are normal components basement membranes. The cell suspension was seeded on top of the matrigel and invasive cells had the opportunity to degrade the matrigel and pass through the membrane to the inner part of the membrane in the Boyden chamber, where they were stained with crystal violet in 70%

v/v ethanol and counted. Again, this assay was used to compare the changes in invasive potential of TIMP-3-down-regulated cells to their un-transfected or non-targeted controls.

2.15.4 Apoptosis Assay

This assay uses Annexin-V-FITC/Propidium Iodide (PI) staining of dead or necrotic cells and measures the amount of stained cells as a percentage of total number of cells assayed. This protocol was first described in 1995 by Vermes *et al* (Vermes et al., 1995). The Annexin-V-FITC and PI kit was bought from BD Biosciences (catalogue no. 556570) and the test kit contained Annexin-V binding buffer (made up of 10 mM Hepes/NaOH, 140 mM NaCl and 2.5 mM $CaCl_2$ pH 7.4). One of the changes that symbolizes the occurrence of early apoptosis in cells is the translocation of a component of the cell membrane; phosphatidyl serine (PS), from the inner part of the membrane to the outer surface. Annexin-V has a strong affinity for PS and will, in the presence of high Calcium concentrations, bind to PS. Propidium iodide (PI) is a fluorescent nucleic acid intercalator that fluoresces upon binding to DNA or RNA. As PI is impermeable to cell membranes, it can be used to detect cells with ruptured cell membranes. Used in combination with Annexin-V-FITC, dead cells and necrotic cells can be excluded from a cell population by flow cytometry. The excitation wavelength for both Annexin-V-FITC and PI are 488nm and the emission wavelengths are 518 nm (detected in the FL1 channel) and 617 nm (detected in the FL2 channel) respectively.

For the apoptosis assay, cells were harvested by trypsinisation, counted and diluted to 1.0 x 10^6cells/mL. Cells were washed with cold PBS by centrifugation at 1500 x *g* for 5 minutes. 100 µL of cell suspension was re-suspended in cold PBS, centrifuged at 1500 x *g* for 5 minutes and re-suspended in 100 µL of 1X annexin-V binding buffer in a small Eppendorf tube. 5 µL of Annexin-V-FITC antibody and 5 µL of PI was added to the cell suspension and vortexed gently for 10 seconds. The mixture was incubated at ambient temperature for 15 minutes. Additional 400 µL of 1X binding buffer was added to each tube and the cells were analysed by flow cytometry for percentage of cells positive for Annexin-V as a measure of the percentage of the cell population that is apoptotic.

2.16 PROTEINASE INHIBITION ASSAY

The total MMP-inhibitory activity of cell lysates, ECM lysates and conditioned medium from LNCaP, PCAF, WPMY-1 and BPH45 cells was assayed using a quenched fluorescence substrate (QF); this is based on the ability of MMPs to break down a quenched fluorescence substrate at its Leu-Gly bond (Mca-Pro-Leu-Gly-Leu-Dpa-Ala-Arg-NH_2) that contains a linked quencher and fluorophore (Bachem). Mca (7-methoxycoumarin-4-yl) is a derivative of 7-methoxycoumarin and is highly fluorescent. Dnp is a dinitrophenyl group, which acts as an internal quencher. This substrate was originally described by Knight *et al* (Knight et al., 1992). For the assay, 3 µL of 5 mM of the QF substrate was diluted in 3 mL of assay buffer (5 µM final concentration) containing 100 mM Tris-HCl, 100 mM NaCl, 10 mM $CaCl_2$ and 0.2% Triton-X-100, pH 7.5 and used to zero the LS-50B fluorimeter (Perkin-Elmer) prior to assaying for MMP activity and MMP-inhibition. The fluorescent peptide, which is released by the action of MMPs, Mca-Pro-Leu-OH, was used to standardise the fluorimeter such that at a concentration of 500 nM (10% substrate hydrolysis) gave a reading of 1000F.

The excitation and emission wavelengths were set at λ_{328} nm and λ_{393} nm. Then 3 µL of 5 µM of either MMP-2 or MMP-9 (final concentration of 5 nM) was added to fresh assay buffer-substrate mixtures and fluorescence was measured and stored in real time using the Flusys software package (Rawlings and Barrett, 1990). The linear rate of substrate conversion was followed for about 100 minutes and recorded as (V_0). Then, 10 µL of protein extracts or 3 µL of 5 µM stock of recombinant human TIMP-3 (control) was added to the reaction and the new linear rate was recorded (V_i). V_i/V_0 was calculated as the amount of matrix metalloproteinase proteolysis. If the value was less than 1, MMP inhibition was occurring but if it was greater than or equal to 1, then MMP activity was present in the sample.

2.17 IMMUNOSTAINING OF CELLS AND TISSUES

Cells were grown on glass slides for 24 hours. Then the slides were rinsed briefly in PBS and cells fixed by submerging slides in 4% paraformaldehyde in PBS, pH 7.5, for 15 minutes at ambient temperature. Afterwards, the slides were washed twice with ice-cold

PBS and then incubated with blocking buffer for 1 hour at ambient temperature, as used in western blotting (Section 2.11). The slides were then incubated in 50 nM of monoclonal TIMP-3 antibody (R&D Systems, MAB973) at 4°C overnight. This monoclonal antibody was used as it gave the best conditions for protein detection in previous optimisation experiments (see Section 2.13). The next day, the slides were removed from the antibody solution, washed with Tris buffered saline with 0.05% tween-20 (TBST) five times at 5 minutes per wash. Then the slides were incubated in 1:1000 dilution of a fluorescent secondary antibody; Alexa-Fluor 488-conjugated goat anti-mouse IgG (Invitrogen, A11011) – this bound to the TIMP-3 mouse monoclonal antibody and fluoresced green with excitation and emission wavelengths of 485-495 nm and 520 nm respectively. The antibody reaction was carried out in the dark, as the fluorescent Alexa-Fluor-488 antibody is light sensitive. The cells were counter-stained by immersing the slides in 1μg/mL DAPI nuclear stain (Thermo Fisher, U.K.) for 5 minutes at ambient temperature. DAPI is a very pure form of diamidino-2-phenylindole dye that is fluorescent and has high affinity for DNA. It binds to nuclear DNA where its fluorescence increases in its bound state (Lawrence and Possingham, 1986). The slides were then rinsed with PBS, allowed to dry and coverslips were mounted on the slides using a drop of mounting medium (DPX mounting medium, BD Biosciences). The coverslips were sealed onto the slides using nail varnish in order to prevent drying and movement under the microscope. The slides were stored in the dark until microscopic examination was carried out.

Tissue samples were obtained as formalin-fixed and paraffin-embedded sections on glass slides. Before IHC staining, the sections were de-paraffinised by immersion twice in xylene for 5 minutes. The sections were then rehydrated by immersion into descending ethanol solutions; 99% for 10 minutes, 95% for 5 minutes, 70% for 5 minutes, and finally into distilled water for 1 minute. This was followed either by H&E staining or antibody incubation, as appropriate. For TIMP-3 antibody, the same protocol as cell immunostaining (above) was used.

H&E is a common histological stain used to differentiate between the nucleic acid components and the cytoplasmic components of cells in a tissue section. Haematoxylin stains nucleic acid blue while eosin stains the intracellular and extracellular proteins found in the cytoplasm and basal laminae red/pink/orange. For H&E staining, the slides were immersed in Gill's II haematoxylin (Sigma Aldrich) for 90 seconds and then into distilled

water for 3 minutes. The slides were immediately immersed in 1% aqueous eosin (Sigma) for 5 minutes and then into distilled water for 30 seconds. The slides were then fixed by immersion into ascending ethanol concentrations; 70% for 10 seconds, 95% for 10 seconds, 99% for 1 minute and finally into xylene for 4 minutes. Coverslips were mounted with DPX mounting medium (BD Biosciences) and images captured using a fluorescent microscope at several objectives.

Dr. Colby Eaton's group kindly donated the prostate tissue microarray samples. Figure 2.2 shows the properties of the tissue microarray used:

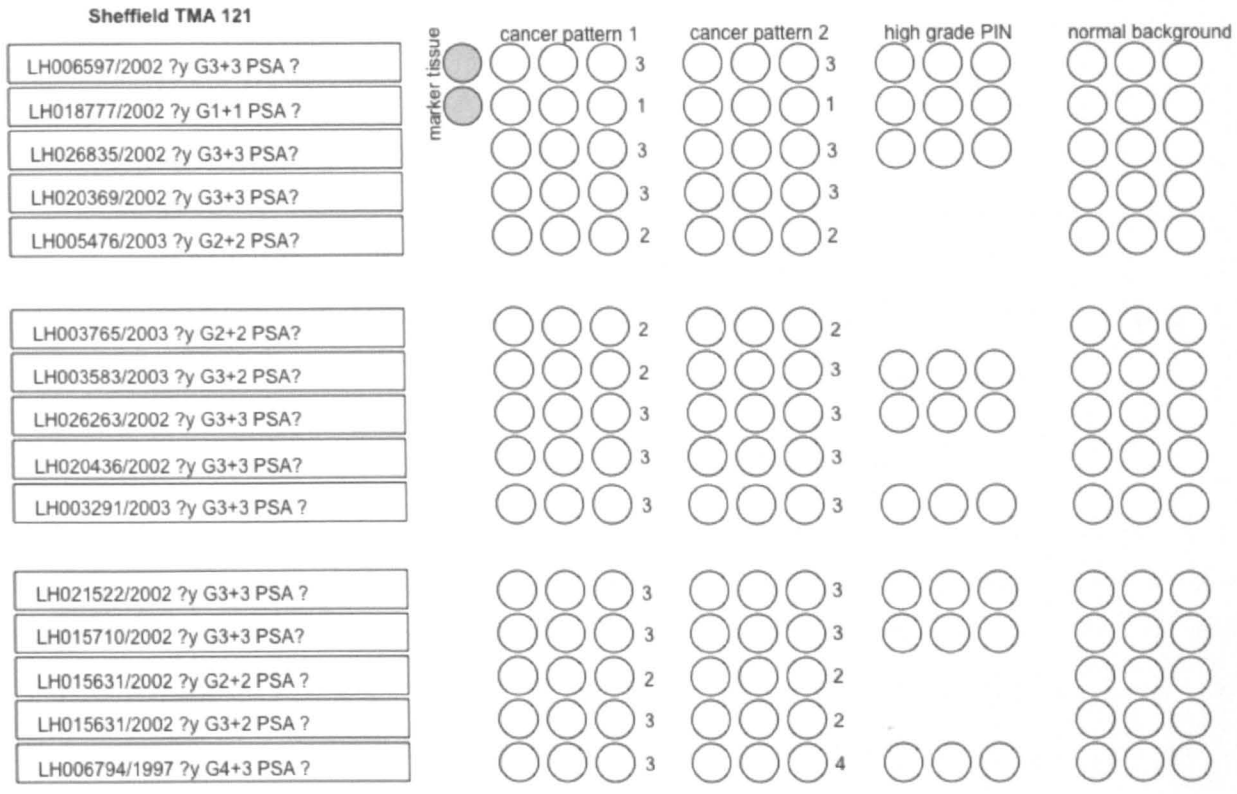

***Figure 2.2: Tissue Micro-array Map**:*
Each row included the samples from a single patient who had been treated by a radical prostatectomy. The clinical data in the first box consisted of: two unique identifier numbers from Sheffield internal coding, the age of the patient in years at the time of prostatectomy, the overall Gleason score for the whole tumour and the PSA level at presentation (if available). The array was orientated by two cores of marker tissue (either liver or spleen) at the beginning of the first two rows (shown as grey shaded circles on the template). The samples from the specimens were in triplicates with all 3 samples adjacent to each other.
The first three cores were samples from cancer pattern 1 of the tumour and the Gleason grade of that area was given after the three circles. The next three cores were samples from cancer pattern 2 of the tumour and the Gleason grade of that area was given after these three circles. Usually these cancer samples represented the two main areas in the overall Gleason score given in the patient data but sometimes were sample from a tertiary or lesser pattern with a different Gleason grade. The next three cores were from areas of high grade PIN if these were present in the specimen, if no PIN was present samples were not taken and the circles were absent from the template. The final three cores were from an area of morphologically normal background prostate epithelium in the specimen.

2.18 STATISTICAL ANALYSES

Several types of statistical analyses were carried out depending on the type of data that needed to be analysed. Parametric analyses were carried out where several repeats of an experiment were carried out as there was sufficient sample number to immediately determine a normal distribution. Non-parametric analyses were done where the data distribution was unknown and/or where sample number was low. The tests used in this project include:

2.18.1 Student t-test

This type of parametric statistical analysis was carried out where the number of experimental repeats was greater than 10 and when distribution was determined to be normal. The paired t-test was carried out to compare differences in paired samples and unpaired t-test for unpaired means of 2 data clusters. $P \leq 0.05$ was considered to be statistically significant. Microsoft excel was used for these calculations.

2.18.2 Mann-Whitney Test

The non-parametric Mann-Whitney two-tailed test was used to test for significant differences in between median values of control and individual samples. It is similar to the unpaired student's t-test but does not assume a normal data distribution. $P \leq 0.05$ was considered to be significant. These were carried out using Graph Pad Prism software.

2.18.3 Wilcoxon Signed-Rank Test

The non-parametric Wilcoxon signed-rank test was used to test for significant differences between median values of control and individual samples. It is similar to the paired students t-test but does not assume a normal data distribution, similar to the Mann-Whitney test. $P \leq 0.05$ was considered to be significant. These were carried out using Graph Pad Prism software.

2.18.4 Kruskal-Wallis Test

This is also a non-parametric statistical analysis, which was used to compare 3 or more groups of data, unlike the Mann-Whitney and Wilcoxon tests, which could only compare 2 groups of data at a time. It is similar to the parametric ANOVA test but instead of using the

means and variances for analysis, the Kruskal-Wallis test replaces it with ranks and reports the differences in the sum of the ranked data as P values. To correct for discrepancies in the ranked sums, a post-test was carried out based on whether the data was paired or unpaired:

- Dunn's Post test for unpaired data sets i.e. extension of the Mann-Whitney test
- Friedman's Post test for paired data sets i.e. extension of the Wilcoxon signed-rank test

Again, $P \leq 0.05$ was considered to be a significant difference, as calculated by Graph Pad Prism software.

CHAPTER 3: EXPRESSION OF TIMP-3 IN PROSTATE CELLS AND TISSUES

3.1 INTRODUCTION

The prostate tissue consists of different types of epithelial cells and a surrounding stromal component, separated from the epithelial component by a basement membrane. This stromal compartment consists of different types of cells such as smooth muscle cells, fibroblasts, nerve cells and lymphocytes, all embedded in the ECM-rich stroma (Wernert, 1997). The basement membrane is semi-permeable and it consists of collagens, elastin, laminin and proteoglycans, all interwoven in a matrix that forms the membrane (Cunha et al., 2002). In the androgen-refractive stage of prostate cancer, there is metastasis of tumour cells from the prostate primary site to other neighbouring and distal organs. This metastasis involves the breakdown of the basement membrane first, invasion of the stromal ECM and possibly co-migration of the cancer cells along with stromal fibroblasts to other organs where they home and form a secondary niche (Kaminski et al., 2006). The process of migration and invasion is aided by proteases secreted by the tumour cells and these degrade substrates such as collagen and proteoglycans to enable passage of the tumour cells. The formation of secondary tumours is an indication of an aggressive cancer phenotype (Cobo Dols et al., 2005, Plancke et al., 1994).

TIMP-3 is a metalloproteinase inhibitor that plays a major role in the regulation of ECM composition (Lee et al., 2007). This leads to regulation of a wide range of physiological processes such as growth (Airola et al., 1998, Baker et al., 1998), apoptosis (Lee et al., 2008, Fata et al., 2001), migration, invasion (Baker et al., 1998), transformation (Yang and Hawkes, 1992) and angiogenesis (Cruz-Munoz et al., 2006). TIMP-3 is unique in that it is the only member of the TIMP family to strongly sequester itself in the ECM by interactions of both its N and C-terminal domains with ECM components (Lee et al., 2007). The localisation of TIMP-3 has been associated with basal lamina and stroma of breast (Mylona et al., 2006, Uria et al., 1994) and prostate cells (Cross et al., 2005). This is as a result of an abundance of ECM in stroma and basal lamina of these tissues as well as stromal cells (Huang et al., 1998, Raga et al., 1999). TIMPs regulates proteinase-mediated ECM and basement membrane degradation in several tumours (Hornebeck, 2003). Low expression of TIMP-3 has been demonstrated in the normal and malignant epithelial components of breast (Mylona et al., 2006), and other tissues relative to the stromal components of the same tissues. This may indicate a negative correlation between TIMP-3 expression and

malignancy *in-vitro*, or may reflect a greater TIMP-3 expression by stromal as compared to epithelial cells. A higher level of expression of ADAMTS proteinases has been reported in malignant epithelial cells relative to expression in normal cells from benign prostatic hyperplasia (Cross et al., 2005, Demircan et al., 2009). This was concomitant with lower expression of the only tissue inhibitor of the ADAMTSs, TIMP-3, in the malignant epithelial cells (Cross et al., 2005). Again, this in-vitro study supports the negative correlation of TIMP-3 with malignancy. In one study (Kotzsch et al., 2005), lower expression of TIMP-3 was correlated with higher nuclear and histological tumour grading of breast cancer, implying that this reduced expression of TIMP-3 correlates with poorer prognosis.

TIMP-3 expression has also been associated with clinical outcome and invasive potential of oesophageal squamous cell carcinoma (Miyazaki, Kato et al. 2004). This study also correlated TIMP-3 expression in tumours with disease stage and patient survival rate, highlighting the importance of TIMP-3 expression in favourable prognosis for patients.

On the other hand, higher levels of TIMP-3 protein were positively correlated with tumour size in laryngeal cancer. Although the majority of TIMP-3 detected by immunohistochemistry in this study was epithelial, some expression was also localised in the stromal cells (Pietruszewska et al., 2008).

Also, methylation of the TIMP-3 promoter, associated with a reduction of TIMP-3 expression, has been observed in oesophageal and gastric cancers (Gu et al., 2008) as well as in hepatocellular carcinoma (Lu et al., 2003). All these studies have, in one way or another, described TIMP-3 expression in tumour samples.

The use of immunohistochemistry is in widespread use for analyses of expression of target protein in tissue samples. It is used extensively to identify expression patterns of known mediators of disease progression in tissue samples obtained from patients (Coons and Kaplan, 1950). It not only shows whether the proteins are expressed in the tissues but also indicates the localisation of the protein within the tissue under investigation. Localisation analyses can also be very informative in elucidating the particular roles that the protein may play in the initiation or progression of the disease. In cancer research, there have been several studies that show the pattern of expression of proteins in tissue samples from patients e.g. expression of PSA and androgen receptor in prostate cancer tissue (Grob et al., 1994, Gregory et al., 1998), of oestrogen receptor in breast cancer (Yang et al., 1991,

Yoshida et al., 1997), to mention but a few. The collated information has proven useful for improvement of therapeutic interventions in clinical management of the progression of cancers as well as identification of target patients for therapy based on the profile of their biopsies and the pattern of expression of the progression marker proteins (Yoshida et al., 1997). The other importance of immunohistochemical analyses of tissues is that it allows pathologists to identify the stage(s) at which the disease is present in the patient as well as giving a snapshot of the degree of tissue damage present, for instance as an indicator of the presence and extent of tumour metastasis that has occurred in the patient. This allows the pathologists to assign a grade to the tumour that allows the oncologists to interpret the immunohistochemical data accurately and proceed to diagnosis and treatment regimes and patient management. In prostate cancer, the use of both Gleason scoring and the TNM method of tumour classification is fundamental to correct grading of tumours from prostate cancer patients (see Section 1.3.3).

TIMP-3 is expressed in different human cell types as described in Chapter 1, Section 1.6. Unique patterns of expression of its transcript and protein have been reported in the literature e.g. TIMP-3 expression in breast (Mylona et al., 2006), liver (Lu et al., 2003), colon (Hilska et al., 2007, Tanaka et al., 2007), ovary (Goldman and Shalev, 2004, Lu et al., 2003), breast (Uria et al., 1994) and prostate (Cross et al., 2005).

One particular study by Su *et al* (Su et al., 2001) looked at the expression of *timp-3* mRNA in a large cohort of tissue samples by Affymetrix GeneChip analyses. Some of the tissue samples they analysed included: normal liver tissues, normal prostate tissues and primary prostate cancer tissues. The mRNA expression results from these 3 tissues were of importance to this project as these were the tissues available at the time for immunohistochemical analyses for the characterisation and localisation studies for TIMP-3. In the Su *et al* study, the fold increase in intensity of *timp-3* mRNA over baseline in several tissues was reported (see Figure 3.1), along with expression data for several other genes. The results were analysed and reported in line with the GCRMA method for analyses of Affymetrix GeneChip array data (Gharaibeh et al., 2008). The interesting and relevant part of the pool of results obtained, was the overall increase in the level of TIMP-3 expression observed in normal prostate tissue compared to primary prostate tissue as well as the higher levels of TIMP-3 expression seen in T2N0M0 (larger) tumours compared to T3N0M0 (smaller) tumours, according to the TNM classification of the tumour (see Figure 3.1 and Figure 3.2).

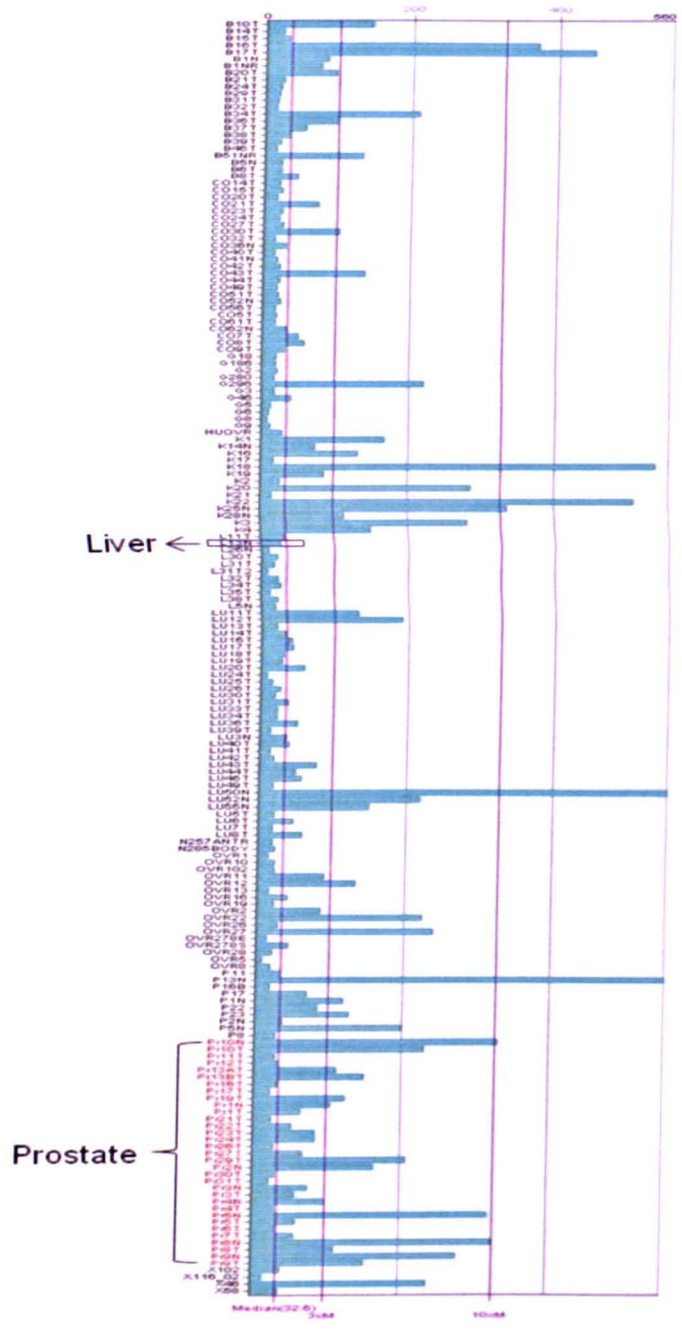

Figure 3.1: Expression Profile of timp-3 mRNA in Tissues.

This is a bar chart obtained via the online BIOGPS gene expression analysis software (Wu et al., 2009a). The data were obtained from results of Affymetrix GeneChip analyses of RNA extracts from various tumours and the results given as normalized fluorescence intensities, which correlate to the levels of timp-3 mRNA present in each sample. See Figure 3.2 for a close-up of the prostate data

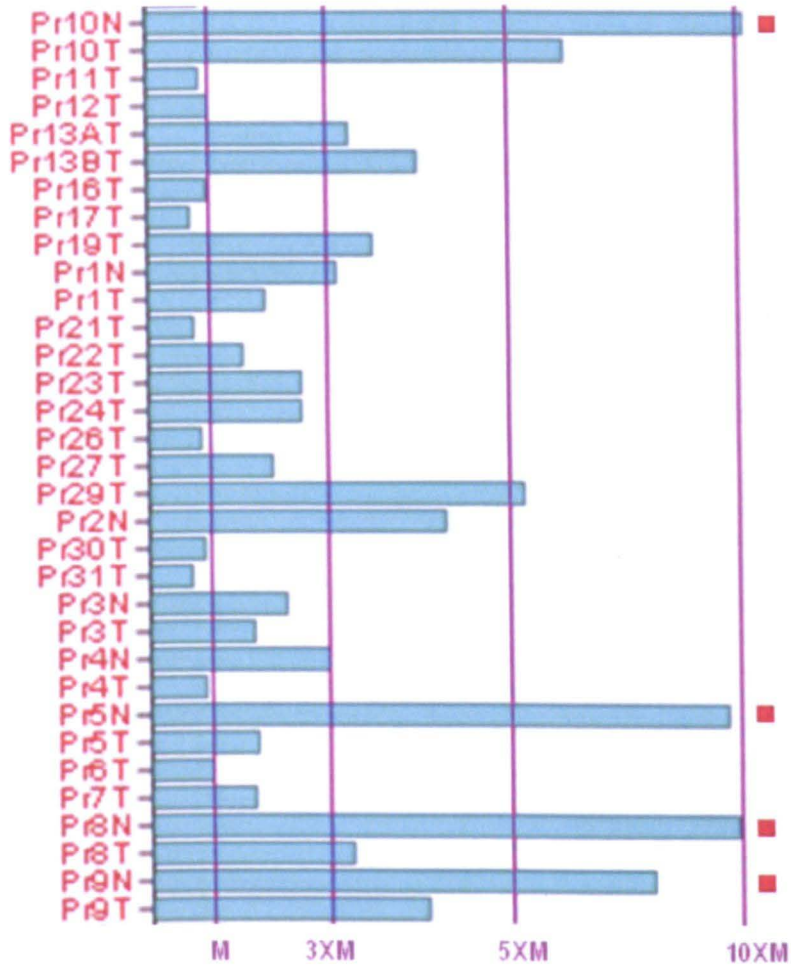

Figure 3.2: Expression Profile of timp-3 mRNA in Prostate Tissue Samples.
These are also results obtained from the Affymetrix GeneChip analyses as in Figure 3.1. The above represents only expression data from prostate tissue samples, magnified from Figure 3.1. The individual bars above represent the different types of prostate tissue analyses. 'Pr' means prostate, the following number is an identifier code specific for the tissue and set by the researcher and the letter following the number is an indicator of whether the tissue is a normal (N) or tumour tissue (T). M stands for the median fold increase in fluorescence intensity, 3XM is 3 times the M value, 5XM is 5 times the M value and 10XM is 10 times the median value. The results from the Su et al study showed greater timp-3 mRNA expression in normal prostate tissues in comparison to prostate tumour tissues (see red dots on bars above) overall.

Annotation	Tissue	Histology	Cancer Stage	Expression
Pr1T	prostate	cancer	T2AN0M0	65.256
Pr5T	prostate	cancer	T2AN0M0	59.719
Pr10T	prostate	cancer	T2AN0M0	232.285
Pr11T	prostate	cancer	T2AN0M0	28.7
Pr29T	prostate	cancer	T2AN0M0	208.023
Pr4T	prostate	cancer	T2bN0M0	30.446
Pr6T	prostate	cancer	T2BN0M0	34.75
Pr3T	prostate	cancer	T2BN0M0	58.229
Pr9T	prostate	cancer	T2BN0M0	153.987
Pr31T	prostate	cancer	T2BN0M0	23.342
Pr16T	prostate	cancer	T2BN0M0	33.249
Pr7T	prostate	cancer	T3AN0M0	57.4
Pr12T	prostate	cancer	T3AN0M0	34.334
Pr13AT	prostate	cancer	T3AN0M0	112.955
Pr13BT	prostate	cancer	T3AN0M0	150.708
Pr22T	prostate	cancer	T3AN0M0	52.721
Pr23T	prostate	cancer	T3AN0M0	84.278
Pr26T	prostate	cancer	T3AN0MX	28.64
Pr30T	prostate	cancer	T3B0M0	30.32
Pr8T	prostate	cancer	T3BN0M0	111.867
Pr19T	prostate	cancer	T3N0M0	124.42
Pr24T	prostate	cancer	TXN0M0	85.311
Pr17T	prostate	cancer	TXN1M0	22.993
Pr21T	prostate	cancer	TXN0MX	24.93
Pr27T	prostate	cancer	TXN0MX	68.262
Pr1N	prostate	normal		104.269
Pr5N	prostate	normal		320.738
Pr3N	prostate	normal		75.261
Pr4N	prostate	normal		100.192
Pr2N	prostate	normal		165.718
Pr8N	prostate	normal		325.356
Pr9N	prostate	normal		279.544
Pr10N	prostate	normal		331.004
L13N	liver	normal		26.372

Table 3.1: Expression Data for timp-3 mRNA in Prostate and Liver Tissue Samples.*-The expression levels were obtained from the Su et al study. These are fold increase in expression levels over the baseline expression levels, measured using the 'GCRMA' method for background correction, normalising and summarisation of results from Affymetrix GeneChip arrays. The annotations are as described in Figure 3.1.*

It was therefore important to investigate whether this expression pattern of *timp-3* mRNA seen in these tissues (as per the above study) translated to expression of the TIMP-3 protein in prostate cancer tissues and normal prostate tissues. To do this, Dr. Colby Eaton's group kindly donated a prostate tissue microarray sample that contained normal liver tissue as well tissue from primary prostate tumour, high grade PIN tumour and normal background prostate epithelium, all 3 tissue types obtained from the same patient. Information on the Gleason Score (GS) of the patients was also supplied. The map of the tissue array is as described in Chapter 2, Section 2.18.

In this project, the first objective was to investigate the expression of TIMP-3 in prostate cells and tissues in order to be able to study its role in the progression of prostate cancer. Normal stromal cells (WPMY-1), prostate cancer-associated fibroblasts (PCAF), benign prostatic hyperplasia stromal cells (BPH45), androgen-dependent prostate cancer cells (LNCaP) and androgen-independent prostate cancer cells (PC3) were analysed for transcript and protein expression of TIMP-3. The TIMP-3 mRNA expression was measured by qPCR and the data were analysed using the Applied Biosystems SDS 2.2.1 analysis software. Protein expression was analysed by western blotting and immuno-cytochemistry. The western blotting was optimised in order to determine the best conditions for analysing protein levels.

The expression of TIMP-3 in normal prostate, primary prostate cancer and BPH tissues was also investigated. Tissues had been obtained from patients and formalin-fixed and paraffin-embedded onto glass slides. Expression and localisation of TIMP-3 was determined by immuno-histochemistry using mouse monoclonal anti-TIMP-3 as the primary antibody (R&D Systems, MAB973) and Alexa-flour-488-conjugated goat anti-mouse secondary antibody (Invitrogen, A11001). The slides were examined using an inverted fluorescence microscope with the 10X objective and the excitation wavelength for observing the Alexa-fluor-488 fluorescent dye was set at 488 nm and emission at 519 nm.

Also, changes in TIMP-3 expression upon co-culturing prostate stromal and prostate cancer cells *in vitro* were investigated as described in Section 2.1.5. Changes in TIMP-3 mRNA expression were analysed by qPCR and protein expression by western blotting. It has been suggested that during migration of cancer epithelial cells from their primary site, they co-migrate with stromal fibroblasts after proteolysis of the basement membrane and ECM in the stromal compartment and co-habit a secondary niche (Kaminski et al., 2006). If TIMP-3

expression is important for metastasis, my hypothesis is that there will be modulation of its expression in coculture.

3.2 RESULTS

3.2.1 Optimisation of Western Blotting

During the course of this project, some protein bands obtained by SDS-PAGE and western blotting were of a higher molecular weight than expected, suggesting post-translational modifications such as glycosylation of proteins or cross-reactivity of antibodies with other non-specific proteins. Several experiments were carried out in order to determine the source of the problem(s). These included: deglycosylation of protein lysates and immune-precipitation of test protein with specific antibody to eliminate cross-reactivity. Therefore, experiments were designed to address these issues, and they are detailed below:

3.2.1.1 De-glycosylation of protein samples

The first possible trouble-shooting experiment was to remove any N-linked glycosyl residues from the proteins. To do this total cell lysates were subject to de-glycosylation using the manufacturer's protocol. N-glycanase (Peptide-N-Glycosidase F) was obtained from Prozyme, UK. N-glycanase releases N-glycans from glycoproteins and so can be used to detach covalently bound sugars (glycosyl groups) from a target protein. First, 20 µl (100 µg) of protein extract was added to 25 µL of reaction buffer (consisting of 100 mM sodium phosphate and 0.1% sodium azide, pH 7.5) (Prozyme) totalling 45 µL of reaction mixture. Then 2.5 µL of denaturation solution (consisting of 2% SDS, 1 M β-mercaptoethanol) (Prozyme) was added. The mixture was maintained at 100°C for 5 minutes and then allowed to cool to ambient temperature. Then 2.5 µL of detergent solution (consisting of 15% NP-40) (Prozyme) was added to the mixture, left for 5 minutes and then 2 µL of N-glycanase stock was added and incubated overnight at 37°C. The next day, sample buffer (as described in Section 2.10) was added to the mixture and the sample was subject to SDS-PAGE and western blotting for protein separation and detection (as described in Section 2.11) This was done for all samples and when not used immediately, was stored at -20°C prior to use. This process of deglycosylation has been previously described (Chu, 1986,

Tarentino et al., 1985, Plummer et al., 1984). Unfortunately, the N-glycanase alone was cross- reacting with antibody and showing as a ~30 kD band (see Figure 3.3).

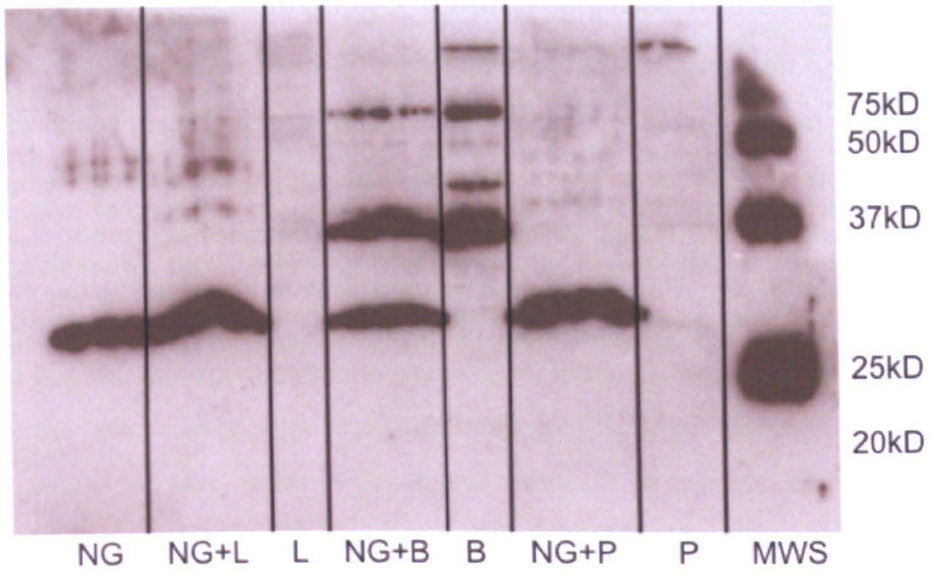

Figure 3.3: Treatment of Proteins with N-Glycanase.
NG = N-Glycanase only, L = Total LNCaP extract, B = Total BPH45 extract, P = Total PCAF extract, MWS = molecular weight standards. For immunoblotting, anti-C-Terminal-TIMP-3 antibody (Sigma) was used as described in Section 2.11. 100 µg protein was loaded per well.

3.2.1.2 Protein A/G Immunoprecipitation

I next attempted immunoprecipitation of the protein using target antibodies. Protein A/G ultralink was obtained from Pierce, UK. Protein A/G binds to all the IgG subclasses with a high affinity and so it has a wider range of binding than either protein A or protein G alone. A protein-antibody complex can therefore be pulled out of solution using Protein A/G bound to Sepharose beads. In this way, I hoped to be able to pull out TIMP-3 specifically from the protein extracts before analysis by western blotting.

For these experiments, protein A/G resin was first diluted 1:2 with immunoprecipitation (IP) buffer (consisting of 25 mM Tris, 150 mM NaCl, pH 7.2) (Pierce, 28379). Then, 50 µg of protein extract was incubated with 250 µg of anti-TIMP-3 mouse monoclonal antibody (R&D Systems, MAB973) made up in IP buffer. The mixture was incubated on a rotor

overnight at 4°C. The next day, 100 µL of the gel suspension was added to the protein-antibody complex and incubated for 2 hours at ambient temperature with gentle mixing. Then 0.5 mL of IP buffer was added to the mixture and centrifuged for 3 minutes at 2500 x *g*. This step was repeated 3 times after which the gel was washed with 0.5 mL of H_20 by centrifugation at 2500 x *g* for 5 minutes. The supernatant was discarded and the immune complex was eluted by adding 50 µl to the gel for 5 minutes and further centrifugation at 2500 x *g* for 3 minutes. 50 µL of loading buffer (as described in Section 2.10) was added to the gel and heated for 15 minutes at 70°C. The resulting supernatant was collected by centrifugation at 2500 x *g* for 5 minutes and cooled to ambient temperature before subjecting to SDS-PAGE and western blotting (as described in Section 2.11) using rabbit anti-TIMP-3 antibody. Unfortunately, this procedure did not resolve the problem and still gave bands of >23 kD molecular weight. It also resulted in non-specific bands across the gel (see Figure 3.4).

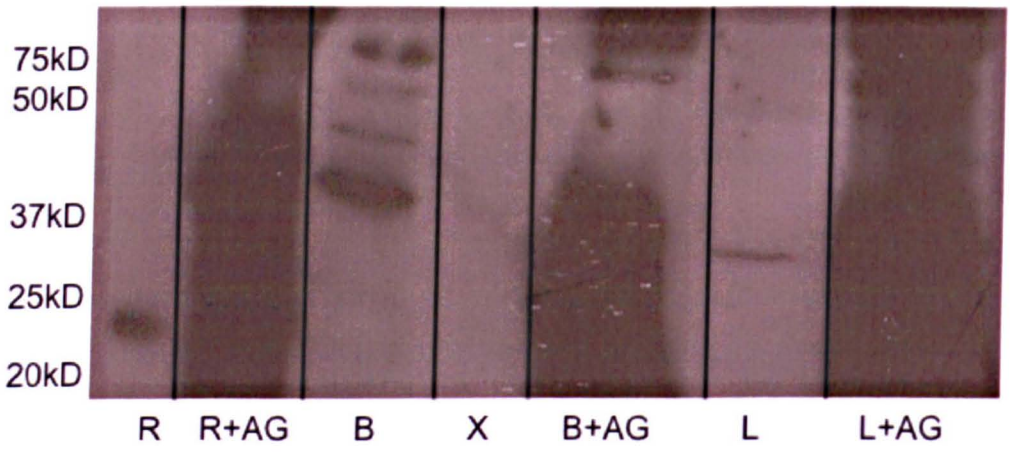

Figure 3.4: Immuno-precipitation of Proteins using Protein A/G Ultralink Beads.
R = recombinant human TIMP-3 only, B = Total BPH45 extract, L = Total LNCaP extract, X = blank well (gel imperfect in this region so well unused). For immunoblotting, anti-C-Terminal-TIMP-3 antibody (Sigma) was used as described in Section 2.13. 10 ng of recombinant human TIMP-3 was loaded – this was seen as ~24 kD as expected. 50 µg of protein extracts was used for immuno-precipitation. Protein A/G beads were cross-reacting with antibody.

3.2.1.3 Monoclonal vs. Polyclonal TIMP-3 Antibody

The problem of potential non-specific bands showing on the western blotting films was still to be tackled and another trouble-shooting experiment was to compare the antibody that I had been using previously (Anti-C-terminal-TIMP-3 from Sigma) for immunoblotting with a mouse monoclonal antibody (R & D systems, MAB973). Total and ECM only proteins were extracted as described in Section 2.10 and subject to SDS-PAGE and western blotting as described in Section 2.11. The results obtained showed the mouse monoclonal anti-TIMP-3 antibody detecting TIMP-3 at ~23 kD (see Figure 3.6) compared to the higher bands seen with the rabbit anti-TIMP-3 antibody (see Figure 3.5) and so led me to the decision to continue other experiments with the antibody since it gave no apparent non-specific bands and TIMP-3 was detected at the correct size. It also buttressed the suggestion in literature (Langton et al., 1998) that TIMP-3 is sequestered predominantly in the ECM, and that the non-specific bands were due to intracellular proteins. It therefore made sense that the better results were seen with loading of ECM proteins and not total proteins. Based on results of this experiment, it was decided to analyse ECM proteins for TIMP-3 expression in all other experiments and to use 50 nM of the anti-TIMP-3 antibody from R&D Systems (MAB973).

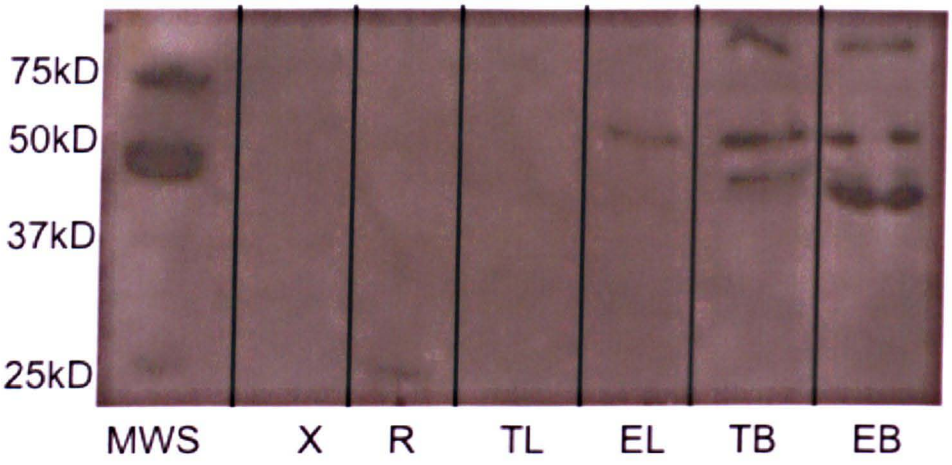

Figure 3.5: Immuno-blotting of Protein Extracts using Rabbit Anti-C-terminal-TIMP-3 antibody.
MWS = molecular weight standards, X = blank well, R = recombinant human TIMP-3, TL = total lysate from LNCaP cells, EL = ECM extract from LNCaP cells, TB = total lysate from BPH45 cells, EB = ECM extract from BPH45 cells. 10 ng of recombinant human TIMP-3 was loaded – this was seen as ~23 kD as expected. For total extracts, 50 µg protein was loaded per well and for ECM extracts, 100,000 cells' worth of ECM was loaded per well. For immunoblotting, anti-C-Terminal-TIMP-3 antibody (Sigma, T7812) was used as described in Section 2.13. This antibody did not detect TIMP-3 at the right size of ~23 kD but showed non-specific bands at ~45 kD and other bands at ~35 kD.

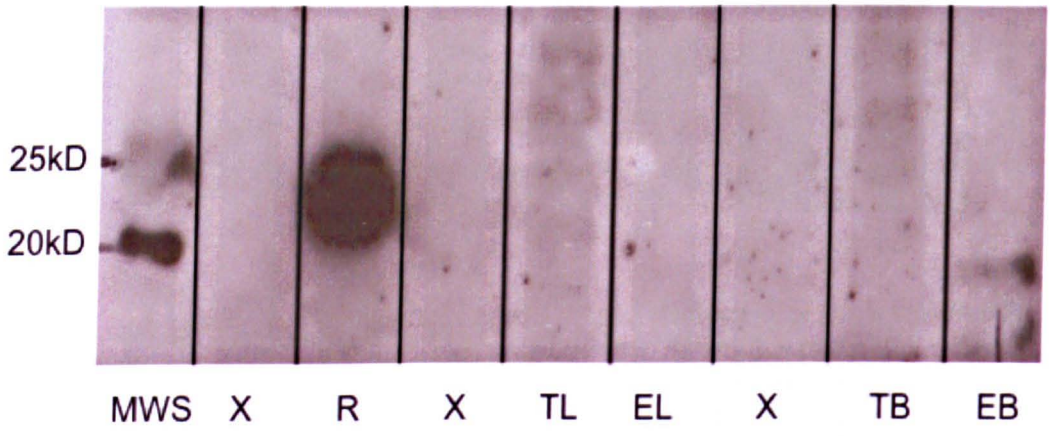

Figure 3.6: Immuno-blotting of Protein Extracts using Mouse Anti-TIMP-3 antibody.
For immunoblotting, anti-TIMP-3 antibody (R&D Systems, MAB973) was used as described in Section 2.13. 100 ng of recombinant human TIMP-3 was loaded – this was seen as ~24 kD as expected. For total extracts, 50 µg protein was loaded per well and for ECM extracts, 100,000 cells' worth of ECM was loaded per well. This antibody detected single TIMP-3 band at ~21 kD in BPH45 ECM extract, closer to its known molecular weight of 22 kD.

3.2.2 TIMP-3 mRNA Expression in Prostate Cells

The relative expression of TIMP-3 mRNA in WPMY-1, PCAF, BPH45, LNCaP and PC3 cell lines was analysed. Total RNA was extracted from cells and quantified as described in Section 2.4. These were reverse-transcribed to make complementary DNA by reverse transciption as described in Section 2.5. mRNA was synthesized from cDNA by qPCR as described in Section 2.6. Results were analysed as described in Section 2.7 using the comparative ΔCt method (Livak and Schmittgen, 2001).

Amplification plots of the different Ct values obtained from qPCR analyses of the expression data are shown in Figure 3.7. BPH45 had the lowest Ct value and highest TIMP-3 mRNA expression, followed by PCAF then WPMY-1 then LNCaP. PC3 had the highest CT value and lowest TIMP-3 mRNA expression. The Ct values were all normalised to the Ct of RNA Polymerase II as a control 'house-keeping' gene.

As summarised in Figure 3.8, all the prostate stromal cells that were analysed expressed significantly higher amounts of TIMP-3 mRNA relative to PC3 cells; about 100,000 – 200,000 fold higher expression ($p=0.0079$ for PCAF, WPMY-1 and BPH45, Mann-Whitney). The androgen-sensitive LNCaP cells produced about 100-fold higher expression of TIMP-3 mRNA than the androgen-resistant PC3 cells but this was also statistically significant ($p=0.012$, Mann-Whitney). The expression levels of TIMP-3 mRNA did not vary significantly between the cancer-associated PCAF and normal WPMY-1 stromal cells but expression level were about 1.5-fold higher in the benign prostatic hyperplasia cells (BPH45) compared to PCAF cells ($p=0.0079$, Mann-Whitney) and about 2-fold higher in BPH45 compared to WPMY-1 cells ($p=0.0079$, Mann-Whitney). The experiment was repeated 4 times.

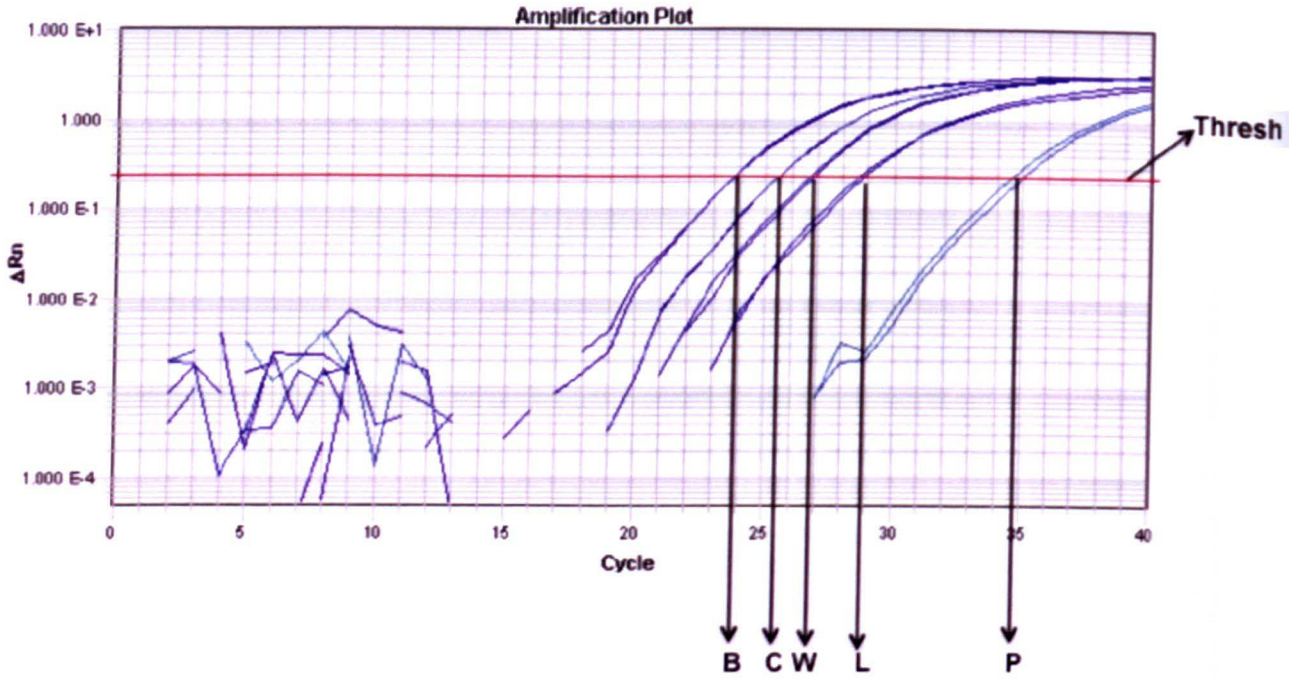

Figure 3.7: Amplification Plot of TIMP-3 mRNA expression in prostate cells.
This is a logarithmic representation of the amplification plot of the mRNA expression in prostatic cells. ΔRn is plotted on the y-axis and it represents the magnitude of the TIMP-3 signal. During the initial cycles of qPCR, there are little or no changes in the fluorescence signal, implying no expression of TIMP-3 mRNA (i.e. between cycles 0 and 15) – this is known as background. Afterwards, the linear and exponential phase of the amplification occurs, where fluorescence is detected, signifying TIMP-3 mRNA detection and amplification. The SDS 2.2.1 analysis software (see Section 2.6) was set to automatically determine a level of ΔRn that is above the baseline and low enough to be within the exponential phase of the curve – this is known as threshold and is the line that intersects with the amplification plot to determine the C_T. The C_T is defined as the cycle number at which the fluorescence signal passes the threshold, and these are indicated by the arrows in the plot. B = C_T of TIMP-3 mRNA in BPH45, C = C_T of TIMP-3 mRNA in PCAF, W = C_T of TIMP-3 mRNA in WPMY-1, L = C_T of TIMP-3 mRNA in LNCaP and P = C_T of TIMP-3 mRNA in PC3 cells. Duplicate curves represent duplicate wells in the assay. Results showed the lowest C_T value in BPH45 cells, indicating that this cell line has the highest TIMP-3 mRNA, followed by PCAF cells, then WPMY-1, then LNCaP and finally PC3 cells with the highest C_T value and the lowest TIMP-3 mRNA expression of all the prostatic cells. n=4

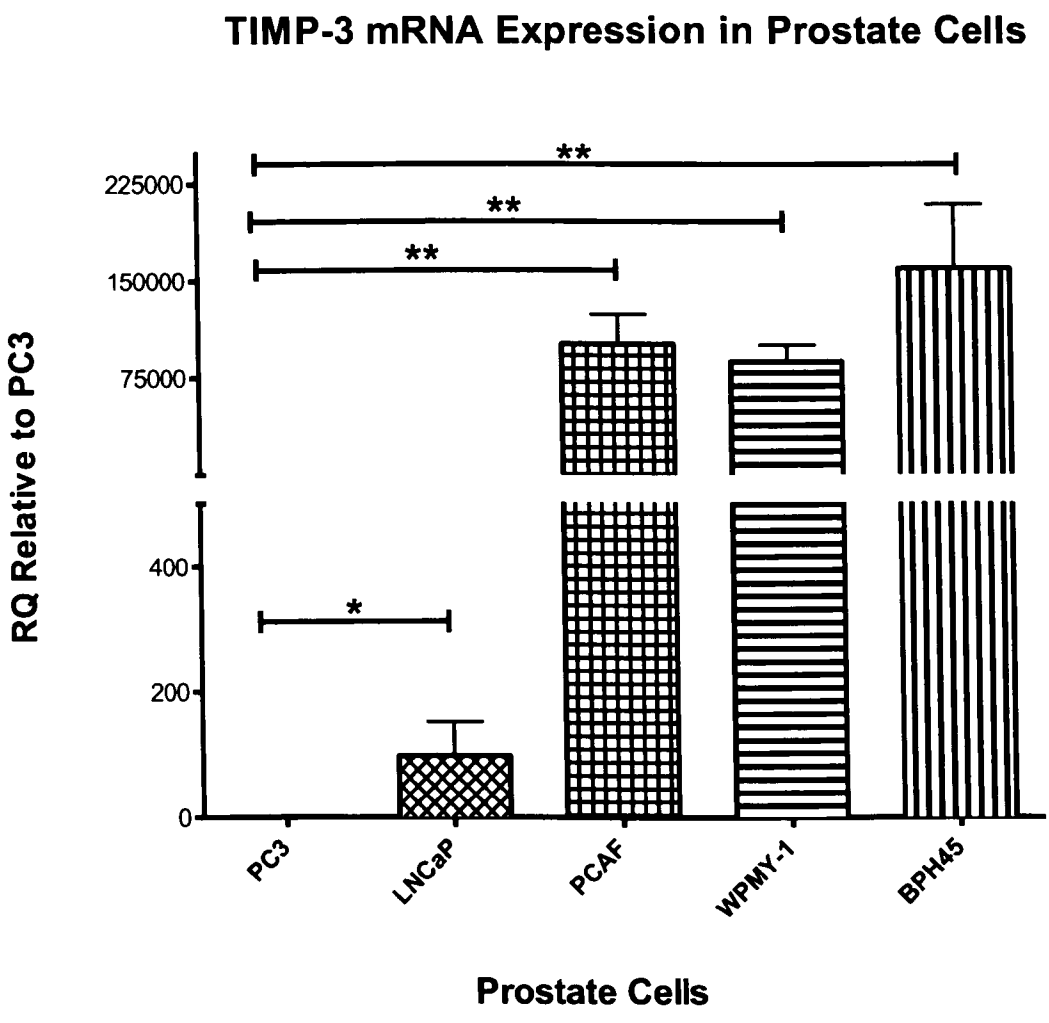

Figure 3.8: TIMP-3 mRNA expression in prostate cells.

*100,000 cells were seeded into 6-well plates using complete DMEM media until they reached ~ 90% confluence. Total RNA was extracted from cells and cDNA synthesized by reverse transcription. TIMP-3 mRNA expression was measured by qPCR and normalised to a housekeeping gene, GAPDH. These procedures are as described in Section 2.6 – 2.9. Columns and bars represent the median and range of values (n=4) y-axis has been segmented to show fold differences between all cell lines relative to expression in PC3 cells. * $p<0.05$ and ** $p<0.01$. Mann-Whitney non-parametric test used to generate p values.*

3.2.3 TIMP-3 Protein Expression in Prostatic Cells

TIMP-3 protein expression was analysed by western blotting of total cell and ECM lysates, separately obtained from all cancer and stromal cells (described in Section 2.11)

As discussed in Section 3.2.1, different antibodies gave different results and so had to be optimised for best TIMP-3 detection. Based on these experiments, anti-TIMP-3 antibody (R&D Systems, MAB973) was chosen for immuno-blotting and ECM lysates were extracted instead of total cell lysates.

For western blotting experiments, 50 nM (1:500 dilution) of anti-TIMP-3 antibody was used for primary incubation. The protocol is as described in Section 3.2.1. As loading control, 1 x 10^5 cells' worth of ECM was loaded per well since the protein concentration could not be measured by BCA assay due to the presence of interfering (high) levels of DTT concentration on the ECM extraction buffer. This meant that the cells had to be counted once they had been uplifted from the ECM with enzyme-free buffer (Section 2.10). Higher levels of TIMP-3 were found in the ECM of the prostate stromal cells BPH45, PCAF and WPMY, compared to very low levels observed in the cancer cells LNCaP (Figure 3.9). This corroborated the mRNA results (Figure 3.8). Densitometric analysis of the blots suggested that BPH45 ECM contained the highest levels of TIMP-3 followed by PCAF ECM and then WPMY-1 ECM. LNCaP ECM had the least amount of TIMP-3. It is important to mention that LNCaP cells did not appear to produce as much ECM as the prostate stromal cells. It was decided not to extract ECM from prostate cancer cells PC3 as they produced negligible levels of TIMP-3 transcripts (Figure 3.8) and also only appeared to produce small amounts of ECM.

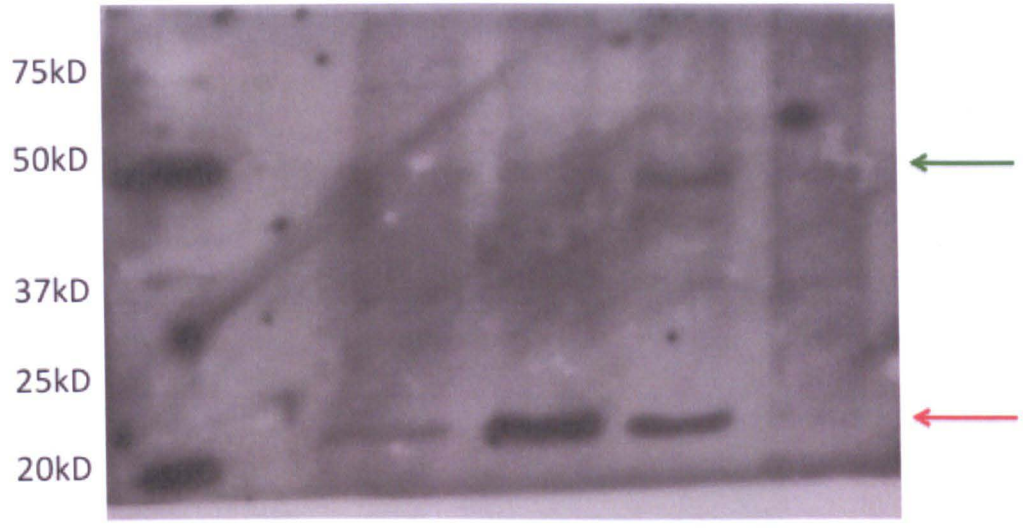

	MWS	X	W	B	P	L
ODmm²	N/A	X	1.3	4.9	2.3	0.2

Figure 3.9: TIMP-3 protein expression in ECM lysates from Prostate Cells. *1 x 10^5 cells' worth of ECM protein was subjected to electrophoresis and transferred onto a PVDF membrane as described in Sections 2.10 - 2.11. The membrane was probed with 1:5000 of monoclonal anti-TIMP-3 overnight at 4°C and afterwards in 1:1000 goat anti-mouse HRP-conjugated secondary antibodies for 1 hour at ambient temperature. ECL detection reagent was applied to the membrane and exposed to x-ray films. TIMP-3 bands were observed as ~ 23 kD bands (red arrow). There also appeared some non-specific bands at about 50kD (green arrow). In row 1, MWS = molecular weight standards, X – blank lane, W = ECM from WPMY-1 cells, B = ECM from BPH45 cells, P = ECM from PCAF cells and L = ECM from LNCaP cells. Semi-quantitative analyses of the bands were carried out by densitometry using the Quantity One software (see Section 2.12). The result of adjusted densitometric volume for each band is reported in row 2.*

Prostate cells were also fixed onto slides and immuno-stained for TIMP-3 as described in Section 2.16. For this, 1:500 (50n M) of mouse monoclonal anti-TIMP-3 was used for primary detection and counter-stained with 1:1000 of Alexa-fluor-488 goat anti-mouse antibody. A 10X or 20X objective on a fluorescence microscope was used for image capture. There was high TIMP-3 staining in stromal cells and low staining in LNCaP cells (Figure 3.10).

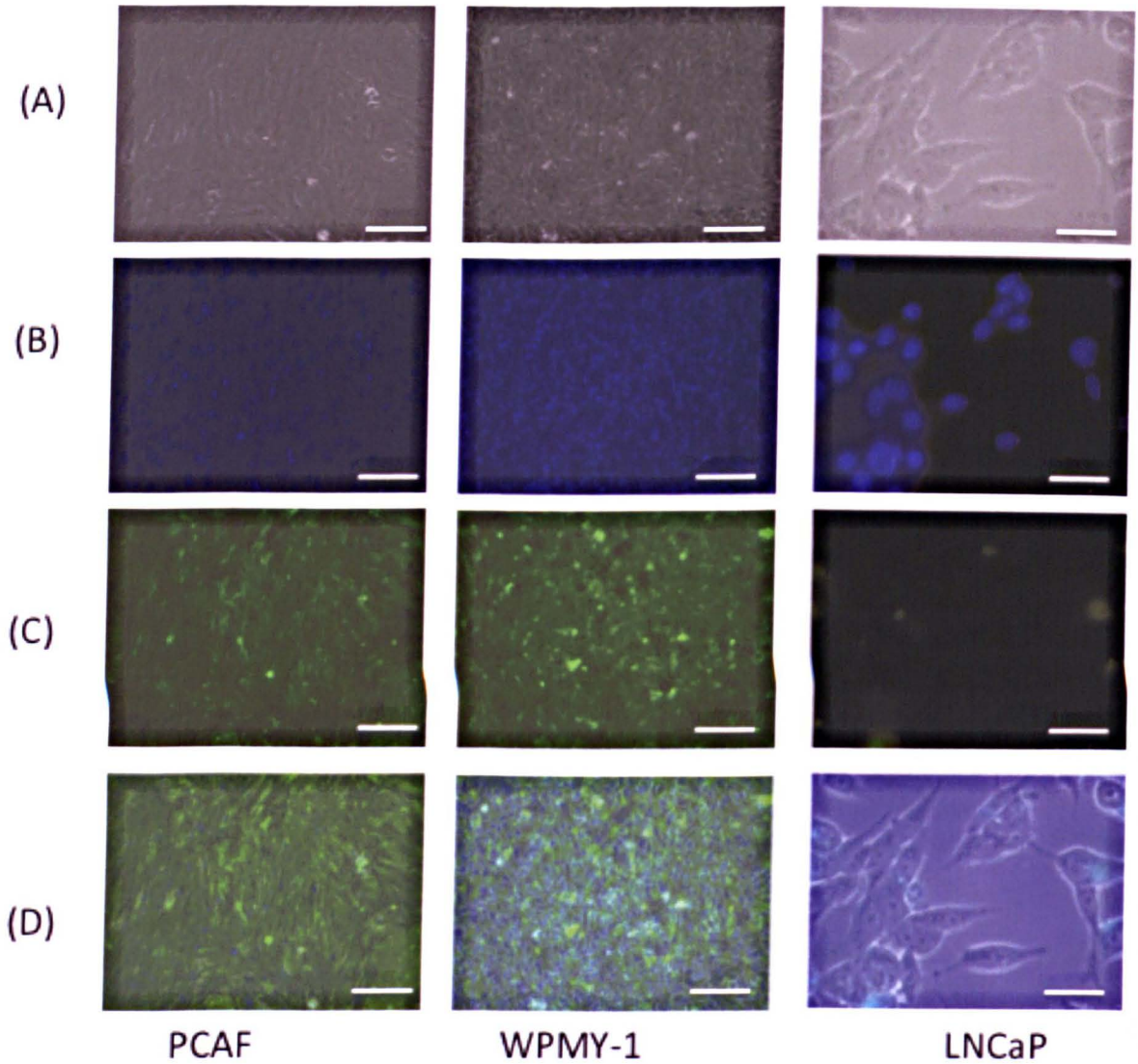

Figure 3.10: TIMP-3 Immunolocalisation in Prostate Cells.
Cells were fixed onto slides as described in Section 2.17. 50 nM (1:500) of mouse monoclonal anti-TIMP-3 antibody and 1:1000 of Alexa-fluor-488 goat anti mouse secondary antibody were used for detection of TIMP-3 in the slide-fixed cells. The slides were incubated overnight at 4˚C in primary antibody, washed with TBS buffer containing 0.05% Tween-20, and then incubated in secondary antibody in the dark at ambient temperature for 1 hour, then washed and counter-stained with DAPI for 5 minutes before mounting the coverslip and visualisation under the microscope. Images from (A) Phase contrast (B) DAPI only (C) Alexa-fluor-488-TIMP-3 staining (D) Super-imposed phase contrast+DAPI+Alexa-fluor-488-TIMP-3 images were taken using a Leica inverted fluorescence microscope and setting to 10X objective (for PCAF and WPMY-1 cells) or 20X objective (for LNCaP cells). Scale bar for PCAF and WPMY-1 = 100 um and for LNCaP = 250 um.

3.2.4 TIMP-3 Protein Expression in Prostatic Tissues

Prostate tissues were obtained as formalin-fixed sections on glass slides. Immunohistochemical analyses of the samples were carried out as described in Section 2.16. Tissues sections were stained with both haematoxylin and eosin (H&E) stains or with mouse anti-TIMP-3 and Alexa-fluor-488 goat anti mouse secondary antibody.

Haematoxylin and eosin (H&E) staining is used routinely to distinguish between the different tissue types and distinguish the nuclear staining from the intracellular and extracellular staining of cytoplasmic and ECM proteins respectively. Haematoxylin dye stains the nuclei of cells blue/violet while eosin stains cytoplasmic and extracellular regions of the cells red/pink.

Images were taken using the Leica inverted fluorescence microscope. Fluorescence was detected at excitation and emission wavelengths of 488 nm and 518 nm respectively. In instances where extra tissue samples were available, control staining was also carried out with the use of only the secondary antibody.

There was pronounced eosin staining in BPH tissue, compared to normal and primary prostate cancer tissue – this indicates a bigger stromal compartment in BPH tissue, and this feature is characteristic of this benign disease (Figure 3.11). There also appears to be glandular infiltration of the extracellular region of the primary prostate tissue characterised by H&E staining in undefined regions – both haematoxylin (nuclear) staining and eosin (intracellular and extracellular protein) staining are evenly distributed in all parts of the tissue section and the tissue has lost much of its glandular structure. In contrast, the haematoxylin staining appears to be defined in the normal prostate and BPH tissue. In these two, the glandular structures have been retained.

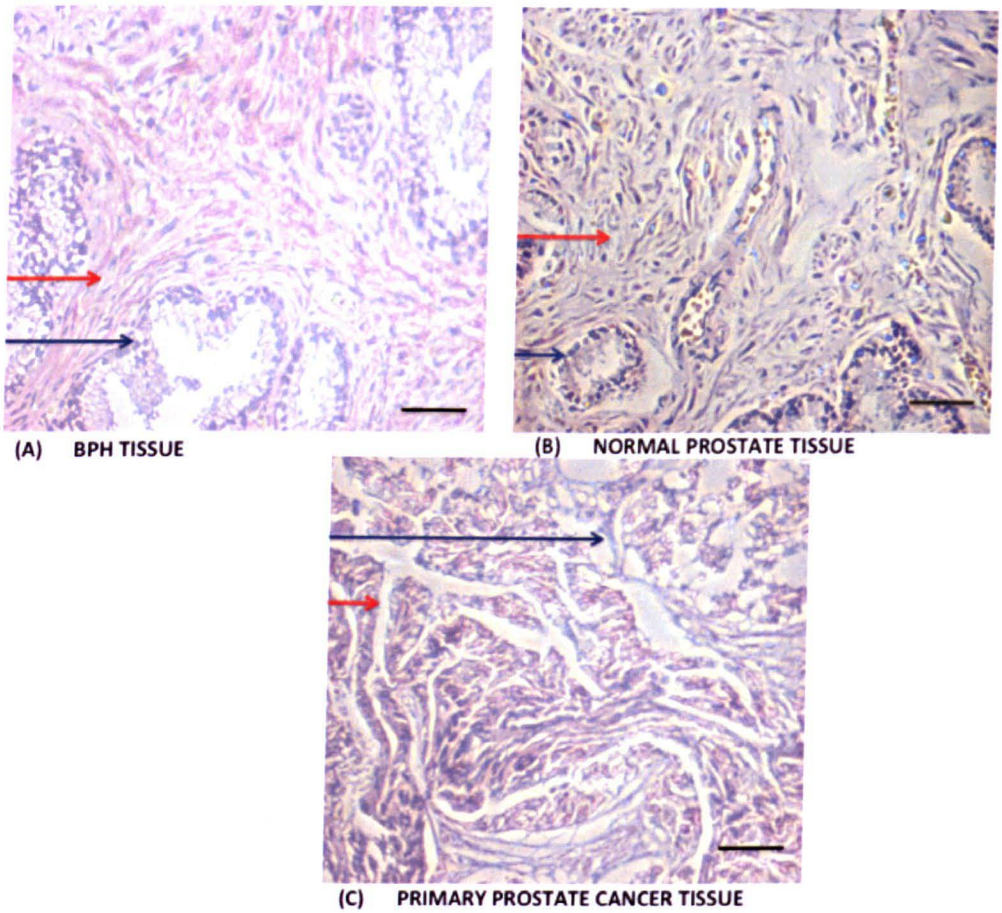

Figure 3.11: H&E Staining in Prostate Tissues.
Staining was performed as described in section 2.17. Images were taken using an inverted microscope. Eosin staining of intracellular and extracellular proteins (red arrow) and haematoxylin staining of cell nuclei (blue arrow) were observed in all tissues with varying levels of each stain. (A) BPH tissue shows high eosin staining as a result of enlarged extracellular stroma and haematoxylin staining allows visualization of the intact glands in the tissue. (B) In normal prostate tissues, there is moderate level of staining of both haematoxylin and eosin staining and the glands appear intact. (C) In primary prostate cancer tissue, there is heterogenous distribution of both stains, and no apparent glandular structure. Scale bar = 100 um.

Slides of tissue sections were also stained with 500 nM (1:50) of mouse monoclonal anti-TIMP-3 antibody and incubated overnight at 4°C. The slides were washed with TBS buffer containing 0.5% Tween-20 and incubated with secondary goat anti-mouse Alexa-Fluor-488 antibody for 1 hour at ambient temperature. Tissues were counter-stained with DAPI nuclear stain and covered with cover slips. Images were taken using an inverted fluorescence microscope at 10X objective.

High expression levels of TIMP-3 were apparent in BPH tissue (Figure 3.12) compared to normal tissue (Figure 3.13) and primary prostate cancer tissue (Figure 3.14). This is in line with the mRNA data from this project, showing higher levels of TIMP-3 mRNA in prostate stromal cells compared to prostate cancer cells (Section 3.2.2). In the primary prostate cancer tissue, the expression of TIMP-3 was generally low.

As control, BPH tissue sections were stained with only secondary antibody so as to ensure that any fluorescence observed was as a result of the antigen-antibody complex formation with the mouse anti-TIMP-3 antibody. Results showed no fluorescence in tissue, confirming that there is no inappropriate staining without the primary antibody (Figure 3.15).

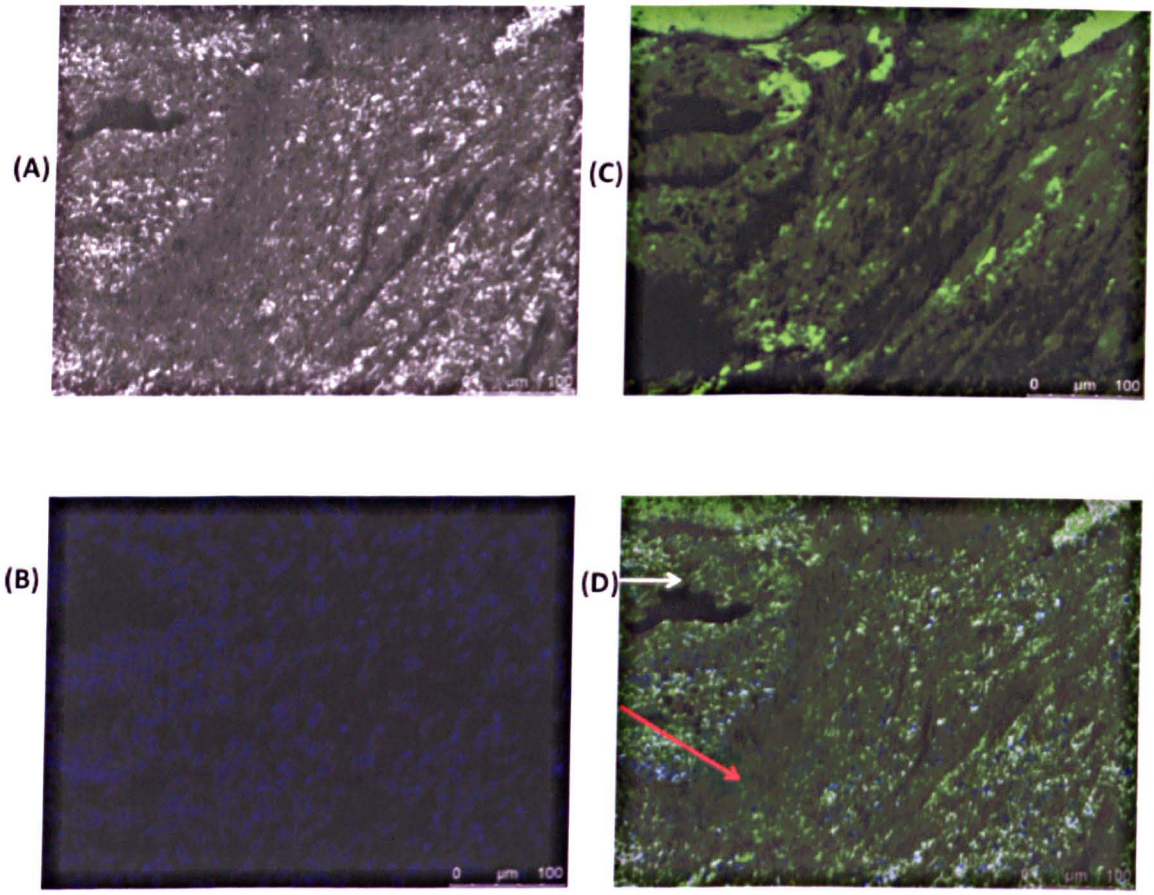

Figure 3.12: TIMP-3 Staining in BPH Tissue.
Samples were stained as described in section 2.17. (A) = phase contrast image (B) = DAPI staining (C) TIMP-3 staining (D) = super-imposed DAPI and TIMP-3 staining. Localization of TIMP-3 observed both in the extracellular (red arrow) and glandular region (white arrow) as seen in (D).

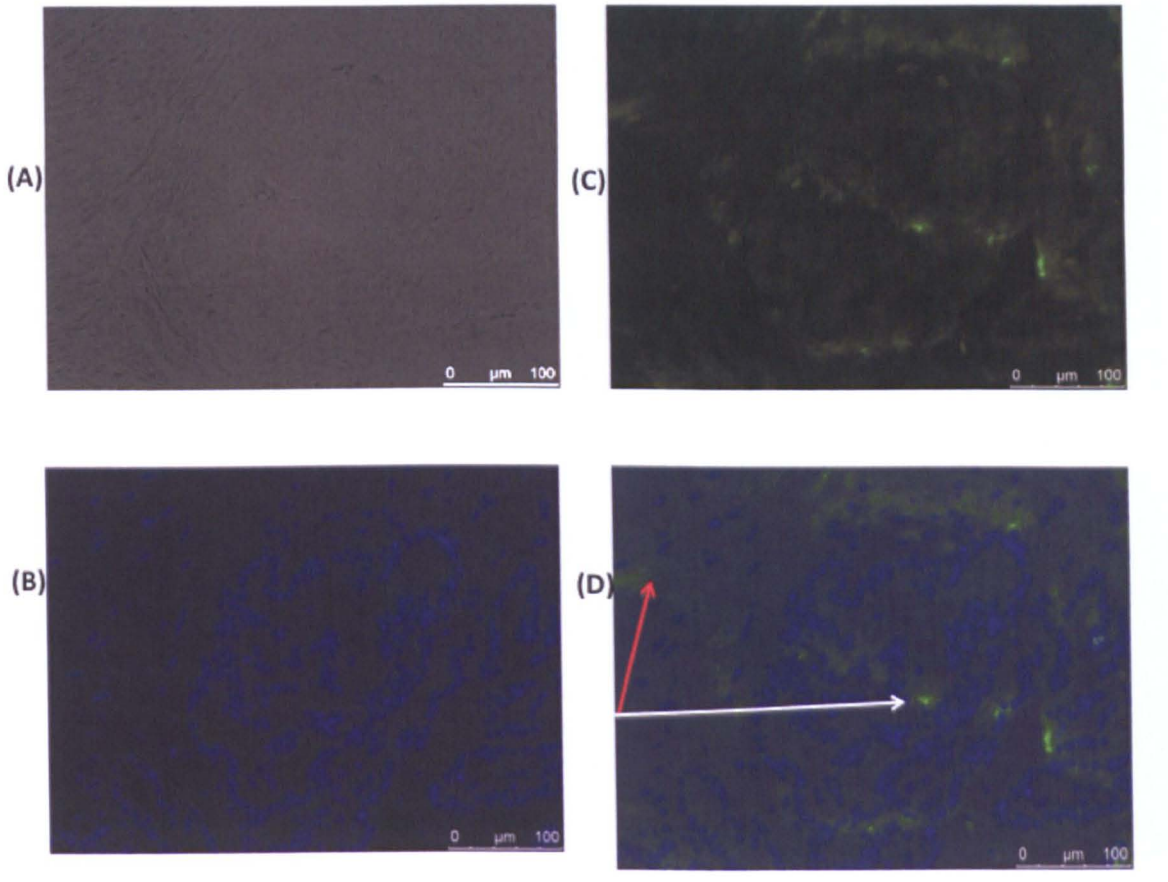

Figure 3.13: TIMP-3 Staining in Normal Prostate Tissue.
Samples were stained as described in section 2.17. (A) = phase contrast image (B) = DAPI staining (C) TIMP-3 staining (D) = super-imposed DAPI and TIMP-3 staining. Localization of TIMP-3 observed both in small proportion of the extracellular (red arrow) and glandular region (white arrow) as seen in (D).

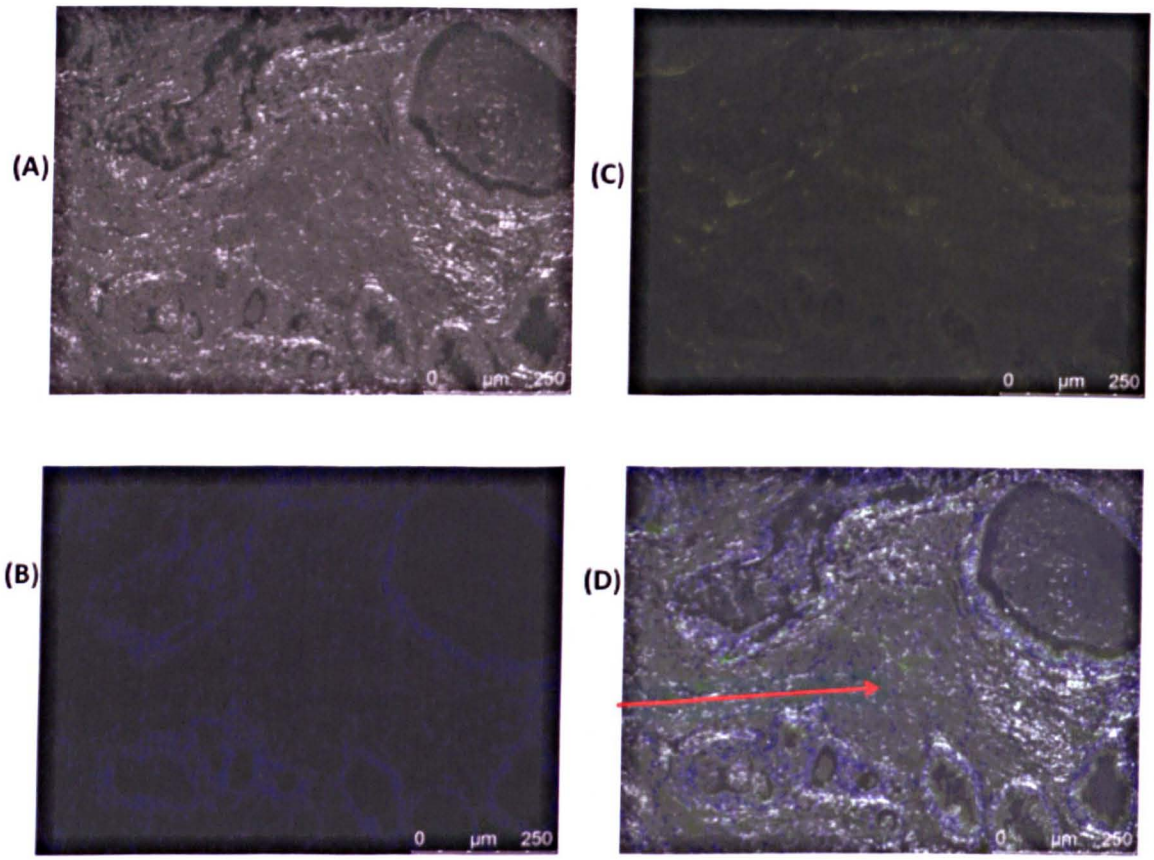

Figure 3.14: TIMP-3 Staining in Primary Prostate Cancer Tissue.
Samples were stained as described in section 2.17. (A) = phase contrast image (B) = DAPI staining (C) TIMP-3 staining (D) = super-imposed DAPI and TIMP-3 staining. Localization of TIMP-3 observed both in small proportion of the extracellular (red arrow) region as seen in (D).

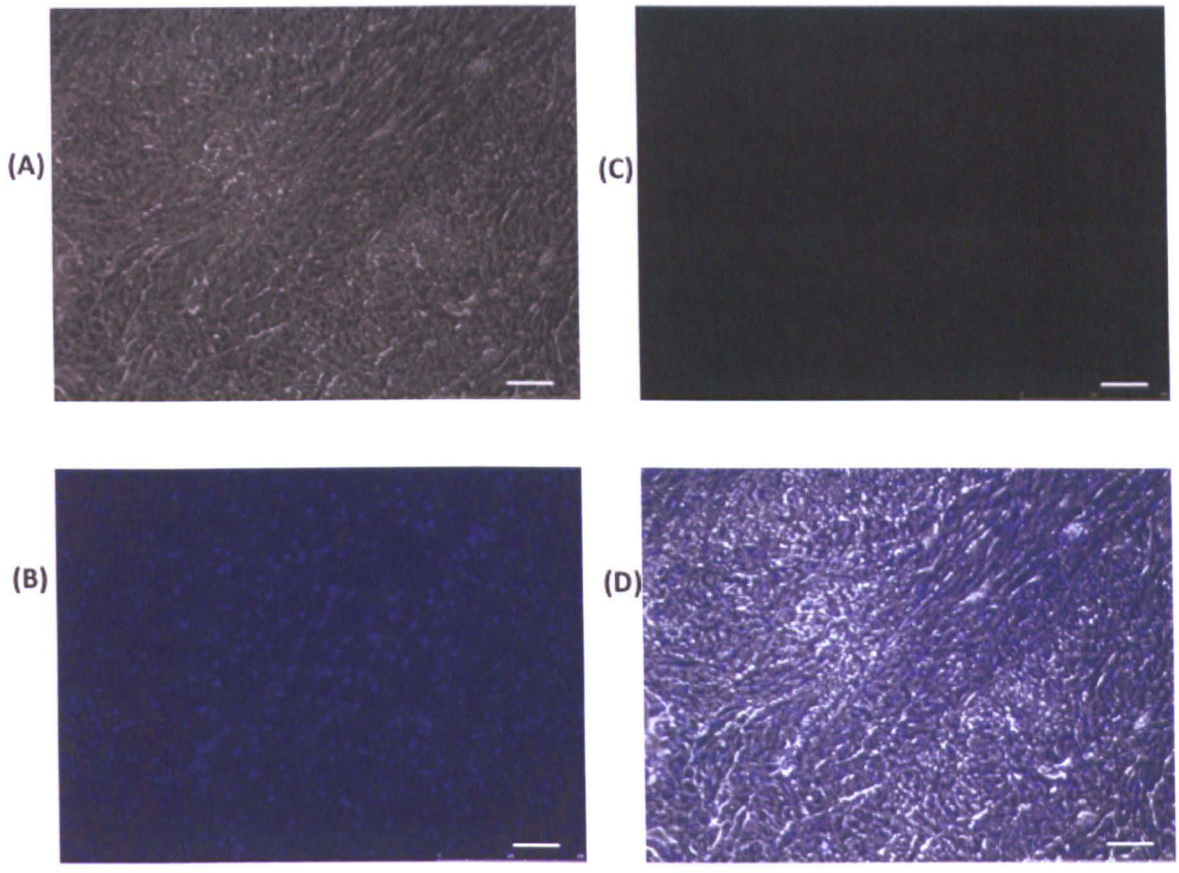

Figure 3.15: Control Staining in BPH Tissue.
Samples were stained as described in section 2.17. (A) = phase contrast image (B) = DAPI staining (C) No TIMP-3 staining (D) = super-imposed DAPI and TIMP-3 staining. No fluorescence observed i.e. no TIMP-3 staining. Scale bar = 100 um

For the tissue microarray analyses, the samples were first checked for their morphological accuracy and were counter-analysed by an in-house pathologist at the University, Dr. Simon Cross. This was to ensure that subsequent analyses were to be carried out using real prostate tissues and no errors were made during their characterisation for the purpose of this study. The pre-fixed tissues obtained were first subjected to haematoxylin and eosin staining, carried out as described in Section 2.17. The results from this research showed a clear difference between normal and prostate cancer tissue as well as difference between the morphology of high GS and low GS primary prostate cancer tissue (see Figure 3.16). All tissue sections were probed with anti-TIMP-3 antibody as described in Section 2.17.

There was also a pair of normal liver sections included on the microarray slide and these were used as control sections. The liver sections showed the occurrence of minute amounts of TIMP-3 expression (Figure 3.17)

There was also a negative correlation between the GS of the prostate cancer tissue and the degree of TIMP-3 staining i.e. more intense staining was observed in tissue with GS of 4 (Figure 3.18) than in tissue with GS of 7 (Figure 3.19).

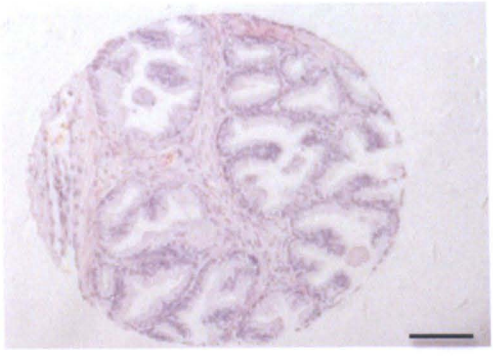

Normal background tissue

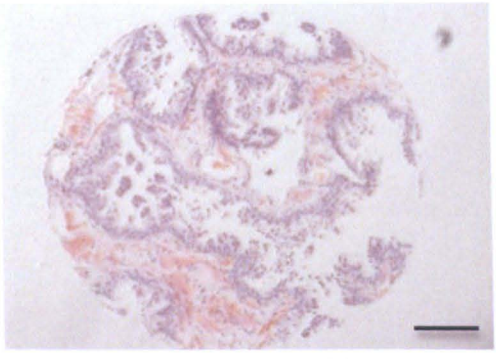

Prostate Cancer Tissue GS 6

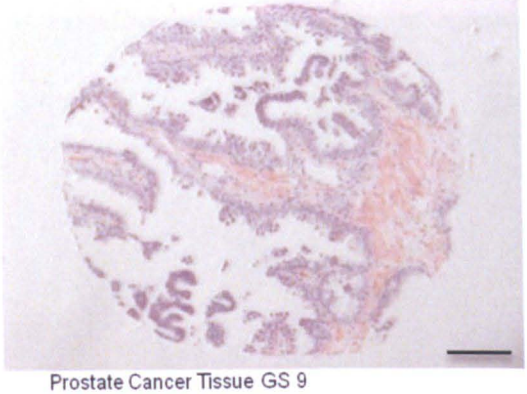

Prostate Cancer Tissue GS 9

Figure 3.16: Haematoxylin & Eosin (H&E) Staining for Morphological Assessment of Prostate Tissue Samples.

The above sample tissues had been previously formalin-fixed onto glass slides and were stained with H&E as described in Section 2.17. The nuclei of the cells are stained blue/purple and cytoplasmic proteins and extracellular matrices are stained red/pink. Scale bar = 100 um.

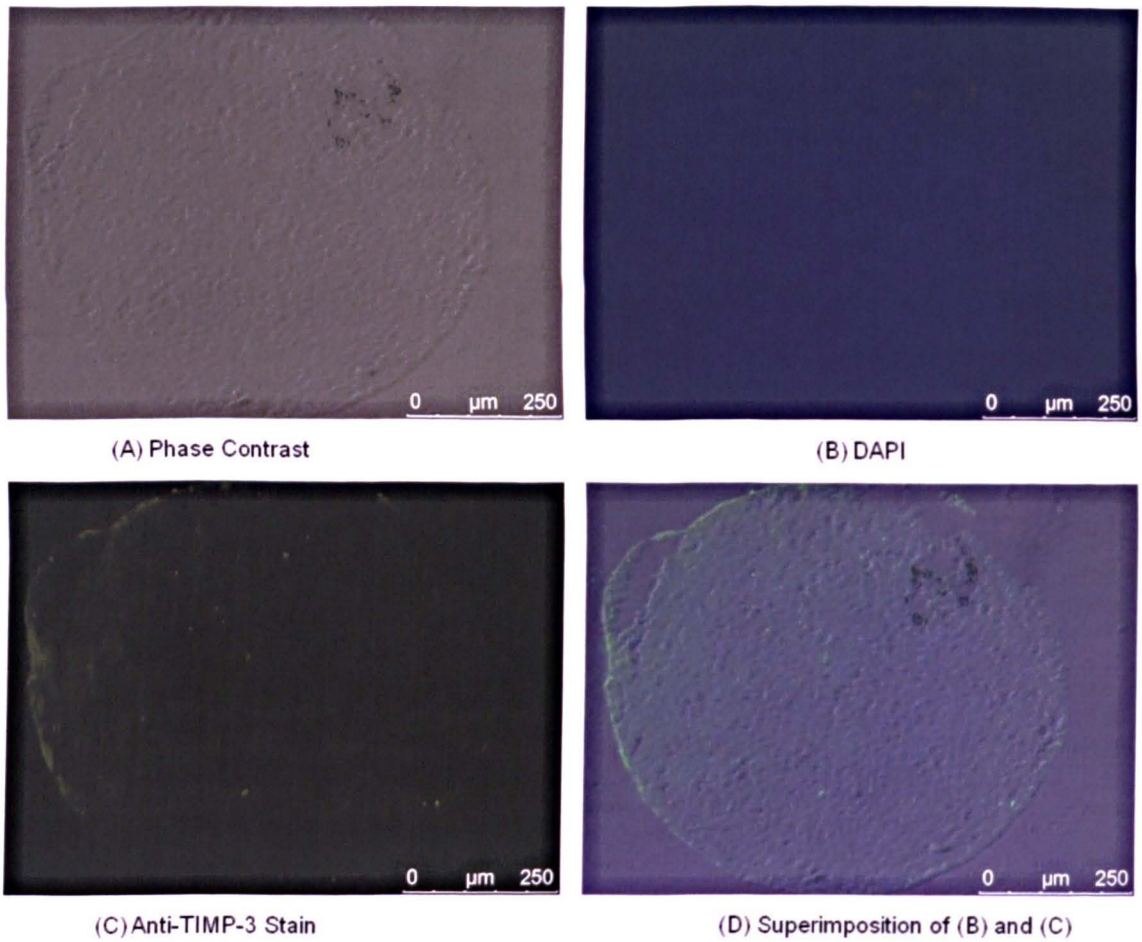

Figure 3.17: Expression of TIMP-3 in Normal Liver

The above sample tissues had been previously formalin-fixed onto glass slides and were stained first with mouse anti-TIMP-3 antibody and then with secondary fluorescent alexa-fluor-488-tagged anti-mouse antibody as described in Section 2.17. (A) shows the phase contrast image of the fixed normal liver (B) is the nuclei staining with DAPI, (C) is the green fluorescence image for TIMP-3 staining and (D) is the superimposition of images (B) and (C). There was virtually no staining for TIMP-3 in both the cytoplasm and extracellular components of the tissue. Images were obtained using a fluorescence microscope and its 20X objective.

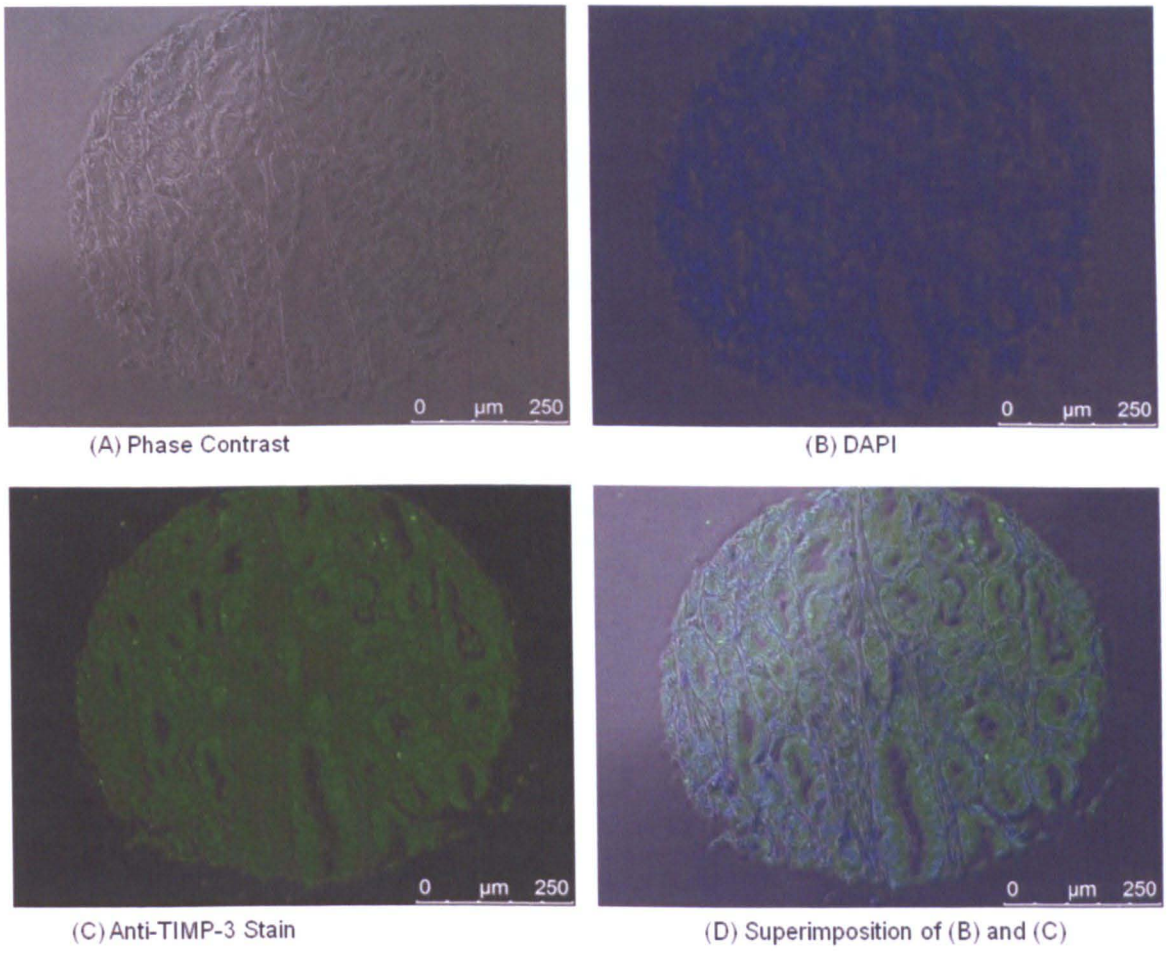

Figure 3.18: TIMP-3 Antibody Probing of Prostate Tissue Sample with GS of 4.
The above sample tissues had been previously formalin-fixed onto glass slides and were stained first with mouse anti-TIMP-3 antibody and then with secondary fluorescent alexa-fluor-488-tagged anti-mouse antibody as described in Section 2.17. (A) shows the phase contrast image of the fixed primary prostate tissue with a GS of 4, (B) is the nuclei staining with DAPI, (C) is the green fluorescence image for TIMP-3 staining and (D) is the superimposition of images (B) and (C). There was detection of staining for TIMP-3 in both the cytoplasm and extracellular components of the tissue as indicated by the green staining in (D). Images were obtained using a fluorescence microscope and its 20X objective.

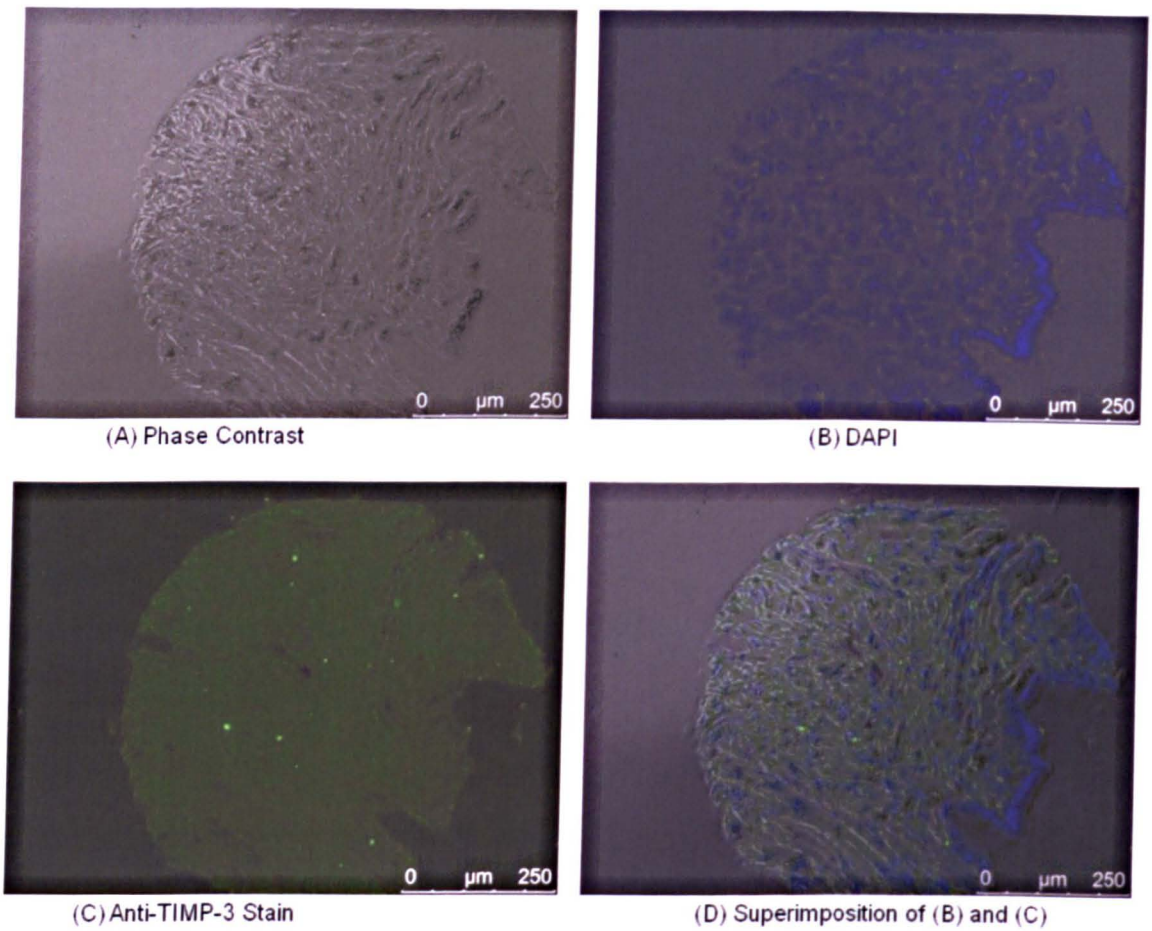

Figure 3.19: TIMP-3 Antibody Probing of Prostate Tissue Sample with GS of 7.
The above sample tissues had been previously formalin-fixed onto glass slides and were stained first with mouse anti-TIMP-3 antibody and then with secondary fluorescent alexa-fluor-488-tagged anti-mouse antibody as described in Section 2.17. (A) shows the phase contrast image of the fixed primary prostate tissue with a GS of 7, (B) is the nuclei staining with DAPI, (C) is the green fluorescence image for TIMP-3 staining and (D) is the superimposition of images (B) and (C). Some staining for TIMP-3 in both the cytoplasm and extracellular components of the tissue as indicated by the green staining in (D). Images were obtained using a fluorescence microscope and its 20X objective.

3.2.5 Changes in TIMP-3 Expression in Co-cultured Cells

Stromal cells PCAF and WPMY-1 were co-cultured with androgen-dependent GFP-transfected LNCaP cells after labelling the stromal cells with a fluorescent dye; PKH26 (as described in Section 2.1.5). The co-cultures were maintained for 48 hours after which FACS was carried out to separate the cells into red stromal cells (PCAF and WPMY-1) and green LNCaP cells (see Section 2.14). The separated cells were then analysed by qPCR for changes in TIMP-3 mRNA expression (see Section 2.6) or by SDS-PAGE and western blotting (see Sections 2.10 and 2.11) for changes in protein expression. The rationale behind the co-culture experiments was that cell-cell contact or cell-derived soluble factors may modulate the expression of TIMP-3 in individual cell cultures and may influence the migratory and invasive pattern of the cancer cells *in vivo*.

Figure 3.20 shows images of cells co-habiting in the same wells and expressing their fluorescent tags; 48 hours was enough time for the cells to settle in the wells and establish cell-cell contact.

Figure 3.21 shows the scatter of co-cultured cells and the separation into different populations by FACS sorting. Only green fluorescent LNCaP cells and only red fluorescent stromal cells were collected from the technicians for further analyses. Cells that did not, or had lost their fluorescence, were excluded from analyses as there was no way to verify their cell type. As a control, mono-cultured cells were also subject to FACS sorting to ensure that there were no other variables between mono-cultured and co-cultured cells other than the fact that the latter had been in contact with another cell type.

Figure 3.22 shows the expression of TIMP-3 mRNA in cells pre- and post-co-culture. Total RNA was extracted from the cells immediately after cell sorting and timp-3 mRNA expression analysed by qPCR. Relative expression of timp-3 mRNA in cells post-sorting was normalised to expression levels in mono-cultured cells. There was an increase in TIMP-3 mRNA expression in both PCAF ($p=0.027$, Mann-Whitney) and WPMY-1 ($p=0.026$, Mann-Whitney) cells 48 hours after culturing with LNCaP cells. In contrast, the relatively low expression of TIMP-3 mRNA in LNCaP cells (see Section 3.1) was lost after co-culture with PCAF cells ($p=0.029$, Mann-Whitney) and after co-culture with WPMY-1 cells ($p=0.05$, Mann-Whitney).

Figure 3.23 shows a representative C_T plot for the data shown in Figure 3.22. Blue curves represent TIMP-3 mRNA expression in mono-cultured cells and green curves represent

TIMP-3 mRNA expression in co-cultured cells. A shift to the right of the plot indicates higher C_T, which is indicative of lower gene expression while a shift to the left of the plot indicates lower C_T and higher gene expression.

Figure 3.24 shows the changes in expression of TIMP-3 in the ECM made by co-cultured cells in comparison to ECM made by mono-cultured cells. Densitometric analyses of the protein blots showed an increase in TIMP-3 expression in ECM from both co-cultured WPMY-1 and PCAF cells when compared to ECM from mono-cultured cells. TIMP-3 was not detected in the lysate from LNCaP cells.

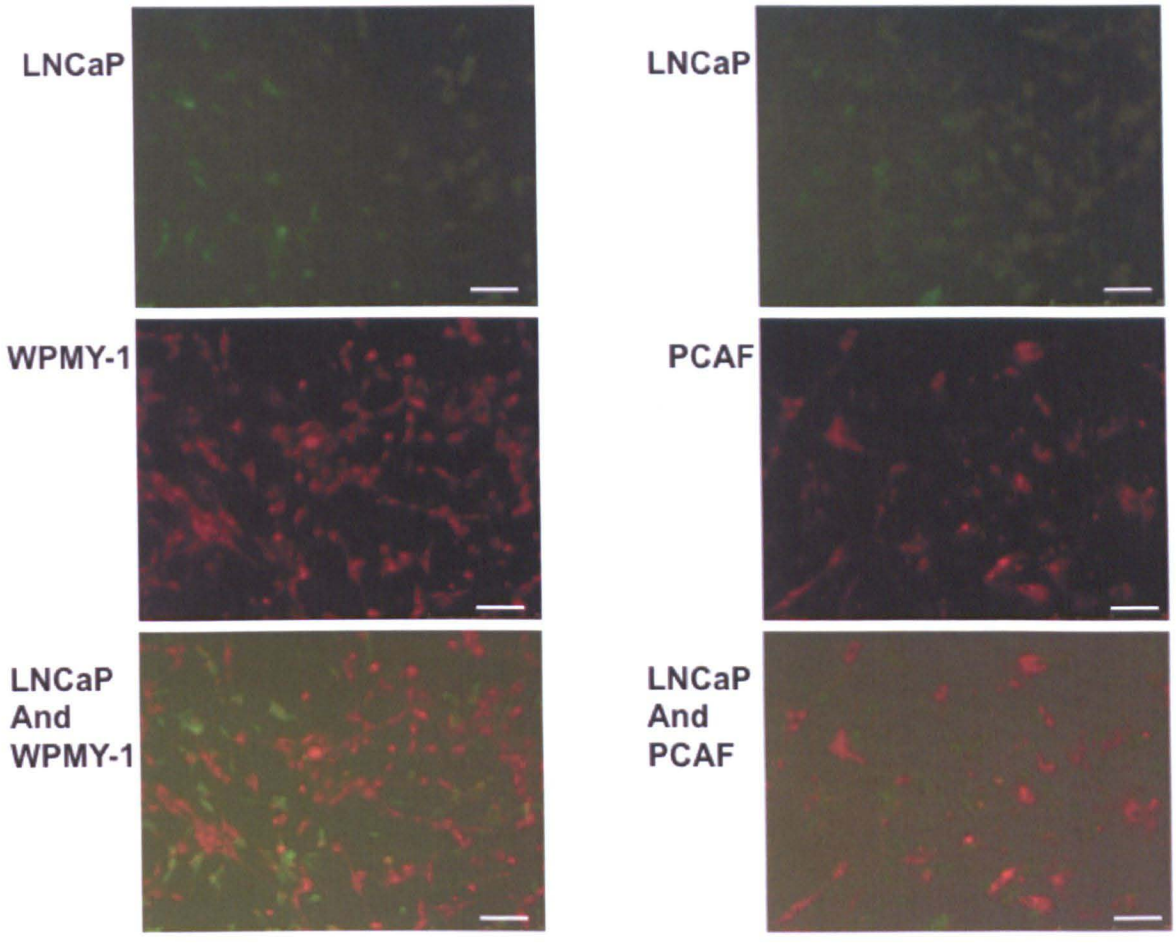

Figure 3.20: Co-cultured prostate stromal and cancer cells.
1 x 10^5 GFP-expressing LNCaP cells were co-cultured with 1 x 10^5 PKH26-labelled PCAF or 1 x 10^5 PKH26-labelled WPMY-1 cells for 48 hours at 37°C/5% CO_2 (see Section 2.1.5). The images were taken with an inverted fluorescence microscope at 10X objective. Scale bar = 100 um.

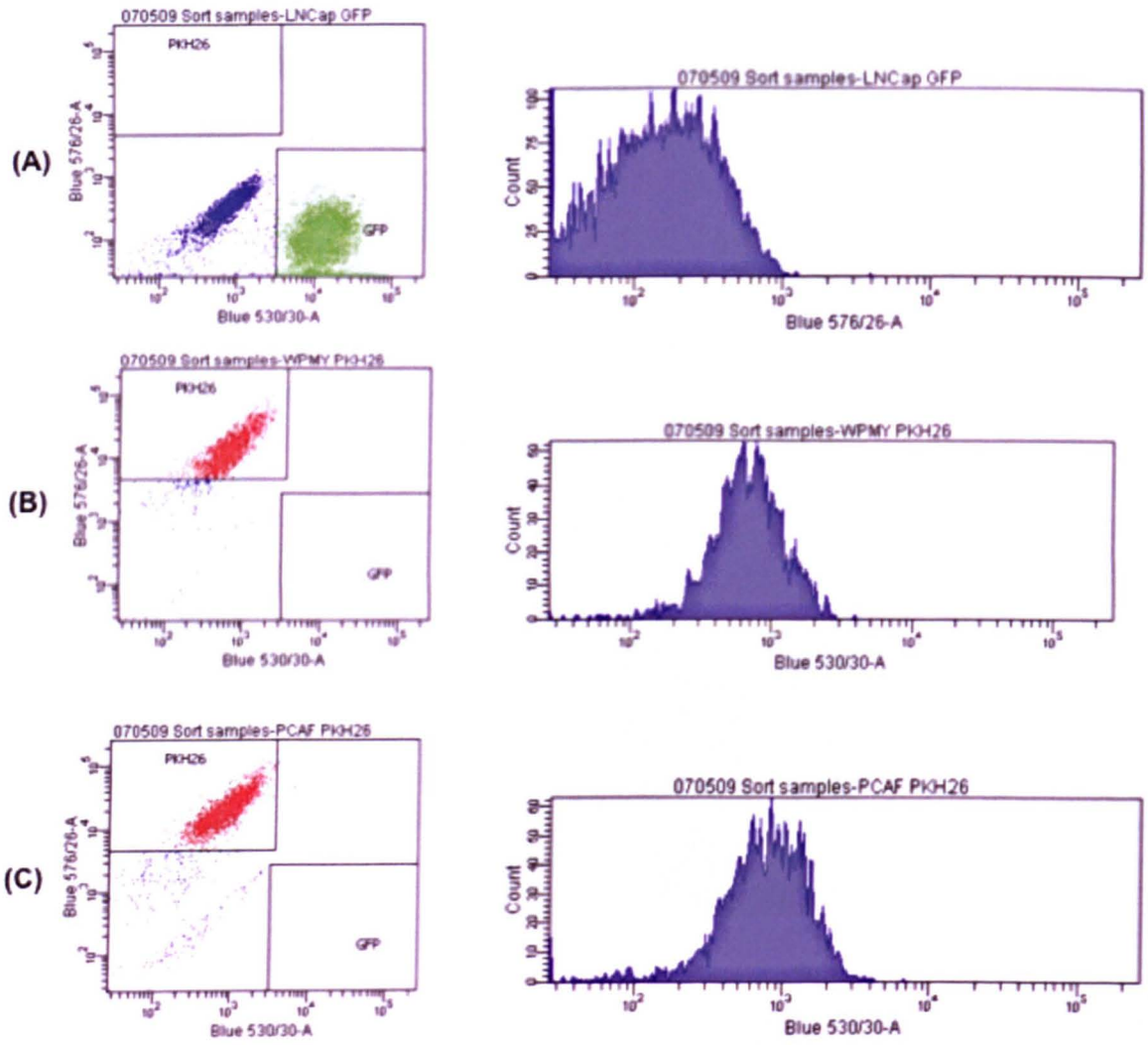
(A)
070509 Sort samples-LNCap GFP
PKH26
GFP
Blue 576/26-A
Blue 530/30-A
070509 Sort samples-LNCap GFP
Count
Blue 576/26-A
(B)
070509 Sort samples-WPMY PKH26
PKH26
GFP
Blue 576/26-A
Blue 530/30-A
070509 Sort samples-WPMY PKH26
Count
Blue 530/30-A
(C)
070509 Sort samples-PCAF PKH26
PKH26
GFP
Blue 576/26-A
Blue 530/30-A
070509 Sort samples-PCAF PKH26
Count
Blue 530/30-A

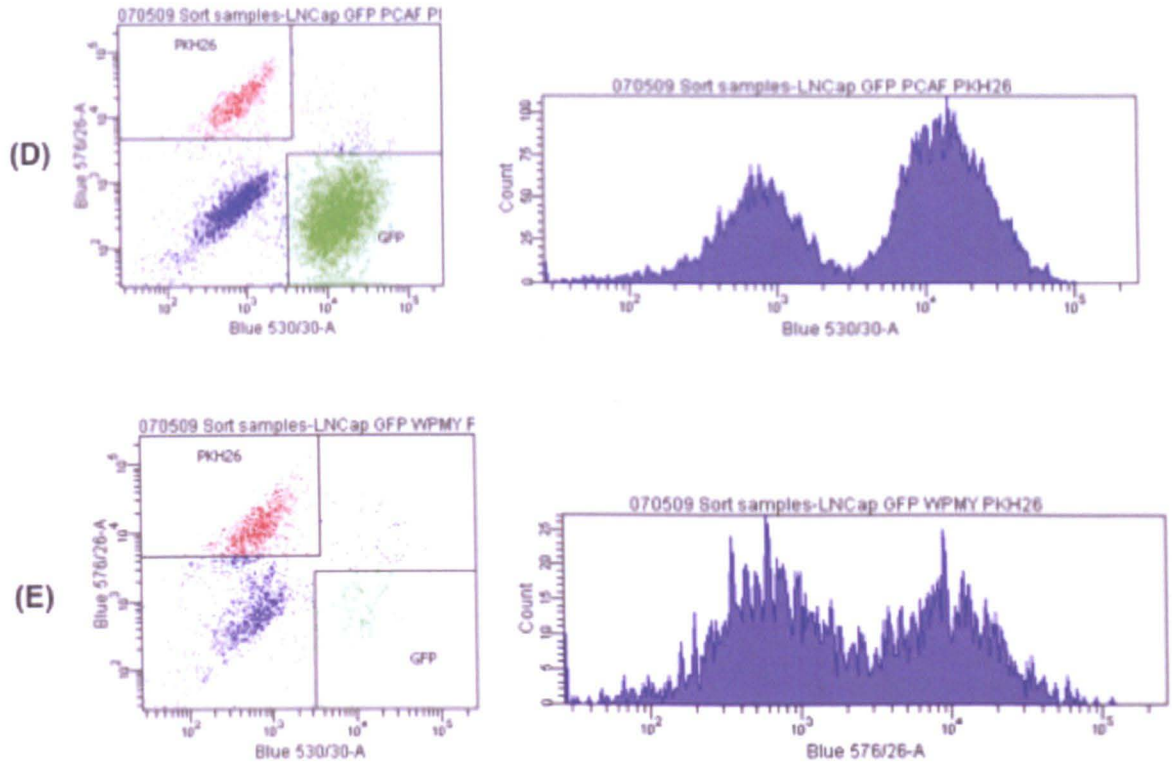

Figure 3.21: FACS sorting results of co-cultured cells.

After the images of cells had been taken, the cells were harvested and suspended in DMEM media with 1% FCS. Cell suspensions were submitted to the FACS technicians for sorting into GFP-positive and PKH26-positive cells.

(A), (B) and (C) are results of sorting of the mono-cultured LNCaP-GFP, PCAF and WPMY-1. (D) and (E) are results of sorting of LNCaP-GFP cells from PCAF and WPMY-1 respectively. As seen on the left hand side of the above representative diagrams, green scatter represents GFP-positive LNCaP-GFP cells and red scatter represents PKH26-positive stromal cells. In the right-hand-side diagrams of (A) – (C), a single population of cells was observed in each case when passing the mono-cultured cells through the FACS sorter, indicating all cells present were fluorescing at the same excitation and emission wavelengths. In (D) and (E), 2 populations of cells were observed, indicating 2 different cell types fluorescing at different excitation and emission wavelengths.

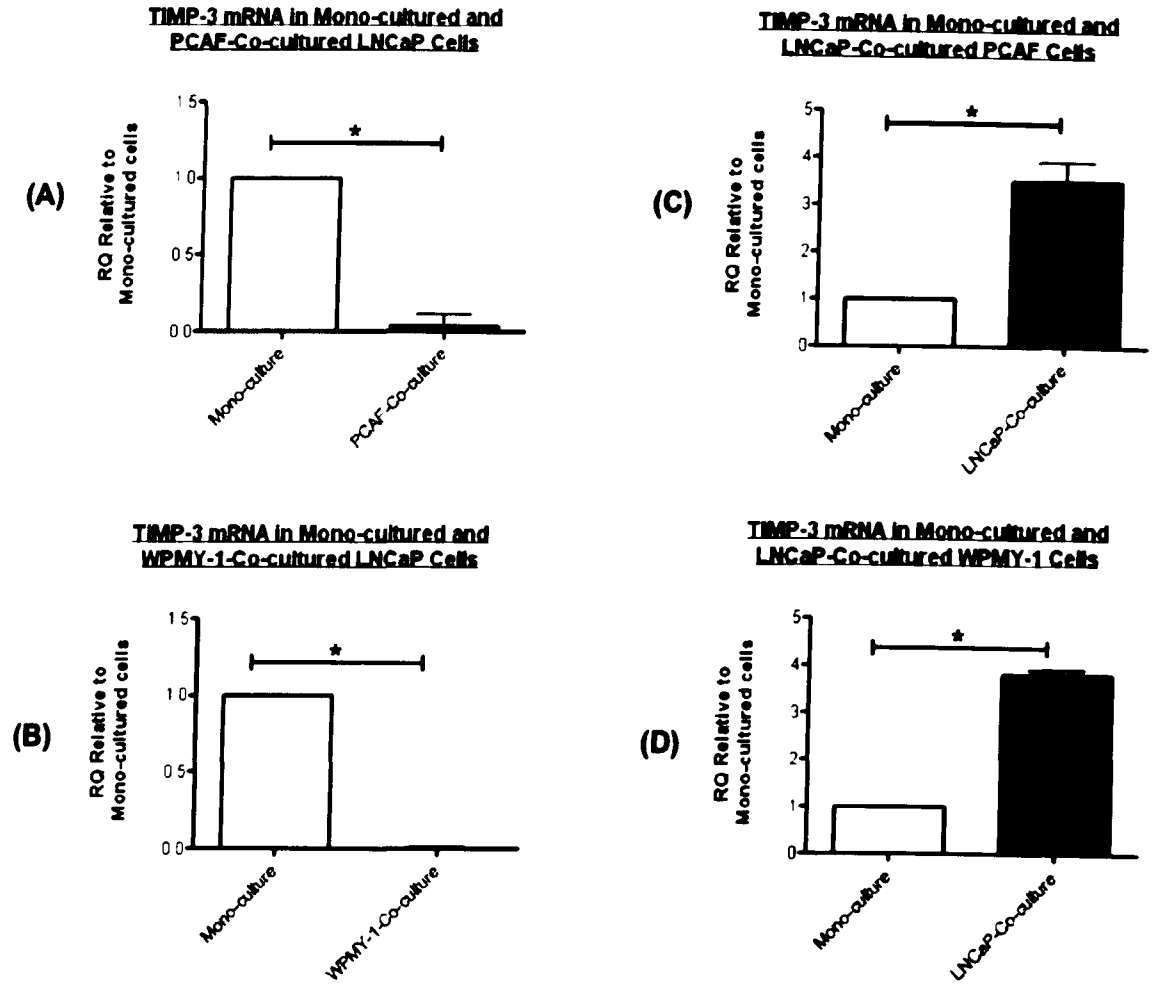

Figure 3.22: Changes in TIMP-3 mRNA expression in co-cultured prostate stromal and cancer cells.

The cells were sorted by FACs then collected and total RNA was extracted from them. cDNA was synthesized and mRNA transcribed as described in Sections 2.6 – 2.8. The data obtained was analysed as described in Section 2.9. All sets of data were analysed relative to data from mono-cultured cells. (n=3).There was a significant decrease in TIMP-3 mRNA in LNCaP cells after co-culture with both PCAF (p=0.029, Mann-Whitney) (A) and WPMY-1 (p=0.05, Mann-Whitney) (B). There was about 3.5-fold higher expression of TIMP-3 mRNA in PCAF cells after co-culture with LNCaP cells (p=0.027, Mann-Whitney) (C) and about 4-fold higher expression in WPMY-1 cells after co-culture with LNCaP (p=0.026, Mann-Whitney) (D).*

(A)

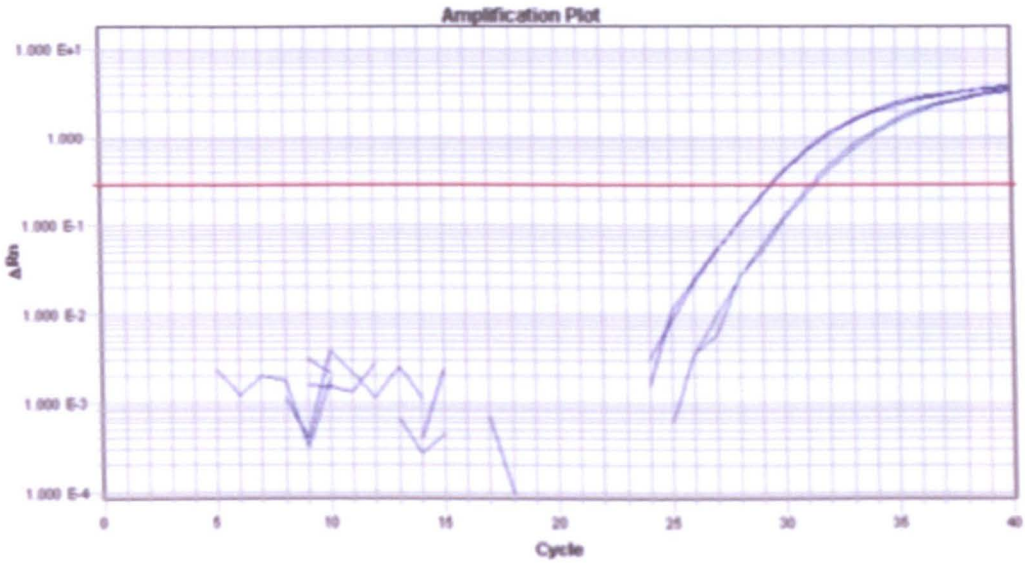
Amplification Plot
1.000 E+1
1.000
1.000 E-1
1.000 E-2
1.000 E-3
1.000 E-4
ΔRn
0
5
10
15
20
25
30
35
40
Cycle

(B)

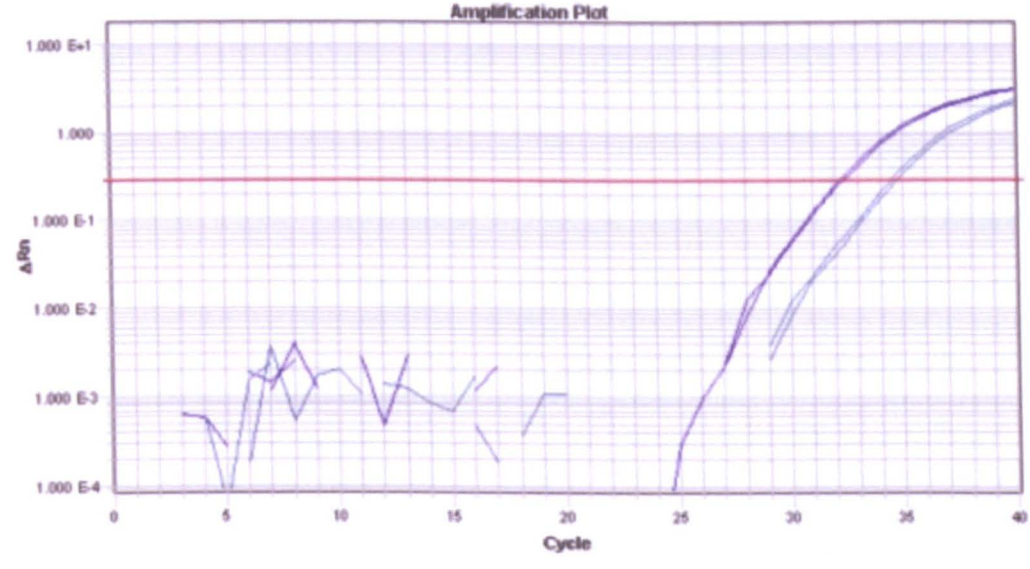
Amplification Plot
1.000 E+1
1.000
1.000 E-1
1.000 E-2
1.000 E-3
1.000 E-4
ΔRn
0
5
10
15
20
25
30
35
40
Cycle

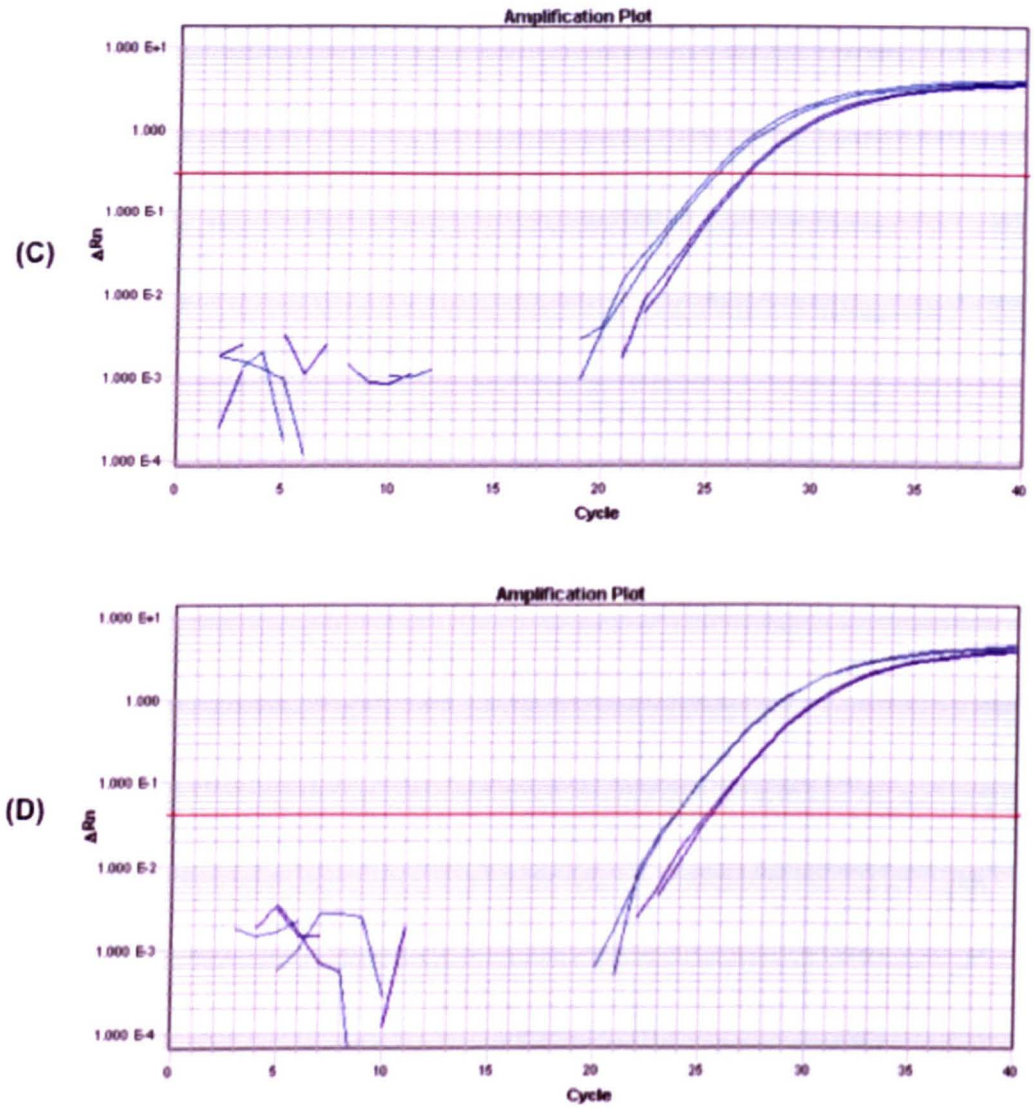

Figure 3.23: Amplification Plot of TIMP-3 mRNA expression in mono-cultured vs. co-cultured prostate stromal and cancer cells.

The graphs labelled A-D are representative diagrams of the amplification of TIMP-3. Both duplicate blue curves represent TIMP-3 mRNA expression in mono-cultured cells and the green curves represent TIMP-3 mRNA expression in co-cultured cells. The cycle at which the curves intersect the threshold (red line) is the C_T for each reaction; the higher the C_T, the more the curve shifts to the right and the lower the expression and vice versa. (A) = changes in TIMP-3 mRNA expression mono-cultured vs. PCAF-co-cultured LNCaP (B) = changes in TIMP-3 mRNA expression mono-cultured vs. WPMY-1-co-cultured LNCaP (C) = changes in TIMP-3 mRNA expression mono-cultured vs. co-cultured PCAF and (D) = changes in TIMP-3 mRNA expression mono-cultured vs. co-cultured WPMY-1. In both A and B, there is a C_T shift to the right of the plot, indicating lower TIMP-3 mRNA expression and in C and D, the C_T shift is to the left, indicating higher TIMP-3 mRNA expression. These results are represented as columns with bars in Figure 3.22.

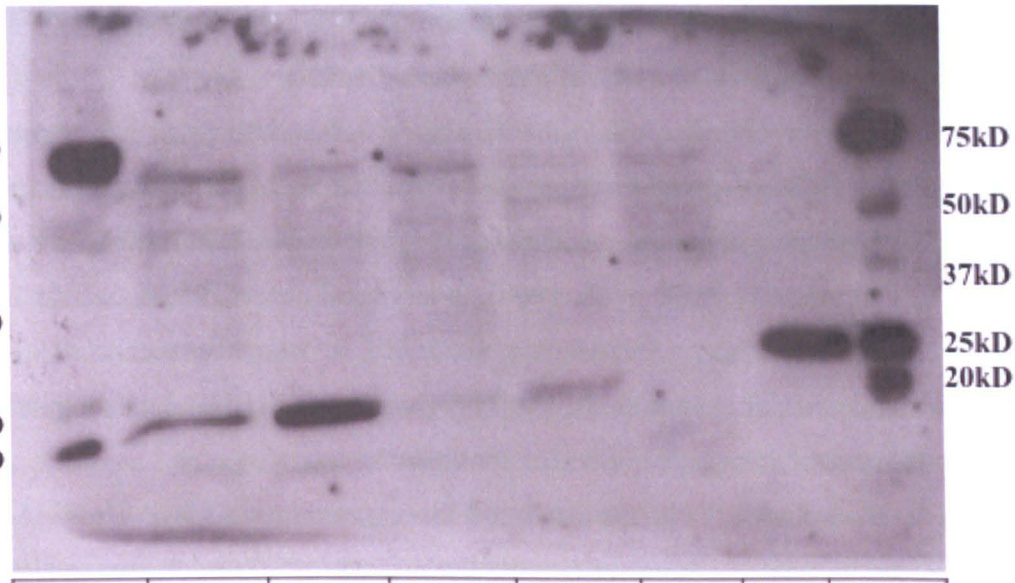

	MWS	EPM	EPC	EWM	EWC	TL	R	MWS
ODmm^2	N/A	1.3	4.7	0.3	0.8	0	6.6	1.3

Figure 3.24: Changes TIMP-3 expression in prostate stromal cells after-co-culture with LNCaP cells.

After 48 hours of either mono-culturing or co-culturing LNCaP cells with PCAF or WPMY-1 cells, they were uplifted using enzyme-free buffer and counted. The ECM laid down by the cells was extracted as described in Section 2.9, using 100 µL of loading buffer. 1 x 10^5 cells' worth of ECM was loaded on the SDS-PAGE, gels run and proteins transferred onto PVDF membrane as described in Section 2.10 – 2.11. Mouse monoclonal anti-TIMP-3 was used for probing the membrane for TIMP-3. MWS = molecular weight standards, EPM = ECM from mono-cultured PCAF, EPC = ECM from co-cultured PCAF, EWM = ECM from mono-cultured WPMY-1 cells. EWC = ECM from co-cultured WPMY-1 cells. TL = Total cell lysate from mono-cultured LNCaP-GFP cells. Optical density (D/A) is in OD mm^2.

3.3 DISCUSSION

To my knowledge, this is the first study demonstrating the expression of TIMP-3 protein in the ECM of prostate cancer cells by western blotting. Other studies have demonstrated expression in breast cancer tissue (Mylona et al., 2006), in stromal cells of squamous cell carcinomas (Airola et al., 1998), in laryngeal cancer (Pietruszewska et al., 2008), in normal CNS white matter (Haddock et al., 2006), in oesophageal cancer (Miyazaki et al., 2004), in endometrial cancer as well as benign endometrial tissue (Tunuguntla et al., 2003) and in hepatocellular carcinoma (Lu et al., 2003).

Other studies have also analysed the expression of TIMP-3 mRNA in different cells and tissue types such as various human prostate cell lines (Karan et al., 2003), in the Bruch's membrane of the eye (Bailey et al., 2001), in normal, neoplastic and hyperplasic endometrium (Maatta et al., 2000), in normal thyrocytes and thyroid carcinoma cell lines (Hofmann et al., 1998), in developing bones, developing kidneys and hair follicles highlighting its importance in foetal development and hair growth cycle (Airola et al., 1998) and in normal colorectal mucosa and colorectal adenocarcinoma (Powe et al., 1997). This highlights the ubiquitous expression of TIMP-3 in nature generally. It is also the first study to show localisation patterns of TIMP-3 in prostate tissue. This is of great importance as it enables the in-depth investigation of the role of this inhibitor in the progression of prostate cancer and raises the possibilities of TIMP-3-targeted therapy for management of the disease.

The results obtained in this study demonstrated a significantly greater TIMP-3 expression mRNA and protein in prostatic stromal cells PCAF, WPMY-1 and BPH45, relative to prostate cancer cells LNCaP and PC3. This correlates with similar findings by Mylona *et al* (Mylona et al., 2006) who showed that TIMP-3 is expressed abundantly in the stromal cells adjacent to the breast tumour, and with studies carried out by Cross *et al* (Cross et al., 2005) showing increased expression of TIMP-3 mRNA in stromal cells BPH31, -33, -44 and –45, relative to the cancer cells PC3 and LNCaP. TIMP-3 is also expressed in cells during foetal development and cancer progression (Airola et al., 1998). Karan *et al* (Karan et al., 2003) also carried out analyses of TIMP-3 expression in prostatic stromal cells, prostatic cancer cells LNCaP-C33 (androgen-dependent) and LNCaP-C81 (androgen independent) - they demonstrated high expression of TIMP-3 in the stromal cells and undetectable expression in the cancer cells LNCaP-C33, LNCaP-C81, MDA PCa 2b,

LNCaP-C51, LNCaP-Pro5, LNCaP-Ln3, LNCaP-C4-2, PC3, and DU145 cells. Riddick *et al* (Riddick et al., 2005) also obtained similar results when analysing the components of prostatic tissue that are associated with prostate cancer. Stromal cells are likely to be important in the control of proteolytic activity due to their increased expression of TIMPs, and as the stromal-epithelial ratio reduces in cancer, this control is less likely to be complete.

It is important to understand how much of TIMP-3 is available in tissue as the disease progresses as it could be a potential marker for prediction of patient outcome. Due to time and financial constraints, the expression of proteinases could not be measured alongside TIMP-3. However, it must be borne in mind that there is homeostasis of proteinase and inhibitors in normal tissue and any modulation in favour of one over the other will lead to altered balance and tissue turnover.

The sequestering of TIMP-3 in the surrounding stroma of many cancers may possibly be a host protective mechanism of preventing tumour migration out of the primary site since more TIMP-3 is available in the stroma to inhibit proteinase-induced degradation of ECM and possibly prevent basement membrane rupture as well. However, analyses of prostate tissue sections (Figures 3.12 – 3.14) demonstrated a reduced expression of TIMP-3 in prostate cancer compared to benign conditions. Thus, the barrier to proteolysis leading to cell migration may be reduced in prostate cancer. The morphology of tissue from prostate cancer samples demonstrated a reduced matrix component in comparison with normal and BPH tissue (Figure 3.11), which may potentially reduce the barrier further.

The results from this project is similar to a study conducted with breast cancer tissue, which showed TIMP-3 staining in both epithelial and stromal compartments of the tissue (Vizoso 2007). The presence of TIMP-3 in the epithelium is contrary to my *in-vitro* findings of higher expression in prostate stromal cells relative to prostate cancer cells (see Section 3.2.2). It is possible that TIMP-3 synthesised by the stromal cells is binding to heparin sulphate proteoglycans in the epithelial compartment, which may be important for its function of inhibiting epithelial-derived metalloproteinases.

Expression of TIMP-3 was very low in the liver marker tissue used as controls for the tissue microarray analyses (Figure 3.17). This is in line with the study by Su *et al* which showed several fold higher expression of TIMP-3 mRNA in prostate tissues in comparison to liver tissue (see Figure 3.1 and 3.3).

The apparent inverse correlation of TIMP-3 expression with GS seen in Figs. 3.18 and 3.19 suggests that the loss of TIMP-3 may result in poorer prognosis and may even encourage disease progression. This finding is in line with studies by Vizoso et al (Vizoso et al., 2007) which showed higher expression of TIMP-3 in ER-positive breast tissue obtained from patients with no metastasis (early stage breast cancer) compared to ER-negative tissues from patients with metastasis (late stage breast cancer). Another study on breast cancer showed higher expression of TIMP-3 in the stromal cells and mononuclear inflammatory cells of the ductal carcinoma (early stage invasive breast cancer) when compared to expression in the distal lobular and medullar carcinomas (late stage invasive breast cancer) (del Casar et al., 2010)

All these results suggest that TIMP-3 may be of use in predicting patient survival. This is buttressed by the results from a study in 2007 (Hilska) which reported strong staining for TIMP-3 in tissues obtained from rectal cancer patients with higher mean survival time and earlier Duke's rectal cancer stage. In another study on breast cancer by Del Casar *et al* (Del Casar et al., 2009) the expression of TIMP-3 was reported to be higher in stromal fibroblasts obtained from within the breast tumour in comparison with fibroblasts obtained from the invasive front of breast cancer. They concluded that higher expression of TIMP-3 was indicative of lower metastasis and *vice versa* and is predictive of more favourable prognosis.

Lower expression of TIMP-3 in cancer has also been reported in breast cancer tissue of an aggressive phenotype – there was lower expression of TIMP-3 and this correlated with high nuclear and histological grading of the tissue (Mylona et al., 2006). Also, TIMP-3 expression has been correlated with oesophageal squamous cell carcinoma invasion and metastasis – immunohistochemical analyses of the carcinoma tissue showed reduced TIMP-3 expression in tumours with higher depth of invasion and patients with lower tissue expression of TIMP-3 had lower survival rates and *vice versa* (Miyazaki et al., 2004).

An interesting and novel finding of my experiments was the apparent up-regulation of TIMP-3 expression both at mRNA transcript and protein level, in stromal fibroblasts following co-culture with tumour epithelial cells. Here, both normal stromal fibroblasts, WPMY-1 and prostatic carcinoma-associated fibroblasts, PCAF, had increased TIMP-3 expression 48 hours after they had been cultured with prostate cancer cells LNCaP (see Figures 3.22 and 3.23). Other studies have demonstrated an increase in TIMP-3 mRNA

expression in stromal fibroblasts adjacent to head and neck cancer patients' tissue samples in comparison with fibroblasts adjacent to normal epithelia (Kornfeld et al., 2011). Also, cancer cells co-migrate with stromal fibroblasts from their primary site of origin to distal organs where they form niches and co-habitate synergistically, with the fibroblasts producing growth factors that enable the cancer cells to home properly and proliferate in this secondary site (Kaminski et al., 2006).

TIMP-3 in the tissue of prostate cancer and other cancers plays a major role in the inhibition of many proteinases, and inhibits angiogenesis, both of which may contribute to the inhibition of cancer growth and metastasis. The molecule may prove a useful diagnostic tool for prediction of patient survival, disease progression and may enable targeted therapeutics for patients with prostate cancer as well as other cancers

In conclusion, this study showed higher expression of TIMP-3 in prostate stromal cells and tissues relative to the prostate cancer cells and tissue as well as an increase in TIMP-3 expression in the stromal cells upon contact with cancer cells. To further understand the impact of this interaction on disease progression, further experiments were designed to investigate changes in expression of TIMP-3 and these are described in subsequent chapters.

CHAPTER 4: MODULATION OF TIMP-3 BY ANDROGEN AND CYTOKINES

4.1 INTRODUCTION

Androgens are steroid hormones that regulate the growth of the prostate and male fertility and they function by binding to androgen receptors (AR) to initiate a signalling cascade that tightly regulates the development of the male sexual organs (Hovenanian and Deming, 1948, Yang et al., 2005). In men, the most important form of androgen is testosterone – this is a circulating androgen that is secreted by Leydig cells found in the testes (Burnstein, 2005). Testosterone is converted by 5-alpha-reductase, into a highly reactive form called dihydrotestosterone (DHT). DHT translocates into the cytoplasm and binds to the androgen receptor via displacement of AR-bound heat shock proteins (HSP) (Brinkmann et al., 1999). The DHT-AR complex becomes dimerized and this results in AR phosphorylation. This phosphorylated complex translocates into the cells' nuclei where they bind to androgen response elements (ARE) in the promoter region of androgen-regulated genes. Once the binding of dimerized AR to AREs occurs, there is a mobilisation of transcription co-regulators to the complex, resulting in the formation of a transcription complex and initiation of the androgen-regulated genes (Gobinet et al., 2002). These genes are essential to the normal growth and development of the prostate. Some of the androgen-regulated genes include prostate specific antigen (KLK-3/PSA), prostate specific membrane antigen (PSMA), kallikrein-2 (hK-2), to mention a few (Xu et al., 2001, Ngan et al., 2009). A schematic representation of the AR signalling pathway is represented in Figure 4.1.

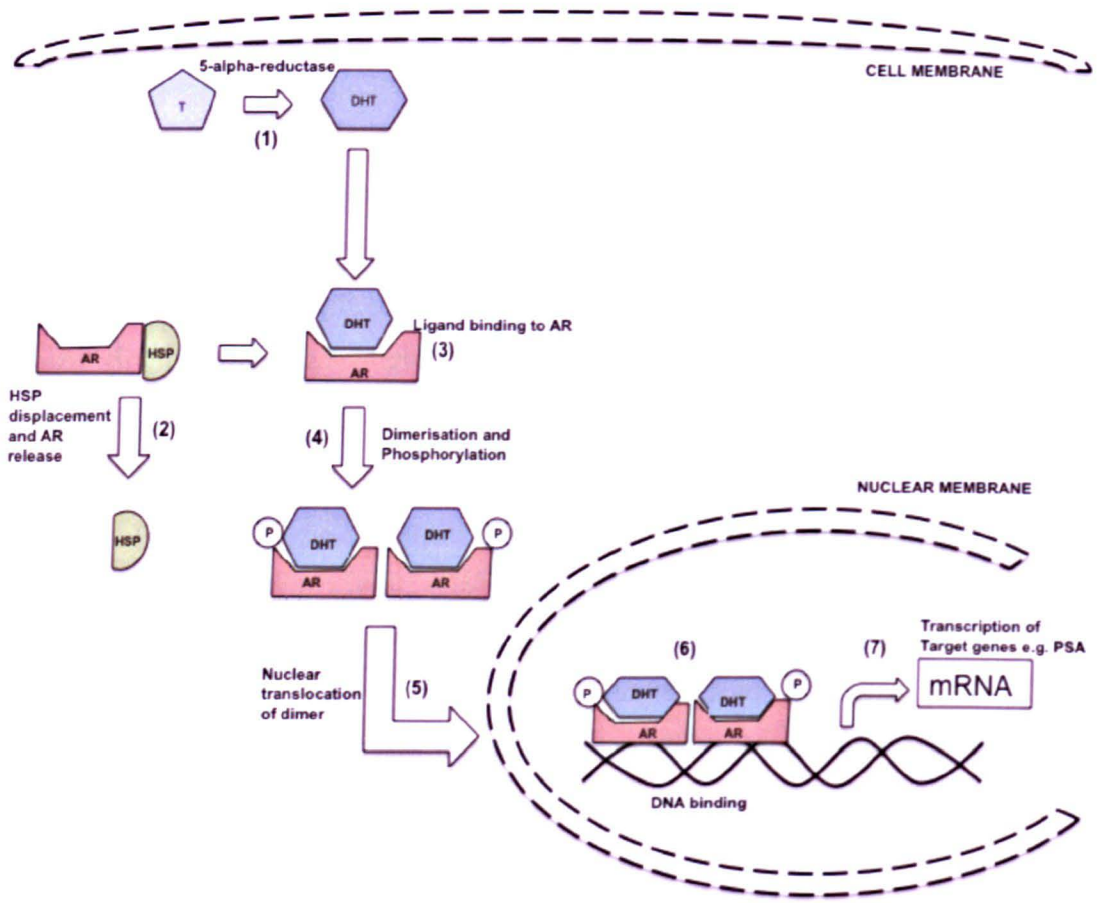

Figure 4.1: DHT Signalling in Prostate Cells.

The above diagram is a schematic representation of DHT signalling cascade in cells. Firstly, soluble circulating testosterone is translocated into the cell via the cell membrane where it is converted into dihydrotestosterone (DHT) by 5-alpha reductase enzyme (1) (Celotti et al., 1991). Binding of DHT to the latent androgen receptor (AR) results in the displacement of heat shock proteins (HSP) from the AR, activation of the DHT-AR complex and subsequent phosphorylation of bound AR. This is followed by dimerization of bound AR (2,3 & 4) (Nazareth and Weigel, 1996). The dimer complex is translocated into the nucleus (5) where it is capable of binding to androgen response elements located on the promoter regions of the DNA sequence of target genes (6), initiating the transcription of target genes such as PSA (7) (Lindzey et al., 1994).

Several mutations have been reported in the AR of prostate cancer patients. This results in the loss of specificity of the AR to androgen, thereby converting it into a promiscuous receptor that will become activated upon binding of other steroids like oestrogen (Yeh et al., 1998) and even anti-androgens like flutamide or making the AR more responsive to DHT (Taplin et al., 2003). There is a point mutation in the AR in the LNCaP cell line, – this mutation is at codon 877 (change of threonine to alanine) located in the ligand-binding domain of the AR and it results in promiscuity of the AR in LNCaP cells (Suzuki et al., 1996, Gaddipati et al., 1994, Suzuki et al., 1993). On the other hand, the PC3 cell line has been reported to have no AR and hence is no longer dependent on androgen for growth and survival. Insertion of the androgen receptor back into the PC3 cells led to androgen-dependence for their growth once again (Yu et al., 2009, Marcelli et al., 1995). This loss of AR expression has been reported in some hormone-refractive prostate cancer patients (Heinlein and Chang, 2004).

Tumours are generally hypoxic, consisting of a highly metabolically active dense population of cells, which causes a local shortage of available oxygen (Phillips, 1998) (Wijffels et al., 2008). The occurrence of tumours results in the initiation of an inflammatory response at the primary site, leading to recruitment of macrophages and subsequent release of cytokines (Murdoch and Lewis, 2005, Murdoch et al., 2004).

Cytokines are secreted proteins that are produced by immune cells, and other cell types such as endothelial cells, epithelial cells and fibroblasts. They function primarily by modulating cellular activities that mediate the inflammatory response and are involved in growth, proliferation, differentiation, survival and apoptosis (Rakesh and Agrawal, 2005, Lentzsch et al., 2004, Benczik and Gaffen, 2004, Klein, 1997). There are different types of cytokines such as interleukins, lymphokines, interferons, colony-stimulating factors, chemokines, polypeptide growth factors and stress proteins. These different types of cytokines have various functions that have independent signalling pathways or inter-related pathways, all of which regulate cellular behaviour and can be grouped as pro-inflammatory or anti-inflammatory cytokines (Roitt I.M. and P.J., 2001).

TNF is implicated in diseases such as rheumatoid arthritis and osteoarthritis (Zangerle et al., 1992), both of which are degenerative diseases of the skeletal system. Membrane-bound pro-TNF is cleaved by a disintegrin and metalloproteinase 17 (ADAM 17) also known as

TNF-alpha-converting enzyme (TACE). This results in the formation of soluble TNF (Black et al., 1997, Moss et al., 1997b).

TNF binds to the extracellular domain of the TNF receptor 1 (TNFR1) - this binding initiates recruitment of an adaptor protein; Tumour necrosis factor receptor type 1-associated DEATH domain protein (TRADD) by the intracellular domain of TNFR1 (Hsu et al., 1995). TRADD recruits TNF receptor associated factor 2 protein (TRAF2) and receptor-interacting serine/threonine protein kinase 1 (RIP) forming a TRADD+TRAF2+RIP complex. This complex subsequently recruits inhibitor of kappa B kinase enzyme complex (IKB). NF-κB is a transcription factor that initiates the transcription of genes involved in regulating the inflammatory response, cell proliferation as well as transcription of anti-apoptotic factors (Roitt I.M. and P.J., 2001). IkB is bound to NF-κB in the cytoplasm. When IkB is inactivated by phosphorylation it leaves nuclear factor kappa enhancer of activated B cells (NF-κB) free to translocate to the nucleus (Baker and Reddy, 1996, Hsu et al., 1996). The complex (TRADD+TRAF2+RIP) can also activate the mitogen-activated protein kinase (MAPK) pathway and initiate transcription of pro-apoptotic factors and genes involved in cell differentiation (Holvoet et al., 2003).

As an alternate pathway, TRADD can also bind to an adaptor protein known as fas-associated protein with death domain (FADD), which binds to caspase 8 - this reaction leads to the activation of caspase 3 and formation of the death inducing signalling complex and subsequent cell apoptosis (Hsu et al., 1996). A schematic diagram summarising the TNF signalling pathways is represented in Figure 4.2.

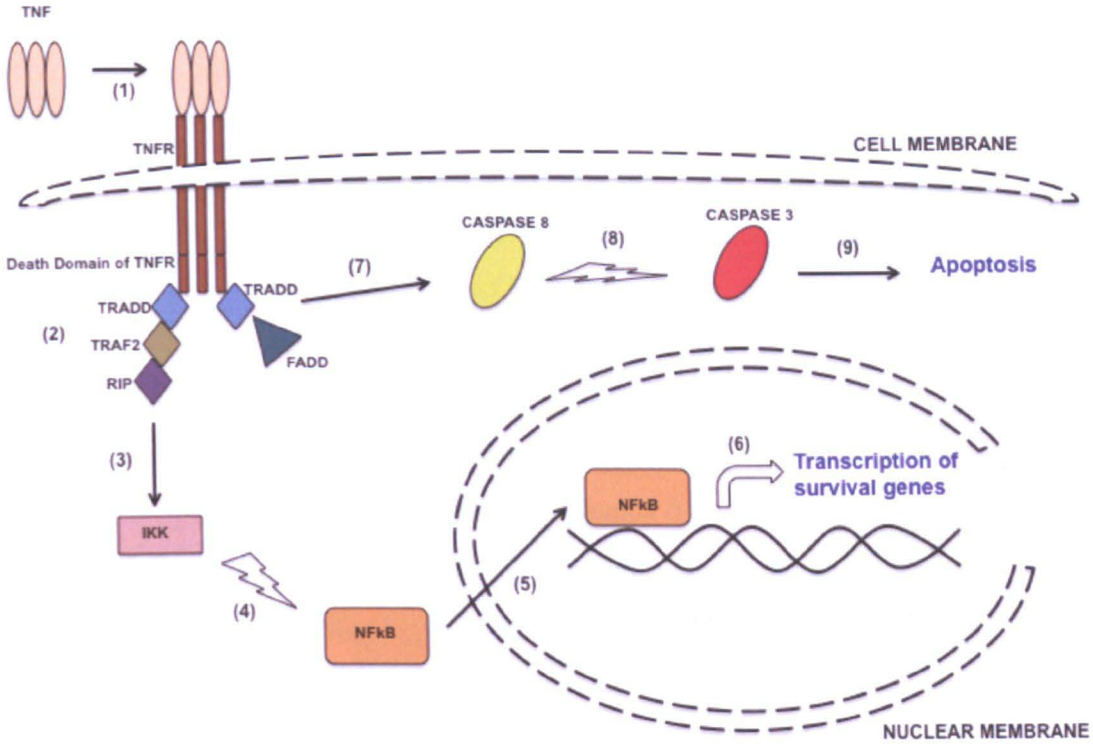

Figure 4.2: TNF Signalling Pathway in Cells.

The above diagram is a schematic representation of the TNF signalling pathway in cells. Soluble trimerised TNF binds to the extracellular domain of TNFR1 (1) and initiates the recruitment of the TRADD+TRAF2+RIP complex by the intracellular death domain of TNFR1 (2). The complex binds to IKK (3), which activates NF-κB (4) and results in its nuclear translocation (5). NF-κB binds to the promoter region of survival genes to initiate their transcription (6). Alternatively, the intracellular death domain of the TNFR1 can initiate the recruitment of a TRADD+FADD complex which binds to caspase 8 (7) and initiates caspase 3 (8), therefore leading to the formation of the death inducing signalling complex and subsequent apoptosis of cells (9).

Transforming growth factors (TGF) are also secreted cytokines belonging to the polypeptide growth factor class of cytokines, which includes activins and bone morphogenic proteins. They are multi-functional cytokines and consist of two members; TGF-α and TGF-β (Wahl, 1992). In particular, TGF-β regulates cell adhesion (Han et al., 1993, Ogata et al., 2007), cell differentiation (Moustakas et al., 2002, Bouche et al., 2000, Sells Galvin et al., 1999) and ECM turnover by increasing the production of ECM proteins (Ballock et al., 1993, Risinger et al., 2010, Chen et al., 2003), and decreasing the production of matrix-degrading proteases (Risinger et al., 2010, Chen et al., 2003) and increasing the production of inhibitors of matrix-degrading proteases (Wu et al., 2000).

In the canonical TGF-β signalling pathway, the ligand, TGF-β, binds to its trans-membrane serine-threonine kinase receptor 2 (TGFβRII) - the bound TGFβRII activates and phosphorylates TGFβRI. Activated TGFβRI then phosphorylates intracellular proteins SMAD 2 and SMAD 3 and subsequently forms a trimeric complex with SMAD 4. The SMAD2+SMAD3+SMAD4 complex translocates and accumulates in the nucleus to activate the transcription of its target genes (Ogata et al., 1997, Roitt I.M. and P.J., 2001). A schematic representation summarising the TGF-β signalling pathway is represented in Figure 4.3.

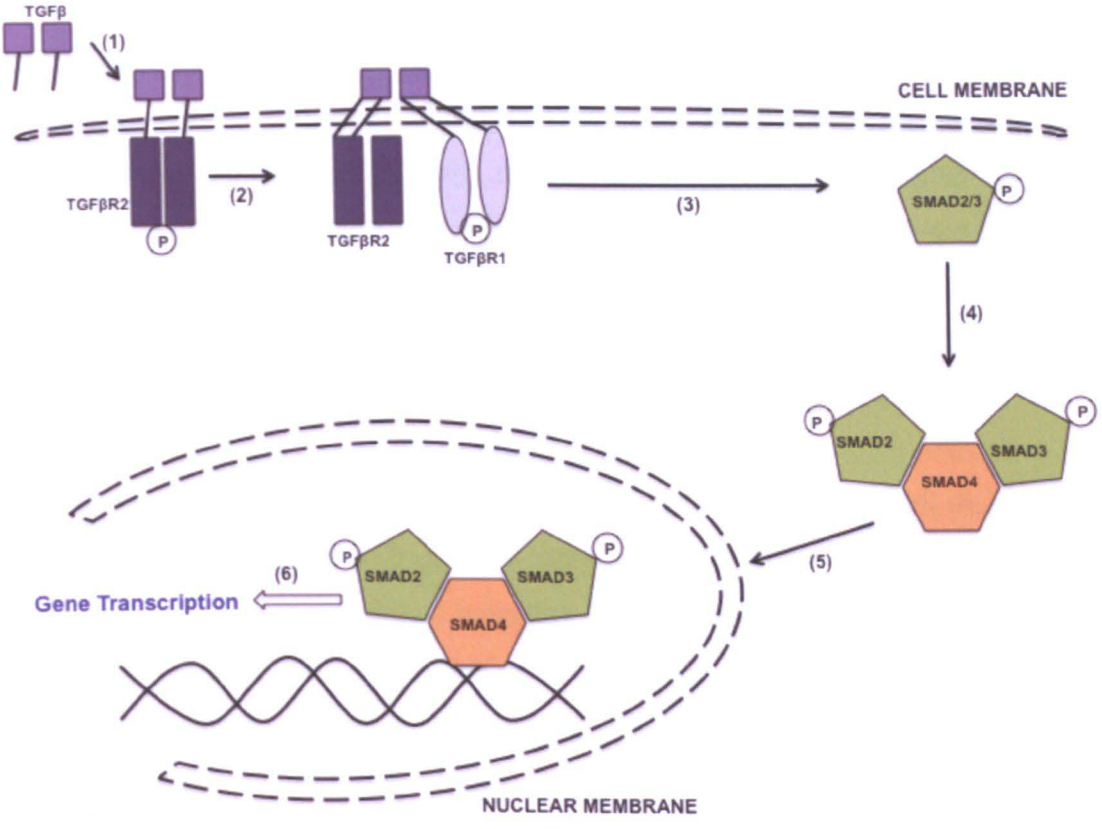

Figure 4.3: TGFβ Signalling in Cells.

The above diagram is a schematic representation of the TGF-β signalling pathway via the TGF-β receptors. TGF-β binds to its trans-membrane receptor TGF-βR2 (1) leading to an activation of a signalling cascade and phosphorylation of TGF-βR1 (2) and subsequent TGF-β receptor-mediated phosphorylation of SMAD2 and SMAD3 (3). The phosphorylated SMAD2 and SMAD3 form a trimeric complex with SMAD4 (4) and the SMAD2+SMAD3+SMAD4 complex translocates into the nucleus (5) where it binds to the promoter regions of the DNA of target genes (6) (Ogata et al., 1997).

There is an interaction between TNF-α and TGF-β signalling pathways and subsequent regulation of one by the other. For instance, TGF-β-mediated ECM deposition is inhibited by TNF-α. This is mediated by the degradation of ECM proteins such as collagen and proteoglycans by proteases recruited as a result of TNF-α signalling (Hui et al., 2001, Knittel et al., 1999, Lee and Rannels, 1998). The relationship between these two cytokines plays an important role in initiation and progression of cancers and therefore genes regulated by any of these signalling pathways may be modulated and cellular homeostasis altered, ultimately resulting in the absence of regulation of cellular growth, leading to cancer.

In this project, the role played by androgens, growth factors and cytokines in the regulation of TIMP-3 expression in prostate cancer cells was explored. Prostatic cells were treated with DHT, TNF-α and TGF-β, followed by measurement of TIMP-3 expression levels.

4.2 RESULTS

4.2.1 Regulation of TIMP-3 mRNA by DHT in Prostate Cells

The stimulation of LNCaP cells with varying doses of DHT as well as flutamide and combinations of DHT plus flutamide, resulted in a significant dose-dependent down-regulation of TIMP-3 mRNA by DHT. This effect was dose-dependent to the highest concentration tested of 10nM. There was no effect of the androgen receptor antagonist flutamide on the expression levels of TIMP-3 mRNA at 100-fold higher concentrations than the highest dose of DHT used, and no significant effect seen when treated alongside DHT i.e. 1000nM flutamide alone or 1000nM flutamide + 10nM DHT (see Figure 4.4).

PSA mRNA increased in a dose-dependent manner in the LNCaP cells, with the greatest effect observed when cells were treated with 10nM DHT. This observation confirmed the known activity of DHT in primary prostate cancer cells (Miniati et al., 1996). As with the effect on TIMP-3 mRNA expression, flutamide did not inhibit PSA mRNA expression (see Figure 4.5). This finding is counter-intuitive as flutamide is clinically prescribed to patients with androgen-insensitive prostate cancer as a therapeutic agent for management of disease progression (Narimoto et al., 2010, Greenway, 1998, Eisenberger et al., 1998, Higano et al., 1996). However, this result is explained by the AR mutation in LNCaP cells, which enable constitutive activation of the AR and subsequent pathway activation regardless of the levels of PSA present (Gaddipati et al., 1994, Suzuki et al., 1993)

TIMP-3 mRNA expression was eliminated in PC3 cells after treatment with DHT, the effect of which was not reversed by flutamide (see Figure 4.6) and PSA mRNA was hardly detected in the PC3 cells (results not shown). It must be borne in mind, though, that PC3 cells produce only very small amounts of TIMP-3 mRNA (see Section 3.2).

TIMP-3 mRNA expression was not significantly different from the control experiments in stromal cells BPH45, PCAF and WPMY-1 after treatment with DHT and there was also no modulation of TIMP-3 mRNA expression by flutamide alone or flutamide and DHT in treated BPH45, PCAF and WPMY-1 cells (see Figures 4.7, 4.8 and 4.9 respectively). These results suggest that modulation of TIMP-3 mRNA by DHT occurs in the prostate carcinoma cells but not in the stromal cells.

Due to limited time and resources and previous results that showed negligible levels of TIMP-3 in the ECM made by LNCaP cells (see Section 3.2), it was not possible to corroborate expression changes seen in LNCaP mRNA by western blotting. Also, as there

were no significant changes in TIMP-3 mRNA expression mediated by DHT in the stromal cells, the TIMP-3 protein expression in these cells was not analysed.

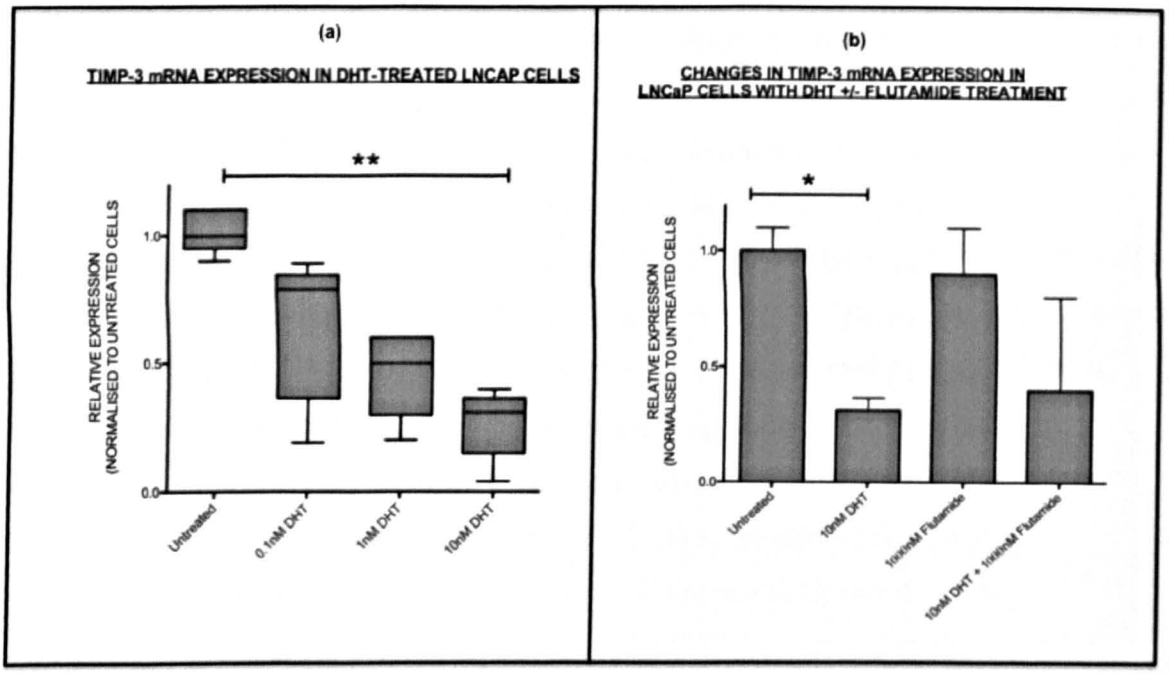

Figure 4.4: TIMP-3 mRNA expression in Treated LNCaP Cells. *Cells were treated for 24 hours, harvested and trypsinised as described in Section 2.6. Total RNA was extracted and cDNA synthesized by reverse transcription as described in Section 2.7. Relative TIMP-3 mRNA was analysed by qPCR (Section 2.8) and expression was normalised to untreated controls. (a) Dose-dependent down-regulation of TIMP-3 mRNA in DHT-treated LNCaP (n=5) **P=0.0037, Kruskal-Wallis test. (b) The significant down-regulation of TIMP-3 mRNA in 10nM DHT-treated cells was not reversed by 1000nM flutamide or a combination of 10nM DHT and 1000nM flutamide.*

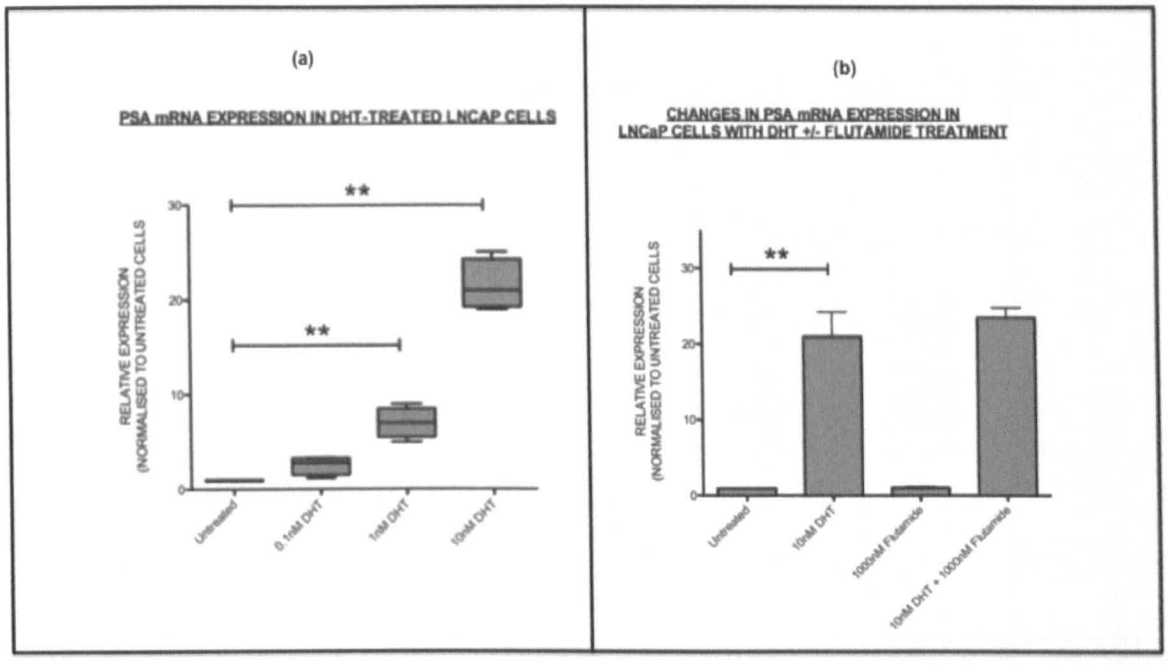

Figure 4.5: PSA mRNA expression in Treated LNCaP Cells.
*(a) Dose-dependent up-regulation of PSA mRNA in DHT-treated LNCaP (n=4) with significant effects seen at 1nM DHT (**P=0.0069, Kruskal-Wallis test) and at 10nM DHT (**P=0.0027, Kruskal-Wallis test) (b) The up-regulation of PSA mRNA in 10nM DHT-treated LNCaP was not reversed by 1000nM flutamide or a combination of 10nM DHT and 1000nM flutamide.*

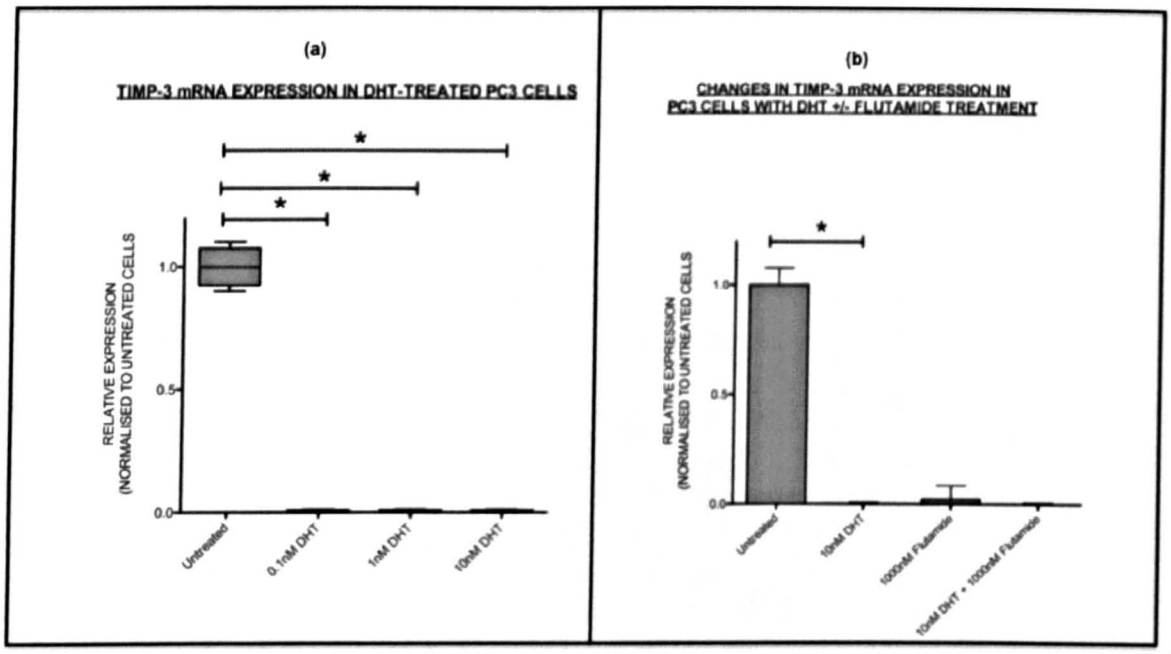

Figure 4.6: TIMP-3 mRNA expression in Treated PC3 Cells.
*(a) Repression of TIMP-3 mRNA in DHT-treated PC3 at all concentrations of DHT tested (n=5, *P=0.0144 for all concentrations tested, Kruskal-Wallis test) (b) The repression of TIMP-3 mRNA in DHT-treated PC3 was not reversed by 1000nM flutamide or a combination of 10nM DHT and 1000nM flutamide. Average C_T for TIMP-3 mRNA from untreated PC3 cells was 36 and for treated cells was 39 (close to detection limit as maximum number of cycles is 40.*

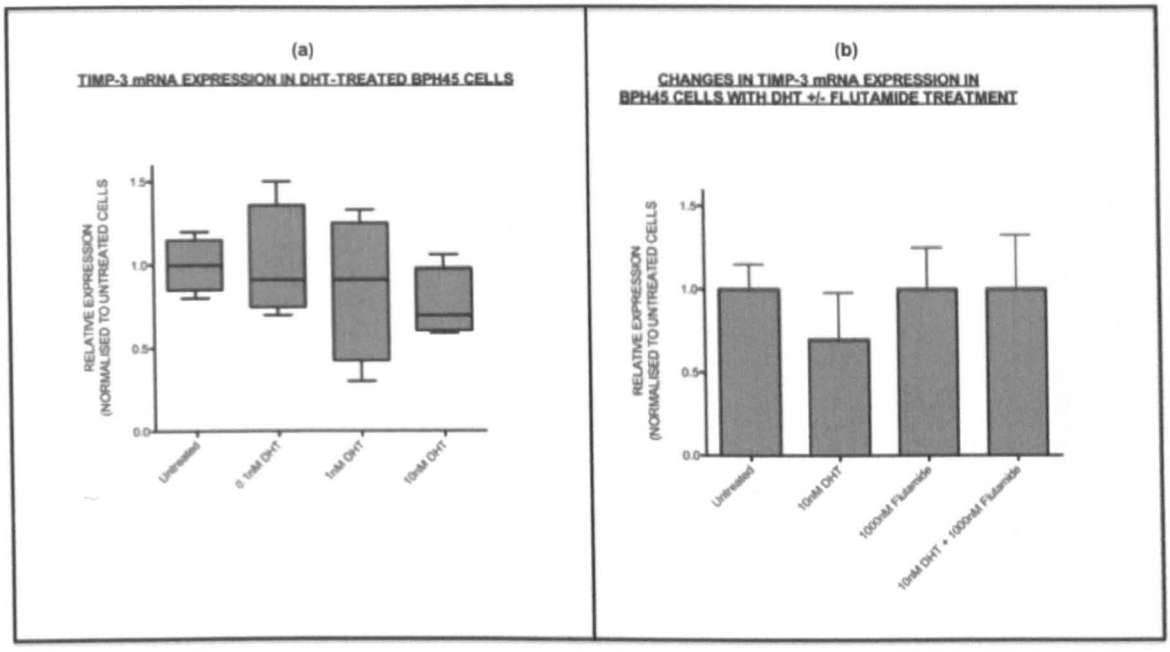

Figure 4.7: TIMP-3 mRNA expression in Treated BPH45 Cells.
(a) There was no significant modulation of TIMP-3 mRNA in DHT-treated BPH45 at all concentrations of DHT tested (n=4) (b) There was no significant modulation of TIMP-3 mRNA expression in BPH45 cells upon treatment with either flutamide alone or with flutamide and DHT (n=4)

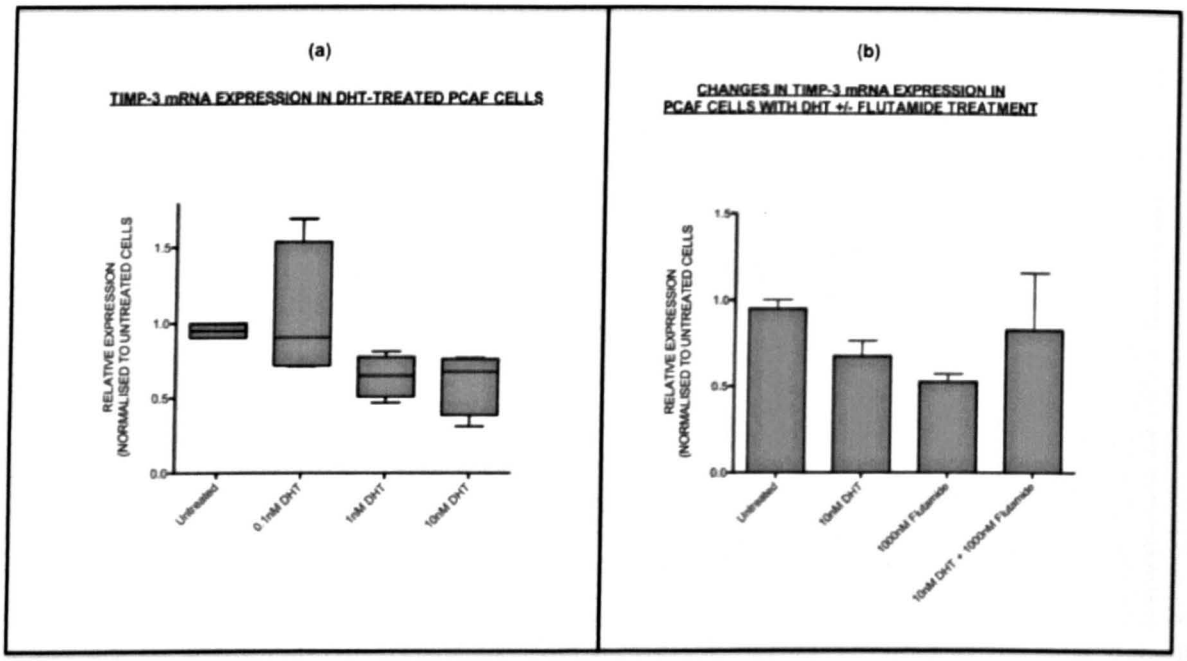

Figure 4.8: TIMP-3 mRNA expression in Treated PCAF Cells.
(a) There was no significant modulation of TIMP-3 mRNA in DHT-treated PCAF at all concentrations of DHT tested (n=4) (b) There was no significant modulation of TIMP-3 mRNA expression in PCAF cells upon treatment with either flutamide alone or with flutamide and DHT (n=4).

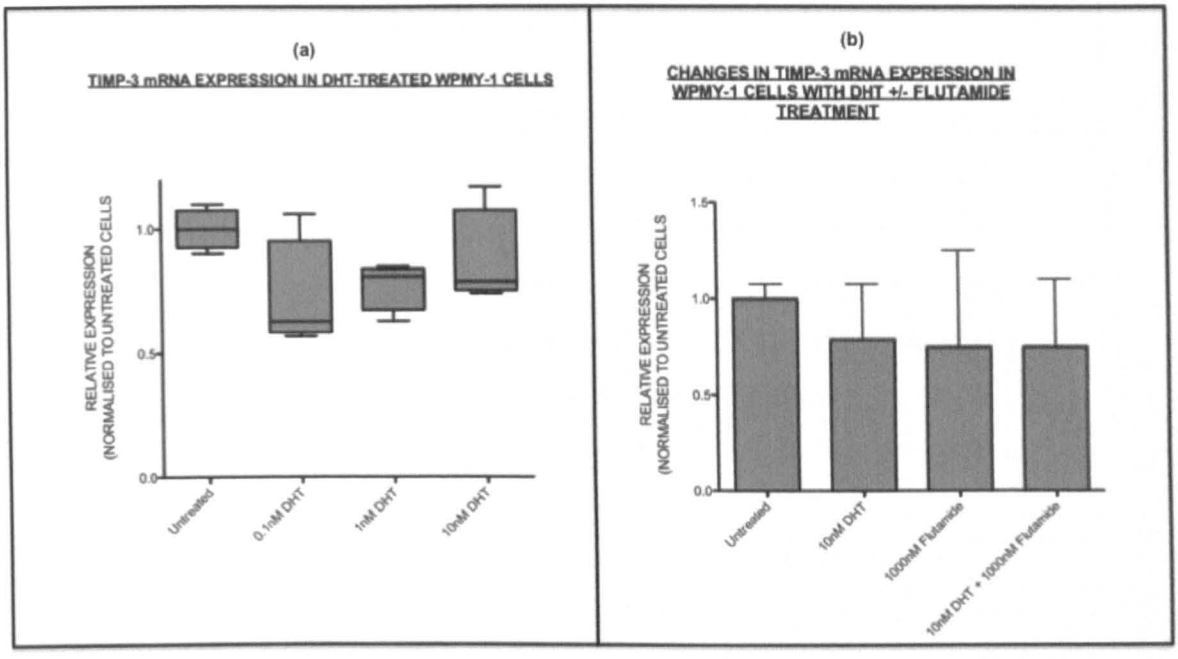

Figure 4.9: TIMP-3 mRNA expression in Treated WPMY-1 Cells.
(a) There was no significant modulation of TIMP-3 mRNA in DHT-treated WPMY-1 at all concentrations of DHT tested (n=4) (b) There was no significant modulation of TIMP-3 mRNA expression in WPMY-1 cells upon treatment with either flutamide alone or with flutamide and DHT (n=4).

4.2.2 Regulation of TIMP-3 by TNF in Prostate Cells

All cells were treated with varying doses of TNF from 0 – 570 pM (0 – 10 ng/mL) TNF. There was no significant changes in TIMP-3 mRNA upon stimulation of LNCaP or PC3 cells with varying doses of TNF (Figure 4.10) but these cells have been shown not to express much TIMP-3 mRNA (see Section 3.2.2). As the mRNA results were not statistically significant, protein expression by western blotting was not done.

In stromal cells BPH45, stimulation with TNF resulted in a down-regulation of TIMP-3 mRNA expression in a dose-dependent manner, with significant down-regulation upon treatment with 5.7 pM TNF (P=0.0072) as well as 570 pM TNF (P=0.003). These results were also corroborated by western blotting of ECM extracts from TNF-treated BPH45 cells as shown by results from densitometric analyses (Figure 4.11). However, there was no significant change in TIMP-3 mRNA expression in the other stromal cells PCAF nor WPMY-1 (Figure 4.12) after TNF stimulation, and so these were not corroborated by western blotting.

The above results suggest modulation by TNF occurs in the cells from the BPH stromal cells from a patient with benign prostatic hyperplasia, but not from cancer-associated stromal cells or cancer cells themselves.

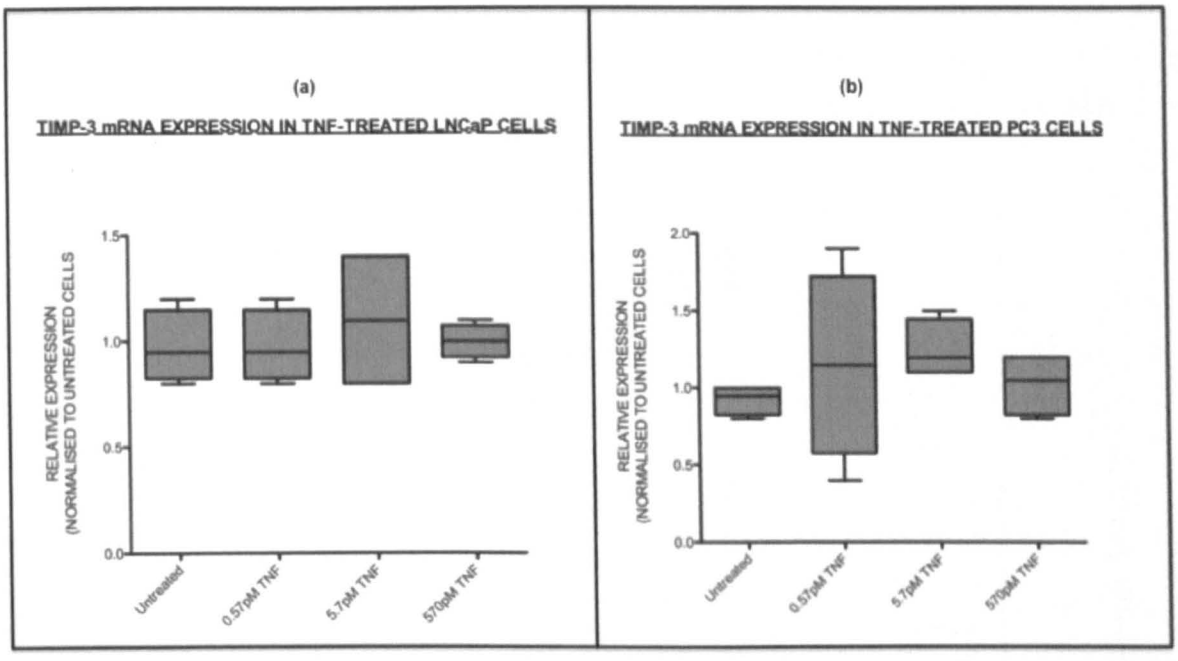

Figure 4.10: TIMP-3 mRNA expression in TNF-treated Prostate Cancer Cells.
Cells were treated for 24 hours, harvested and trypsinised as described in Section 2.3. Total RNA was extracted and cDNA synthesized by reverse transcription as described in Section 2.7. Relative TIMP-3 mRNA was analysed by qPCR (Section 2.6) and expression was normalised to untreated controls. (a) There was no significant modulation of TIMP-3 mRNA in TNF-treated LNCaP cells at all concentrations of TNF tested (n=4) (b) There was no significant modulation of TIMP-3 mRNA in TNF-treated PC3 cells at all concentrations of TNF tested (n=3).

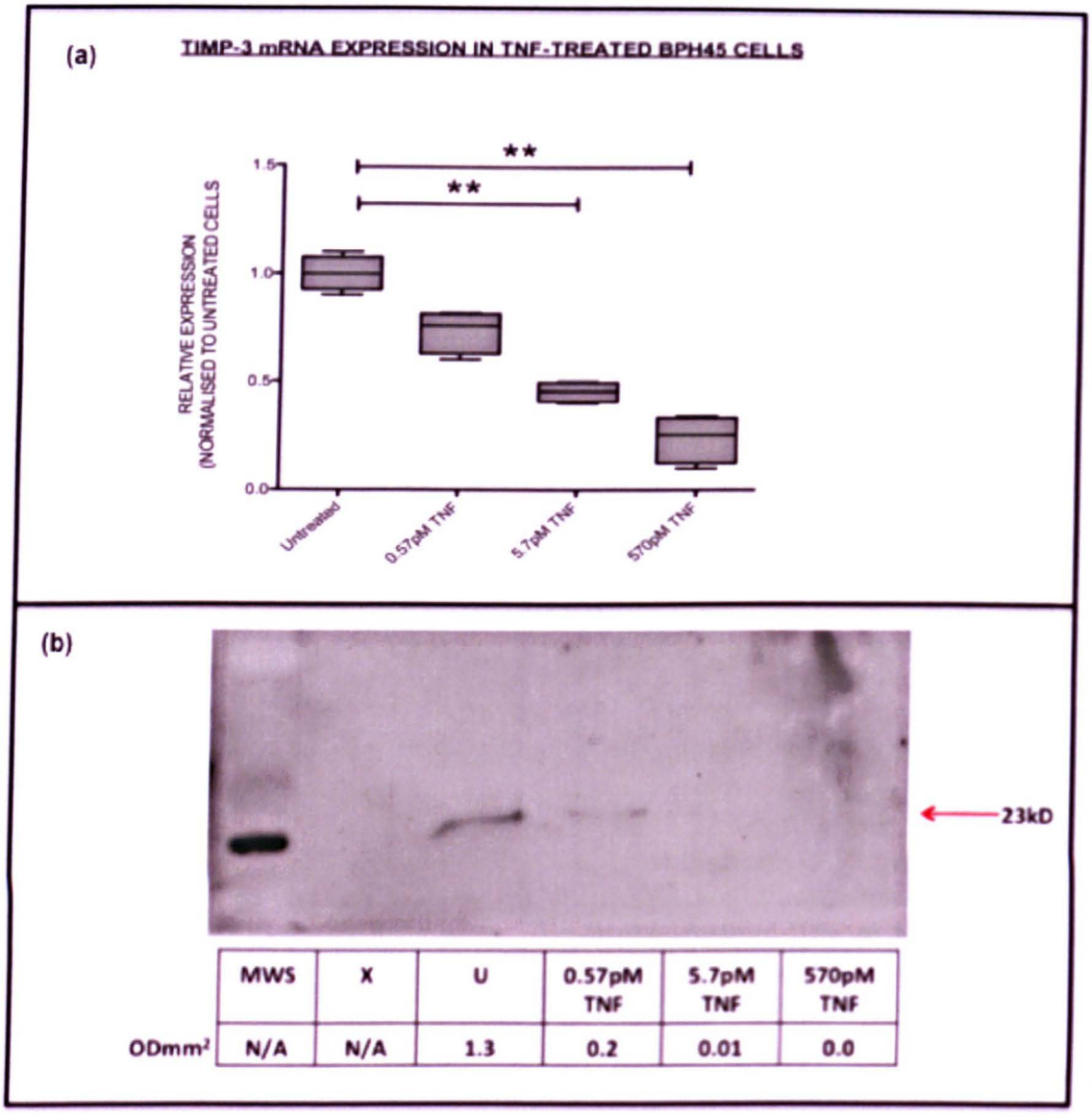

	MWS	X	U	0.57pM TNF	5.7pM TNF	570pM TNF
ODmm²	N/A	N/A	1.3	0.2	0.01	0.0

Figure 4.11: TIMP-3 expression in TNF-treated BPH Cells.

*Cells were treated for 24 hours, harvested and trypsinised as described in Section 2.3. Total RNA was extracted and cDNA synthesized by reverse transcription as described in Section 2.7. Relative TIMP-3 mRNA was analysed by qPCR (Section 2.6) and expression was normalised to untreated controls. (a) There was a dose-dependent down-regulation of TIMP-3 mRNA with significant decrease observed both at 5.7 pM TNF (**P=0.0072, Kruskal-Wallis) and 570pM TNF (**P=0.0072, Kruskal-Wallis) (n=4) (b) Representative blot showing ECM proteins from treated cells were extracted as described in Section 2.10. 100,000 cells' worth of ECM proteins were subject to SDS-PAGE, western blotting and densitometric analyses as described in Sections 2.12 – 2.14. Results showed down-regulation of TIMP-3 protein as shown by less dense bands of 23kD (see red arrow for bands) after treatment with all doses of TNF tested. MWS = molecular weight standards, U = untreated, X = empty lane. Results of densitometric analyses are in OD mm² (n=2)*

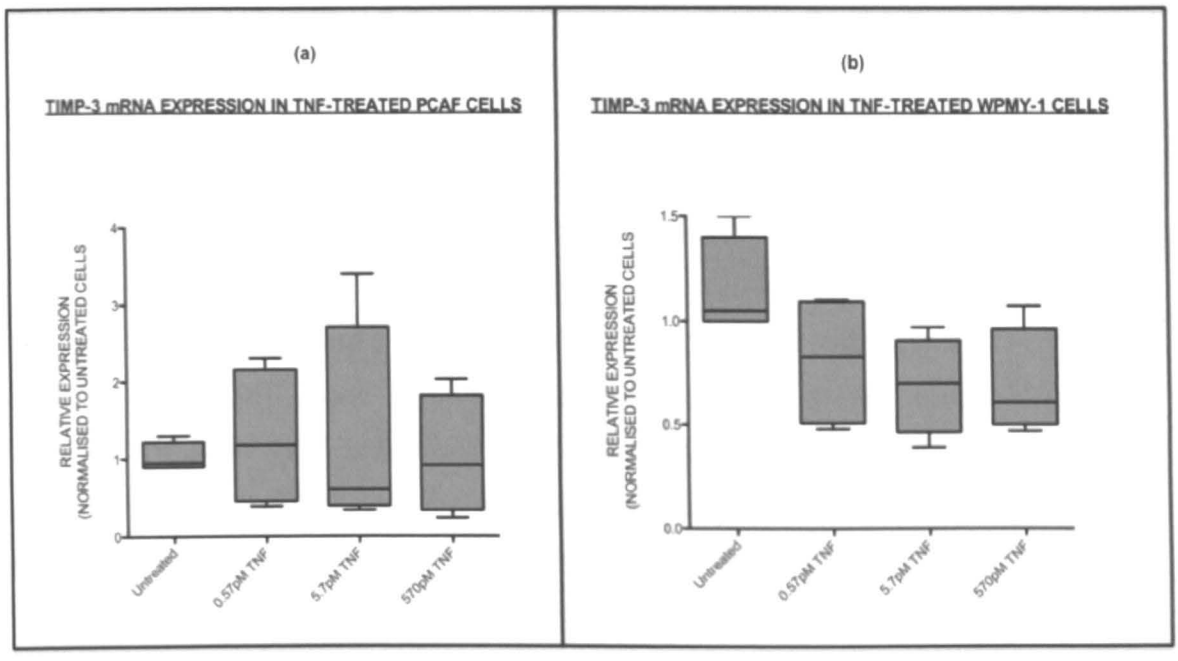

Figure 4.12: TIMP-3 mRNA expression in TNF-treated Prostate Stromal Cells.
Cells were treated for 24 hours, harvested and trypsinised as described in Section 2.3. Total RNA was extracted and cDNA synthesized by reverse transcription as described in Section 2.7. Relative TIMP-3 mRNA was analysed by qPCR (Section 2.6) and expression was normalised to untreated controls. (a) There was no significant modulation of TIMP-3 mRNA in TNF-treated PCAF cells at all concentrations of TNF tested (n=4) (b) There was no significant modulation of TIMP-3 mRNA in TNF-treated WPMY-1 cells at all concentrations of TNF tested (n=4).

4.2.3 Regulation of TIMP-3 by TGF-β in Prostate Cells

All cells were treated with varying doses of TGF-β from 0 – 50nM (0 – 10ng/mL) TGF-β. There was no significant changes in TIMP-3 mRNA upon treatment of LNCaP nor PC3 cells with varying doses of TGF-β (Figure 4.13) but these cells have been shown not to express much TIMP-3 mRNA (see Section 3.2). As the mRNA results were not statistically significant, the proteins were not analysed by western blotting.

The expression of TIMP-3 mRNA in BPH45 after treatment with TGF-β significantly increased in a dose-dependent manner with about 10-fold up-regulation at 50nM concentration after 24 hours. This was corroborated by western blotting (Figure 4.14). There was also a dose-dependent up-regulation of TIMP-3 mRNA in treated PCAF cells with about 3-fold increase observed with 50nM concentration. Western blotting results of treated PCAF proteins also showed an increase in TIMP-3 after treatment with TGF-β (Figure 4.15).

There was no statistically significant effect of TGF-β treatment on the expression of TIMP-3 mRNA in WPMY-1 cells (Figure 4.16) and so western blotting was not carried out on the WPMY-1 proteins.

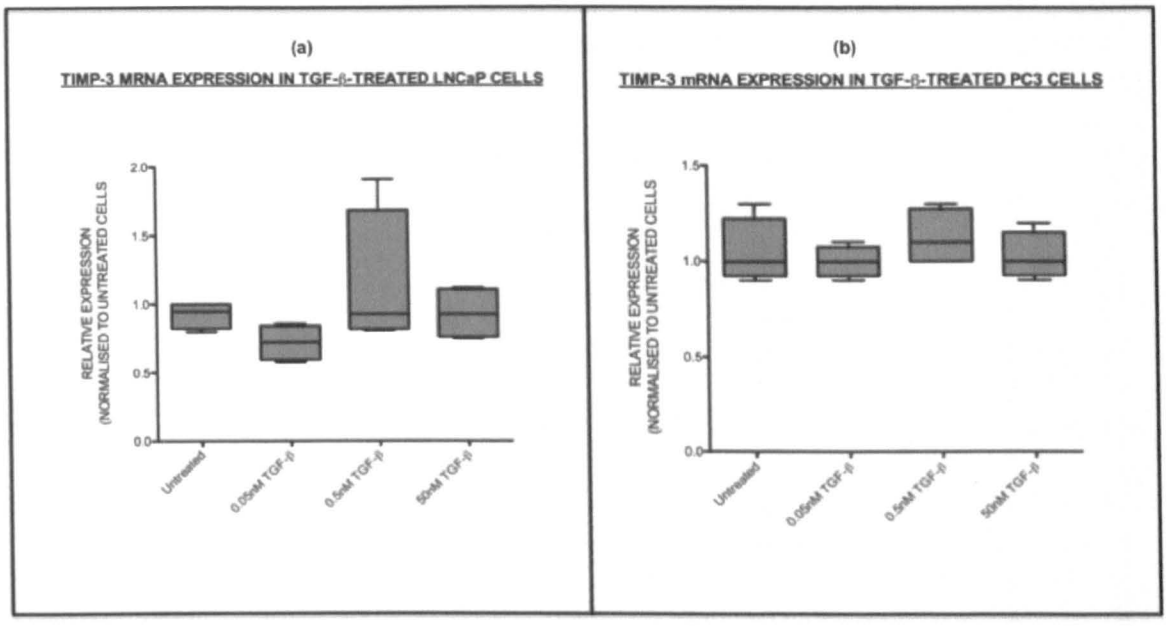

Figure 4.13: TIMP-3 mRNA expression in TGF-β-treated Prostate Cancer Cells. *Cells were treated for 24 hours, harvested and trypsinised as described in Section 2.3. Total RNA was extracted and cDNA synthesized by reverse transcription as described in Section 2.5. Relative TIMP-3 mRNA was analysed by qPCR (Section 2.6) and expression was normalised to untreated controls. (1) There was no modulation of TIMP-3 mRNA in TGF-β -treated LNCaP cells at all concentrations of TNF tested (n=4) (2) There was no modulation of TIMP-3 mRNA in TGF-β-treated PC3 cells at all concentrations of TNF tested (n=3).*

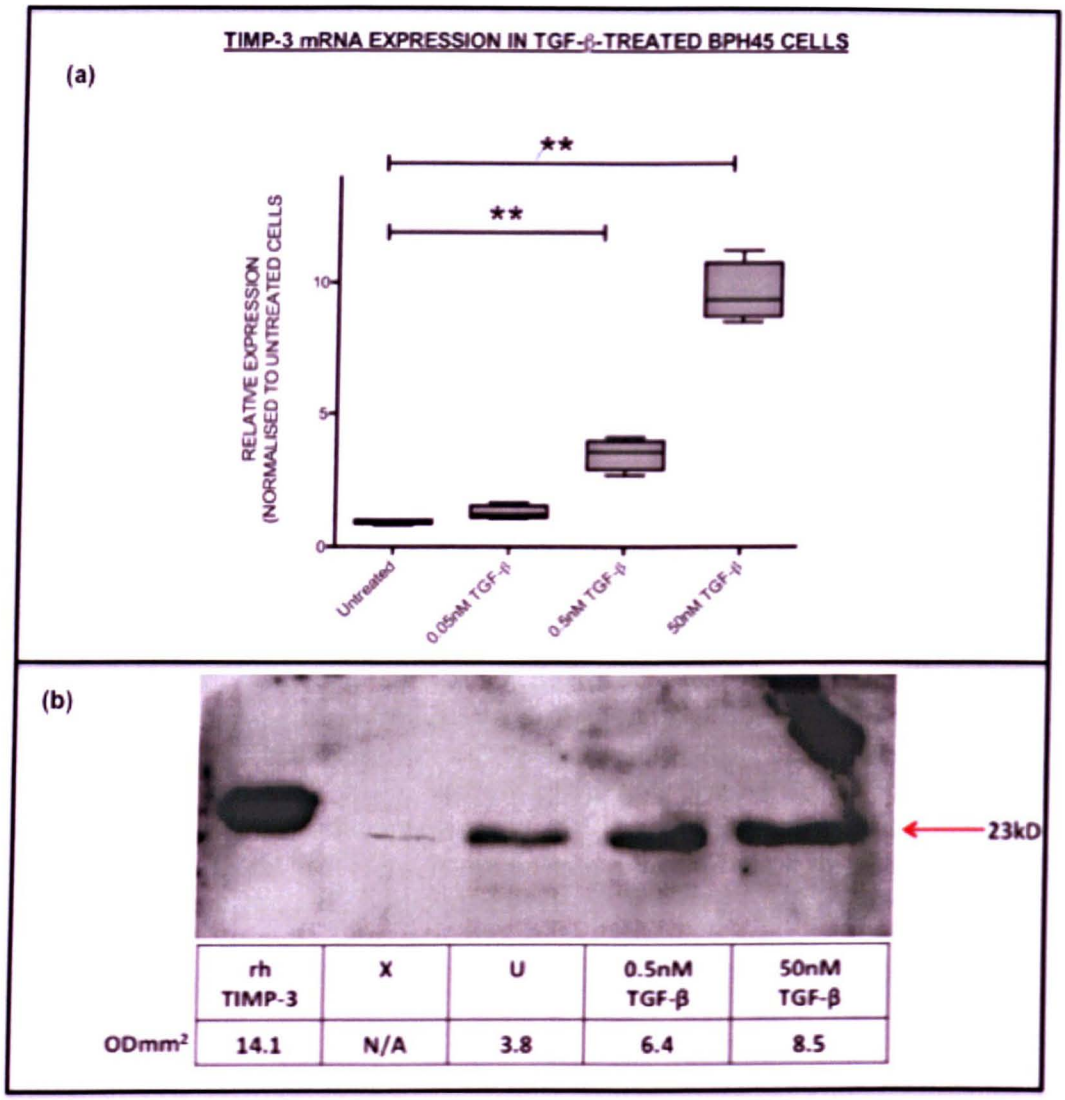

Figure 4.14: TIMP-3 expression in TGF-β -treated BPH45 Cells.

*(a) There was a dose-dependent up-regulation of TIMP-3 mRNA in BPH45 cells, with significant increase observed both at 0.5nM TGF-β (**P=0.0065, Kruskal-Wallis) and 50nM TNF (**P=0.0026, Kruskal-Wallis) (n=4)*

(b) ECM proteins from treated cells were extracted as described in Section 2.9. 100,000 cells' worth of ECM proteins were subject to SDS-PAGE, western blotting and densitometric analyses as described in Sections 2.10 – 2.12. Results showed up-regulation of TIMP-3 protein as shown by denser bands at ~23kD (see red arrow) after treatment with both doses of TGF-β tested. rhTIMP-3 = recombinant human TIMP-3 protein, U = untreated, X = blank lane. Results of densitometric analyses are in ODmm² (n=2)

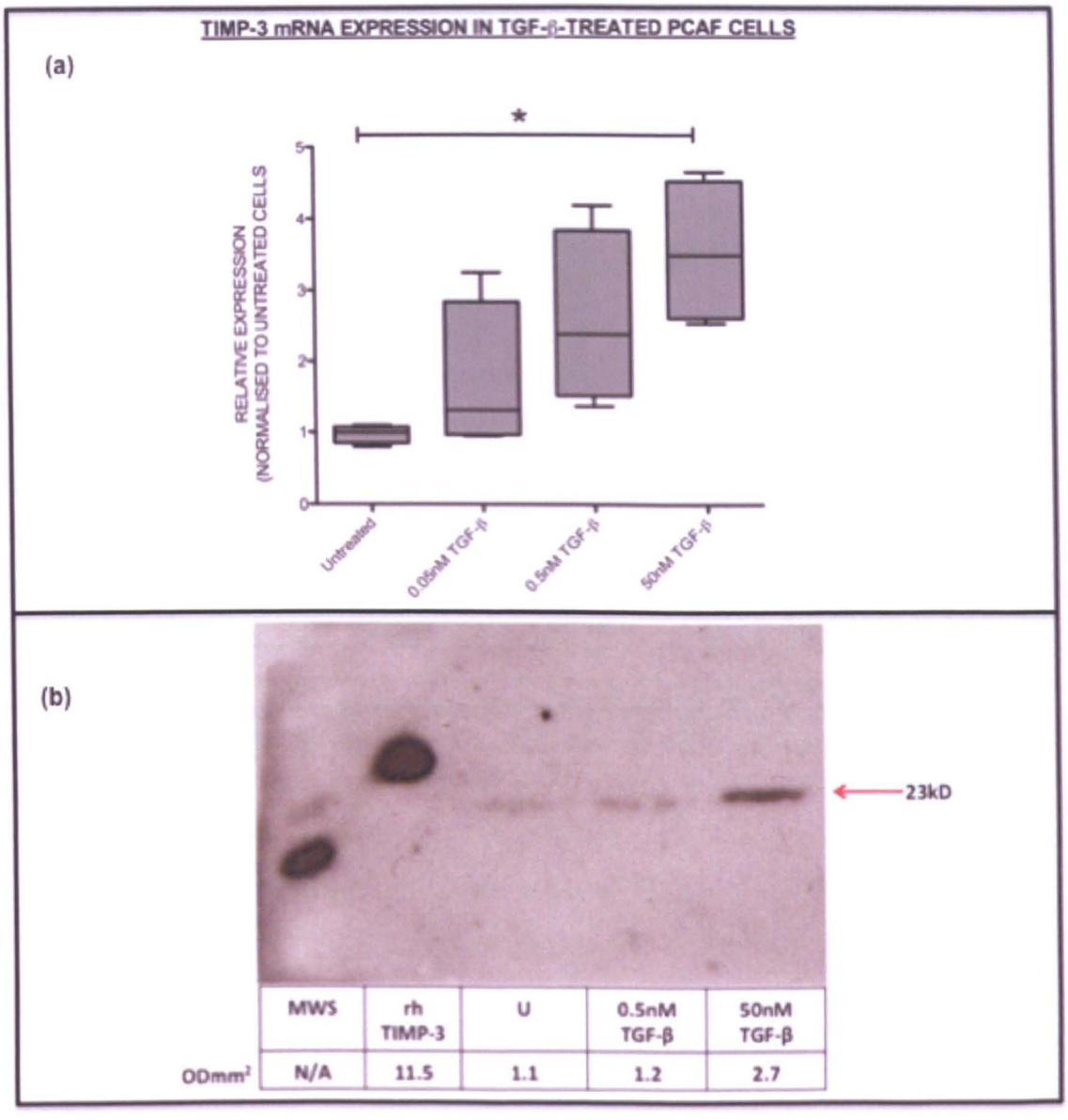

Figure 4.15: TIMP-3 expression in TGF-β -treated PCAF Cells

*(4a) There was a dose-dependent up-regulation of TIMP-3 mRNA in PCAF cells, with significant increase observed at 50 nM TGF-β (**P=0.0313, Kruskal-Wallis) (n=4).*

(4b) There was an up-regulation of TIMP-3 protein as shown by denser bands at ~23kD (see red arrow) after treatment with 50nM TGF-β. MWS = molecular weight standards, rhTIMP-3 = recombinant human TIMP-3 protein, U = untreated Results of densitometric analyses are in ODmm² (n=2)

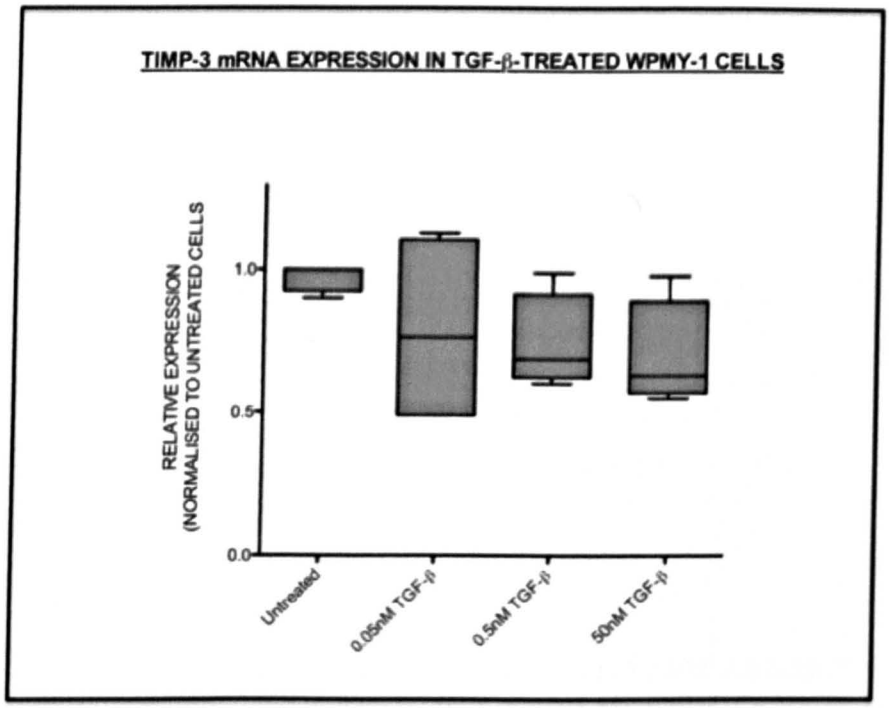

Figure 4.16: TIMP-3 mRNA expression in TGF-β-treated WPMY-1 Cells.
(5) There was no significant modulation of TIMP-3 mRNA in TGF-β-treated WPMY-1 cells at all concentrations of TNF tested (n=3)

4.2.4 *In-silico* analyses of *timp-3*

This chapter has described the regulation of TIMP-3 gene expression by androgen DHT in prostate cancer cell LNCaP and by TNF in prostate stromal cells BPH45 and by TGF-β in prostate stromal cells PCAF and BPH45. In the light of these results it seemed essential to try to determine whether a secondary hypothesis was derived at this stage – does the TIMP-3 gene have androgen, TNF or TGF-β response elements in its promoter region. This would suggest direct transcriptional regulation of the gene via androgen, TNF or TGF-β binding to a specific DNA sequence motif upstream of the promoter region of the gene. The promoter region of DNA is known to enhance the transcription of the genes close to it and is usually located on the same strand at 5' upstream of the gene to be regulated. Proximal promoters are usually 250bp upstream of the transcription start site of the gene and are characterised by the presence of CpG islands very near the beginning of the first exon of target regulated genes (Iannello et al., 1997, Koutsodontis et al., 2002, Desmoucelles et al., 1999). Nuclear receptors and transcription regulators will bind to specific response elements within the promoter region to initiate recruitment of co-activators or co-repressors for regulation of gene transcription.

TIMP-3 is located on chromosome 22: 33192687 – 33197686. For *in-silico* analyses, an area of 5,000bp upstream of the 5' position of the TIMP-3 gene was investigated, in order to identify the presence of known androgen response elements, TNF response elements or TGF-β response elements.

The general motif sequence for androgen response elements (ARE) is a loosely palindromic sequence consisting of 15bp arranged as 2 half sites of 6bp each divided by a 3bp spacer region: 5'-GGA/TACA nnn TGTTCT-3' (Roche et al., 1992). This sequence has been shown to be specific for androgen receptor binding and activation of gene transcription. Other AREs that have some of the matching nucleotides as the consensus ARE, have been discovered in promoter regions of genes and have been shown to be functional e.g.

5'-AGAACA gca AGTGCT-3' and 5'-AGCACT tgc TGTTCT-3' are functional AREs found in the proximal promoter of PSA (Cleutjens et al., 1997, Cleutjens et al., 1996), 5'-TGAAGT tcc TGTTCT-3' in the proximal promoter of mouse vas deferens protein gene (MVDP) (Fabre et al., 1994), 5'-CAACTT cta TGTACA-3' in distal promoter of human protease activated receptor 1 (hPar1) (Salah et al., 2005) to mention but a few. Other putative AREs have also been discovered in the promoter regions of genes e.g. 5'-

GGAACA taa GGTGCG-3' in the promoter of ADAMTS15 gene (Molokwu et al., 2010) although the functionality is yet to be tested.

The sequences for TIMP-3 and 5,000bp upstream of TIMP-3 were obtained from ENSEMBL genome database (Hubbard et al., 2002). Only exonal sequences for TIMP-3 were analysed. 10 putative AREs were found in the 5000bp sequence upstream of the TIMP-3 gene upon analysis. This 5000bp region contains the promoter region of TIMP-3 as characterised by GC-rich region close to the transcription start site and transcription start point on exon 1. The AREs were detected using the NUBISCAN software (Podvinec et al., 2002) and imputing the functional ARE half sites: AGAACA, TGTAAC, TGTACA, TGTTCT, GGTACA, AGTGCT, TGGTCA, AGTTCT, AGTACG and GGAACA (Monge et al., 2006). The search criteria imputed into NUBISCAN for ARE prediction ensured that only sequences with at least 70% similarity to these functional half sites were reported. The putative AREs have been highlighted in Figure 4.2.4.1. Also, a CpG island was identified in the 5000bp sequence using the CPGPLOT software (Rice et al., 2000) – the island was proximal to the first exon and the transcription start point. This is also highlighted in the Figure 4.17.

Table 4.1 shows a comparison of the AREs in the *timp-3* gene promoter region to other known AREs in androgen-regulated genes. The percentage of nucleotide similarity of the timp-3 AREs to these reported AREs is also reported on the table. This analysis showed that there was 40 – 75% sequence similarity between the *timp-3* AREs and the AREs of known androgen-regulated genes.

GCTTGGGGGAAGGCATCGTGGCTAGGGTCTGGAGGGGAAGAGGGAGGAAAGCAAAGAGGA
GCTTCCCTATGAGGCAACAGAAATGACAGTACCTTCTCCAGGTTGAATTTCCAAAACCCA
GCTCTGCCCTGGAAGACTGGGACTGTGGCATCCTCTGCAGTGTTCCCAGACCGCCCTAAG
GCCCCCAAACCAATGATTCACAACTATGTTGCTTCCCCAGAGAGCATCTCCCCCTTTGGT
TGACATGTGGCCAGCTCAGGGGTGGAGGAGCTCCGGCAGCCACGAACCCAGACGGGATGT
TGACTGAGAGCTTTGTGGCCATGGCAGATGGGAGGGGTGAGCTTCACCCACTCAAAGGCA
CCCGCACCCCACCGATGAGTGTGGAATTGTGCTCTCCCGCCCTCGCAGTGAGACGACCGA
CCAGGACTGCAGGCTGAGCAAATGGGTGTTCTCTGGCTTATAGCGCCCCCTAGCACCAGC
CAGCGGGATAGAGCTCCCTGAACTCTCCAAGGAGCCACCACCTGCCTGTCTGAATGCTGG
AAAGGGGTCGGTGGTGCTGATCATTGGACCCATTCAACCAATACTTATTAAACTCGTTGT
TACCAACACTTAATCCCTGTTCTAGGGGCTTAGACTCCAGCAAGGGAAACAGATGGGT
AAATAATCACATTAGAGTCAGCTAAGTATTGTCAAAGAAGTTGATACAGGGTGTTGTGGG
GATACATGGGAGGGGAATCAGAGGAGGTTTCCCGGAGGAGGTGACATCTAAGCTGAGGTC
TGAAGGATGTGGAAGAGTTCAGTAACTCCTGAAGACCAAAAAAATGGTGATAAAAAAGAC
ACCTTCCTAACTTTTTAGTGCTACGATCCAAGAGACAAACAAGCAGGTGAACGCATAACT
ACACTGGGCTCCACCATAAGCCAGAGCCTGTCTCTCCTAGGACTTTGGCATCACAATCTT

CTCTGAAATTCTGTTTTCGGCATTGATTCTTGGGGGAGGTAGCAATATAGGAACTCAGTG
TTCGTTGCGAAACTGATGGATGGTCTTCAGTCTTGGGTACGTTCCCATGTGTCAAACCTG
TTTAAATGGCAGGACCCATCTCCCCTTCAGAAGCATTCACTTGTCCTACAGGATTCCCCA
TGGAATCTTGGAGTTTTTGAGGCGAGAGGGATCCTGGATACCACTGAGTTCTATCTTTCA
TCCAATAAACACAGAAGTGGACGCCTGGACAGGCAAAGTGACTTGACCAAGGCAGGTGCA
CAGCTATTCTGCAACATTGGGAACAAATCTCAGGTCTTTTGATTTTTTGTTTCCACTTTA
CTCTCTTTTCATTTCCCAGAAACAAAGTTTTCATGTGCTTTTTTTTATAGTGATATGTTT
GGAATGCATTAGCTAGTAATTTAGGAAGGGAAAAAAATAAACACACAAGAGATAAACCTG
TCAGGAGGACAAACCTGTATTGCTTCTGATTGGCTCAGAGGGTGATTATTATCATGGTAG
AGAATTATTTAATCAGTGTAAGTAAAATTTCTCTGTGGGCTGGGCACTGTACAAAGACTC
AAACGAATCTGTCTACAGATCTGAAAAGCAGATACGAGATCTGTGAATGGCTGGGGTTTC
CAAGCCCACAGTACAAGCATGGGCCACACCTTACAGCTTGGAGGACTGAGCCCTGAAAAT
GGGCAAGTTCCTTCACTTCTCTGAACCTTATTTTTCCCACATTTAAAACAAGGATGAGTA
GTTTCTGAGGTCCTTTTTACGACTTCTCTTCCTACAGACTCTAGCATCCTATAACTTGAT
ACAAAGAGGGTGGATATGAACTCACCTTTCCTAGAAAAGTTCCAGGAAAGAGAATACCAG
GTCATCCTAGTAGGTGTGTAGACAGGCCAGATAGATCTTGAAACTTACTCAGTTCTTCCC
AGATGTATAACTCTATCATTGTTCTTAGCTGTCAAGAGAAAGCAGGAGAGCCTGCATCTT
CATTCTTTTTTTTTTTTTTTTTTTTTTTTGGAGACGGAGTCTCACTCCATCACCTAGGCTA
GAGTGCAGTGGCATGATCTCAGCTCACTGCAAGCTCCGCCTCCCAGGTTCACGCCATTCT
CCTGCCTCAGCCTCCCAAGTAACTGGGACTACAGGCGCCCACCACCACACCTGGCTAATT
TTTTGTGTTGTTAGTACAGACGGGGTTTCACCATGTTAGCCAGGATGGTCTCGATCTCCT
GACCTCGTGATCCGCCCACCTTGGCCTCTCAAAGTGCTGGGATTACAGGCGTGAGCCACC
GCACCCAGCCTGCATCTTCATTCTTACTGTTAGCCTCAGGTTCACCCCACCTAGCTTATT
AAGTGATGTTGAATAACCAATTCTTACATATTATTAGGCTCATGGACACCATGACATCCA
GACTGATGGGTGCCTGCTGAAGGGGGTGACCCTAGCAGGAGGACTCCCCTACGCAAGGAT
TCATGGAGTTTGCTGTTTCTTTTCCTTAGGGTGAGAACCAAACTGCCTTCACACGGTGGG
CAGAGGGGAACTGACTCAGGTTTGGAATAAGAGAGAACATCCCAACTGAAAAGCTCTTGG
AATTCGCTGAACTTCAAGACACTGTGTGGACCAGCTTAGGATAGGGAGTGAGAAGAAATT
AACCAAAAGGTAATTTCGTTACTTTTCAGCTGGAAAAAAGATCAGATTATACTTGTGCTT
TCATAATTAAGTAGCTGCTGGAAAAAAACGCTTCAGATGCTTTCTATGAGAAAACTGCTG
CTTGAAGTTCAGCAGAAGTTATCTACTTGATACTTATATTCCAGGCAAGGCCTTCCGTTG
GAGAAAATATCGGCACTTTGGACAAAACTGAAATGTGAAAAGAAAGGGAAGAGAGGGCCT
CTATCATGTAAGATGCTTATCCAAAGTGGATTTGGTCTGGAAAGTCTTCTAAAACCTTCC
ACATGACTGTGGAATAAGTCATGTGGGGCGCGGGGATAAGCGAATCTCTCAAATTCCACC
ACGTATGCCCTCATTCAACCTGGATCCTTAGAGTGGCCTCCAGGGCACTCTGCTCAGGAC
TCAGTCAGCTGTTGGCCACACCCATGCTCTCCAGTCTCCTGAGACCCTATTTGGTTCTGA
GAGGGCTAAAAAGCAGTGTGGCTAAATATCCCAGGCCTCAAAGTATTCCTACTGTGGTTG
GGGAAGCAATAGAATCATACCCCATAAAACAATGAAAACAGTGCTAGAAAAACATCGAGA
GACAGAAACATCTCTACGAGTTAGGCCACAGTTAGAGTGAAGGCAGGGAAGGTTTTTAAA
GCTGGGTGGAGGGGACAAGTCAAAAAGATGTGGAAACTGGTTTCCCTTTCCTATGGCTAA
AGTGCTCAAAGGGGAAAAAGGAGTTTCAAAAATGTTCTTGGAAATACCATCTCTCACGAA
TTCTTCGGCCTCTGCTGTCCCAATGTCACTTGTCTGAGATGTAAACAGAGGAGTTCTGAG
AAAGAAGCTGAACTTGCATTTCTCCCTGTTTCTATTTGTTCCAAACTTGTGGCATTTCTA
ACAGGATGAAGCGGAAGAGAAAGGGAAAGAGACAAAAGTGTAGAAAGATGGAAGATCCCA
GCTGCAAATGGCCATTTGCAGTTAGATGGAACAGCTGCTGACGTTCAGGGAAATGCATGT
CTCTCTTCAGATGGGAAGGAGCAGTGGAAAGGGGTGACGAGTTCCTGGCTGGCCACCAAT
CATCCCATCTTTCTGTGCCGGTTCCTCATCTGGAAAGTGGGAGTGATACTTGTGCTTGCT
TTTCCTACCCACAAAGATTATTGTGAGAGCTATAATACGGTGAGATACAGAATCCTGCTT
TTAAAAATACAAAGCAGAATCAAGATGTCAATAATAAGGATAGTAATTGTGTTAGTTATC
TGCAATCATCTATTATAGCTAGTCGTCTAGGATCCTGGATCGTTCTCCTGGTTTTACTAC
AGTTTTGGATCAGCTCACCCCCAAATCCCTTGCTGAAGGGTGGAGCTCTGTCAGCCATGG
GCAGGGAACCACTTCCTCTTGCCTTTCTACTTTCTGTCTTTCAAACATGCCCAGGGTCTT
TGCACTTGCTGTTCCCCCTGCCTGGTACCTCTCTCCTGTGGCTTGCCCCAGAGCTGATCC
TTGTCTTTGTCCACTTCTCAGCGAGGATGGCACTTCAGGGAGCCCTTCCCTTACTATCGC
AGAGAGAGCAGGCCCTCCCCAGTCATGTCCAACCCAGAACTCTGTTTTGTTTTCTTCATA

GCCCTAGCATCACAGAAAATCACCCTGTGCATTCATGGATGTCCACGGGGGCAAGGGCTT
TGTGTTGCTTAACCCAGCATCCTGAACCGTGTTTGTTGAATGAATACAGAACCCCGTTTG
CTCTGGGAGAGCACAGAAAACAGTCTTCTATCATATATCATAGCCAGCTGCAAACAGCAG
ATGGCTTCCCATATCCCAGAGAGTAAGAACCAGAGAGAGAGAGAAAGAGAGAGTTTGG
GTCTTTCTCCTCTGTGCCTGCTCTCTCCAGAGAAACTGGAGGGGTAGCAGTTAGCATTCC
CCCGCTGGTTCCACCAAGCACAGTCAAGGTCTCTAGGACATGGCCACCCCTCACCTGTGG
AAGCGGTCCTGCTGGGGTGGGTGGGTGTTAGTTGGTTCTGGTTTGGGTCAGAGACACCCA
GTGGCCCAGGTGGGCGTGGGGCCAGGGCGCAGACGAGAAGGGGCACGAGGGCTCCGCTCC
GAGGACCCAGCGGCAAGCACCGGTCCCGGGCGCGCCCCAGCCCACCCACTCGCGTGCCCA
CGGCGGCATTATTCCCTATAAGGATCTGAACGATCCGGGGGCGGCCCCGCCCCGTTACCC
CTTGCCCCCGGCCCCGCCCCCTTTTTGGAGGGCCGATGAGGTAATGCGGCTCTGCCATTG
GTCTGAGGGGGCGGGCCCCAACAGCCCGAGGCGGGGTCCCCGGGGGCCCAGCGCTATATC
ACTCGGCCGCCCAGGCAGCG

ATGACCCCTTGGCTCGGGCTCATCGTGCTCCTGGGCAGCTGGAGCCTGGGGGACTGGGGC
GCCGAGGCGTGCACATGCTCGCCCAGCCACCCCCAGGACGCCTTCTGCAACTCCGACATC
G

TGATCCGGGCCAAGGTGGTGGGGAAGAAGCTGGTAAAGGAGGGGCCCTTCGGCACGCTGG
TCTACACCATCAAGCAGATGAAG

ATGTACCGAGGCTTCACCAAGATGCCCCATGTGCAGTACATCCATACGGAAGCTTCCGAG
AGTCTCTGTGGCCTTAAGCTGGAGGTCAACAAGTACCAGTACCTGCTGACAG

GTCGCGTCTATGATGGCAAGATGTACACGGGGCTGTGCAACTTCGTGGAGAGGTGGGACC
AGCTCACCCTCTCCCAGCGCAAGGGGCTGAACTATCGGTATCACCTGGGTTGTAACTGCA
AG

ATCAAGTCCTGCTACTACCTGCCTTGCTTTGTGACTTCCAAGAACGAGTGTCTCTGGACC
GACATGCTCTCCAATTTCGGTTACCCTGGCTACCAGTCCAAACACTACGCCTGCATCCGG
CAGAAGGGCGGCTACTGCAGCTGGTACCGAGGATGGGCCCCCCCGGATAAAAGCATCATC
AATGCCACAGACCCCTGA

Figure 4.17: Results of in silico analysis of timp-3 plus 5,000bp upstream of the gene. *Blue sequences are 5,000bp upstream of the gene. Black sequences are the 5 exons (translated region) that make up the TIMP-3 gene. ATG underlined in exon 1 is the start codon while TGA in exon 5 is the stop codon. Red sequences are the CG repeats characteristic of CpG islands that are found in promoter regions of genes. The grey area highlighted represents the CpG Island proximal to the first exon of the TIMP-3 gene, and was identified by CPGPLOT software. The CpG island was 258bp long with an observed/expected ratio of > 0.6 and a %C + %G of > 50%. The green areas highlighted represent the AREs both proximal and distal to the promoter region of TIMP-3 gene. (Key characteristics of general ARE consensus = always C at position 5 and always G at position 11 of the sequence.)*

.

SEQUENCE	H-S1	SR	H-S2	% OF CONSENSUS
CONSENSUS 1	GGAACA	nnn	TGTTCT	
CONSENSUS 2	GGTACA	nnn	TGTTCT	
PSA	AGAACA	nnn	AGTGCT	75, 67
MVDP	TGAAGT	nnn	TGTTCT	75, 67
hPAR1	CAACTT	nnn	TGTACA	42, 33
1	TAATCC	nnn	TGTCCT	67, 58
2	AGAGCT	nnn	TGAACT	58, 50
3	GGAACT	nnn	TGTTCG	83, 75
4	GTTTCA	nnn	TGTTAG	67, 67
5	CTGACC	nnn	TGATCC	50, 50
6	GCCTCT	nnn	AGTGCT	50, 50
7	GTTTCT	nnn	TGTTCC	67, 67
8	GGAACC	nnn	GGCAAG	50, 42
9	GGATCT	nnn	CGATCC	58, 50
10	TGCACT	nnn	TGTTCC	67, 67

Table 4.1: Comparison of the putative AREs found in the 5000bp promoter region upstream of timp-3 gene and known AREs in androgen-regulated genes to consensus ARE as defined by Roche et al (Roche et al., 1992).

Nucleotide similarity of the 10 predicted/putative AREs in the promoter region of TIMP-3 (labelled as 1 – 10) was compared to the nucleotide sequence of the consensus ARE. The functional AREs of PSA, MVDP and hPAR1 were also compared to the consensus ARE. H-S1 = half-site 1, H-S2 = half-site 2, SR = 3bp spacer region, n = any base. The % of nucleotide similarity in the putative AREs in TIMP-3 promoter ranged from 50% to 83% for consensus 1 and from 42% to 75% for consensus 2 – this is designated as x, x comparing sequences versus consensus 1, consensus 2. The conserved C at position 5 of H-S1 and conserved G at position 2 of H-S2 are both underlined for emphasis

In the TNF signalling cascade, NF-kB binds to its binding site within the promoter region of regulated genes to initiate transcription (Borset et al., 1996). The consensus for the binding site is:

5'-GGGRNNYYCC-3' where N = any base, R = purine (A/G), Y = pyrimidine (T/C) (Wang et al., 2000, Parry and Mackman, 1994). The results of the analysis showed no sequence matching the consensus for the binding site for NF-kB – this implies that the regulation of TIMP-3 expression by TNF as seen in prostate stromal cells BPH45 is not as a direct result of modulation of TNF/NF-kB-mediated gene transcription, but could be using a different pathway such as MAPK.

There are two TGF-β response elements reported in the literature, with the following specific motifs:

5'-ATCACGTGGCTGGCTGCATGCCCTGTGGCT-3 (Datto et al., 1995)

5'-TAGACAATCACGTGGCTGGCTG-3' (Riccio et al., 1992)

None of the above motifs was found in the 5,000bp region upstream of TIMP-3 gene, implying that the regulation of TIMP-3 expression by TGF-β as seen in prostate stromal cells BPH45 and PCAF is due to other, as yet uncharacterised, response elements, or is an indirect result of modulation of TGF-β-mediated gene transcription.

4.3 DISCUSSION

This is the first study to look for modulation of TIMP-3 by DHT in prostate stromal and cancer cells. For the role of TIMP-3 in the progression of prostate cancer to be fully understood, it was important to investigate the alterations in expression of this metalloproteinase inhibitor since metalloproteinase expression has been shown to correlate with disease progression of prostate and other cancers (Mylona et al., 2006, Vazquez-Ortiz et al., 2005, Iwata et al., 1995, Ellerbroek et al., 1998, Islekel et al., 2007, Riddick et al., 2005)

TIMP-3 mRNA expression was significantly down regulated in LNCaP cells after treatment with DHT (Figure 4.4). The loss of TIMP-3 in LNCaP cells may be the reason for their known increase in their expression of metalloproteinases compared to normal prostate cells (Aalinkeel et al., 2011). DHT-mediated prostate cancer cell proliferation and cell survival is androgen receptor (AR)-dependent (Arnold et al., 2007, Wu et al., 2007, Klus et al., 1996). However, there was no reversal of the effect of DHT on TIMP-3 mRNA expression when LNCaP cells were treated with flutamide, an anti-androgen (see Figure 4.4). This result is counter-intuitive as flutamide is clinically administered to patients with lymph node metastatic prostate cancer as an androgen receptor antagonist, the mode of action of which is inhibiting the binding of androgen to the AR (Eisenberger et al., 1998, Greenway, 1998, Higano et al., 1996). Although the down-regulation of TIMP-3 mRNA by DHT was not verified by western blotting due to difficulty in detecting the TIMP-3 protein in LNCaP cells, the loss of the transcript may be contributing to the loss of TIMP activity observed with LNCaP protein extracts as discussed in the next chapter.

The activity of the DHT used in these experiments was confirmed by analysing the expression of PSA (Figure 4.5) – a serine protease that is androgen-dependent and is used as a diagnostic marker for prostate cancer progression (Downing et al., 2003). PSA mRNA was up-regulated by DHT in a dose-dependent manner in LNCaP cells, as previously demonstrated (Montgomery et al., 1992). This result also confirms that the activity of the mutant androgen receptor in the LNCaP cells can be enhanced in-vitro by addition of DHT, and this in turn enhances the signalling cascade involved in transcription of androgen-regulated genes such as PSA (see figure 4.1). Flutamide did not reduce PSA mRNA expression in LNCaP cells (see Figure 4.5) - again, this is counter-intuitive as PSA is

routinely measured in patients' serum for evidence of decreased levels as an indication of better prognosis of prostate cancer (Yu and Lai, 1998, Mettlin et al., 1994).

Also, in this study, the expression of the small amount of TIMP-3 mRNA expressed by PC3 cells was completely eliminated after DHT treatment (Figure 4.6). This result was unexpected, as these cells do not possess an AR (Marcelli et al., 1995) and should not respond to nuclear receptor activation by DHT ligand. The existence of alternative pathways by which these cancer cells are able to respond to androgen treatment has been investigated, one of which is transcriptional activation by a cell surface receptor (Kampa et al., 2002, Hatzoglou et al., 2005), where the inhibition of LNCaP cell growth by BSA-coupled testosterone was demonstrated to occur via a membrane androgen receptor *in-vitro* and in nude mice. Their results suggest that the potentially pro-tumourigenic AR-independent effect of DHT-mediated reduction in TIMP-3 mRNA expression in the prostate cancer cell line PC3 may be via a membrane receptor. As with LNCaP cells, there was no reversal of the effect of DHT on TIMP-3 mRNA expression when the PC3 cells were treated with flutamide (Figure 4.6).

In the stromal cell lines BPH45, PCAF and WPMY-1, there was no statistical difference in TIMP-3 mRNA expression between treated and untreated cells nor between untreated, DHT-treated and DHT+flutamide-treated (see Figures 4.7, 4.8 and 4.9 respectively), implying that DHT-mediated regulation of TIMP-3 may be cancer cell-specific.

Elevated levels of TNF have been observed in the serum of prostate cancer patients (Nakashima et al., 1998) and this may be as a result of recruitment and activation of macrophages by necrotic cells in the tumour mass in response to the hypoxic conditions. The macrophages subsequently elicit the production of pro-inflammatory cytokines in tumours. In this study, TIMP-3 expression was down regulated in prostate stromal cells BPH45 by TNF treatment, in a dose-dependent and statistically significant manner (see Figure 4.11). There were no significant changes in TIMP-3 mRNA expression after cell treatment in the cancer cells LNCaP and PC3 (see Figure 4.10), nor stromal cells WPMY-1 and PCAF cells (see Figure 4.12). It is likely that that the stromal cells produce the bulk of the TIMP-3 in the tumour microenvironment, as has been reported previously (Mylona et al., 2006). A decrease in TIMP-3 expression in response to increased TNF expression may favour increased proteolytic activity and subsequent tumour metastasis and disease progression. The effect seen in BPH45 (Figure 4.11) is probably due to the fact that these

cells produce large amounts of TIMP-3 and they originate from a highly fibrotic condition that results in hyperplasia and hypoxia.
Despite the name "tumour necrosis factor", the levels of circulating TNF required to antagonise tumour growth may be toxic to the patient (Balkwill, 1992) and could also act as an agonist under certain conditions (Szlosarek et al., 2006).

The expression of TIMP-3 was significantly up regulated by 5 ng/mL (50 nM) TGF-β in the prostatic stromal cells PCAF (Figure 4.15) and at 50 pg/mL (0.5 nM) and 5 ng/mL (50 nM) concentrations in BPH45 (Figure 4.14). These results are in line with studies undertaken by Cross et al (Cross et al., 2005) who showed a dose-dependent up-regulation of versican, a component of ECM, and TIMP-3 in the prostate stromal cells BPH 31, 33, 44 and 45 after TGF-β treatment. Increase in ECM deposition will subsequently lead to increase in sequestering of TIMP-3 and may alter the proteinase: inhibitor balance in favour of the inhibitor, TIMP-3.

In-silico analysis of TIMP-3 revealed 10 putative AREs in the promoter region (Figure 4.17). A key feature of the putative AREs obtained was the conserved C at position 5 of H-S1 and conserved G at position 2 of H-S2. This occurrence is also seen with the PSA ARE but only the G is conserved in MVDP and hPAR1 AREs. This conserved G has been shown to be essential for the binding of androgen receptor to the DNA sequence for functionality of ARE and activation of gene transcription to occur (Fabre et al., 1994, Claessens et al., 1989, Crossley et al., 1992). The results from this project showed down-regulation of TIMP-3 transcript by 10nM DHT. The presence of putative AREs in the promoter region of this gene could mean that it is directly regulated by androgen. Although functional studies have not been carried out to validate these putative AREs as a result of limited time and resources, the presence of the conserved G at position 2 of the second half-site makes it more likely that these AREs are functional and may be regulating the transcription of TIMP-3. Also, the degree of sequence similarity of the putative AREs to the consensus ARE plus their conserved G further increases their chances of being actual AREs.
There was no identified TNF/NF-kB response elements or TGF-β response elements in the promoter region of TIMP-3, suggesting that the regulation of TIMP-3 expression by TNF and TGF-β occur via mechanisms other than those investigated.

In conclusion, the effects of DHT, TNF and TGF-β on the expression of TIMP-3 in normal prostate, prostate stromal cells and prostate cancer cells clearly reflect two different patterns; a DHT-mediated cancer-cell specific modulation of TIMP-3 and a cytokine-mediated stromal cell-specific modulation of TIMP-3. The results from this project are important in light of the fact that the tumour microenvironment consists of both cancer and stromal cells co-existing and co-migrating and an overall increase in TIMP-3 will favour reduced proteinase activity and subsequently may prevent metastasis of the tumour and *vice versa*.

In the next chapter, the effect of artificial TIMP-3 modulation was investigated in order to understand if reduction of TIMP-3 expression has functional consequences for the cells indeed affect migration of the tumour as well as other biological functions.

CHAPTER 5: siRNA-MEDIATED DOWN-REGULATION OF TIMP-3 FOR FUNCTIONAL STUDIES

5.1. INTRODUCTION

The occurrence of short interfering double-stranded RNA molecules in living cells plays a vital role in the regulation of gene expression and control of biological processes. Short interfering RNAs (siRNAs) are small double-stranded molecules of about 25 nucleotides that have been important in the analyses of gene functions. They were first observed in plants as regulators of post-translational modifications and have since been widely studied in other organisms, including humans (Hamilton and Baulcombe, 1999). siRNAs act by binding to specific mRNA molecules in living cells and effectively blocking the transcription of the target gene and down-regulating the expression of the gene products. This involves a cascade of reactions that are important for successful gene regulation (Lipardi et al., 2001).

The knowledge obtained from studying these natural dsRNA molecules has led to the production of commercially available siRNAs that have been designed to target different genes in humans (Gruber et al., 2004, Davidson and Harper, 2005, Grayson et al., 2006, Endsley et al., 2008). These have now been widely used for mode of action as well as loss of function studies (Endsley et al., 2008, Molhoek et al., 2011, Elbashir et al., 2002) and for the study of the role(s) played by different genes in disease progression. For use in *in-vitro* studies, siRNA is introduced into the cells by the process of transfection. There are several ways to achieve effective transfection, some of which have already been discussed in Section 5.2. In the course of this study, several optimization experiments were carried out to obtain the best transfection efficiency with minimal toxicity to the cells. The best protocol was the calcium phosphate transfection method as described in Section 5.2.1.

For this project, commercially available TIMP-3 silencing siRNA was purchased so as to silence the gene and study the changes in biological functions in prostate cells. The *timp-3* silencer siRNA (AM16708, Ambion) targets the fifth exon of *timp-3* gene and was shown by the manufacturer to effectively down regulate *timp-3*.

First, the gene silencer siRNA is introduced into the cells by the calcium phosphate transfection. It enters the cells and binds to an RNA-induced silencing complex (RISC), which contains active RNAse. One strand of the siRNA is incorporated into the complex and the other strand is degraded. With siRNA incorporated, the RISC is now active (aRISC) and able to recognize *timp-3* mRNA, which it binds to and degrades via the action

of RNAse. aRISC dissociates from the destroyed mRNA and is available to bind to more mRNA for destruction, thereby continuing the silencing cycle (Elbashir et al., 2001b, Elbashir et al., 2002, Elbashir et al., 2001a). Eventually, there is sufficient inhibition of gene transcription leading to inhibition of translation and protein expression. The cells can then be analysed for changes in biological behaviour and compared to control un-transfected cells or cells that have been transfected with non-targetting siRNA.

A schematic representation of the process of gene down regulation is shown in Figure 5.1.

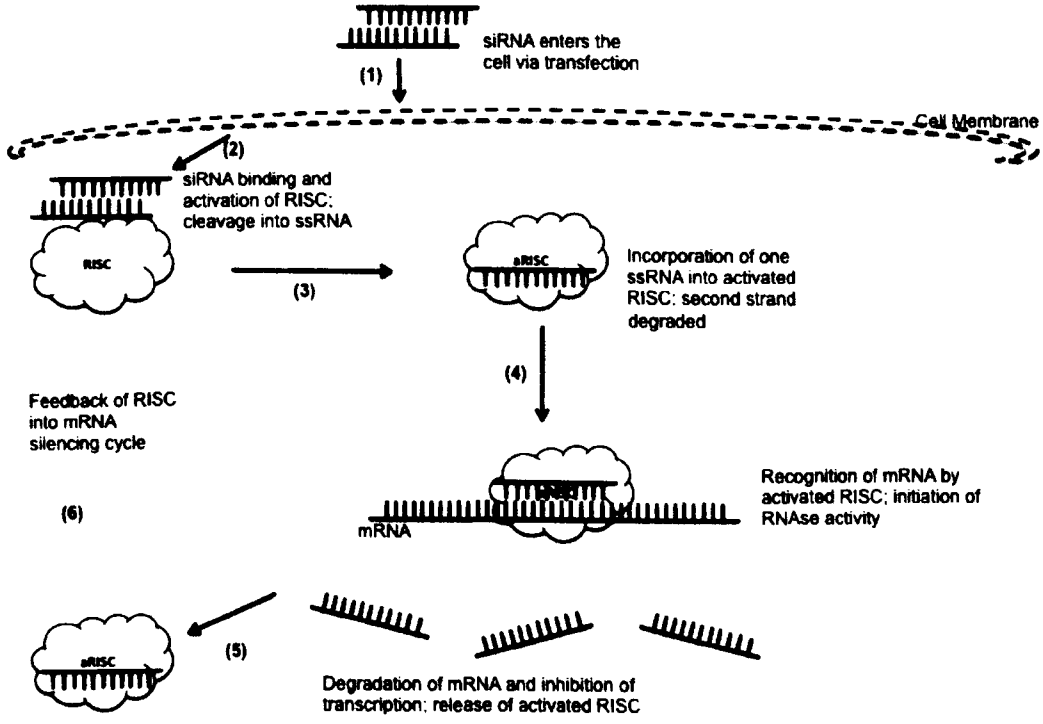

***Figure 5.1*: Schematic Diagram of the mode of action of siRNA in gene silencing.** *siRNA is introduced into the cells (1) and this binds to RISC (2), leading to its activation and subsequent cleavage of double stranded siRNA; one strand is completely degraded and the other is incorporated into the activated RISC (aRISC) complex (3). aRISC recognizes and binds to a specific mRNA and initiates the degradation activity of RNAse, leading to inhibition of transcription (4) and release of aRISC (5), which is recycled back into the mRNA silencing cycle (6).*

Several biological functions are important in the survival of a cell. There should be homeostasis between proliferation and apoptosis in tissues and this is made possible by the inherent characteristics of the individual cells that make up the tissue. In cancer, there is an altered balance in the tissue in favour of proliferation (Backus et al., 2002, Evan and Vousden, 2001, Butler et al., 1999) and this causes uncontrolled growth of the tissue and formation of a tumour. If malignant, the tumour grows in size and cancer epithelial cells break out of the primary site with the help of the increased proteinases present in them and those produced by the accompanying stromal cells (Wroblewski et al., 2002, Itoh and Nagase, 2002, Cockett et al., 1998). The cells intravasate into the blood stream and migrate to neighbouring regions and other organs of the body. Some studies have also shown that the cancer epithelial cells also co-migrate with some stromal fibroblast cells. Eventually, the cells extravasate and invade other organs and form a secondary site and co-habit with the cells in that part of the body (Vande Broek et al., 2008, Wernert, 1997). Proteinases are thought to play a key role in the migratory and invasive potential of several cancers. An increase in their expression has been observed in several advanced stage cancers (Porter et al., 2004, Molokwu et al., 2010). Again, the balance between these proteinases and their inhibitors is altered in favour of the former. As TIMP-3 is a tissue inhibitor of many extracellular metalloproteinases, the effects of siRNA-mediated down regulation of this inhibitor on biological functions such as proliferation, cell survival and apoptosis, migration, invasion and proteinase inhibition were investigated. In previous experiments in Chapter 3, it was observed that the prostate stromal cells produce very high levels of TIMP-3 compared to prostate cancer cells and that this expression was reproducible across 3 different types of stromal cells. The effect of down regulation of TIMP-3 in the prostate cancer-associated fibroblasts (PCAF) and compared the results to those obtained from non-prostate cancer-associated fibroblasts (WPMY-1) was therefore investigated. As the availability of BPH stromal cells was limited, the effect of down regulation of TIMP-3 could not be investigated in these cells, even though they had previously been available and had been used for previous experiments (Chapters 3 and 4). The experiments set up to investigate any changes in biological functions post-TIMP-3 down-regulation included: proliferation assay, apoptosis assay, migration assay, invasion assay and MMP inhibition assay.

5.2. RESULTS

5.2.1 Optimisation of Transfection

There were three methods of reverse transfection employed in this study, as described in Section 2.13. These were carried out in order to determine the optimal conditions of siRNA transfection that gave the best gene knockdown. The methods include: electroporation, lipid-based Dharmafect-2 and calcium phosphate transfection methods. With all three, there was a degree of transfection complex-mediated loss of gene transcript compared to untransfected control (see Figure 5.2 and 5.3) in both PCAF and WPMY-1 cells.

The calcium phosphate transfection gave the best results, with <20% toxicity of the transfection complex and so this was used for subsequent transfection experiments. In PCAF (Figure 5.2) and WPMY-1 (Figure 5.3) cells, there was ~19% knockdown of timp-3 mRNA with the calcium phosphate transcription complex alone and ~ 85-89% knockdown of timp-3 mRNA with timp-3 targeted siRNA (n=4). The net knockdown, taking the effect of transfection complex into consideration, was therefore ~70% - this level of knockdown was still sufficient for protein depletion in the ECM of cells, as measured by western blotting (see Figures 5.4 and 5.5). The electroporation and Dharmafect-2 transfection transfection methods gave unfavourable loss of gene transcript with transfection complex alone (between 35 and 45% loss) in both cell lines so were not pursued further.

The data sets for these optimisation experiments were n=2 (Figures 5.2 and 5.3) so it was not possible to do reliable statistical analyses on the results. However, for the subsequent experiments, the data sets were at least n=3 (Figures 5.4 onwards) and statistical analyses were carried out.

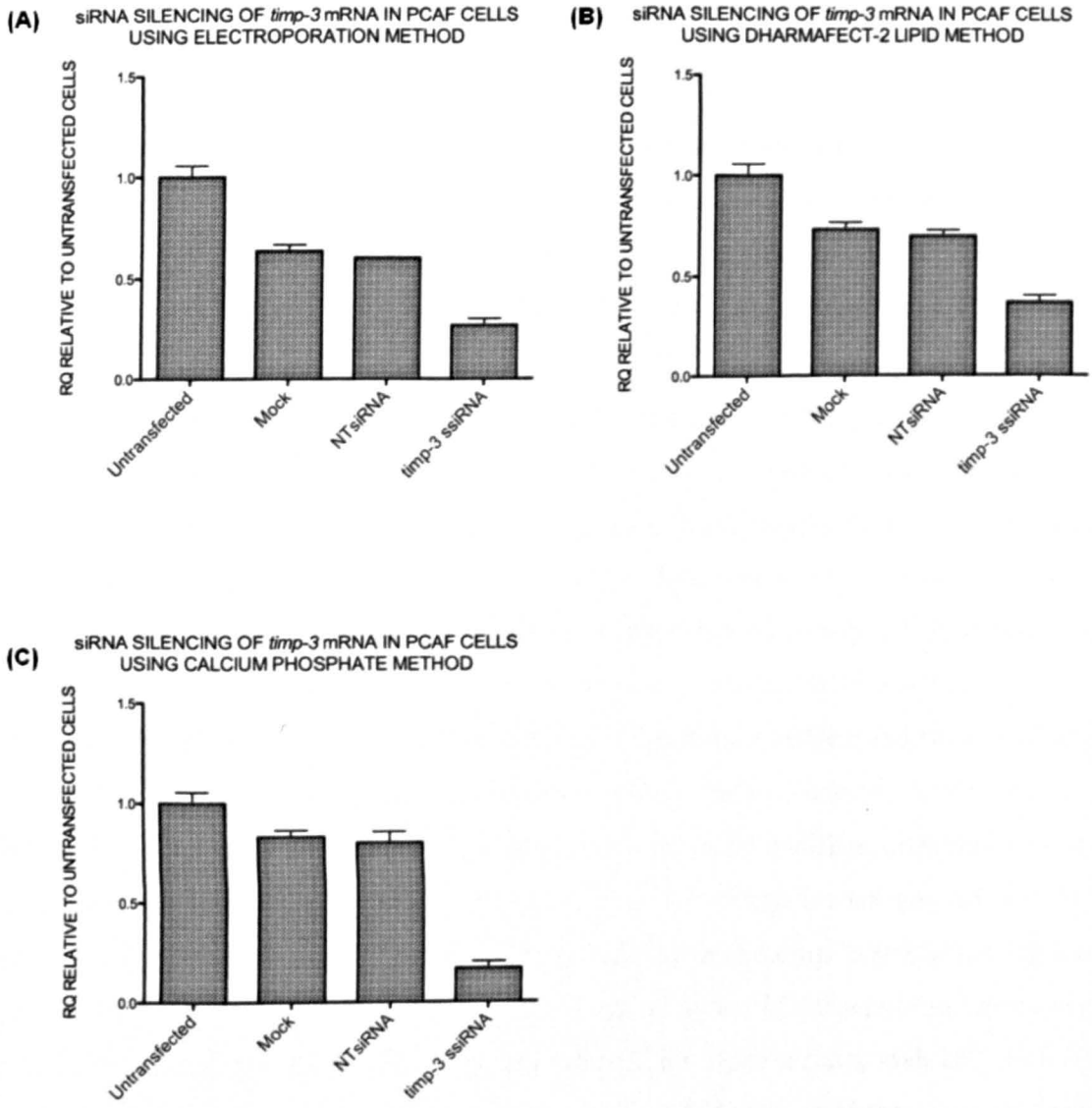

Figure 5.2: Transfection of PCAF cells using different transfection methods.
100,000 cells were reverse-transfected as described in Section 2.13 and the transcription complex was maintained in the cells for 24 hours after which the medium was changed to antibiotic-free, serum-containing media for another 3 days. The cells were then uplifted from the ECM, RNA extracted, cDNA prepared and mRNA produced via qPCR as described in Section 2.6 – 2.9. (A) There was ~40% down-regulation of timp-3 mRNA with the transfection complex alone (Mock) and this remained unchanged with the non-targeting siRNA (NTsiRNA). There was ~ 70% down-regulation of timp-3 mRNA with timp-3 targeting silencer siRNA (timp-3 ssiRNA) (n=2). (B) There was ~25% down-regulation of timp-3 mRNA with the transfection complex alone (Mock) and this remained unchanged with the non-targeting siRNA (NTsiRNA). There was ~ 70% down-regulation of timp-3 mRNA with timp-3 targeting silencer siRNA (timp-3 ssiRNA) (n=2) (C) There was ~19% down-regulation of timp-3 mRNA with the transfection complex alone (Mock) and this remained unchanged with the non-targeting siRNA (NTsiRNA). There was ~ 85% down-regulation of timp-3 mRNA with timp-3 targeting silencer siRNA (timp-3 ssiRNA) (n=2).

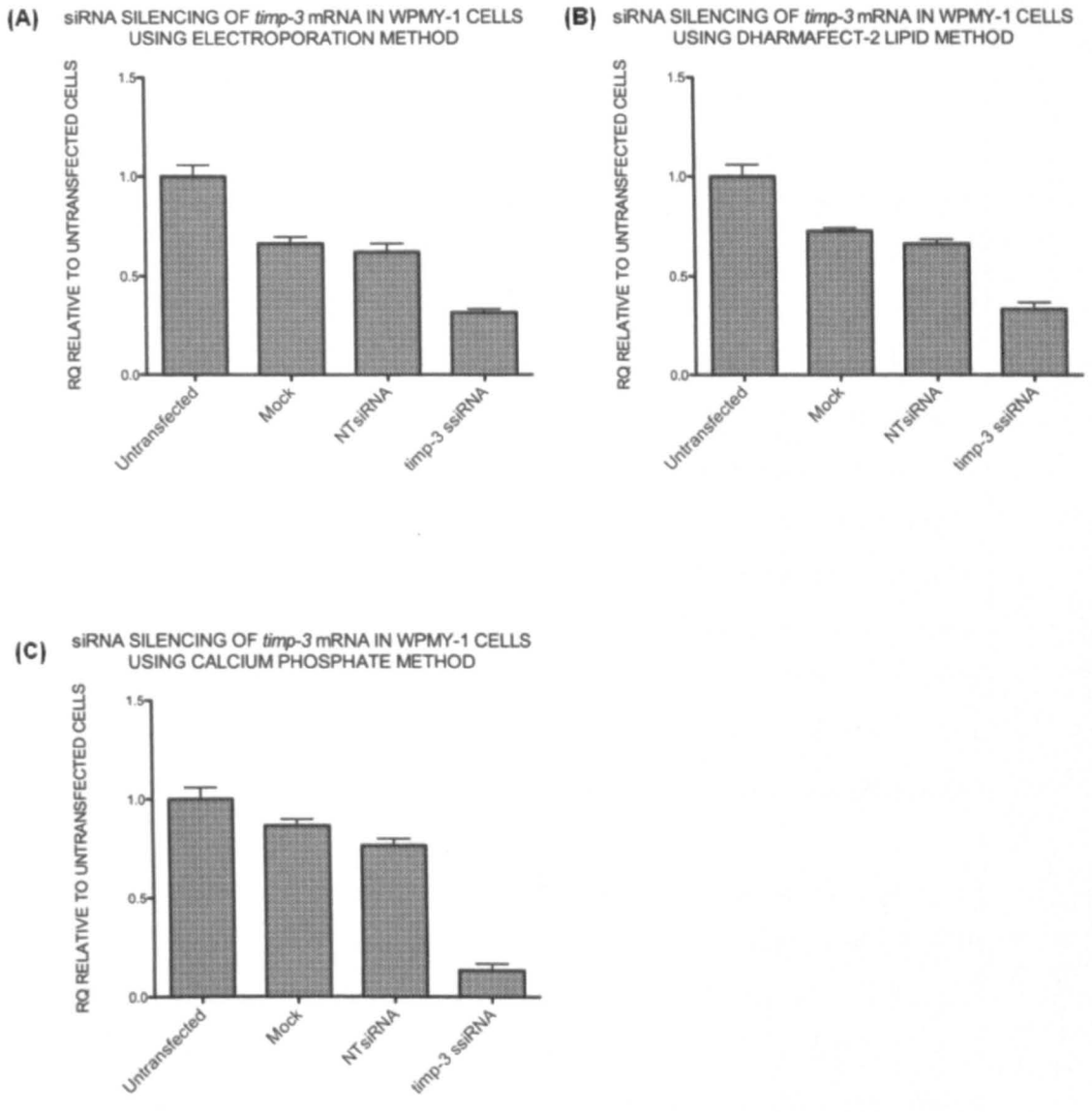

Figure 5.3: Transfection of WPMY-1 cells using different transfection methods.
(A) There was ~45% down-regulation of timp-3 mRNA with the transfection complex alone (Mock) and this remained unchanged with the non-targeting siRNA (NTsiRNA). There was ~ 70% down-regulation of timp-3 mRNA with timp-3 targeting silencer siRNA (timp-3 ssiRNA) (n=2). (B) There was ~30% down-regulation of timp-3 mRNA with the transfection complex alone (Mock) and this remained unchanged with the non-targeting siRNA (NTsiRNA). There was ~ 70% down-regulation of timp-3 mRNA with timp-3 targeting silencer siRNA (timp-3 ssiRNA) (n=2) (C) There was ~20% down-regulation of timp-3 mRNA with the transfection complex alone (Mock) and this remained unchanged with the non-targeting siRNA (NTsiRNA). There was ~ 89% down-regulation of timp-3 mRNA with timp-3 targeting silencer siRNA (timp-3 ssiRNA) (n=2).

5.2.2 Down regulation of TIMP-3 in Prostate Cells

PCAF and WPMY-1 cells were grown to ~80% confluence and afterwards harvested for reverse transfection using the calcium phosphate method. The transfection complex was maintained in the cells for 4 days to allow for better silencing effects and afterwards the cells were uplifted from the ECM and counted. The ECM was harvested as described in Section 2.10 and subjected to SDS-PAGE and western blotting. RNA was extracted from the cells and subjected to reverse transcriptase PCR for cDNA production and qPCR for quantification of timp-3 mRNA. The controls for these sets of experiments were the cells transfected with the non-targetting siRNA (NTsiRNA) and the test experiments were the cells transfected with *timp-3* silencer siRNA (timp-3 ssiRNA).

Duplicate experiments were also set up in order to monitor changes in TIMP-3 expression by immunocytochemistry as previously described in Section 2.17. The cells were grown on glass slides after reverse transfection for 4 days and formaldehyde-fixed onto the slides prior to staining with primary mouse anti-TIMP-3 antibody and counterstained with fluorescent anti-mouse antibody. The fixed cells were also counter-stained with the DAPI nuclear stain to differentiate nuclear from cytoplasmic and ECM staining.

The results from the experiments showed a significant down regulation of timp-3 mRNA in PCAF cells (n=4, p=0.0286 Mann-Whitney) and in WPMY-1 cells (n=4, p=0.0294 Mann-Whitney) transfected with timp-3 ssiRNA when compared to cells transfected with NTsiRNA. These results were also corroborated at the protein level by western blotting of PCAF and WPMY-1 ECM extracts (see Figures 5.4 and 5.5 respectively) and by immunostaining of duplicate PCAF and WPMY-1 cells (see Figure 5.6 and 5.7 respectively). The expression of TIMP-3 in immunostained cells was cytoplasmic to a small extent and largely extracellular, supporting its expression predominantly in the ECM.

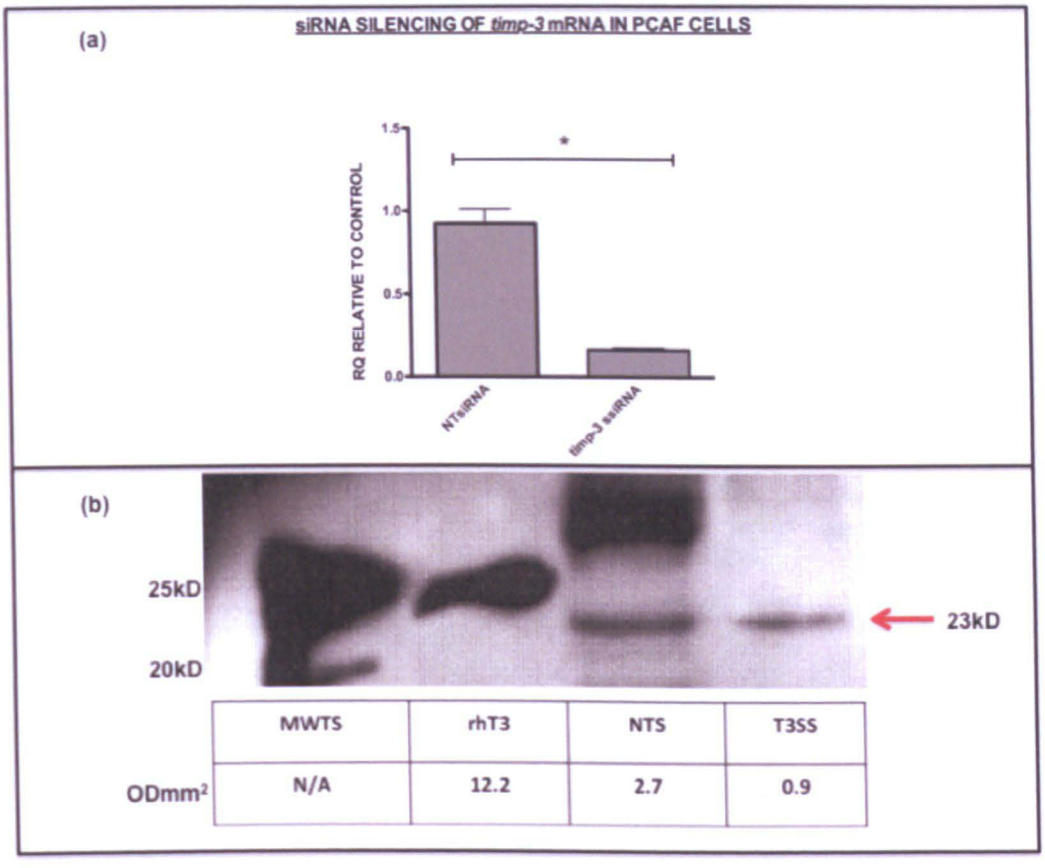

Figure 5.4: siRNA Silencing of timp-3 in PCAF cells.

100,000 cells were reverse-transfected as described in Section 2.13 and the transcription complex was maintained in the cells for 24 hours after which the medium was changed to antibiotic-free, serum-containing media for another 3 days. The cells were then uplifted from the ECM, RNA extracted, cDNA prepared and mRNA produced via qPCR as described in Section 2.6 – 2.9. (a) There was significant down regulation of timp-3 mRNA in timp-3 ssiRNA transfected PCAF cells compared to NTsiRNA transfected (control) cells (n=4, p=0.0286, Mann-Whitney).

(b) ECM was extracted as described in Section 2.10 and 100,000 cells' worth of ECM was immuno-blotted for TIMP-3 as described in Section 2.11. 5 nM of recombinant human TIMP-3 was also loaded as control. The western blots were analysed by densitometry as described in Section 2.12. There was a loss of TIMP-3 protein in the ECM after TIMP-3 down regulation in PCAF cells (see red arrow at the 23 kD area) when compared to ECM from NTsiRNA transfected control cells. MWTS = Molecular weight standards, rhT3 = recombinant human TIMP-3, NTS = ECM from Non-targetting siRNA transfected cells, T3SS = ECM from timp-3 silencer siRNA transfected cells (n=3)

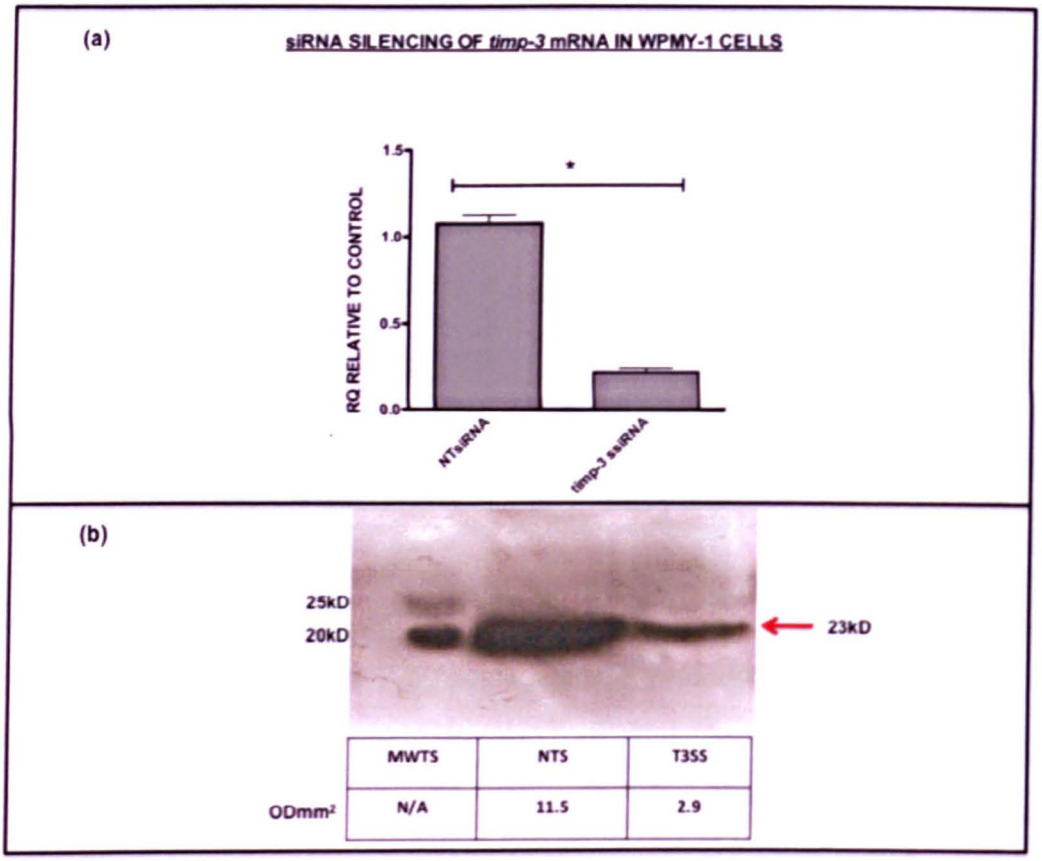

Figure 5.5: siRNA Silencing of timp-3 in WPMY-1 cells.
(a) There was significant down regulation of timp-3 mRNA in timp-3 ssiRNA transfected WPMY-1 cells compared to NTsiRNA transfected (control) cells (n=4, p=0.0294, Mann-Whitney), n=3
(b) There was a loss of TIMP-3 protein in the ECM after TIMP-3 down regulation in WPMY-1 cells (see red arrow at the 23 kD area) when compared to ECM from NTsiRNA transfected control cells. MWTS = Molecular weight standards, NTS = ECM from Non-targetting siRNA transfected cells, T3SS = ECM from timp-3 silencer siRNA transfected cells. n=3

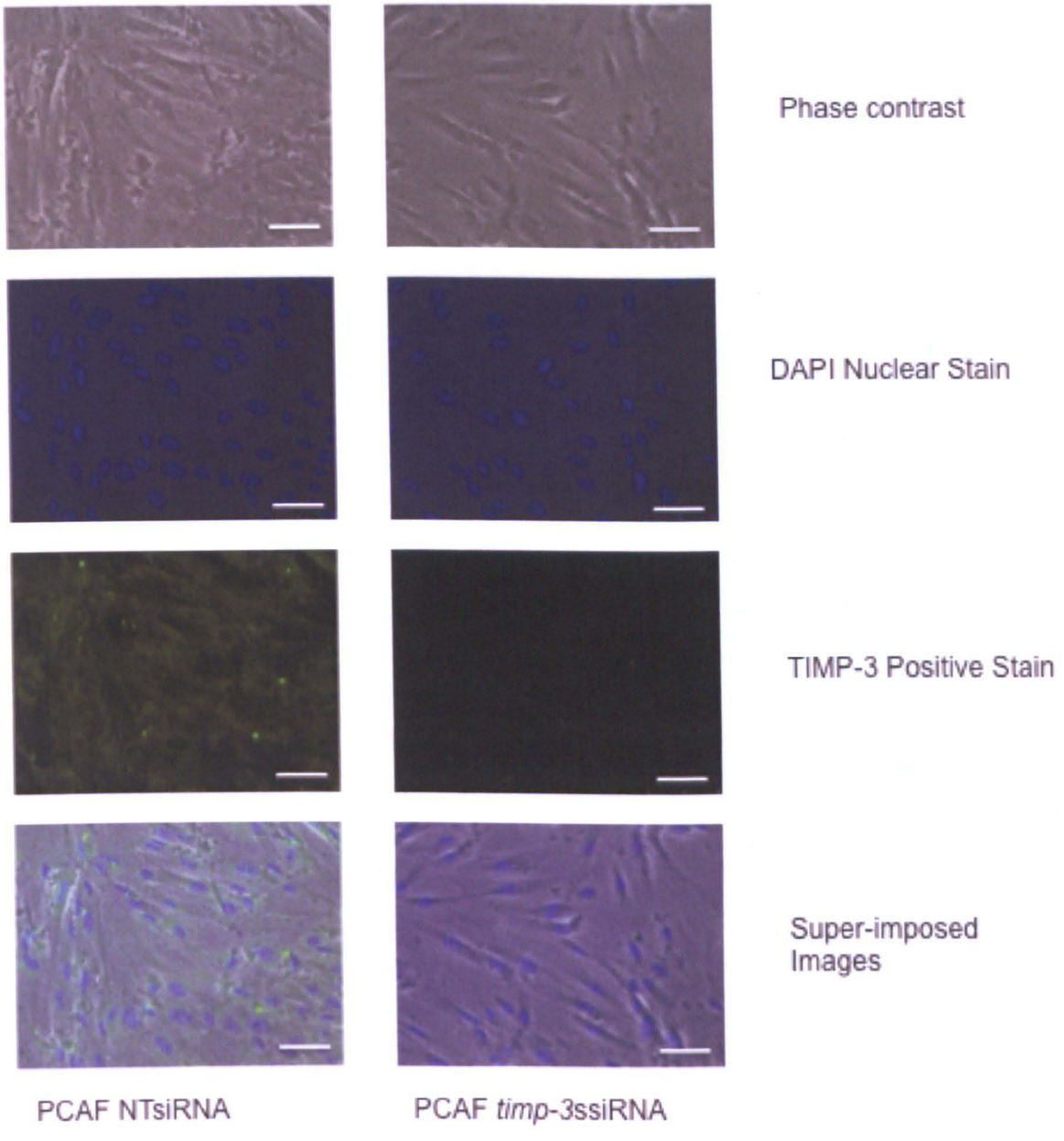

Figure 5.6: Immunocytochemistry and Imaging of Transfected PCAF Cells.
The above is a representative example of results from 4 experimental repeats. 25,000 cells were reverse transfected as described in Section 2.13 and seeded into chambers on a glass slide. The transcription complex was maintained in the cells for 24 hours after which the media was changed to antibiotic-free, serum-containing media for another 3 days. Afterwards, the cells were subjected to immunocytochemistry as described in Section 2.17. The cells were incubated with mouse anti-TIMP-3 antibody for 24 hours and green fluorescent anti-mouse secondary antibody for 1 hour. The cells were imaged using a fluorescent microscope at 10X objective. There was loss of the green fluorescence in timp-3 ssiRNA transfected PCAF cells compared to the control NTsiRNA transfected cells as shown in the bottom 4 images. Scale bar = 100 um.

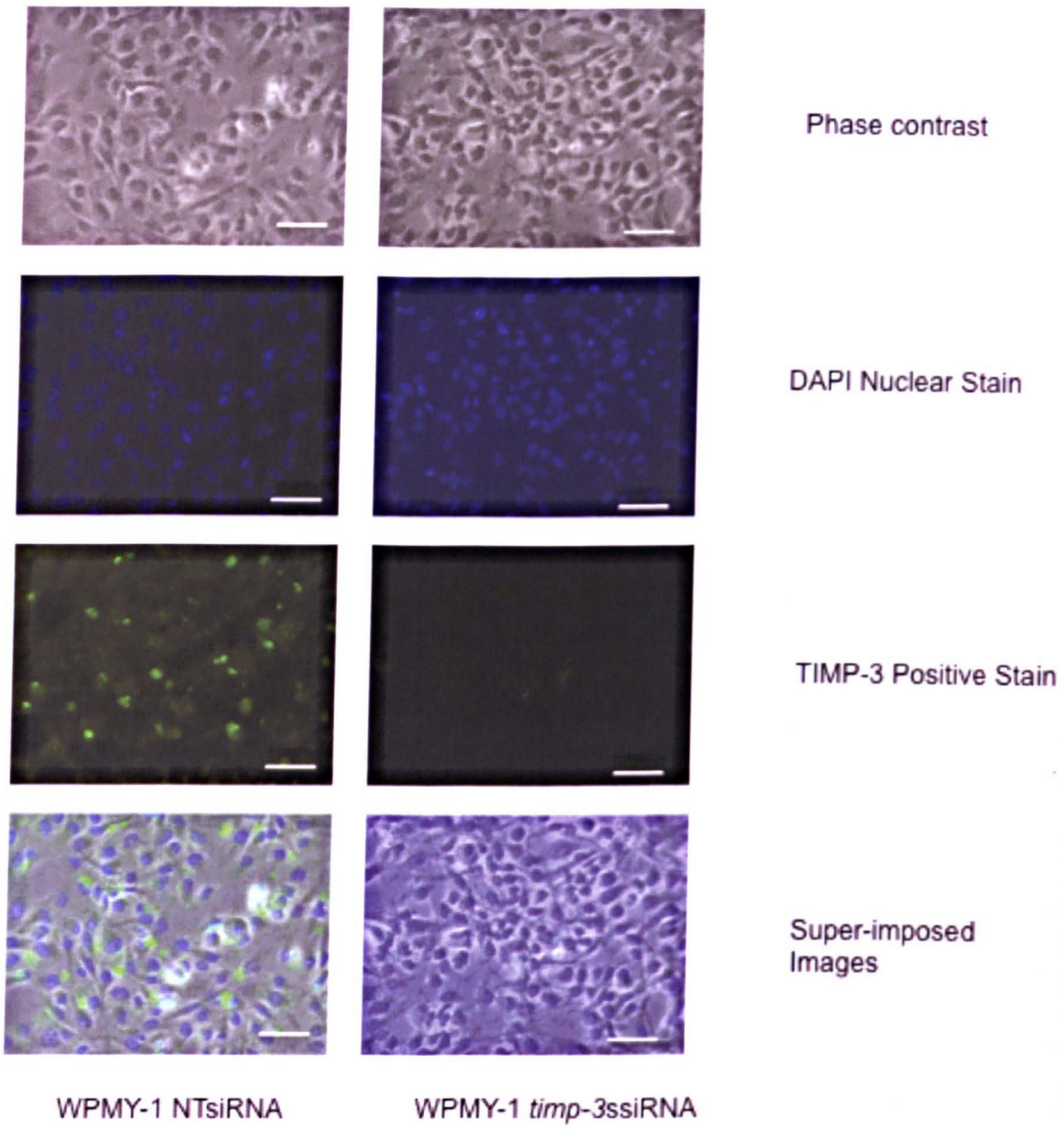

Figure 5.7: Immunocytochemistry and Imaging of Transfected WPMY-1 Cells.
The above is a representative example of results from 4 experimental repeats. 25,000 cells were reverse transfected as described in Section 2.13 and seeded into chambers on a glass slide. The transcription complex was maintained in the cells for 24 hours after which the media was changed to antibiotic-free, serum-containing media for another 3 days. Afterwards, the cells were subjected to immunocytochemistry as described in Section 2.17. The cells were incubated with mouse anti-TIMP-3 antibody for 24 hours and green fluorescent anti-mouse secondary antibody for 1 hour. The cells were imaged using a fluorescent microscope at 10X objective. There was a loss of the green fluorescence in timp-3 ssiRNA transfected WPMY-1cells compared to the control NTsiRNA transfected cells as shown in the bottom 4 images. Scale bar = 100 um.

The proliferation assay was carried out using the coulter counter method as described in Section 2.16.1. The cells were counted after being uplifted from the ECM using the coulter counter 4 days post transfection. There was no significant difference in the number of NTsiRNA and timp-3 ssiRNA transfected PCAF and WPMY-1 cells (see Figure 5.8).

The apoptosis assay was carried out using the Annexin-v-FITC/PI method as discussed in Section 2.16.4. The cells, 48 hours post-transfection were stained with Annexin-V/FITC to detect apoptotic cells and counter-stained with PI to exclude cells that were necrotic. The results from this project showed a significant increase in apoptosis in PCAF cells after down regulation of TIMP-3 (n=3, p=0.0265 Mann-Whitney) compared to cells that had been transfected with NTsiRNA (see Figure 5.9). This increase in cellular apoptosis was not detected in timp-3 ssiRNA-transfected WPMY-1 cells (see Figure 5.10).

The migration assay was carried out using the 3D trans-well Boyden chamber method without Matrigel as described in Section 2.15.2. After transfection with timp-3 ssiRNA, the cells were seeded onto the upper compartment of the Boyden chamber and were allowed to migrate towards the chemo-attractant (complete medium with serum) in the lower chamber. The number of cells that migrated was counted 48 hours post-seeding via cellular staining with crystal violet. These results showed significantly lower migration of timp-3 down-regulated PCAF cells when compared to the control NTsiRNA cells (n=4, p=0.0294, Mann-Whitney) (see Figure 5.11). The opposite result was observed in timp-3 down regulated WPMY-1 cells where a significant increase in the migration potential was seen in comparison to the control cells (n=4, p=0.0294, Mann-Whitney) (see Figure 5.12). It is worth mentioning, at this point, that the PCAF cells are cancer-associated fibroblasts and the WPMY-1 cells are non-cancer associated fibroblasts.

The invasion assay was carried out using the modified Boyden chamber method as described in Section 2.15.3. - this is similar to the migration assay as above but the membrane dividing the upper and the lower compartments of the Boyden chamber is layered with growth factor-reduced Matrigel. This system therefore artificially mimics the barrier that cells will come across when invading tissues by crossing a basement membrane. There was significantly lower invasion of timp-3 down-regulated PCAF cells when compared to the control cells (n=4, p= 0.0265, Mann-Whitney) (see Figure 5.13). Again, the opposite result was observed in timp-3 down-regulated WPMY-1 cells where a

significant increase in the invasive potential was seen in comparison to the control cells (n=4, p=0.0265, Mann-Whitney) (see Figure 5.14).

The proteinase inhibition assay was carried out as described in Section 2.16. The ECM was extracted from transfected cells and analysed for its MMP-inhibitory properties. The rate of MMP inhibition was measured using the Flusys Software, where a deviation from a Vi/V_0 of <1 was regarded as inhibition of MMP activity. The NDLB buffer used had little or no MMP inhibitory property (see Figure 5.15). As a positive control, 5 nM rhTIMP-3 was also made up in NDLB and tested for its activity on MMP and inhibited MMP-2 by 79% (see Figure 5.15). ECM extracts from PCAF and WPMY-1 cells inhibited MMP-2, by 48% and 45%. When the timp-3 mRNA was knocked down, these values were reduced to 17% and 20% respectively. The results from PCAF cells are shown in Figure 5.16.

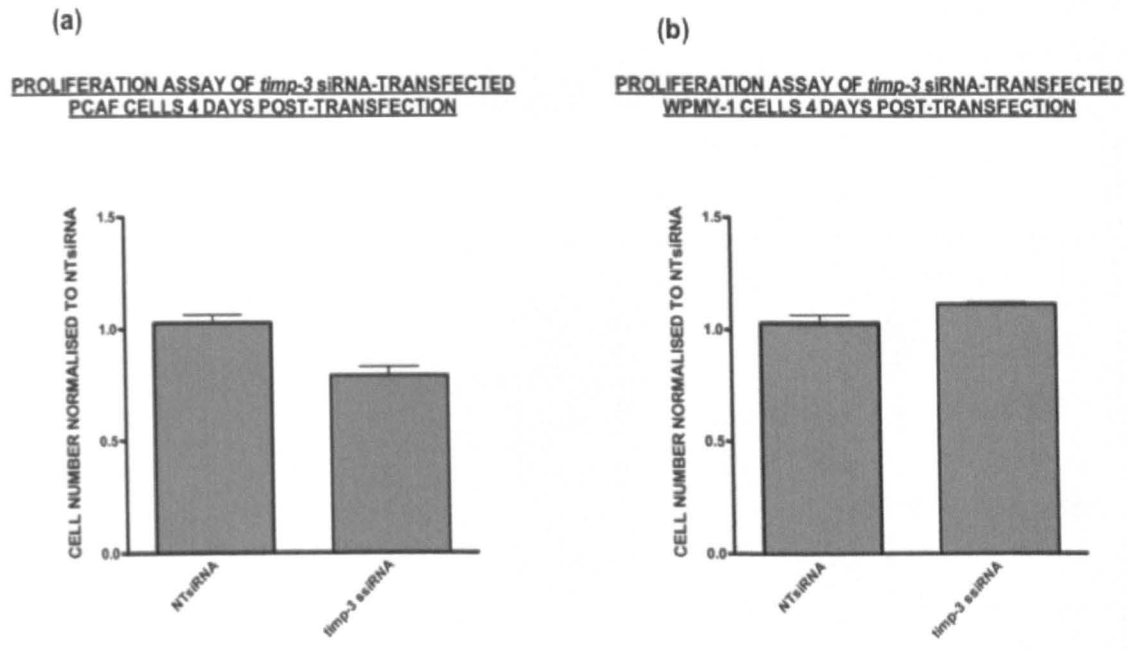

Figure 5.8: Coulter Counter Proliferation Assay of Transfected PCAF and WPMY-1 cells. *100,000 cells were reverse-transfected as described in Section 2.13 and the transcription complex was maintained in the cells for 24 hours after which the media was changed to antibiotic-free, serum-containing media for another 3 days. Afterwards, the cells were uplifted from the ECM and counted as described in Section 2.15.1. The counts from timp-3 ssiRNA transfected cells were normalized to counts from NTsiRNA transfected cells. Results showed no significant proliferative difference between timp-3 ssiRNA transfected cells when compared to control for both PCAF and WPMY-1 cells (a) and (b) respectively.*

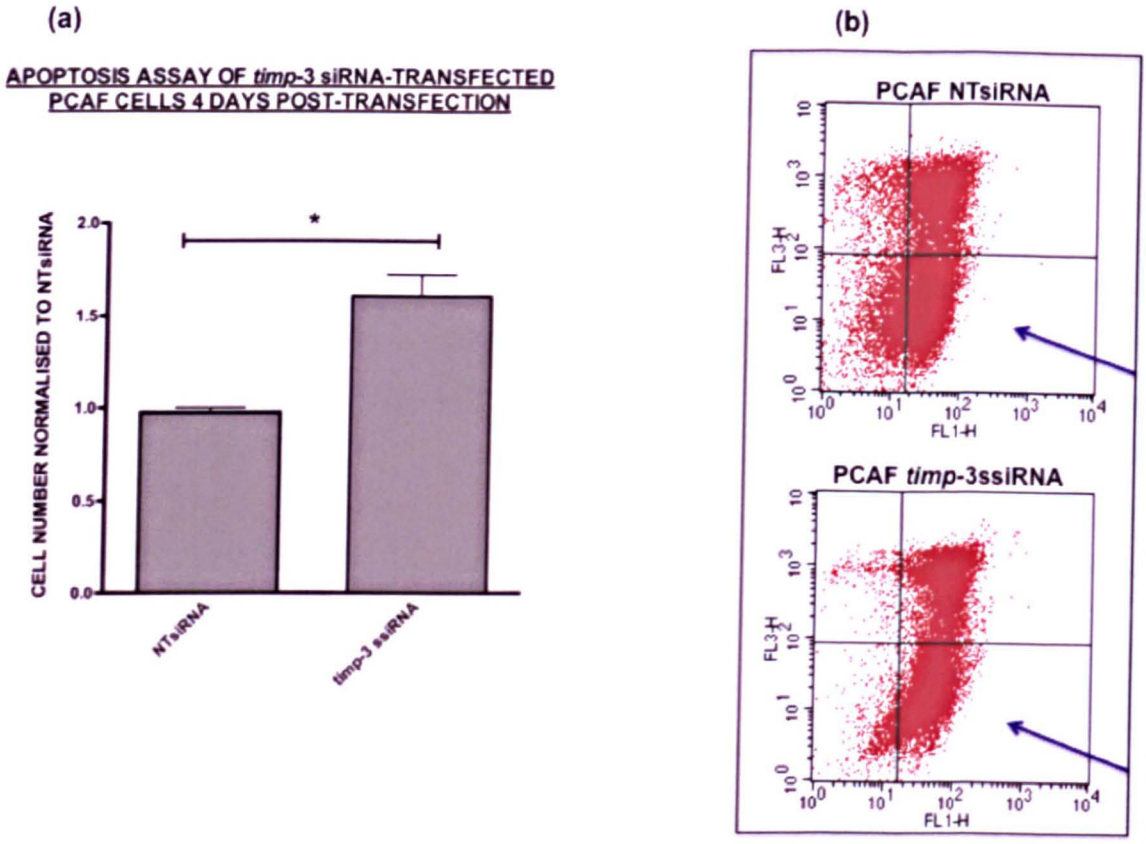

Figure 5.9: Apoptosis Assay of Transfected PCAF Cells.
100,000 cells were reverse-transfected as described in Section 2.13 and the transcription complex was maintained in the cells for 24 hours after which the media was changed to antibiotic-free, serum-containing media for another 3 days. Afterwards, the cells were uplifted from the ECM and stained with Annexin-V-FITC and Propidium Iodide (PI) for FACS analysis as described in Section 2.15.4. (a) The counts from timp-3 ssiRNA transfected cells were normalized to counts from NTsiRNA transfected cells. There was a significant increase in the number of apoptotic PCAF cells after transfection with timp-3 ssiRNA relative to NTsiRNA control cells (n=3, p=0.0265, Mann-Whitney).
(b) A shift to the right side of the graph represents an increase in apoptotic Annexin-V-FITC positive cells while a shift to the top of the graph represents an increase in necrotic PI-positive cells. In both NTsiRNA and timp-3ssiRNA transfected PCAF cells, a proportion of the cells displayed a necrotic profile (top left and right quadrant) but in the latter, there was a shift of non-apoptotic (bottom left) towards apoptosis (bottom right – indicated by blue arrow). This population of cells were analysed and counts graphically represented as in (a). n=3

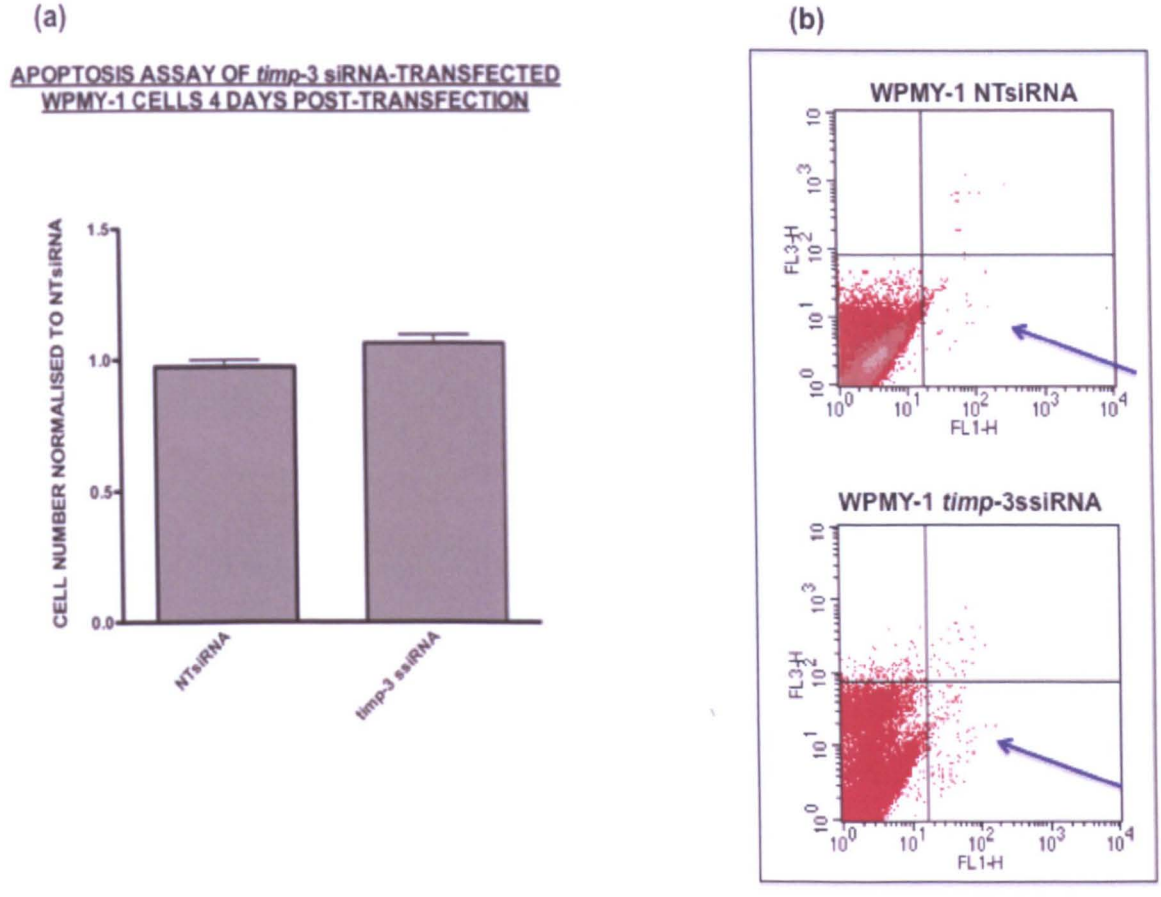

Figure 5.10: Apoptosis Assay of Transfected WPMY-1 Cells.

(a) There was no significant level of apoptosis in NTsiRNA and timp-3ssiRNA-transfected WPMY-1 cells. This is also indicated by the minimal number of counts in the bottom right quadrant (blue arrow) of timp-3 ssiRNA transfected WPMY-1 cells when compared to NTsiRNA transfected control cells

(b) In both NTsiRNA and timp-3ssiRNA transfected WPMY-1 cells, there were minimal necrotic cells (top left and right quadrant) but in the latter, there was a slight but non-statistically significant shift of non-apoptotic (bottom left) towards apoptosis (bottom right – indicated by blue arrow). This population of cells were analysed and counts graphically represented in (a). n=3

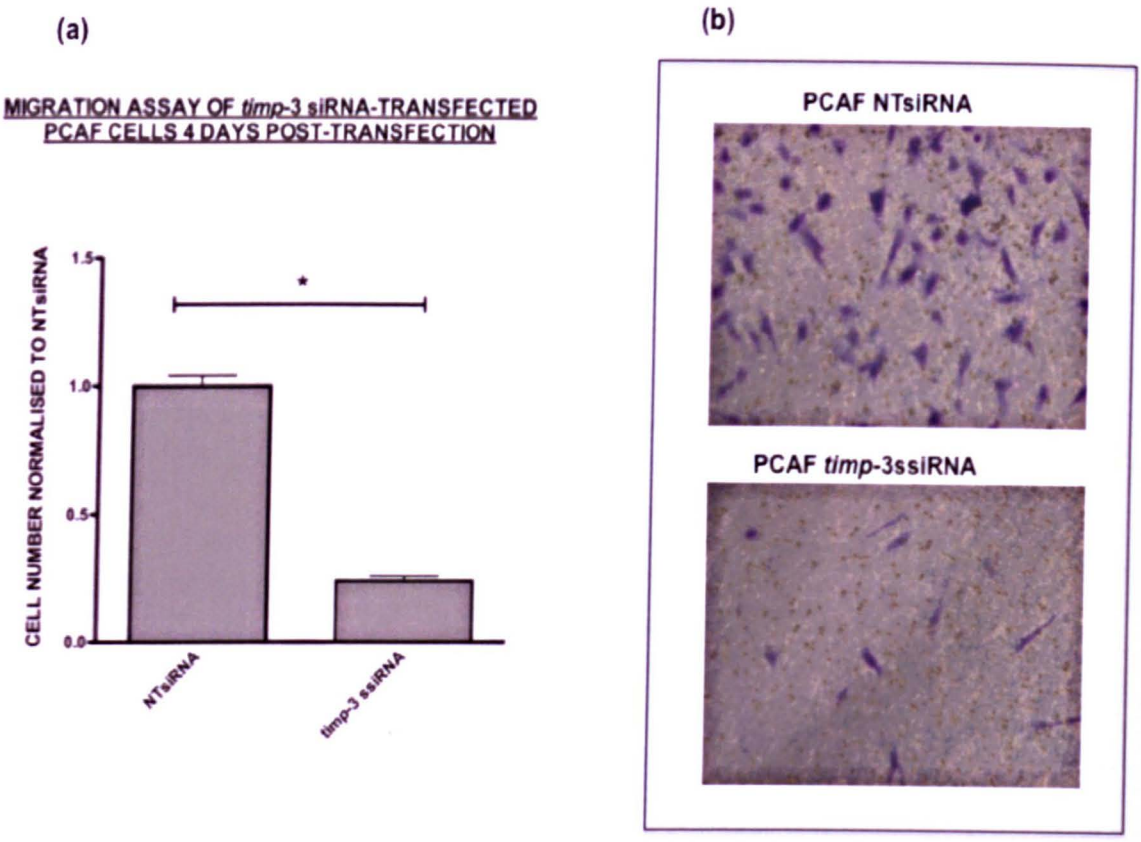

Figure 5.11: Migration Assay of Transfected PCAF Cells.
After reverse transfection of the cells for 4 days, the cells were uplifted and counted. 25,000 transfected cells were seeded onto the upper compartment of the Boyden chamber, as described in Section 2.15.2. The migrated cells were stained 48 hours post-seeding. The counts from timp-3 ssiRNA transfected cells were normalized to counts from NTsiRNA transfected cells. There was a significant decrease in the number of migrated PCAF cells after transfection with timp-3 ssiRNA relative to NTsiRNA control cells (n=4, p=0.0294, Mann-Whitney) – this is represented graphically in (a) and pictorially in (b) n=3

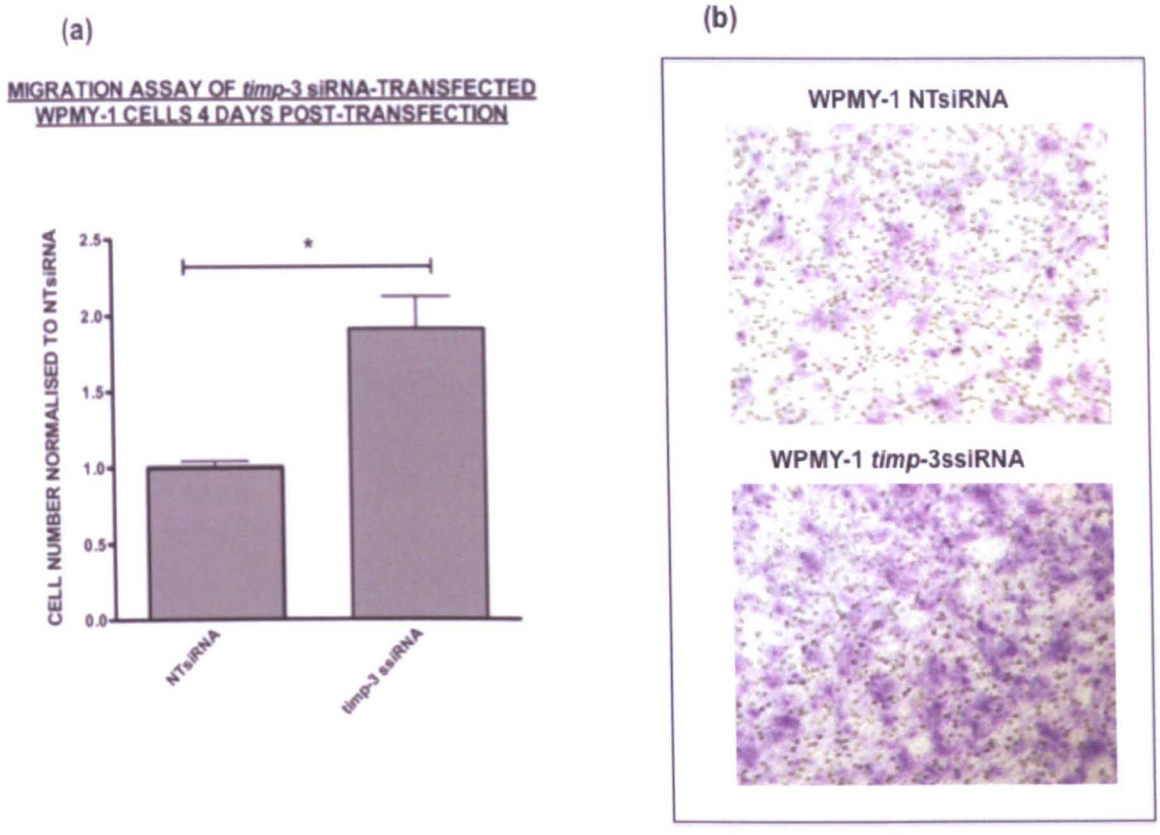

Figure 5.12: Migration Assay of Transfected WPMY-1 Cells.
After reverse transfection of the cells for 4 days, the cells were uplifted and counted. 25,000 transfected cells were seeded onto the upper compartment of the Boyden chamber, as described in Section 2.15.2. The migrated cells were stained 48 hours post-seeding. The counts from timp-3 ssiRNA transfected cells were normalized to counts from NTsiRNA transfected cells. Results showed a significant increase in the number of migrated WPMY-1 cells after transfection with timp-3 ssiRNA relative to NTsiRNA control cells (n=4, p=0.0294, Mann-Whitney) – this is represented graphically in (a) and pictorially in (b). n=3

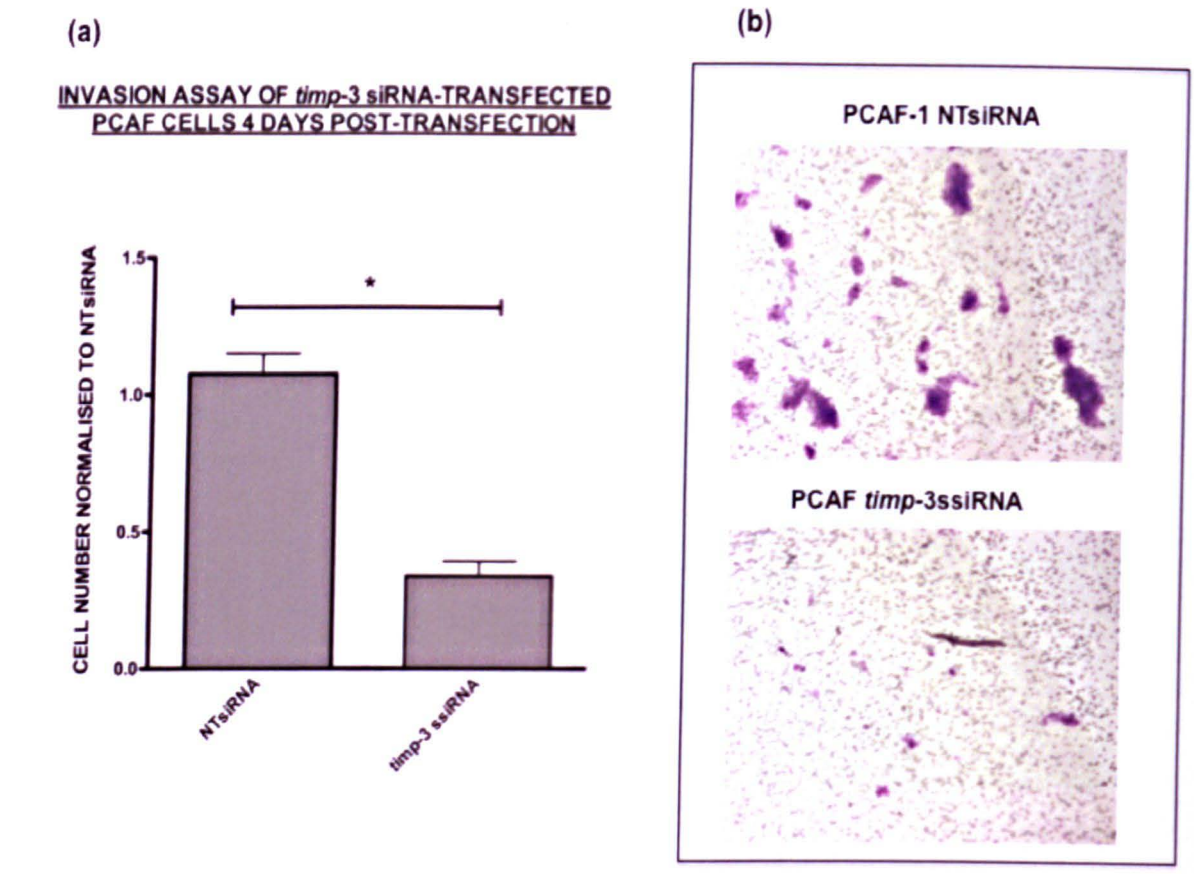

Figure 5.13: Invasion Assay of Transfected PCAF Cells.
After reverse transfection of the cells for 4 days, the cells were uplifted and counted. 25,000 transfected cells were seeded onto the upper compartment of the Boyden chamber, as described in Section 2.15.3. The cells that passed through the matrigel were stained 48 hours post-seeding. The counts from timp-3 ssiRNA transfected cells were normalized to counts from NTsiRNA transfected cells. Results showed a significant decrease in the number of invasive PCAF cells after transfection with timp-3 ssiRNA relative to NTsiRNA control cells (n=4, p=0.0265, Mann-Whitney) – this is represented graphically in (a) and pictorially in (b) n=3

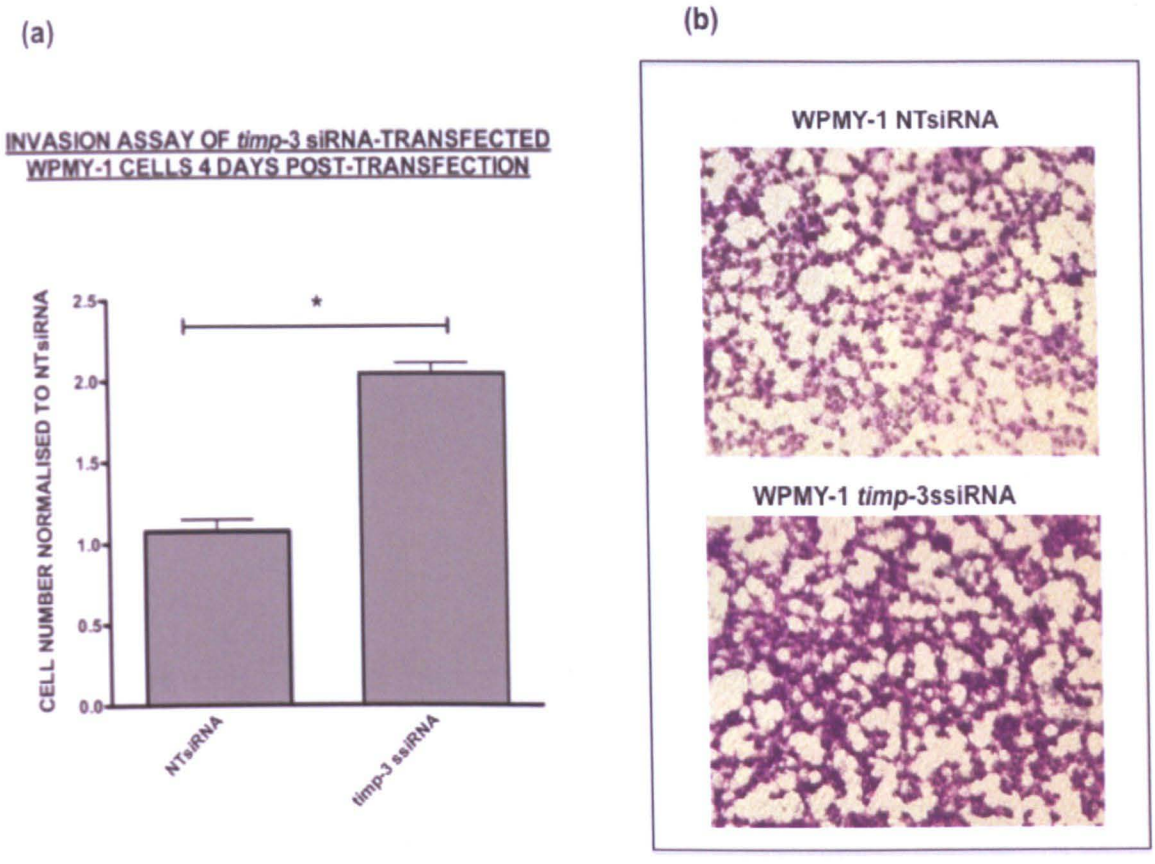

Figure 5.14: Invasion Assay of Transfected WPMY-1 Cells.
After reverse transfection of the cells for 4 days, the cells were uplifted and counted. 25,000 transfected cells were seeded onto the upper compartment of the Boyden chamber, as described in Section 2.15.3. The cells that passed through the matrigel were stained 48 hours post-seeding. The counts from timp-3 ssiRNA transfected cells were normalized to counts from NTsiRNA transfected cells. Results showed a significant increase in the number of invasive WPMY-1 cells after transfection with timp-3 ssiRNA relative to NTsiRNA control cells (n=4, p=0.0265, Mann-Whitney) – this is represented graphically in (a) and pictorially in (b) n=3

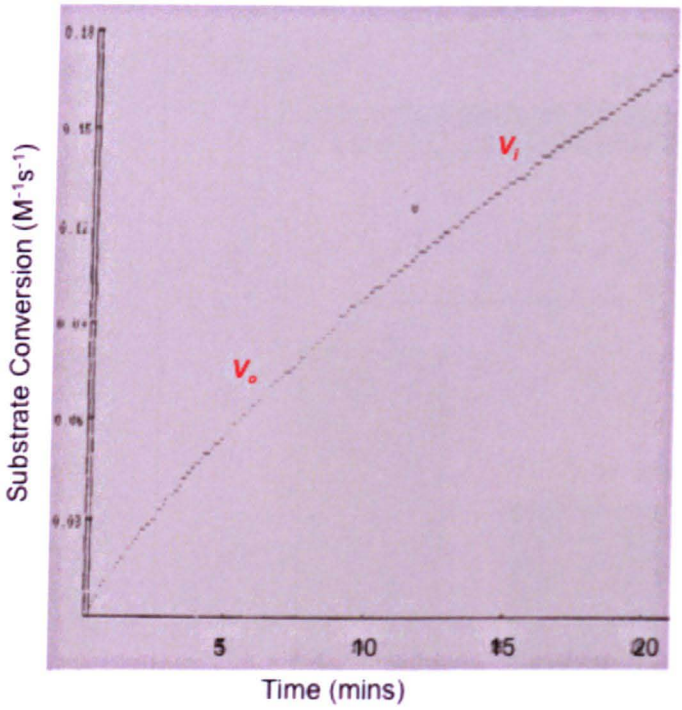

Figure 5.15: Control Experiment for the Proteinase Inhibition Assay.
3 uM of the non-denaturing lysis buffer (NDLB) was added to the cuvette at v on the graph and had minimal effect on the activity of MMP-2

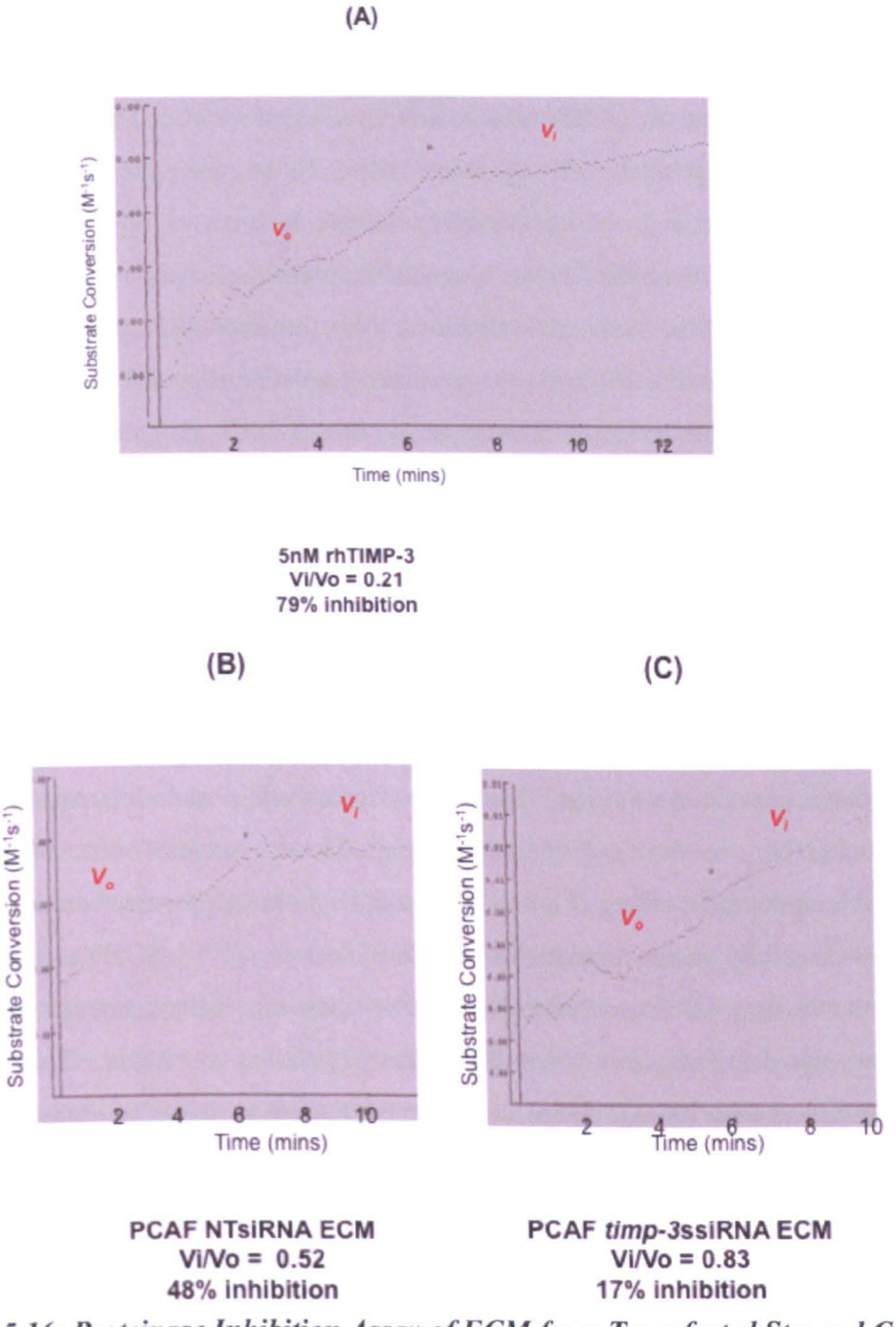

Figure 5.16: Proteinase Inhibition Assay of ECM from Transfected Stromal Cells.
Cells were reverse transfected and after 4 days, ECM was extracted and subjected to the proteinase inhibition assay as described in Section 2.16. 5 nM of recombinant human TIMP-3 (rhTIMP-3)(A) or 100,000 cells' worth of ECM was added to the substrate-MMP-2 mixture and the change in rate of substrate breakdown measured (V_1). A V_i/V_0 value of 0.21 was achieved by rhTIMP-3, meaning that there was 79% inhibition of MMP-2 activity. A Vi/V_0 value of 0.52 with ECM of PCAF transfected with control NTsiRNA., implying a 48% inhibition of MMP-2 activity. With ECM from the timp-3 ssiRNA transfected PCAF and WPMY-1 cells, the V_1/V_0 was 0.83, implying 17% inhibition.

5.3. DISCUSSION

To my knowledge, this is the first investigation of the role of TIMP-3 in biological functions in prostate cells by using siRNA to down-regulate the expression of TIMP-3. It enhances the body of knowledge available to improve on therapy by focusing on other factors apart from the known 'culprits' responsible for poor prognosis of prostate cancer. It is also the first study to look closer into the expression patterns and role(s) played by prostate stromal cells in the progression of prostate cancer. TIMP-3 is an endogenous tissue inhibitor of many metalloproteinases involved in the progression of many cancers, and the study of its pattern of expression and modulation would greatly enhance our understanding and management.

In this project, siRNA-mediated down regulation of *timp-3* in cancer-associated PCAF and non-cancer associated WPMY-1 prostate stromal cells was carried out successfully using the calcium phosphate reverse transfection method (Figure 5.2 and 5.3), with significant down-regulation of timp-3 gene transcription and protein expression (Figure 5.4 and 5.5) achieved 4 days post-transfection. These results were also corroborated by immunocytochemistry (Figure 5.6 and 5.7). Although the expression of *timp-3* mRNA was successfully down-regulated in prostate cancer cells LNCaP at the first trial (data not shown as n=1), it was decided not to carry out further experiments with these down-regulated cells as only about 50% down regulation was achieved and the LNCaP cells do not produce a lot of TIMP-3 in the first instance, as shown in Figure 3.8. The LNCaP cells also do not lay down much ECM and TIMP-3 has been undetected in the little ECM that they make. PC3 cells produce negligible *timp-3* mRNA and protein as well, so it was not feasible to use them in these sets of experiments. Instead, the readily available PCAF and WPMY-1 prostate stromal cells were studied, in light of the literature at the time that suggested a tumour-stroma migration and interaction, and in light of previous results from this project showing a decrease in the expression of TIMP-3 in both of the prostate stromal cells PCAF and WPMY-1 after co-culturing with prostate cancer cells LNCaP (see Figures 3.22 and 3.23). It was important to understand the implication of the loss of this endogenous proteinase inhibitor on certain physiological processes in the stromal cells that were the major producers of this inhibitor.

Proliferation is an important biological occurrence in all living cells and a major factor in the initiation and progression of all cancers. Cells have inherent mechanisms by which they regulate their rate of growth and an outcome of one of several possible alterations in these mechanisms can cause uncontrolled proliferation of epithelial cells, leading to the first stage of cancer e.g. in prostate cancer, the cells develop androgen independence via mutations in their androgen receptor, leading to uncontrolled cell growth (Kabalin et al., 1995, Morote et al., 1997). These cells co-habit with surrounding stromal cells and may influence their behaviour and their protein expression profile (Olumi et al., 1999, Shimao et al., 1999, Stuelten et al., 2005, Kaminski et al., 2006, Paland et al., 2009). Therefore, I wanted to investigate whether TIMP-3 had any direct role to play in the rate of growth of the prostate stromal cells, especially as they produce more TIMP-3 than prostate cancer cells. The results of the proliferation assay showed no significant difference in the rate of growth of cells with down regulated TIMP-3 expression when compared to control cells. Although there was always a lower number of a PCAF cell after TIMP-3 down regulation in comparison to the control cells, the numbers were never statistically different (see Figure 5.8). This implied that the reduction of available TIMP-3 in the tumour microenvironment might not affect the total number of cells present. This is somewhat contrary to other results in the literature where an over-expression of TIMP-3 in tumour cells led to a reduction in overall tumour cell size (Vizoso et al., 2007) Although this was an in vivo study, one would expect that under-expression would give the opposite result i.e. increase in the rate of growth of cells with lower levels of TIMP-3. It must be borne in mind that some cells also have compensatory mechanisms whereby the loss of a pathway partner/protein could lead to the production of a substitute or increased production of a co-pathway partner, such that the absence or reduction of the protein does not manifest in an early alteration in physiological processes. As the transfections set up in this project were transient, it was not possible to investigate changes in the rate of proliferation outside of 4 days post transfection.

Apoptosis is also a regulated process necessary for the balanced homeostasis of cells in an organ. Alterations in the mechanism of regulation of cell death may result in a 'switch off' of cell death and 'switch on' of unchecked cell survival. The results obtained in this project showed a significant increase in the number of apoptotic PCAF cells after down regulation of TIMP-3 (See Figure 5.9). This implied that the loss of TIMP-3 sensitised the cells and

initiated apoptosis in these cells. This result is in line with studies that showed an increase in the rate of cellular apoptosis in the epithelial mammary gland of TIMP-3-deficient mice (Fata et al., 2001), highlighting its role as an important survival factor, albeit in mouse cells. The results from this project are contrary to other studies that show TIMP-3 as a pro-apoptotic protein in several cancers such as fibro sarcoma, lung cancer (Baker et al., 1999, Finan et al., 2006, Lee et al., 2008). However, cancer cells are mostly epithelial (excluding fibrosarcomas) and this assay involved stromal cells – this may account for the counter-intuitive results obtained with these cells. It could also be that by virtue of the previous proximity of these cells to prostate cancer cells, they may no longer be able to efficiently regulate their cell cycle balance, leading to the increase in apoptotic cells observed.
There was no significant apoptosis in the WPMY-1 cells after down regulation of TIMP-3 when compared to the control cells (see Figure 5.10). As these cells are not malignant, the compensatory mechanisms that regulate the cell cycle balance may still be intact, allowing for recovery of the imbalance caused as a result of the loss of TIMP-3.

Migration and invasion are important processes observed in advanced cancers where the cancer cells detach from the primary tumour, are released into the blood stream and migrate to neighbouring parts of the primary site as well as to distal organs. It is therefore important to understand the factors that mediate these processes. When cancer cells migrate, they carry along with them stromal fibroblast cells from the primary site and these stromal fibroblasts enable the cancer cells to invade and 'home' in their new secondary site (Shimao et al., 1999, Eck et al., 2009). With this in mind, I set out to investigate the changes in migratory and invasive potential of TIMP-3 down regulated stromal cells. The results from this project showed a significant down regulation of both migration and invasive potentials of PCAF cells when compared to their control cells (see Figs. 5.11 and 5.13 respectively) and, on the opposite hand, a significant increase in the migration and invasive potentials in WPMY-1 cells (see Figs. 5.12 and 5.14 respectively). There is not much data available in literature on expression pattern of TIMP-3 in prostate stromal cells grown in vitro and while the results from the WPMY-1 cells in this project are in line with other studies that show a decrease in the invasive potential of cancer cells that were over-expressing TIMP-3 (Miyazaki et al., 2004, Baker et al., 1999), the results from the PCAF cells are contrary to literature. In one study where thyroid tumour cells were subjected to TIMP-3 silencing, an increase was observed in the migration and invasive potential of

NIM1 thyroid carcinoma cell line when compared to control cells (Anania et al., 2011) – this is in line with the increase in invasive potential seen in TIMP-3 down regulated WPMY-1 cells. The reason for the contrary behaviour of the PCAF cells upon down regulation of TIMP-3 remains unclear – again it may be that their previous proximity to cancer cells has altered their mechanism of maintenance of the proteinase-inhibitor balance.

A proteinase inhibition assay was carried out as previously described (Knight et al., 1992). Due to the age of the Flusys machine and lack of availability of reagents and printing facilities to connect to the machine, the amount of data collected was small, compared to the other assays in this project. Because similar results were obtained from ECM of PCAF and WPMY-1 cells, only the PCAF experiment data are shown, as these were the only ones that could be printed from the machine. These have been scanned and reported in this Chapter. As shown, there was no interference of the buffer on the assay, indicating that the results obtained from the protein extracts were real effects of the contents of the extracts see Figure 5.15). Commercial recombinant human TIMP-3 was also able to show an inhibitory effect on the MMP-2 activity on the QF substrate, up to approximately 80% inhibition. The ECM extracts from the control cells transfected with NTsiRNA showed a total MMP-2 inhibitory effect of approximately 50% while the ECM from the TIMP-3 down regulated cells showed only approximately 20% inhibition of total MMP-2 activity (see Figure 5.16). This implied that the reduction of the amount of TIMP-3 present in the ECM of the stromal cells after TIMP-3 down regulation resulted in an overall loss of inhibition of MMP-2 activity. TIMP-3 is strongly sequestered in the ECM (Langton et al., 1998, Leco et al., 1994, Anand-Apte et al., 1996) and so it can be inferred that the loss of MMP-2 activity seen in this assay may be as a result of the siRNA-mediated reduction in TIMP-3 levels in the ECM of transfected cells. This is in line with the study where an increase in the levels of TIMP present in conditioned medium from prostate stromal cells resulted in an increase in MMP inhibition (Cross et al., 2005).

In conclusion, the importance of TIMP-3 in the tumour microenvironment is key to elucidating better diagnosis and treatment or management of prostate cancer. The stromal cells that produce the bulk of the available TIMP-3 that is in the ECM may play a role in progression of prostate cancer. The complexity of events within a tumour makes it difficult to pin point one determining factor for tumour development, migration and invasion out of

the primary site. Direct and indirect feedback mechanisms are all at work in ensuring continuity of cancer progression and TIMP-3 has proven a worthy protein to be studied as a potential anti-tumourigenic agent and a candidate for new therapy.

CHAPTER 6: GENERAL CONCLUSIONS AND LIMITATIONS OF RESEARCH

This research has focused primarily on investigating the role(s) of tissue inhibitor of metalloproteinases-3 (TIMP-3) in prostate cancer. The first sets of experiments were carried out in order to investigate the expression levels of TIMP-3 in prostate cells, both at the transcript and protein levels. The first port of call was to compare the TIMP-3 levels in available androgen-dependent LNCaP and androgen-independent PC3 prostate cancer cell lines as well as benign prostatic hyperplasia stromal cell line BPH45 as a control. As a result of emerging literature at the time, which showed higher expression of TIMP-3 in stromal compartments of several cancers, it was important to investigate whether TIMP-3 was expressed in normal stromal cells as an additional control. Therefore, a transformed prostate stromal cell line, WPMY-1 was purchased from ATCC and profiled for expression of stromal markers in order to confirm its reported stromal fibroblast characteristics (Webber et al., 1999). True to the literature, WPMY-1 cells expressed vimentin, which is a marker for fibroblasts (Webber et al., 1999) (see Appendix). At the time of the project, our collaborator at the University of Sheffield, Dr. Colby Eaton, kindly donated some stromal fibroblast cells isolated from primary prostate tissue, designated as PCAF cells so in total, there were 3 stromal cell lines and 2 cancer cell lines available for comparison.

Our collaborators also kindly donated prostate tissue samples comprising normal prostate tissues, BPH tissue and primary prostate cancer tissues for analyses and so this enabled immunohistochemical analyses to be carried out alongside the immunocytochemical analyses using the cell lines available.

The first set of experiments involved analysis of modulating factors on the expression of TIMP-3. The effect of androgen, TNF and TGF-β on the levels of TIMP-3 in all the cell lines was analysed. Also, siRNA-mediated down-regulation of TIMP-3 was employed in order to study the changes in migration and invasive potential of the cells and to investigate the effect of loss of this inhibitor on proliferation and apoptotic processes in the cells. The primary function of TIMP-3 in tissues is the inhibition of metalloproteinases and so it was also important to study the effects of siRNA-mediated down-regulation of TIMP-3 on its proteinase inhibitory characteristics. This was carried out using a previously described method (Knight et al., 1992).

Part of the tissue samples donated included tissue microarray samples collected from patients with different Gleason scores. This proved very useful in experiments aimed at correlating the expression of TIMP-3 with tissue Gleason grading and progression of prostate cancer. There were also other tissue samples available – these were obtained from

liver and spleen samples and were very useful as control tissues for the immunohistochemical analyses of the prostate tissues.
There were limitations to this project and these are discussed later on in this Chapter.

6.1 TIMP-3 EXPRESSION IS HIGHER IN PROSTATE STROMAL CELLS THAN IN PROSTATE CANCER CELLS

To my knowledge, this is the first report showing the expression of TIMP-3 in the prostate stromal cells WPMY-1 and the first report to compare the levels of TIMP-3 in this cell line to other prostate cell lines *in vitro* (see Section 3.2.2).
The results obtained in this study showed significantly greater TIMP-3 mRNA expression in prostatic stromal cells, PCAF, WPMY-1 and BPH45, relative to LNCaP and PC3 cells (Figure 3.4). There was also higher expression of TIMP-3 mRNA in the BPH45 stromal cell line compared to the normal stromal cells WPMY-1 and the cancer associated stromal cells PCAF. This may be as a result of the fibromatous characteristics of BPH which results in an overgrowth of the stromal compartment of the prostate (Di Silverio et al., 1993) suggesting differentiation of the stromal fibroblasts to myofibroblasts (Lovelock et al., 2005, Tuxhorn et al., 2002) thereby leading to concomitant increase in the total amount of TIMP-3 sequestered in the BPH cell line. Studies by Mylona *et al* (Mylona et al., 2006) have showed that TIMP-3 is expressed abundantly in the stromal cells adjacent to the breast tumour. Also, studies carried out by Cross *et al* (Cross et al., 2005) demonstrated increased expression of TIMP-3 mRNA in stromal cells BPH31, -33, -44 and –45, relative to the cancer cells PC3 and LNCaP. As shown in this study, the expression of TIMP-3 in the androgen-dependent prostate cancer cell line LNCaP was 100-fold higher than expression in androgen-independent prostate cancer cell line PC3 (see Figure 3.4) This suggests that expression of TIMP-3 may inversely relate to staging of prostate cancer as the LNCaP cells were originally obtained from a patient with local metastasis and the PC3 cells from a patient with distant metastasis (Sobel and Sadar, 2005b). Also corroborating the results from this project, when TIMP-3 was cloned and transfected into the metastatic breast cancer cell line MDA-MB-453, there was a reduction in its metastatic potential, in comparison to untransfected cells (Han et al., 2004). The results from this project showing higher expression of TIMP-3 in prostate stromal cells compared to prostate cancer cells, are also in line with studies by Karan *et al* (Karan et al., 2003) who carried out analyses of

TIMP-3 expression in prostatic stromal cells, prostatic cancer cells LNCaP-C33 (androgen-dependent) and LNCaP-C81 (androgen independent). They demonstrated greater expression of TIMP-3 in the stromal cells, relative to the LNCaP-C33 cells, and expression was undetectable in the LNCaP-C81 cells. Riddick *et al* (Riddick et al., 2005) also obtained similar results when analysing the components of prostatic tissue that are associated with prostate cancer. Stromal cells are likely to be important in the control of proteolytic activity within the tumour microenvironment, perhaps as a result of their increased expression of TIMP-3, and as the stromal-epithelial ratio reduces in cancer, this control is less likely to be complete. At the protein level, the expression of TIMP-3 is corroborated in the stromal cells relative to expression in LNCaP. As a result of the negligible levels of TIMP-3 mRNA in PC3 cells, comparative western blotting was not carried out on their cell lysates. Immunocytochemical analyses also corroborated the expression of TIMP-3 in prostate stromal cells PCAF and WPMY-1, with negligible levels of TIMP-3 detected in the LNCaP prostate cancer cells (see Figure 3.6). TIMP-3 staining was also localised primarily in the ECM – this is in line with its known ECM-adherent characteristics (Lee et al., 2007)

6.2 TIMP-3 EXPRESSION IS CONTROLLED BY PARACRINE SIGNALING IN CO-CULTURES OF PROSTATE STROMAL AND CANCER CELLS.

In this study, the levels of TIMP-3mRNA expressed in stromal cells PCAF and WPMY-1 more than doubled significantly upon co-culturing with prostate cancer cells LNCaP (see Chapter 3, Figure 3.22) and the low expression of TIMP-3 in the LNCaP cells was completely lost post-co-culture with both PCAF and WPMY-1 stromal cells (see Figures 3.22 and 3.23). There appear to be some paracrine crosstalk between the cells, making them behave differently, as opposed to when the cells are grown independently. This type of paracrine effect has been previously reported (Arnold et al., 2008) whereby the expression levels of PSA were significantly increased in androgen-dependent LAPC-4 prostate cancer cells when co-cultured with cancer-associated prostate stromal cells. It is also possible that the cancer cells LNCaP may be secreting excess proteinases and, via paracrine signalling, activating the defence mechanism in stromal cells, resulting in an increase in the amount of TIMP-3 expressed by the cells. TIMP-3 will sequester in the ECM and protect the tissue from proteinase degradation. It is also likely that TGF-β normally produced by prostate

cancer cells LNCaP (Ishii et al., 2011) resulted in an increase in TIMP-3 expression by the stromal cells due to transformation to myofibroblasts. The results from this study show a significant up-regulation of TIMP-3 expression in PCAF cells by TGF-β in a dose-dependent manner. Another example of paracrine synergy between stromal and cancer cells was demonstrated by Hinsley *et al* who showed that when pro-tumourigenic endothelin-1 is elevated, as is the case in several cancer epithelial cells (Granchi et al., 2001), there is a concomitant up-regulation of ADAM-17/TACE activation and/or expression which in turn stimulates the production of epidermal growth factor receptor ligands amphiregulin and HB-EGF in oral fibroblasts. These ligands activate EGF signalling in neighbouring head and neck squamous cancer cells by binding and activating the EGF receptor on the cell surface of the cancer cells which in turn mediates elevated motility, increase in pro-migratory COX-2 expression and migration of the cancer cells out of the tumour micro-environment (Hinsley et al., 2012). These reports support the importance of tumour-stromal interactions in the initiation of cellular migration leading to tumour progression. However, the results from this project suggest that this interaction is likely to inhibit overall tumour migration as a result of the increase in stromal cell production of TIMP-3 upon contact with cancer cells (see Section 3.2.5).

6.3 TIMP-3 EXPRESSION IS HIGHER IN NORMAL AND BPH PROSTATE TISSUES THAN IN PROSTATE CANCER TISSUE

The expression of TIMP-3 in BPH tissue was higher than in normal prostate tissue (see Figures 3.12 and 3.13). In primary prostate cancer tissue, the expression of TIMP-3 was low (see Figure 3.10). Upon analysis of the normal prostate tissue, the localization of TIMP-3 was observed both in the ECM and cytoplasm (see Figure 3.13). However, the cytoplasmic expression of TIMP-3 was much lower in primary prostate cancer tissue (see Figure 3.14). This suggests that the transformation of normal epithelial cells to malignant carcinoma cells may inversely correlate with expression of TIMP-3. This also corroborates the results obtained in cell lines where there was a significantly higher level of TIMP-3 expression in LNCaP cells (early lymph node metastatic cell line) in comparison to PC3 cells (advanced bone metastatic cell line).

Tissue microarray samples were kindly donated by our collaborators and information such as patient Gleason score, tissue Gleason grade and PSA levels of the patient was also supplied. As a control, liver tissue samples were also made available. Results from this study showed the expression of TIMP-3 in all tissue samples, irrespective of disease state. However, the intensity of expression and localisation patterns varied with disease state and tissue Gleason grade. There was negligible expression of TIMP-3 in the liver tissues in comparison to prostate tissue (see Figure 3.17). This is in line with results obtained in previous studies that investigated the expression of genes in several tissue types and showed TIMP-3 gene transcripts were expressed at a higher degree in prostate tissues, when compared to liver tissue (Wu et al., 2009a). There was higher expression of TIMP-3 in cancer tissue with Gleason grade of 4, in comparison to tissue with Gleason grade of 7 (see Figures 3.18 and 3.19 respectively). This suggests there is an inverse correlation between expression of TIMP-3 and malignancy in prostate cancer. The localisation of TIMP-3 was primarily glandular, although staining was still observed in the stromal compartment. The lower expression of TIMP-3 in the prostate cancer tissue with high Gleason grade was concomiatant with loss of a huge amount of epithelial glandular expression of TIMP-3 in the prostate cancer tissue. This predominantly epithelial expression of TIMP-3 has also been demonstrated in breast carcinoma tissue where expression of TIMP-3 correlated inversely with histological grading of the tissue (Mylona et al., 2006) as well as non-small cell lung cancer (Mino et al., 2007) and glioblastoma samples (non-epithelial cancer) (Nakamura et al., 2005a). It is possible that the epithelial localisation of proteinases responsible for glandular degradation results in co-localisation of TIMP-3 inside the epithelium as well as in the stromal cells where it is produced in high quantities. Upon loss of glandular epithelia, there could possibly be a concommitant loss of TIMP-3, leading to results such as ones seen in this project. However, as co-localisation experiments of proteinases with TIMP-3 in these prostate tissues were not done, it is not possible to confirm that the epithelial localisation of TIMP-3 is as a response to presence of proteinases.

Taken together, the importance of TIMP-3 in progression of cancer, including cancer of the prostate, cannot be over-emphasized. Measures targeting cancer associated fibroblasts, as well as increasing total levels of TIMP-3 in the prostate microenvironment may prove invaluable for the management of prostate cancer. This may also be applicable to other

cancers that have shown an inverse correlation between TIMP-3 expression and malignancy.

6.4 TIMP-3 IS MODULATED BY DHT IN PROSTATE CANCER CELLS

The down-regulation of TIMP-3 mRNA in LNCaP cells after treatment with DHT (Figure 4.4) and its elimination in PC3 cells (Figure 4.6) suggests that there may be an increase in metastatic potential of prostate cancer cells with loss of TIMP-3. The LNCaP cells are less metastatic than the PC3 cells (Sobel and Sadar, 2005b), and their loss of this inhibitor may increase proteolysis and initiate tumour metastasis. DHT-mediated prostate cancer cell proliferation is androgen receptor (AR)-dependent. However, in this study, there was no reversal of the DHT effect on TIMP-3 expression by flutamide. This agent is clinically administered to patients with lymph node metastatic prostate cancer, as they are androgen receptor antagonists that act by inhibiting the binding of androgen to the AR. The IC_{50} of Flutamide with regards to inhibition of the androgen receptor, is approximately 175nM (Peets et al., 1974) so at approximately 5x IC_{50} concentration, there was no inhibition of the AR by Flutamide in LNCaP cells. The caveat to this experiment is that the activity of the stock of flutamide used cannot be verified, as there was no reversal of the increase in PSA mRNA levels observed after DHT treatment in LNCaP cells (see Figure 4.5).

In this project, the expression of TIMP-3 mRNA in the PC3 cells was completely depleted after DHT treatment (Figure 4.6). This result was unexpected, as these cells do not possess an AR (Marcelli et al., 1995). The results suggest that the potentially pro-tumourigenic effect of DHT-mediated reduction in TIMP-3 expression might be AR-independent. The effect of DHT on down regulation of TIMP-3 was seen at 10nM; a concentration that allows for optimal proliferation of LNCaP cells (Lin et al., 1998, Zhu et al., 2003). At concentrations that only allow for binding of DHT to the AR (dissociation constant of approximately 0.1nM) (Wilson and French, 1976), there was no significant effect on the levels of TIMP-3. This suggests that the DHT-mediated effect on TIMP-3 down regulation was 'switched on' where there are higher levels of circulating DHT, to enhance cellular proliferation and not just for the binding of the DHT ligand to its receptor. The existence of alternative pathways by which these cancer cells are able to respond to androgen treatment has been investigated and could be due to aromatase action (Tsugaya et al., 1996) or a cell surface receptor, as shown by Hatzoglu *et al* (Hatzoglou et al., 2005); they carried out

studies that demonstrated the inhibition of LNCaP cell growth by BSA-coupled testosterone via a membrane androgen receptor *in-vitro* and in nude mice. TIMP-3 is implicated in cell cycle progression (Airola et al., 1998) and inhibition of cell growth may correlate with a reduction in TIMP-3 expression in the LNCaP cells treated with DHT in the Hatzoglu et al study. The activity of DHT used in this project experiments was confirmed by co-analysing the expression of PSA – a serine protease that is androgen-dependent and is clinically used as a diagnostic marker for prostate cancer progression (Downing et al., 2003) (Figure 4.5).

In the stromal cells, there was no statistical difference in TIMP-3 mRNA expression between treated and untreated cells (Figures 4.7, 4.8 and 4.9), implying that DHT-mediated regulation may be cancer cell-specific. As the levels of TIMP-3 in protein extracts from LNCaP cells were undetectable, it was not possible to corroborate the DHT-mediated down-regulation of TIMP-3 mRNA observed.

In silico analyses of the promoter region of the *TIMP-3* gene revealed 10 putative androgen response elements (ARE) in its promoter region (see Figure 4.17). The sequence similarity was comparable to AREs found in known androgen-regulated genes like PSA (Cleutjens et al., 1997, Cleutjens et al., 1996), hPAR1 (Salah et al., 2005) and MVDP (Fabre et al., 1994), all of which had 40 – 85% sequence similarity to the general ARE consensus (Table 4.1). This result opens the possibility that *TIMP-3* may be an androgen-regulated gene specifically in prostate cancer cells. TIMP-3 may also be androgen-regulated in prostate epithelial cells, although I did not test this. The results from this project also showed that the prostate stromal cells did not alter their TIMP-3 mRNA expression upon treatment with DHT, again buttressing the cancer cell or perhaps epithelial specific modulation of *TIMP-3* in prostate. Also, the functionality of the putative AREs discovered in the promoter regions was not validated as a result of financial and time constraints during the course of the project. Several studies have shown the occurrence of putative AREs in the promoter region of genes and have validated their functionality. These include the Janne *et al* study which showed that ornithine decarboxylase was regulated by androgen in murine epithelial cells and demonstrated the functionality of the putative ARE in murine epithelial cells (Janne et al., 1991). Also, the putative 5' ARE half site of ARE in the promoter region of human kallikrein-2 gene *hKLK-2* was shown to be functional in PC3 cells upon transfection with AR and the promoter region of the *hKLK-2* gene (Murtha et al., 1993). Work with our collaborators also revealed that the *ADAMTS-15* gene was modulated by DHT and we

found that within the proximal and distal promoter regions of the *ADAMTS-15* gene, there were several putative AREs, although their functionality was not confirmed (Molokwu et al., 2010). There has also been a study by Villar *et al* who discovered novel putative AREs in the promoter region of the gonadotropin regulated testicular RNA helicase gene (*GRTH*) and demonstrated that treatment with an AR antagonist prevented the transcription and production of GRTH and also that point mutating one of the AREs resulted in repression of androgen-mediated transcription of GRTH (Villar et al., 2012).

Taken together, the existence of AREs in the promoter region of TIMP-3 may be indicative of its androgen-regulation. Further experiments targeted at demonstrating the functionality of the 10 putative AREs discovered would be necessary in order to confirm this hypothesis.

6.5 TIMP-3 IS MODULATED BY TNF IN PROSTATE STROMAL CELLS

Elevated levels of TNF have been observed in the serum of prostate cancer patients (Nakashima et al., 1998) and this may be as a result of recruitment and activation of macrophages by necrotic cells in the tumour mass as a result of hypoxic conditions and subsequent production of pro-inflammatory cytokines in response. In this project, TIMP-3 mRNA and protein expression were down regulated in prostate stromal cells BPH45 by TNF treatment, in a dose-dependent and statistically significant manner (see Figure 4.11). There were no apparent changes in TIMP-3 mRNA expression after cell treatment in the stromal cells PCAF and WPMY-1 cells nor in cancer cells LNCaP and PC3 (see Figures 4.10 and 4.12). As NF-κB signalling is elevated by stromal fibroblasts in BPH, it is possible that TNF signalling is driving the cells' resistance to apoptosis and promoting hyper-proliferation. As TNF induces the expression of MMP-2 in BPH tissue (Konig et al., 2004), it is quite possible that the balance between MMPs and TIMPs has been altered in favour of proteolysis.

In silico analysis of the TIMP-3 gene did not reveal the presence of any of the known NF-κB response elements (Section 4.2.) implying that the TNF-driven modulation of TIMP-3 in the stromal cells BPH45 may be an indirect effect on other mediators in the non-canonical TNF/ NF-κB signalling pathway in the cells, leading to a possible inhibitory effect on the production of TIMP-3 in these.

Overall, it is possible to include TIMP-3 as a potential target for the management of BPH by gene therapy to incorporate or activate the pro-apoptotic TIMP-3 gene in BPH tissue.

6.6 TIMP-3 IS MODULATED BY TGF-B IN PROSTATE STROMAL CELLS

The expression of TIMP-3 mRNA was significantly up-regulated by 50nM TGF-β1 in the prostatic stromal cells BPH45 and PCAF (see Figures 4.14 and 4.15). This result is in line with studies undertaken by Cross et al (Cross et al., 2005) who showed the up-regulation of *versican* and *TIMP-3* transcripts in the prostate stromal cells BPH 31, 33, 44 and 45. The results from this project suggest there may be an altered balance in favour of higher TIMP-3 expression in the stromal cells in the prostate, which could potentiate inhibition of proteolysis and subsequent metastasis of tumours from the prostatic primary site. There was no effect of TGF-β on TIMP-3 expression in normal prostate stromal cells WPMY-1 after TGF-β treatment, implying that the up-regulation of TIMP-3 by this cytokine is related to pathology (disease) rather than physiology (normal tissue homeostasis).

In *silico* analysis of the *TIMP-3* gene did not reveal any TGF-β response elements in the promoter region of the gene, implying that the effect of TGF-β on TIMP-3 expression was not via direct modulation of transcription or was via unknown direct mechanisms. One hypothesis is that TGF-β may modulate other proteins that interact with TIMP-3 thereby modulating the total levels in the stromal cells. One such example is demonstrated in bovine chondrocytes where TGF-β significantly increased the expression of TIMP-3 via a mechanism thought to involve protein kinases, and also showed that inhibition of serine and tyrosine kinases in the cells reversed the increased TIMP-3 expression observed (Su et al., 1998). Other examples have also been published for TIMP-3 modulation by TGF-β (Airola et al., 1998, Canovas et al., 2008) so this potential indirect modulation of TIMP-3 is not novel.

6.7 DOWN-REGULATION OF TIMP-3 IN PROSTATE STROMAL CELLS RESULTS IN ALTERED BIOLOGICAL FUNCTIONS

The RNAi-mediated down-regulation of TIMP-3 mRNA expression in both prostate stromal and cancer cells was successful via previously described electroporation, lipid and calcium phosphate transfection methods (see Section 2.13). As the total level of TIMP-3 in

LNCaP cells was negligible, it was not possible to validate the down regulation by western blotting in LNCaP cells. However, this was successfully done in stromal cells PCAF and WPMY-1 (see Figures 5.4 and 5.5). To follow up on this, the effect of down-regulation of TIMP-3 in the stromal cells on biological functions such as cell proliferation, apoptosis, migration, and invasion and proteinase inhibition was investigated. This was important in elucidating the role(s) TIMP-3 plays in prostate cancer progression, since stromal cells have been shown to secrete soluble factors that enhance the migration and invasive potential of cancer cells from their primary site to distal sites (Kaminski et al., 2006, Mi et al., 2011, Nomura et al., 2008, Barone et al., 2012). Stromal fibroblasts play an anti-tumourigenic role in normal tissues but once activated during carcinogenesis, activated stromal fibroblasts have also been shown to co-exist with migrated cancer cells from several cancers e.g. ovarian cancer (Zhang et al., 2011) and multiple myeloma (Vande Broek et al., 2008).

Proliferation of the stromal cells PCAF did not change after siRNA-mediated down regulation of TIMP-3 although there was a trend towards slight loss of cell number in PCAF cells (see Figure 5.8). There was, however, a significant increase in the number and percentage of apoptotic PCAF cells (Figure 5.9), which may explain the slight decrease in number of PCAF cells counted, post-transfection. This suggests that the effect of TIMP-3 is not primarily by enhancement of the proliferation of activated stromal fibroblasts in the tumour microenvironment. In contrast, there were no changes in number of proliferating WPMY-1 cells post TIMP-3 down-regulation (Figure 5.8) and no increase in the percentage of apoptotic cells when compared to the control cells with non-targeting siRNA (Figure 5.9). The results from this research are in direct opposition to the known anti-tumourigenic effects of TIMP-3 in cancer cells and have not previously been reported in any other cancer-associated fibroblasts. It is possible that epigenetic changes have occurred in the PCAF cells due to their previous existence with cancer cells and, whilst the inhibitor TIMP-3 is still being expressed, it may be interacting with pathways that mediate cell survival in the cancer associated fibroblasts. Human fibroblasts are characteristically known to secrete elevated levels of growth factors such as TGF-β (Thannickal et al., 1998, Strutz et al., 2001) and FGF (Yamazaki et al., 1997) so their proliferation may have become overly dependent on the survival pathways mediated by these secreted factors.

This effect may not be present in normal fibroblasts like the WPMY-1 cells that still have their regulatory pathways intact.

Migratory and invasive potential of activated cancer-associated fibroblasts PCAF was significantly inhibited after siRNA-mediated down regulation of TIMP-3 (see Figures 5.11 and 5.13). This is in contrast to previously described studies such as one by Coulson-Thomas *et al* who demonstrated an increase in activated stromal cell migration after being in contact with metastatic prostate cancer cells DU145 and PC3 (Coulson-Thomas et al., 2010). However, in their studies, the fibroblasts used were normal non-cancer associated but attained an activated myofibroblastic phenotype when co-cultured with bone-metastatic PC3 and brain-metastatic DU-145 prostate cancer cell lines. Also in this project, the origin of the fibroblasts is prostatic so whether this confers alternate characteristics to the fibroblasts in comparison to what prostate cancer cells would confer to bone marrow and brain-derived fibroblasts used in the Coulson-Thomas study, is unknown. It would be interesting to investigate the effect on migration on these brain and bone marrow derived fibroblasts upon down regulation of TIMP-3. The migration of cancer associated fibroblasts is not alien and has been reported in colon carcinoma associated fibroblasts via FGF-mediated 'switch on' of migration (Sonvilla et al., 2008) as well as in a directed fibroblast-led matrix-degrading and migratory pattern (Gaggioli et al., 2007). Therefore, inhibition of matrix-degrading proteinases should, in theory, reduce this migration of cells and vice versa. In this project, TIMP-3 down regulation in the cancer associated fibroblasts resulted in decreased migration. There was an increase in the migratory and invasive potential observed in the normal prostate stromal fibroblasts WPMY-1 after down-regulation of TIMP-3 (see Figure 5.12 and 5.14). This would support the anti-migratory properties of MMP inhibitors and would subsequently result in reduced invasion of cells. As these WPMY-1 cells have not undergone any previous oncogenic selection leading to potential epigenetic alterations, they may not have the 'over-compensatory' mechanism in them. This, however, is speculatory. In order to confirm that the down-regulation of TIMP-3 in the prostate cells also resulted in an increase of total MMP activity, an in vitro proteinase assay was carried out to test this. As TIMP-3 is a known MMP-2 inhibitor (Visse and Nagase, 2003), it was chosen for the assay. Recombinant MMP-2 was shown to cleave the substrate leading to release of a fluorescent group (see Figure 5.15) as previously described (Knight et al., 1992). Apparent MMP-2 inhibition was observed with control recombinant TIMP-3 (79% inhibition) as well as ECM lysates from NTsiRNA-transfected PCAF and WPMY-1 cells (48% inhibition) while only 17% inhibition remained in ECM lysates from TIMP-3 ssiRNA-transfected PCAF and WPMY-1 cells (Figure 5.16). This confirmed that

TIMP-3, the only TIMP to be sequestered in the ECM, was functioning as an MMP-2 inhibitor in prostate stromal cells and that the loss of the expression of TIMP-3 in the stromal cells led to a loss of MMP-2 inhibition. This result supports the previously characterized MMP-inhibitory function of TIMP-3 and strengthens the proposal for therapies targeted at increasing the levels of TIMP-3 as a means of management of cancer.

6.8 LIMITATIONS OF THIS RESEARCH

There were some limitations that prevented additional experiments to be carried out. The major limitation was time and it would have been interesting to do several follow-up experiments to further understand the mechanism of regulation of TIMP-3 in prostate cancer and its specific role(s) in the cancer progression. Also, it would have been ideal to carry out some xenograft studies *in vivo,* including injection of LNCaP cells into athymic mice so as to follow their growth, migration and invasion of tissues upon siRNA or shRNA-mediated modulation of TIMP-3 *in-vivo*, in comparison to wild type LNCaP cells. These LNCaP cells have been previously successfully injected into mice and they successfully grew into tumours (Ryo et al., 2005)

Also, it would have been useful to carry out more comprehensive prostate tissue microarray analyses to have a diverse comparison of TIMP-3 expression and Gleason grades 1, 2, 3 4 and 5. Comparison of the expression of TIMP-3 and clinical PSA level would have proved useful as well but both of these actions were hindered by the limited availability of time and tissue samples for me to carry out the experiments. The limited experiments carried out using the available tissue microarray were not included in the main body of my thesis due the loss of nuclear images obtained from the microscope (see Appendix).

6.9 PROPOSALS FOR FOLLOW-UP RESEARCH

The following experiments are proposed as follow-up research to complete the body of work already carried out in this project and would enable better understanding of the role(s) of TIMP-3 in prostate cancer progression:

- Investigation of the expression of TIMP-3 in normal prostate epithelial cells such as RPWE cells (CRL 2853, ATCC). This would enable better comparison of TIMP-3 expression between non-malignant and malignant prostate cancer cells, and verify if

the DHT-mediated modulation was cancer cell specific or characteristic of all prostate epithelial cells.

- Investigation of paracrine modulation of TIMP-3 expression in co-cultures of prostate cancer and prostate stromal cells. This is to determine if the co-culture-mediated modulation of expression of TIMP-3 required cell-cell contact or if it was as a result of cancer cells secreting soluble factors that stimulated the elevation of TIMP-3 in cancer cells.
- Investigation of the pattern of growth, migration and metastasis of LNCaP cells with and without accompanying stromal cells in athymic mice with and without inducible shRNA-mediated down regulation of TIMP-3 in the cells using commercially available lentiviral vectors like TRIPZ shRNA vectors (Thermo Fisher Scientific, U.S.A>). This would enable transfer of the *in vitro* experiments to *in vivo* scenario and demonstration of the differences seen in migration and invasion between normal and cancer associated stromal fibroblasts.

BIBLIOGRAPHY

AALINKEEL, R., NAIR, B. B., REYNOLDS, J. L., SYKES, D. E., MAHAJAN, S. D., CHADHA, K. C. & SCHWARTZ, S. A. 2011. Overexpression of MMP-9 Contributes to Invasiveness of Prostate Cancer Cell Line LNCaP. *Immunol Invest,* 40, 447-64.

ABEL, S., HUNDHAUSEN, C., MENTLEIN, R., SCHULTE, A., BERKHOUT, T. A., BROADWAY, N., HARTMANN, D., SEDLACEK, R., DIETRICH, S., MUETZE, B., SCHUSTER, B., KALLEN, K. J., SAFTIG, P., ROSE-JOHN, S. & LUDWIG, A. 2004. The transmembrane CXC-chemokine ligand 16 is induced by IFN-gamma and TNF-alpha and shed by the activity of the disintegrin-like metalloproteinase ADAM10. *J Immunol,* 172, 6362-72.

AFONSO, S., ROMAGNANO, L. & BABIARZ, B. 1997. The expression and function of cystatin C and cathepsin B and cathepsin L during mouse embryo implantation and placentation. *Development,* 124, 3415-25.

AIROLA, K., AHONEN, M., JOHANSSON, N., HEIKKILA, P., KERE, J., KAHARI, V. M. & SAARIALHO-KERE, U. K. 1998. Human TIMP-3 is expressed during fetal development, hair growth cycle, and cancer progression. *J Histochem Cytochem,* 46, 437-47.

ALGABA ARREA, F., TRIAS PUIG-SUREDA, I., LOPEZ DUESA, L., RODRIGUEZ-VALLEJO, J. M. & GONZALEZ-ESTEBAN, J. 1997. [Relationship of prostatic carcinoma of the peripheral zone with glandular atrophy and prostatic intraepithelial neoplasia]. *Actas Urol Esp,* 21, 40-3.

ALLAN, J. A., DOCHERTY, A. J., BARKER, P. J., HUSKISSON, N. S., REYNOLDS, J. J. & MURPHY, G. 1995. Binding of gelatinases A and B to type-I collagen and other matrix components. *Biochem J,* 309 (Pt 1), 299-306.

ALTWEIN, J. E. & ORESTANO, F. 1975. A systematic study of testosterone metabolism in benign prostatic hypertrophy (BPH): in vitro results. *Urol Res,* 2, 143-8.

AMOUR, A., KNIGHT, C. G., ENGLISH, W. R., WEBSTER, A., SLOCOMBE, P. M., KNAUPER, V., DOCHERTY, A. J., BECHERER, J. D., BLOBEL, C. P. & MURPHY, G. 2002. The enzymatic activity of ADAM8 and ADAM9 is not regulated by TIMPs. *FEBS Lett,* 524, 154-8.

AMOUR, A., KNIGHT, C. G., WEBSTER, A., SLOCOMBE, P. M., STEPHENS, P. E., KNAUPER, V., DOCHERTY, A. J. & MURPHY, G. 2000. The in vitro activity of ADAM-10 is inhibited by TIMP-1 and TIMP-3. *FEBS Lett,* 473, 275-9.

ANAND-APTE, B., BAO, L., SMITH, R., IWATA, K., OLSEN, B. R., ZETTER, B. & APTE, S. S. 1996. A review of tissue inhibitor of metalloproteinases-3 (TIMP-3) and experimental analysis of its effect on primary tumor growth. *Biochem Cell Biol,* 74, 853-62.

ANANIA, M. C., SENSI, M., RADAELLI, E., MIRANDA, C., VIZIOLI, M. G., PAGLIARDINI, S., FAVINI, E., CLERIS, L., SUPINO, R., FORMELLI, F., BORRELLO, M. G., PIEROTTI, M. A. & GRECO, A. 2011. TIMP3 regulates migration, invasion and in vivo tumorigenicity of thyroid tumor cells. *Oncogene,* 30, 3011-23.

APTE, S. S. 2004. A disintegrin-like and metalloprotease (reprolysin type) with thrombospondin type 1 motifs: the ADAMTS family. *Int J Biochem Cell Biol,* 36, 981-5.

APTE SS, BR, O. & G, M. 1995. The gene structure of tissue inhibitor of metalloproteinases (TIMP)-3 and its inhibitory activities define the distinct TIMP gene family. *J Biol Chem,* 270, 14313 - 14318.

APTE, S. S., HAYASHI, K., SELDIN, M. F., MATTEI, M. G., HAYASHI, M. & OLSEN, B. R. 1994. Gene encoding a novel murine tissue inhibitor of metalloproteinases (TIMP), TIMP-3, is expressed in developing mouse epithelia, cartilage, and muscle, and is located on mouse chromosome 10. *Dev Dyn,* 200, 177-97.

ARNOLD, J. T., GRAY, N. E., JACOBOWITZ, K., VISWANATHAN, L., CHEUNG, P. W., MCFANN, K. K., LE, H. & BLACKMAN, M. R. 2008. Human prostate stromal cells stimulate increased PSA production in DHEA-treated prostate cancer epithelial cells. *J Steroid Biochem Mol Biol,* 111, 240-6.

ARNOLD, J. T., LIU, X., ALLEN, J. D., LE, H., MCFANN, K. K. & BLACKMAN, M. R. 2007. Androgen receptor or estrogen receptor-beta blockade alters DHEA-, DHT-, and E(2)-induced proliferation and PSA production in human prostate cancer cells. *Prostate,* 67, 1152-62.

AUMULLER, G. & SEITZ, J. 1990. Protein secretion and secretory processes in male accessory sex glands. *Int Rev Cytol,* 121, 127-231.

BACHMAN KE, HERMAN JG, CORN PG & AL, E. 1999. Methylation-associated Silencing of the tissue inhibitor of metalloproteinase-3 Gene suggests a suppressor role in kidney, brain, and other human cancers. *Cancer Research,* 59, 798 - 802.

BACKUS, H. H., VAN GROENINGEN, C. J., VOS, W., DUKERS, D. F., BLOEMENA, E., WOUTERS, D., PINEDO, H. M. & PETERS, G. J. 2002. Differential expression of cell cycle and apoptosis related proteins in colorectal mucosa, primary colon tumours, and liver metastases. *J Clin Pathol,* 55, 206-11.

BAILEY, T. A., ALEXANDER, R. A., DUBOVY, S. R., LUTHERT, P. J. & CHONG, N. H. 2001. Measurement of TIMP-3 expression and Bruch's membrane thickness in human macula. *Exp Eye Res,* 73, 851-8.

BAIROCH, A. 1994. The ENZYME data bank. *Nucleic Acids Res,* 22, 3626-7.

BAKER AH, EDWARDS DR & 3719-3727, M. G. J. O. C. S. 2002. Metalloproteinase inhibitors: biological actions and therapeutic opportunities. *J Cell Sci,* 115, 3719 - 3727.

BAKER, A. H., GEORGE, S. J., ZALTSMAN, A. B., MURPHY, G. & NEWBY, A. C. 1999. Inhibition of invasion and induction of apoptotic cell death of cancer cell lines by overexpression of TIMP-3. *Br J Cancer,* 79, 1347-55.

BAKER, A. H., ZALTSMAN, A. B., GEORGE, S. J. & NEWBY, A. C. 1998. Divergent effects of tissue inhibitor of metalloproteinase-1, -2, or -3 overexpression on rat vascular smooth muscle cell invasion, proliferation, and death in vitro. TIMP-3 promotes apoptosis. *J Clin Invest,* 101, 1478-87.

BAKER, S. J. & REDDY, E. P. 1996. Transducers of life and death: TNF receptor superfamily and associated proteins. *Oncogene,* 12, 1-9.

BALK, S. P. 2002. Androgen receptor as a target in androgen-independent prostate cancer. *Urology,* 60, 132-8; discussion 138-9.

BALKWILL, F. R. 1992. Tumour necrosis factor and cancer. *Prog Growth Factor Res,* 4, 121-37.

BALLOCK, R. T., HEYDEMANN, A., WAKEFIELD, L. M., FLANDERS, K. C., ROBERTS, A. B. & SPORN, M. B. 1993. TGF-beta 1 prevents hypertrophy of epiphyseal chondrocytes: regulation of gene expression for cartilage matrix proteins and metalloproteases. *Dev Biol,* 158, 414-29.

BARONE, I., CATALANO, S., GELSOMINO, L., MARSICO, S., GIORDANO, C., PANZA, S., BONOFIGLIO, D., BOSSI, G., COVINGTON, K. R., FUQUA, S. A. & ANDO, S. 2012. Leptin mediates tumor-stromal interactions that promote the invasive growth of breast cancer cells. *Cancer Res,* 72, 1416-27.

BARRETT, A. J. & STARKEY, P. M. 1973. The interaction of alpha 2-macroglobulin with proteinases. Characteristics and specificity of the reaction, and a hypothesis concerning its molecular mechanism. *Biochem J,* 133, 709-24.

BASILE, J. R., HOLMBECK, K., BUGGE, T. H. & GUTKIND, J. S. 2007. MT1-MMP controls tumor-induced angiogenesis through the release of semaphorin 4D. *J Biol Chem,* 282, 6899-905.

BAXTER, A., CAMPBELL, C. J., GRINHAM, C. J., KEANE, R. M., LAWTON, B. C. & PENDLEBURY, J. E. 1990. Substrate and inhibitor studies with human gastric aspartic proteinases. *Biochem J,* 267, 665-9.

BENCZIK, M. & GAFFEN, S. L. 2004. The interleukin (IL)-2 family cytokines: survival and proliferation signaling pathways in T lymphocytes. *Immunol Invest,* 33, 109-42.

BENOIT, G., JARDIN, A. & GILLOT, C. 1993. Reflections and suggestions on the nomenclature of the prostate. *Surg Radiol Anat,* 15, 325-32.

BIGG, H. F., SHI, Y. E., LIU, Y. E., STEFFENSEN, B. & OVERALL, C. M. 1997. Specific, high affinity binding of tissue inhibitor of metalloproteinases-4 (TIMP-4) to the COOH-terminal hemopexin-like domain of human gelatinase A. TIMP-4 binds progelatinase A and the COOH-terminal domain in a similar manner to TIMP-2. *J Biol Chem,* 272, 15496-500.

BISHOP, J. M. 1991. Molecular themes in oncogenesis. *Cell,* 64, 235-48.

BISSETT, D., O'BYRNE, K. J., VON PAWEL, J., GATZEMEIER, U., PRICE, A., NICOLSON, M., MERCIER, R., MAZABEL, E., PENNING, C., ZHANG, M. H., COLLIER, M. A. & SHEPHERD, F. A. 2005. Phase III study of matrix metalloproteinase inhibitor prinomastat in non-small-cell lung cancer. *J Clin Oncol,* 23, 842-9.

BLACK, R. A., RAUCH, C. T., KOZLOSKY, C. J., PESCHON, J. J., SLACK, J. L., WOLFSON, M. F., CASTNER, B. J., STOCKING, K. L., REDDY, P., SRINIVASAN, S., NELSON, N., BOIANI, N., SCHOOLEY, K. A., GERHART, M., DAVIS, R., FITZNER, J. N., JOHNSON, R. S., PAXTON, R. J., MARCH, C. J. & CERRETTI, D. P. 1997. A metalloproteinase disintegrin that releases tumour-necrosis factor-alpha from cells. *Nature,* 385, 729-33.

BODE, W., FERNANDEZ-CATALAN, C., TSCHESCHE, H., GRAMS, F., NAGASE, H. & MASKOS, K. 1999. Structural properties of matrix metalloproteinases. *Cell Mol Life Sci,* 55, 639-52.

BOEL, E., KRISTENSEN, T., PETERSEN, C. M., MORTENSEN, S. B., GLIEMANN, J. & SOTTRUP-JENSEN, L. 1990. Expression of human alpha 2-macroglobulin cDNA in baby hamster kidney fibroblasts: secretion of high levels of active alpha 2-macroglobulin. *Biochemistry,* 29, 4081-7.

BORDER, W. A., BREES, D. & NOBLE, N. A. 1994. Transforming growth factor-beta and extracellular matrix deposition in the kidney. *Contrib Nephrol,* 107, 140-5.

BORDER, W. A. & NOBLE, N. A. 1994. Transforming growth factor beta in tissue fibrosis. *N Engl J Med,* 331, 1286-92.

BORSET, M., MEDVEDEV, A. E., SUNDAN, A. & ESPEVIK, T. 1996. The role of the two TNF receptors in proliferation, NF-kappa B activation and discrimination between TNF and LT alpha signalling in the human myeloma cell line OH-2. *Cytokine,* 8, 430-8.

BOSTWICK, D. G., QIAN, J. & FRANKEL, K. 1995. The incidence of high grade prostatic intraepithelial neoplasia in needle biopsies. *J Urol,* 154, 1791-4.

BOUCHE, M., CANIPARI, R., MELCHIONNA, R., WILLEMS, D., SENNI, M. I. & MOLINARO, M. 2000. TGF-beta autocrine loop regulates cell growth and myogenic differentiation in human rhabdomyosarcoma cells. *FASEB J,* 14, 1147-58.

BOYD, S., VIROLAINEN, S., PARSSINEN, J., SKOOG, T., VAN HOGERLINDEN, M., LATONEN, L., KYLLONEN, L., TOFTGARD, R. & SAARIALHO-KERE, U. 2009. MMP-10 (Stromelysin-2) and MMP-21 in human and murine squamous cell cancer. *Exp Dermatol,* 18, 1044-52.

BREW, K. & NAGASE, H. 2010. The tissue inhibitors of metalloproteinases (TIMPs): an ancient family with structural and functional diversity. *Biochim Biophys Acta,* 1803, 55-71.

BRINKMANN, A. O., BLOK, L. J., DE RUITER, P. E., DOESBURG, P., STEKETEE, K., BERREVOETS, C. A. & TRAPMAN, J. 1999. Mechanisms of androgen receptor activation and function. *J Steroid Biochem Mol Biol,* 69, 307-13.

BURNSTEIN, K. L. 2005. Regulation of androgen receptor levels: implications for prostate cancer progression and therapy. *J Cell Biochem,* 95, 657-69.

BUTLER, G. S., WILL, H., ATKINSON, S. J. & MURPHY, G. 1997. Membrane-type-2 matrix metalloproteinase can initiate the processing of progelatinase A and is regulated by the tissue inhibitors of metalloproteinases. *Eur J Biochem,* 244, 653-7.

BUTLER, L. M., HEWETT, P. J., FITRIDGE, R. A. & COWLED, P. A. 1999. Deregulation of apoptosis in colorectal carcinoma: theoretical and therapeutic implications. *Aust N Z J Surg,* 69, 88-94.

CANOVAS, D., RENNIE, I. G., NICHOLS, C. E. & SISLEY, K. 2008. Local environmental influences on uveal melanoma: vitreous humor promotes uveal melanoma invasion, whereas the aqueous can be inhibitory. *Cancer,* 112, 1787-94.

CARDOSO, L. E., FALCAO, P. G. & SAMPAIO, F. J. 2004. Increased and localized accumulation of chondroitin sulphate proteoglycans in the hyperplastic human prostate. *BJU Int,* 93, 532-8.

CARMELIET, P. & JAIN, R. K. 2000. Angiogenesis in cancer and other diseases. *Nature,* 407, 249-57.

CELOTTI, F., MELCANGI, R. C., NEGRI-CESI, P. & POLETTI, A. 1991. Testosterone metabolism in brain cells and membranes. *J Steroid Biochem Mol Biol,* 40, 673-8.

CHAIN, B. M., FREE, P., MEDD, P., SWETMAN, C., TABOR, A. B. & TERRAZZINI, N. 2005. The expression and function of cathepsin E in dendritic cells. *J Immunol,* 174, 1791-800.

CHAN, K. C., KO, J. M., LUNG, H. L., SEDLACEK, R., ZHANG, Z. F., LUO, D. Z., FENG, Z. B., CHEN, S., CHEN, H., CHAN, K. W., TSAO, S. W., CHUA, D. T., ZABAROVSKY, E. R., STANBRIDGE, E. J. & LUNG, M. L. 2010. Catalytic activity of matrix metalloproteinase-19 is essential for tumor suppressor and anti-angiogenic activities in nasopharyngeal carcinoma. *Int J Cancer.*

CHANDELE, A., PRASAD, V., JAGTAP, J. C., SHUKLA, R. & SHASTRY, P. R. 2004. Upregulation of survivin in G2/M cells and inhibition of caspase 9 activity enhances resistance in staurosporine-induced apoptosis. *Neoplasia,* 6, 29-40.

CHEN, H., LI, D., SALDEEN, T. & MEHTA, J. L. 2003. TGF-beta 1 attenuates myocardial ischemia-reperfusion injury via inhibition of upregulation of MMP-1. *Am J Physiol Heart Circ Physiol,* 284, H1612-7.

CHONG, N. H., ALEXANDER, R. A., GIN, T., BIRD, A. C. & LUTHERT, P. J. 2000. TIMP-3, collagen, and elastin immunohistochemistry and histopathology of Sorsby's fundus dystrophy. *Invest Ophthalmol Vis Sci,* 41, 898-902.

CHU, F. K. 1986. Requirements of cleavage of high mannose oligosaccharides in glycoproteins by peptide N-glycosidase F. *J Biol Chem,* 261, 172-7.

CHU, L. W., RITCHEY, J., DEVESA, S. S., QURAISHI, S. M., ZHANG, H. & HSING, A. W. 2011. Prostate cancer incidence rates in Africa. *Prostate Cancer,* 2011, 947870.

CLAESSENS, F., CELIS, L., PEETERS, B., HEYNS, W., VERHOEVEN, G. & ROMBAUTS, W. 1989. Functional characterization of an androgen response element in the first intron of the C3(1) gene of prostatic binding protein. *Biochem Biophys Res Commun,* 164, 833-40.

CLARK, R. A., MCCOY, G. A., FOLKVORD, J. M. & MCPHERSON, J. M. 1997. TGF-beta 1 stimulates cultured human fibroblasts to proliferate and produce tissue-like fibroplasia: a fibronectin matrix-dependent event. *J Cell Physiol,* 170, 69-80.

CLEUTJENS, K. B., VAN DER KORPUT, H. A., VAN EEKELEN, C. C., VAN ROOIJ, H. C., FABER, P. W. & TRAPMAN, J. 1997. An androgen response element in a far upstream enhancer region is essential for high, androgen-regulated activity of the prostate-specific antigen promoter. *Mol Endocrinol,* 11, 148-61.

CLEUTJENS, K. B., VAN EEKELEN, C. C., VAN DER KORPUT, H. A., BRINKMANN, A. O. & TRAPMAN, J. 1996. Two androgen response regions cooperate in steroid hormone regulated activity of the prostate-specific antigen promoter. *J Biol Chem,* 271, 6379-88.

COBO DOLS, M., MUNOZ GALLARDO, S., PELAEZ ANGULO, J., ALGARRA GARCIA, R., FUENTE LUPIANEZ, C., GIL CALLE, S., VILLAR CHAMORRO, E., MONTESA PINO, A., ALCAIDE GARCIA, J., ALES DIAZ, I., GUTIERREZ CALDERON, V., CARABANTE OCON, F. & BENAVIDES ORGAZ, M. 2005. Secondary signet-ring cell tumour of the prostate derived from a primary gastric malignancy. *Clin Transl Oncol,* 7, 409-12.

COCKETT, M. I., MURPHY, G., BIRCH, M. L., O'CONNELL, J. P., CRABBE, T., MILLICAN, A. T., HART, I. R. & DOCHERTY, A. J. 1998. Matrix metalloproteinases and metastatic cancer. *Biochem Soc Symp,* 63, 295-313.

COLIGE, A., LI, S. W., SIERON, A. L., NUSGENS, B. V., PROCKOP, D. J. & LAPIERE, C. M. 1997. cDNA cloning and expression of bovine procollagen I N-proteinase: a new member of the superfamily of zinc-metalloproteinases with binding sites for cells and other matrix components. *Proc Natl Acad Sci U S A,* 94, 2374-9.

COLIGE, A., VANDENBERGHE, I., THIRY, M., LAMBERT, C. A., VAN BEEUMEN, J., LI, S. W., PROCKOP, D. J., LAPIERE, C. M. & NUSGENS, B. V. 2002. Cloning and characterization of ADAMTS-14, a novel ADAMTS displaying high homology with ADAMTS-2 and ADAMTS-3. *J Biol Chem,* 277, 5756-66.

CONDON, T. P., FLOURNOY, S., SAWYER, G. J., BAKER, B. F., KISHIMOTO, T. K. & BENNETT, C. F. 2001. ADAM17 but not ADAM10 mediates tumor necrosis factor-alpha and L-selectin shedding from leukocyte membranes. *Antisense Nucleic Acid Drug Dev,* 11, 107-16.

COONS, A. H. & KAPLAN, M. H. 1950. Localization of antigen in tissue cells; improvements in a method for the detection of antigen by means of fluorescent antibody. *J Exp Med,* 91, 1-13.

COULSON-THOMAS, V. J., GESTEIRA, T. F., COULSON-THOMAS, Y. M., VICENTE, C. M., TERSARIOL, I. L., NADER, H. B. & TOMA, L. 2010. Fibroblast and prostate tumor cell cross-talk: fibroblast differentiation, TGF-beta, and extracellular matrix down-regulation. *Exp Cell Res,* 316, 3207-26.

COUSSENS, L. M., RAYMOND, W. W., BERGERS, G., LAIG-WEBSTER, M., BEHRENDTSEN, O., WERB, Z., CAUGHEY, G. H. & HANAHAN, D. 1999. Inflammatory mast cells up-regulate angiogenesis during squamous epithelial carcinogenesis. *Genes Dev,* 13, 1382-97.

CRAFT, N., SHOSTAK, Y., CAREY, M. & SAWYERS, C. L. 1999. A mechanism for hormone-independent prostate cancer through modulation of androgen receptor signaling by the HER-2/neu tyrosine kinase. *Nat Med,* 5, 280-5.

CRESCIOLI, C., VILLARI, D., FORTI, G., FERRUZZI, P., PETRONE, L., VANNELLI, G. B., ADORINI, L., SALERNO, R., SERIO, M. & MAGGI, M. 2002. Des (1-3) IGF-I-stimulated growth of human stromal BPH cells is inhibited by a vitamin D3 analogue. *Mol Cell Endocrinol,* 198, 69-75.

CROSS, N. A., CHANDRASEKHARAN, S., JOKONYA, N., FOWLES, A., HAMDY, F. C., BUTTLE, D. J. & EATON, C. L. 2005. The expression and regulation of ADAMTS-1, -4, -5, -9, and -15, and TIMP-3 by TGFbeta1 in prostate cells: relevance to the accumulation of versican. *Prostate,* 63, 269-75.

CROSSLEY, M., LUDWIG, M., STOWELL, K. M., DE VOS, P., OLEK, K. & BROWNLEE, G. G. 1992. Recovery from hemophilia B Leyden: an androgen-responsive element in the factor IX promoter. *Science,* 257, 377-9.

CRUZ-MUNOZ, W., KIM, I. & KHOKHA, R. 2006. TIMP-3 deficiency in the host, but not in the tumor, enhances tumor growth and angiogenesis. *Oncogene,* 25, 650-5.

CUNHA, G. R., HAYWARD, S. W. & WANG, Y. Z. 2002. Role of stroma in carcinogenesis of the prostate. *Differentiation,* 70, 473-85.

D'ANTONIO, J. M., VANDER GRIEND, D. J., ANTONY, L., NDIKUYEZE, G., DALRYMPLE, S. L., KOOCHEKPOUR, S. & ISAACS, J. T. 2010. Loss of androgen receptor-dependent growth suppression by prostate cancer cells can occur independently from acquiring oncogenic addiction to androgen receptor signaling. *PLoS One,* 5, e11475.

DATTO, M. B., YU, Y. & WANG, X. F. 1995. Functional analysis of the transforming growth factor beta responsive elements in the WAF1/Cip1/p21 promoter. *J Biol Chem,* 270, 28623-8.

DAVIDSON, B. L. & HARPER, S. Q. 2005. Viral delivery of recombinant short hairpin RNAs. *Methods Enzymol,* 392, 145-73.

DE WEVER, O. & MAREEL, M. 2003. Role of tissue stroma in cancer cell invasion. *J Pathol,* 200, 429-47.

DEL CASAR, J. M., CARRENO, G., GONZALEZ, L. O., JUNQUERA, S., GONZALEZ-REYES, S., GONZALEZ, J. M., BONGERA, M., MERINO, A. M. & VIZOSO, F. J. 2010. Expression of metalloproteases and their inhibitors in primary tumors and in local recurrences after mastectomy for breast cancer. *J Cancer Res Clin Oncol,* 136, 1049-58.

DEL CASAR, J. M., GONZALEZ, L. O., ALVAREZ, E., JUNQUERA, S., MARIN, L., GONZALEZ, L., BONGERA, M., VAZQUEZ, J. & VIZOSO, F. J. 2009. Comparative analysis and clinical value of the expression of metalloproteases and their inhibitors by intratumor stromal fibroblasts and those at the invasive front of breast carcinomas. *Breast Cancer Res Treat,* 116, 39-52.

DEMIRCAN, K., GUNDUZ, E., GUNDUZ, M., BEDER, L. B., HIROHATA, S., NAGATSUKA, H., CENGIZ, B., CILEK, M. Z., YAMANAKA, N., SHIMIZU, K. & NINOMIYA, Y. 2009. Increased mRNA expression of ADAMTS metalloproteinases in metastatic foci of head and neck cancer. *Head Neck,* 31, 793-801.

DENAULT, J. B. & SALVESEN, G. S. 2002. Caspases. *Curr Protoc Protein Sci,* Chapter 21, Unit 21 8.

DESMOUCELLES, C., VAUDRY, H., EIDEN, L. E. & ANOUAR, Y. 1999. Synergistic action of upstream elements and a promoter-proximal CRE is required for neuroendocrine cell-specific expression and second-messenger regulation of the gene encoding the human secretory protein secretogranin II. *Mol Cell Endocrinol,* 157, 55-66.

DI CARLO, E., FORNI, G., LOLLINI, P., COLOMBO, M. P., MODESTI, A. & MUSIANI, P. 2001. The intriguing role of polymorphonuclear neutrophils in antitumor reactions. *Blood,* 97, 339-45.

DI SILVERIO, F., D'ERAMO, G., FLAMMIA, G. P., CAPONERA, M., FRASCARO, E., BUSCARINI, M., MARIANI, M. & SCIARRA, A. 1993. Pathology of BPH. *Minerva Urol Nefrol,* 45, 135-42.

DICKINSON, S. I. 2010. Premalignant and malignant prostate lesions: pathologic review. *Cancer Control,* 17, 214-22.

DOWNING, S., BUMAK, C., NIXDORF, S., OW, K., RUSSELL, P. & JACKSON, P. 2003. Elevated levels of prostate-specific antigen (PSA) in prostate cancer cells expressing mutant p53 is associated with tumor metastasis. *Mol Carcinog,* 38, 130-40.

DUBAIL, J., KESTELOOT, F., DEROANNE, C., MOTTE, P., LAMBERT, V., RAKIC, J. M., LAPIERE, C., NUSGENS, B. & COLIGE, A. 2010. ADAMTS-2 functions as anti-angiogenic and anti-tumoral molecule independently of its catalytic activity. *Cell Mol Life Sci,* 67, 4213-32.

DUFFY, M. J. & MCCARTHY, K. 1998. Matrix metalloproteinases in cancer: prognostic markers and targets for therapy (review). *Int J Oncol,* 12, 1343-8.

DUFOUR, E. K., DENAULT, J. B., HOPKINS, P. C. & LEDUC, R. 1998. Serpin-like properties of alpha1-antitrypsin Portland towards furin convertase. *FEBS Lett,* 426, 41-6.

DUNN, J. R., REED, J. E., DU PLESSIS, D. G., SHAW, E. J., REEVES, P., GEE, A. L., WARNKE, P. & WALKER, C. 2006. Expression of ADAMTS-8, a secreted protease with antiangiogenic properties, is downregulated in brain tumours. *Br J Cancer,* 94, 1186-93.

EATON, C. L. 2003. Aetiology and pathogenesis of benign prostatic hyperplasia. *Curr Opin Urol,* 13, 7-10.

ECK, S. M., COTE, A. L., WINKELMAN, W. D. & BRINCKERHOFF, C. E. 2009. CXCR4 and matrix metalloproteinase-1 are elevated in breast carcinoma-associated fibroblasts and in normal mammary fibroblasts exposed to factors secreted by breast cancer cells. *Mol Cancer Res,* 7, 1033-44.

EGEVAD, L., ALLSBROOK, W. C. & EPSTEIN, J. I. 2006. Current practice of diagnosis and reporting of prostatic intraepithelial neoplasia and glandular atypia among genitourinary pathologists. *Mod Pathol,* 19, 180-5.

EISENBERGER, M. A., BLUMENSTEIN, B. A., CRAWFORD, E. D. & AL, E. 1998. Bilateral Orchiectomy with or without Flutamide for Metastatic Prostate Cancer. *N Engl J Med,* 339.

EKMAN, P., GRONBERG, H., MATSUYAMA, H., KIVINEVA, M., BERGERHEIM, U. S. & LI, C. 1999. Links between genetic and environmental factors and prostate cancer risk. *Prostate,* 39, 262-8.

ELBASHIR, S. M., HARBORTH, J., WEBER, K. & TUSCHL, T. 2002. Analysis of gene function in somatic mammalian cells using small interfering RNAs. *Methods,* 26, 199-213.

ELBASHIR, S. M., LENDECKEL, W. & TUSCHL, T. 2001a. RNA interference is mediated by 21- and 22-nucleotide RNAs. *Genes Dev,* 15, 188-200.

ELBASHIR, S. M., MARTINEZ, J., PATKANIOWSKA, A., LENDECKEL, W. & TUSCHL, T. 2001b. Functional anatomy of siRNAs for mediating efficient RNAi in Drosophila melanogaster embryo lysate. *EMBO J,* 20, 6877-88.

ELLERBROEK, S. M., HUDSON, L. G. & STACK, M. S. 1998. Proteinase requirements of epidermal growth factor-induced ovarian cancer cell invasion. *Int J Cancer,* 78, 331-7.

ENDSLEY, M. P., THILL, R., CHOUDHRY, I., WILLIAMS, C. L., KAJDACSY-BALLA, A., CAMPBELL, W. B. & NITHIPATIKOM, K. 2008. Expression and function of fatty acid amide hydrolase in prostate cancer. *Int J Cancer,* 123, 1318-26.

EVAN, G. I. & VOUSDEN, K. H. 2001. Proliferation, cell cycle and apoptosis in cancer. *Nature,* 411, 342-8.

FABRE, S., MANIN, M., PAILHOUX, E., VEYSSIERE, G. & JEAN, C. 1994. Identification of a functional androgen response element in the promoter of the gene for the androgen-regulated aldose reductase-like protein specific to the mouse vas deferens. *J Biol Chem,* 269, 5857-64.

FARISS, R. N., APTE, S. S., LUTHERT, P. J., BIRD, A. C. & MILAM, A. H. 1998. Accumulation of tissue inhibitor of metalloproteinases-3 in human eyes with Sorsby's fundus dystrophy or retinitis pigmentosa. *Br J Ophthalmol,* 82, 1329-34.

FATA JE, LECO KJ, VOURA EB & AL, E. 2001. Accelerated apoptosis in the TIMP-3 – deficient mammary gland. *J Clin Invest,* 108, 831 - 841.

FATA, J. E., LECO, K. J., VOURA, E. B., YU, H. Y., WATERHOUSE, P., MURPHY, G., MOOREHEAD, R. A. & KHOKHA, R. 2001. Accelerated apoptosis in the Timp-3-deficient mammary gland. *J Clin Invest,* 108, 831-41.

FERLAY, J., SHIN, H. R., BRAY, F., FORMAN, D., MATHERS, C. & PARKIN, D. M. 2010. Estimates of worldwide burden of cancer in 2008: GLOBOCAN 2008. *Int J Cancer,* 127, 2893-917.

FERNANDES, R. J., HIROHATA, S., ENGLE, J. M., COLIGE, A., COHN, D. H., EYRE, D. R. & APTE, S. S. 2001. Procollagen II amino propeptide processing by ADAMTS-3. Insights on dermatosparaxis. *J Biol Chem,* 276, 31502-9.

FERNANDEZ-GOMEZ, J., ESCAF, S., GONZALEZ, L. O., SUAREZ, A., GONZALEZ-REYES, S., GONZALEZ, J., MIRANDA, O. & VIZOSO, F. 2011. Relationship between metalloprotease expression in tumour and stromal cells and aggressive behaviour in prostate carcinoma: Simultaneous high-throughput study of multiple metalloproteases and their inhibitors using tissue array analysis of radical prostatectomy samples. *Scand J Urol Nephrol,* 45, 171-6.

FINAN, K. M., HODGE, G., REYNOLDS, A. M., HODGE, S., HOLMES, M. D., BAKER, A. H. & REYNOLDS, P. N. 2006. In vitro susceptibility to the pro-apoptotic effects of TIMP-3 gene delivery translates to greater in vivo efficacy versus gene delivery for TIMPs-1 or -2. *Lung Cancer,* 53, 273-84.

FOLGUERAS, A. R., PENDAS, A. M., SANCHEZ, L. M. & LOPEZ-OTIN, C. 2004. Matrix metalloproteinases in cancer: from new functions to improved inhibition strategies. *Int J Dev Biol,* 48, 411-24.

FOLKMAN, J. 1995. Angiogenesis in cancer, vascular, rheumatoid and other disease. *Nat Med,* 1, 27-31.

FONTANA, S., HOVINGA, J. A., STUDT, J. D., ALBERIO, L., LAMMLE, B. & TALEGHANI, B. M. 2004. Plasma therapy in thrombotic thrombocytopenic purpura: review of the literature and the Bern experience in a subgroup of patients with severe acquired ADAMTS-13 deficiency. *Semin Hematol,* 41, 48-59.

FRANOVIC, A., ROBERT, I., SMITH, K., KURBAN, G., PAUSE, A., GUNARATNAM, L. & LEE, S. 2006. Multiple acquired renal carcinoma tumor capabilities abolished upon silencing of ADAM17. *Cancer Res,* 66, 8083-90.

FREIJE, J. P., ABRAHAMSON, M., OLAFSSON, I., VELASCO, G., GRUBB, A. & LOPEZ-OTIN, C. 1991. Structure and expression of the gene encoding cystatin D, a novel human cysteine proteinase inhibitor. *J Biol Chem,* 266, 20538-43.

FRIDMAN, R., FUERST, T. R., BIRD, R. E., HOYHTYA, M., OELKUCT, M., KRAUS, S., KOMAREK, D., LIOTTA, L. A., BERMAN, M. L. & STETLER-STEVENSON, W. G. 1992. Domain structure of human 72-kDa gelatinase/type IV collagenase. Characterization of proteolytic activity and identification of the tissue inhibitor of metalloproteinase-2 (TIMP-2) binding regions. *J Biol Chem,* 267, 15398-405.

GABUEV, A. & OELKE, M. 2011. [Latest trends and recommendations on epidemiology, diagnosis, and treatment of benign prostatic hyperplasia (BPH)]. *Aktuelle Urol,* 42, 167-78.

GADDIPATI, J. P., MCLEOD, D. G., HEIDENBERG, H. B., SESTERHENN, I. A., FINGER, M. J., MOUL, J. W. & SRIVASTAVA, S. 1994. Frequent detection of codon 877 mutation in the androgen receptor gene in advanced prostate cancers. *Cancer Res,* 54, 2861-4.

GAGGIOLI, C., HOOPER, S., HIDALGO-CARCEDO, C., GROSSE, R., MARSHALL, J. F., HARRINGTON, K. & SAHAI, E. 2007. Fibroblast-led collective invasion of carcinoma cells with differing roles for RhoGTPases in leading and following cells. *Nat Cell Biol,* 9, 1392-400.

GALL, A. L., RUFF, M., KANNAN, R., CUNIASSE, P., YIOTAKIS, A., DIVE, V., RIO, M. C., BASSET, P. & MORAS, D. 2001. Crystal structure of the stromelysin-3 (MMP-11) catalytic domain complexed with a phosphinic inhibitor mimicking the transition-state. *J Mol Biol,* 307, 577-86.

GAUDIN, P. B., SESTERHENN, I. A., WOJNO, K. J., MOSTOFI, F. K. & EPSTEIN, J. I. 1997. Incidence and clinical significance of high-grade prostatic intraepithelial neoplasia in TURP specimens. *Urology,* 49, 558-63.

GHARAIBEH, R. Z., FODOR, A. A. & GIBAS, C. J. 2008. Background correction using dinucleotide affinities improves the performance of GCRMA. *BMC Bioinformatics,* 9, 452.

GLASEL, J. A. 1995. Validity of nucleic acid purities monitored by 260nm/280nm absorbance ratios. *Biotechniques,* 18, 62-3.

GLEASON, D. F. 1977. The Veteran's Administration Cooperative Urologic Research Group: histologic grading and clinical staging of prostatic carcinoma. *Urologic Pathology: The Prostate,* 171-198.

GOBINET, J., POUJOL, N. & SULTAN, C. 2002. Molecular action of androgens. *Mol Cell Endocrinol,* 198, 15-24.

GOLDMAN, S. & SHALEV, E. 2004. MMPS and TIMPS in ovarian physiology and pathophysiology. *Front Biosci,* 9, 2474-83.

GRAHAM, F. L. & VAN DER EB, A. J. 1973. A new technique for the assay of infectivity of human adenovirus 5 DNA. *Virology,* 52, 456-67.

GRANCHI, S., BROCCHI, S., BONACCORSI, L., BALDI, E., VINCI, M. C., FORTI, G., SERIO, M. & MAGGI, M. 2001. Endothelin-1 production by prostate cancer cell lines is up-regulated by factors involved in cancer progression and down-regulated by androgens. *Prostate,* 49, 267-77.

GRAYSON, A. C., MA, J. & PUTNAM, D. 2006. Kinetic and efficacy analysis of RNA interference in stably and transiently expressing cell lines. *Mol Pharm,* 3, 601-13.

GREENWAY, B. A. 1998. Effect of flutamide on survival in patients with pancreatic cancer: results of a prospective, randomised, double blind, placebo controlled trial. *Bmj,* 316, 1935-8.

GREGORY, C. W., HAMIL, K. G., KIM, D., HALL, S. H., PRETLOW, T. G., MOHLER, J. L. & FRENCH, F. S. 1998. Androgen receptor expression in androgen-independent prostate cancer is associated with increased expression of androgen-regulated genes. *Cancer Res,* 58, 5718-24.

GROB, B. M., SCHELLHAMMER, P. F., BRASSIL, D. N. & WRIGHT, G. L., JR. 1994. Changes in immunohistochemical staining of PSA, PAP, and TURP-27 following irradiation therapy for clinically localized prostate cancer. *Urology,* 44, 525-9.

GRUBER, J., BOESE, G., TUSCHL, T., OSBORN, M. & WEBER, K. 2004. RNA interference by osmotic lysis of pinosomes: liposome-independent transfection of siRNAs into mammalian cells. *Biotechniques,* 37, 96-102.

GU, P., XING, X., TANZER, M., ROCKEN, C., WEICHERT, W., IVANAUSKAS, A., PROSS, M., PEITZ, U., MALFERTHEINER, P., SCHMID, R. M. & EBERT, M. P. 2008. Frequent loss of TIMP-3 expression in progression of esophageal and gastric adenocarcinomas. *Neoplasia,* 10, 563-72.

GUZMAN, J. R., FUKUDA, S. & PELUS, L. M. 2009. Inhibition of caspase-3 by Survivin prevents Wee1 Kinase degradation and promotes cell survival by maintaining phosphorylation of p34Cdc2. *Gene Ther Mol Biol,* 13B, 264-273.

HADDOCK, G., CROSS, A. K., PLUMB, J., SURR, J., BUTTLE, D. J., BUNNING, R. A. & WOODROOFE, M. N. 2006. Expression of ADAMTS-1, -4, -5 and TIMP-3 in normal and multiple sclerosis CNS white matter. *Mult Scler,* 12, 386-96.

HAMILTON, A. J. & BAULCOMBE, D. C. 1999. A species of small antisense RNA in posttranscriptional gene silencing in plants. *Science,* 286, 950-2.

HAN, E. K., GUADAGNO, T. M., DALTON, S. L. & ASSOIAN, R. K. 1993. A cell cycle and mutational analysis of anchorage-independent growth: cell adhesion and TGF-beta 1 control G1/S transit specifically. *J Cell Biol,* 122, 461-71.

HAN, X., ZHANG, H., JIA, M., HAN, G. & JIANG, W. 2004. Expression of TIMP-3 gene by construction of a eukaryotic cell expression vector and its role in reduction of metastasis in a human breast cancer cell line. *Cell Mol Immunol,* 1, 308-10.

HAQ, I., LOWREY, G. E., KALSHEKER, N. & JOHNSON, S. R. 2011. Matrix metalloproteinase-12 (MMP-12) SNP affects MMP activity, lung macrophage infiltration and protects against emphysema in COPD. *Thorax,* 66, 970-6.

HARTLEY, B. S. 1970. Homologies in serine proteinases. *Philos Trans R Soc Lond B Biol Sci,* 257, 77-87.

HASHIMOTO, G., AOKI, T., NAKAMURA, H., TANZAWA, K. & OKADA, Y. 2001. Inhibition of ADAMTS4 (aggrecanase-1) by tissue inhibitors of metalloproteinases (TIMP-1, 2, 3 and 4). *FEBS Lett,* 494, 192-5.

HASHIMOTO, H., TAKEUCHI, T., KOMATSU, K., MIYAZAKI, K., SATO, M. & HIGASHI, S. 2011. Structural basis for matrix metalloproteinase-2 (MMP-2)-selective inhibitory action of beta-amyloid precursor protein-derived inhibitor. *J Biol Chem,* 286, 33236-43.

HASSELL, J. R., SCHRECENGOST, P. K., RADA, J. A., SUNDARRAJ, N., SOSSI, G. & THOFT, R. A. 1992. Biosynthesis of stromal matrix proteoglycans and basement membrane components by human corneal fibroblasts. *Invest Ophthalmol Vis Sci,* 33, 547-57.

HATZOGLOU, A., KAMPA, M., KOGIA, C., CHARALAMPOPOULOS, I., THEODOROPOULOS, P. A., ANEZINIS, P., DAMBAKI, C., PAPAKONSTANTI, E. A., STATHOPOULOS, E. N., STOURNARAS, C., GRAVANIS, A. & CASTANAS, E. 2005. Membrane androgen receptor activation induces apoptotic regression of human prostate cancer cells in vitro and in vivo. *J Clin Endocrinol Metab,* 90, 893-903.

HEDSTROM, L. 2002. An overview of serine proteases. *Curr Protoc Protein Sci,* Chapter 21, Unit 21 10.

HEGE, T. & BAUMANN, U. 2001. The conserved methionine residue of the metzincins: a site-directed mutagenesis study. *J Mol Biol,* 314, 181-6.

HEINLEIN, C. A. & CHANG, C. 2004. Androgen receptor in prostate cancer. *Endocr Rev,* 25, 276-308.

HEMMINKI, K., RAWAL, R. & BERMEJO, J. L. 2005. Prostate cancer screening, changing age-specific incidence trends and implications on familial risk. *Int J Cancer,* 113, 312-5.

HEYNS, C. F., MATHEE, S., ISAACS, A., KHARWA, A., DE BEER, P. M. & PRETORIUS, M. A. 2003. Problems with prostate specific antigen screening for prostate cancer in the primary healthcare setting in South Africa. *BJU Int,* 91, 785-8.

HIGANO, C. S., ELLIS, W., RUSSELL, K. & LANGE, P. 1996. Intermittent Androgen Supression with Leuprolide and Flutamide for Prostate Cancer: A Pilot Study. *Urology,* 48, 800-804.

HILSKA, M., ROBERTS, P. J., COLLAN, Y. U., LAINE, V. J., KOSSI, J., HIRSIMAKI, P., RAHKONEN, O. & LAATO, M. 2007. Prognostic significance of matrix metalloproteinases-1, -2, -7 and -13 and tissue inhibitors of metalloproteinases-1, -2, -3 and -4 in colorectal cancer. *Int J Cancer,* 121, 714-23.

HINSLEY, E. E., HUNT, S., HUNTER, K. D., WHAWELL, S. A. & LAMBERT, D. W. 2012. Endothelin-1 stimulates motility of head and neck squamous carcinoma cells by promoting stromal-epithelial interactions. *Int J Cancer,* 130, 40-7.

HOFMANN, A., LAUE, S., ROST, A. K., SCHERBAUM, W. A. & AUST, G. 1998. mRNA levels of membrane-type 1 matrix metalloproteinase (MT1-MMP), MMP-2, and MMP-9 and of their inhibitors TIMP-2 and TIMP-3 in normal thyrocytes and thyroid carcinoma cell lines. *Thyroid,* 8, 203-14.

HOLVOET, S., VINCENT, C., SCHMITT, D. & SERRES, M. 2003. The inhibition of MAPK pathway is correlated with down-regulation of MMP-9 secretion induced by TNF-alpha in human keratinocytes. *Exp Cell Res,* 290, 108-19.

HORNEBECK, W. 2003. Down-regulation of tissue inhibitor of matrix metalloprotease-1 (TIMP-1) in aged human skin contributes to matrix degradation and impaired cell growth and survival. *Pathol Biol (Paris),* 51, 569-73.

HOVENANIAN, M. S. & DEMING, C. L. 1948. The heterologous growth of cancer of the human prostate. *Surg Gynecol Obstet,* 86, 29-35.

HSING, A. W. & CHOKKALINGAM, A. P. 2006. Prostate cancer epidemiology. *Front Biosci,* 11, 1388-413.

HSU, H., SHU, H. B., PAN, M. G. & GOEDDEL, D. V. 1996. TRADD-TRAF2 and TRADD-FADD interactions define two distinct TNF receptor 1 signal transduction pathways. *Cell,* 84, 299-308.

HSU, H., XIONG, J. & GOEDDEL, D. V. 1995. The TNF receptor 1-associated protein TRADD signals cell death and NF-kappa B activation. *Cell,* 81, 495-504.

HSU, Y. P., STATON, C. A., CROSS, N. & BUTTLE, D. J. 2012. Anti-angiogenic properties of ADAMTS-4 in vitro. *Int J Exp Pathol,* 93, 70-7.

HUANG, H. Y., WEN, Y., IRWIN, J. C., KRUESSEL, J. S., SOONG, Y. K. & POLAN, M. L. 1998. Cytokine-mediated regulation of 92-kilodalton type IV collagenase, tissue inhibitor or metalloproteinase-1 (TIMP-1), and TIMP-3 messenger ribonucleic acid expression in human endometrial stromal cells. *J Clin Endocrinol Metab,* 83, 1721-9.

HUANG, W., YU, L. F., ZHONG, J., QIAO, M. M., JIANG, F. X., DU, F., TIAN, X. L. & WU, Y. L. 2007. Angiotensin II Type 1 Receptor Expression in Human Gastric Cancer and Induces MMP2 and MMP9 Expression in MKN-28 Cells. *Dig Dis Sci.*

HUBBARD, T., BARKER, D., BIRNEY, E., CAMERON, G., CHEN, Y., CLARK, L., COX, T., CUFF, J., CURWEN, V., DOWN, T., DURBIN, R., EYRAS, E., GILBERT, J., HAMMOND, M., HUMINIECKI, L., KASPRZYK, A., LEHVASLAIHO, H., LIJNZAAD, P., MELSOPP, C., MONGIN, E., PETTETT, R., POCOCK, M., POTTER, S., RUST, A., SCHMIDT, E., SEARLE, S., SLATER, G., SMITH, J., SPOONER, W., STABENAU, A., STALKER, J., STUPKA, E., URETA-VIDAL, A., VASTRIK, I. & CLAMP, M. 2002. The Ensembl genome database project. *Nucleic Acids Res,* 30, 38-41.

HUI, W., ROWAN, A. D. & CAWSTON, T. 2001. Modulation of the expression of matrix metalloproteinase and tissue inhibitors of metalloproteinases by TGF-beta1 and IGF-1 in primary human articular and bovine nasal chondrocytes stimulated with TNF-alpha. *Cytokine,* 16, 31-5.

HUSSAINI, I. M., SRIKUMAR, K., QUESENBERRY, P. J. & GONIAS, S. L. 1990. Colony-stimulating factor-1 modulates alpha 2-macroglobulin receptor expression in murine bone marrow macrophages. *J Biol Chem,* 265, 19441-6.

IANNELLO, R. C., YOUNG, J., SUMARSONO, S., TYMMS, M. J., DAHL, H. H., GOULD, J., HEDGER, M. & KOLA, I. 1997. Regulation of Pdha-2 expression is mediated by proximal promoter sequences and CpG methylation. *Mol Cell Biol,* 17, 612-9.

IKONOMIDIS, J. S., HENDRICK, J. W., PARKHURST, A. M., HERRON, A. R., ESCOBAR, P. G., DOWDY, K. B., STROUD, R. E., HAPKE, E., ZILE, M. R. & SPINALE, F. G. 2005. Accelerated LV remodeling after myocardial infarction in TIMP-1-deficient mice: effects of exogenous MMP inhibition. *Am J Physiol Heart Circ Physiol,* 288, H149-58.

ILLMAN, S. A., LOHI, J. & KESKI-OJA, J. 2008. Epilysin (MMP-28)--structure, expression and potential functions. *Exp Dermatol,* 17, 897-907.

INAOKA, T., BILBE, G., ISHIBASHI, O., TEZUKA, K., KUMEGAWA, M. & KOKUBO, T. 1995. Molecular cloning of human cDNA for cathepsin K: novel cysteine proteinase predominantly expressed in bone. *Biochem Biophys Res Commun,* 206, 89-96.

IRVING, J. A., PIKE, R. N., DAI, W., BROMME, D., WORRALL, D. M., SILVERMAN, G. A., COETZER, T. H., DENNISON, C., BOTTOMLEY, S. P. & WHISSTOCK,

J. C. 2002. Evidence that serpin architecture intrinsically supports papain-like cysteine protease inhibition: engineering alpha(1)-antitrypsin to inhibit cathepsin proteases. *Biochemistry,* 41, 4998-5004.

ISHII, K., MIZOKAMI, A., TSUNODA, T., IGUCHI, K., KATO, M., HORI, Y., ARIMA, K., NAMIKI, M. & SUGIMURA, Y. 2011. Heterogenous induction of carcinoma-associated fibroblast-like differentiation in normal human prostatic fibroblasts by co-culturing with prostate cancer cells. *J Cell Biochem,* 112, 3604-11.

ISLEKEL, H., OKTAY, G., TERZI, C., CANDA, A. E., FUZUN, M. & KUPELIOGLU, A. 2007. Matrix metalloproteinase-9,-3 and tissue inhibitor of matrix metalloproteinase-1 in colorectal cancer: relationship to clinicopathological variables. *Cell Biochem Funct,* 25, 433-41.

ITO, A., NAKAJIMA, S., SASAGURI, Y., NAGASE, H. & MORI, Y. 1995. Co-culture of human breast adenocarcinoma MCF-7 cells and human dermal fibroblasts enhances the production of matrix metalloproteinases 1, 2 and 3 in fibroblasts. *Br J Cancer,* 71, 1039-45.

ITOH, Y. & NAGASE, H. 2002. Matrix metalloproteinases in cancer. *Essays Biochem,* 38, 21-36.

IWATA, H., KOBAYASHI, S., IWASE, H. & OKADA, Y. 1995. [The expression of MMPs and TIMPs in human breast cancer tissues and importance of their balance in cancer invasion and metastasis]. *Nippon Rinsho,* 53, 1805-10.

IYER, S., WEI, S., BREW, K. & ACHARYA, K. R. 2007. Crystal structure of the catalytic domain of matrix metalloproteinase-1 in complex with the inhibitory domain of tissue inhibitor of metalloproteinase-1. *J Biol Chem,* 282, 364-71.

JANNE, O. A., CROZAT, A., PALVIMO, J. & EISENBERG, L. M. 1991. Androgen-regulation of ornithine decarboxylase and S-adenosylmethionine decarboxylase genes. *J Steroid Biochem Mol Biol,* 40, 307-15.

JANOSSY, J., UBEZIO, P., APATI, A., MAGOCSI, M., TOMPA, P. & FRIEDRICH, P. 2004. Calpain as a multi-site regulator of cell cycle. *Biochem Pharmacol,* 67, 1513-21.

JARVINEN, M., RINNE, A. & HOPSU-HAVU, V. K. 1987. Human cystatins in normal and diseased tissues--a review. *Acta Histochem,* 82, 5-18.

JECHLINGER, M., SOMMER, A., MORIGGL, R., SEITHER, P., KRAUT, N., CAPODIECCI, P., DONOVAN, M., CORDON-CARDO, C., BEUG, H. & GRUNERT, S. 2006. Autocrine PDGFR signaling promotes mammary cancer metastasis. *J Clin Invest,* 116, 1561-70.

JOVIN, T. M. 1973a. Multiphasic zone electrophoresis. I. Steady-state moving-boundary systems formed by different electrolyte combinations. *Biochemistry,* 12, 871-9.

JOVIN, T. M. 1973b. Multiphasic zone electrophoresis. II. Design of integrated discontinuous buffer systems for analytical and preparative fractionation. *Biochemistry,* 12, 879-90.

KABALIN, J. N., MCNEAL, J. E., JOHNSTONE, I. M. & STAMEY, T. A. 1995. Serum prostate-specific antigen and the biologic progression of prostate cancer. *Urology,* 46, 65-70.

KAMEI, M. & HOLLYFIELD, J. G. 1999. TIMP-3 in Bruch's membrane: changes during aging and in age-related macular degeneration. *Invest Ophthalmol Vis Sci,* 40, 2367-75.

KAMINSKI, A., HAHNE, J. C., HADDOUTI EL, M., FLORIN, A., WELLMANN, A. & WERNERT, N. 2006. Tumour-stroma interactions between metastatic prostate cancer cells and fibroblasts. *Int J Mol Med,* 18, 941-50.

KAMPA, M., PAPAKONSTANTI, E. A., HATZOGLOU, A., STATHOPOULOS, E. N., STOURNARAS, C. & CASTANAS, E. 2002. The human prostate cancer cell line LNCaP bears functional membrane testosterone receptors that increase PSA secretion and modify actin cytoskeleton. *FASEB J,* 16, 1429-31.

KARAN, D., LIN, F. C., BRYAN, M., RINGEL, J., MONIAUX, N., LIN, M. F. & BATRA, S. K. 2003. Expression of ADAMs (a disintegrin and metalloproteases) and TIMP-3 (tissue inhibitor of metalloproteinase-3) in human prostatic adenocarcinomas. *Int J Oncol,* 23, 1365-71.

KASHIWAGI M, TORTORELLA M, NAGASE H & K, B. 2001. TIMP-3 is a potent inhibitor of aggrecanase-1 (ADAMTS-4) and aggrecanase-2 (ADAMTS-5). *J Biol Chem,* 276, 12501 - 12504.

KASHIWAGI, M., ENGHILD, J. J., GENDRON, C., HUGHES, C., CATERSON, B., ITOH, Y. & NAGASE, H. 2004. Altered proteolytic activities of ADAMTS-4 expressed by C-terminal processing. *J Biol Chem,* 279, 10109-19.

KAUSHAL, G. P. & SHAH, S. V. 2000. The new kids on the block: ADAMTSs, potentially multifunctional metalloproteinases of the ADAM family. *J Clin Invest,* 105, 1335-7.

KEHINDE, E. O. 1995. The geography of prostate cancer and its treatment in Africa. *Cancer Surv,* 23, 281-6.

KEMPPAINEN, J. A., LANGLEY, E., WONG, C. I., BOBSEINE, K., KELCE, W. R. & WILSON, E. M. 1999. Distinguishing androgen receptor agonists and antagonists: distinct mechanisms of activation by medroxyprogesterone acetate and dihydrotestosterone. *Mol Endocrinol,* 13, 440-54.

KENFIELD, S. A., CHANG, S. T. & CHAN, J. M. 2007. Diet and lifestyle interventions in active surveillance patients with favorable-risk prostate cancer. *Curr Treat Options Oncol,* 8, 173-96.

KERN, C. B., WESSELS, A., MCGARITY, J., DIXON, L. J., ALSTON, E., ARGRAVES, W. S., GEETING, D., NELSON, C. M., MENICK, D. R. & APTE, S. S. 2010. Reduced versican cleavage due to Adamts9 haploinsufficiency is associated with cardiac and aortic anomalies. *Matrix Biol,* 29, 304-16.

KEVORKIAN, L., YOUNG, D. A., DARRAH, C., DONELL, S. T., SHEPSTONE, L., PORTER, S., BROCKBANK, S. M., EDWARDS, D. R., PARKER, A. E. & CLARK, I. M. 2004. Expression profiling of metalloproteinases and their inhibitors in cartilage. *Arthritis Rheum,* 50, 131-41.

KHOO, V. S., PADHANI, A. R., TANNER, S. F., FINNIGAN, D. J., LEACH, M. O. & DEARNALEY, D. P. 1999. Comparison of MRI with CT for the radiotherapy planning of prostate cancer: a feasibility study. *Br J Radiol,* 72, 590-7.

KIRKIN, V., CAHUZAC, N., GUARDIOLA-SERRANO, F., HUAULT, S., LUCKERATH, K., FRIEDMANN, E., NOVAC, N., WELS, W. S., MARTOGLIO, B., HUEBER, A. O. & ZORNIG, M. 2007. The Fas ligand intracellular domain is released by ADAM10 and SPPL2a cleavage in T-cells. *Cell Death Differ,* 14, 1678-87.

KLEIN, B. 1997. GP130 cytokines, interferon, survival and proliferation of human myeloma cells. *Eur Cytokine Netw,* 8, 323.

KLEIN, T. & BISCHOFF, R. 2011. Active metalloproteases of the A Disintegrin and Metalloprotease (ADAM) family: biological function and structure. *J Proteome Res,* 10, 17-33.

KLUS, G. T., NAKAMURA, J., LI, J. S., LING, Y. Z., SON, C., KEMPPAINEN, J. A., WILSON, E. M. & BRODIE, A. M. 1996. Growth inhibition of human prostate cells in vitro by novel inhibitors of androgen synthesis. *Cancer Res,* 56, 4956-64.

KNAUPER, V., LOPEZ-OTIN, C., SMITH, B., KNIGHT, G. & MURPHY, G. 1996. Biochemical characterization of human collagenase-3. *J Biol Chem,* 271, 1544-50.

KNIGHT, C. G., WILLENBROCK, F. & MURPHY, A. G. 1992. A novel Coumarin-labelled Peptide for Sensitive Continuous Assays of the Matrix Metalloproteinases. *FEBS Lett,* 296, 263-266.

KNITTEL, T., MEHDE, M., KOBOLD, D., SAILE, B., DINTER, C. & RAMADORI, G. 1999. Expression patterns of matrix metalloproteinases and their inhibitors in parenchymal and non-parenchymal cells of rat liver: regulation by TNF-alpha and TGF-beta1. *J Hepatol,* 30, 48-60.

KNOWLES, J. P., SHI-WEN, X., HAQUE, S. U., BHALLA, A., DASHWOOD, M. R., YANG, S., TAYLOR, I., WINSLET, M. C., ABRAHAM, D. J. & LOIZIDOU, M. 2012. Endothelin-1 stimulates colon cancer adjacent fibroblasts. *Int J Cancer,* 130, 1264-72.

KOHRMANN, A., KAMMERER, U., KAPP, M., DIETL, J. & ANACKER, J. 2009. Expression of matrix metalloproteinases (MMPs) in primary human breast cancer and breast cancer cell lines: New findings and review of the literature. *BMC Cancer,* 9, 188.

KOLB, C., MAUCH, S., PETER, H. H., KRAWINKEL, U. & SEDLACEK, R. 1997. The matrix metalloproteinase RASI-1 is expressed in synovial blood vessels of a rheumatoid arthritis patient. *Immunol Lett,* 57, 83-8.

KOMIYAMA, T., RAY, C. A., PICKUP, D. J., HOWARD, A. D., THORNBERRY, N. A., PETERSON, E. P. & SALVESEN, G. 1994. Inhibition of interleukin-1 beta converting enzyme by the cowpox virus serpin CrmA. An example of cross-class inhibition. *J Biol Chem,* 269, 19331-7.

KONIG, J. E., SENGE, T., ALLHOFF, E. P. & KONIG, W. 2004. Analysis of the inflammatory network in benign prostate hyperplasia and prostate cancer. *Prostate,* 58, 121-9.

KORNFELD, J. W., MEDER, S., WOHLBERG, M., FRIEDRICH, R. E., RAU, T., RIETHDORF, L., LONING, T., PANTEL, K. & RIETHDORF, S. 2011. Overexpression of TACE and TIMP3 mRNA in head and neck cancer: association with tumour development and progression. *Br J Cancer,* 104, 138-45.

KOTZSCH, M., FARTHMANN, J., MEYE, A., FUESSEL, S., BARETTON, G., TJAN-HEIJNEN, V. C., SCHMITT, M., LUTHER, T., SWEEP, F. C., MAGDOLEN, V. & SPAN, P. N. 2005. Prognostic relevance of uPAR-del4/5 and TIMP-3 mRNA expression levels in breast cancer. *Eur J Cancer,* 41, 2760-8.

KOUTSODONTIS, G., MOUSTAKAS, A. & KARDASSIS, D. 2002. The role of Sp1 family members, the proximal GC-rich motifs, and the upstream enhancer region in the regulation of the human cell cycle inhibitor p21WAF-1/Cip1 gene promoter. *Biochemistry,* 41, 12771-84.

KRAUT, J. 1977. Serine proteases: structure and mechanism of catalysis. *Annu Rev Biochem,* 46, 331-58.

KUFE, D. W., POLLOCK, R. E., WEICHSELBAUM, R. R. & AL, E. 2003. Neoplasms of the Prostate. *Cancer Medicine.* BC Decker Inc. Ohio, U.S.A.

KUIVANEN, T., AHOKAS, K., VIROLAINEN, S., JAHKOLA, T., HOLTTA, E., SAKSELA, O. & SAARIALHO-KERE, U. 2005. MMP-21 is upregulated at early

stages of melanoma progression but disappears with more aggressive phenotype. *Virchows Arch,* 447, 954-60.

KUMAR, V. L. & MAJUMDER, P. K. 1995. Prostate gland: structure, functions and regulation. *Int Urol Nephrol,* 27, 231-43.

KUNO, K. & MATSUSHIMA, K. 1998. ADAMTS-1 protein anchors at the extracellular matrix through the thrombospondin type I motifs and its spacing region. *J Biol Chem,* 273, 13912-7.

KUNO, K., OKADA, Y., KAWASHIMA, H., NAKAMURA, H., MIYASAKA, M., OHNO, H. & MATSUSHIMA, K. 2000. ADAMTS-1 cleaves a cartilage proteoglycan, aggrecan. *FEBS Lett,* 478, 241-5.

LAMBERT, E., DASSE, E., HAYE, B. & PETITFRERE, E. 2004. TIMPs as multifacial proteins. *Crit Rev Oncol Hematol,* 49, 187-98.

LANGTON, K. P., BARKER, M. D. & MCKIE, N. 1998. Localization of the functional domains of human tissue inhibitor of metalloproteinases-3 and the effects of a Sorsby's fundus dystrophy mutation. *J Biol Chem,* 273, 16778-81.

LANGTON, K. P., MCKIE, N., SMITH, B. M., BROWN, N. J. & BARKER, M. D. 2005. Sorsby's fundus dystrophy mutations impair turnover of TIMP-3 by retinal pigment epithelial cells. *Hum Mol Genet,* 14, 3579-86.

LAWRENCE, M. E. & POSSINGHAM, J. V. 1986. Direct measurement of femtogram amounts of DNA in cells and chloroplasts by quantitative microspectrofluorometry. *J Histochem Cytochem,* 34, 761-8.

LECO, K. J., KHOKHA, R., PAVLOFF, N., HAWKES, S. P. & EDWARDS, D. R. 1994. Tissue inhibitor of metalloproteinases-3 (TIMP-3) is an extracellular matrix-associated protein with a distinctive pattern of expression in mouse cells and tissues. *J Biol Chem,* 269, 9352-60.

LEE, J. K., SHIN, J. H., SUH, J., CHOI, I. S., RYU, K. S. & GWAG, B. J. 2008. Tissue inhibitor of metalloproteinases-3 (TIMP-3) expression is increased during serum deprivation-induced neuronal apoptosis in vitro and in the G93A mouse model of amyotrophic lateral sclerosis: a potential modulator of Fas-mediated apoptosis. *Neurobiol Dis,* 30, 174-85.

LEE, M. H., ATKINSON, S. & MURPHY, G. 2007. Identification of the extracellular matrix (ECM) binding motifs of tissue inhibitor of metalloproteinases (TIMP)-3 and effective transfer to TIMP-1. *J Biol Chem,* 282, 6887-98.

LEE, Y. C. & RANNELS, D. E. 1998. Regulation of extracellular matrix synthesis by TNF-alpha and TGF-beta1 in type II cells exposed to coal dust. *Am J Physiol,* 275, L637-44.

LENTZSCH, S., CHATTERJEE, M., GRIES, M., BOMMERT, K., GOLLASCH, H., DORKEN, B. & BARGOU, R. C. 2004. PI3-K/AKT/FKHR and MAPK signaling cascades are redundantly stimulated by a variety of cytokines and contribute independently to proliferation and survival of multiple myeloma cells. *Leukemia,* 18, 1883-90.

LEUNG-TOUNG, R., LI, W., TAM, T. F. & KARIMIAN, K. 2002. Thiol-dependent enzymes and their inhibitors: a review. *Curr Med Chem,* 9, 979-1002.

LILJA, H. 1993. Structure, function, and regulation of the enzyme activity of prostate-specific antigen. *World J Urol,* 11, 188-91.

LIN, M. F., MENG, T. C., RAO, P. S., CHANG, C., SCHONTHAL, A. H. & LIN, F. F. 1998. Expression of human prostatic acid phosphatase correlates with androgen-stimulated cell proliferation in prostate cancer cell lines. *J Biol Chem,* 273, 5939-47.

LINDZEY, J., KUMAR, M. V., GROSSMAN, M., YOUNG, C. & TINDALL, D. J. 1994. Molecular mechanisms of androgen action. *Vitam Horm,* 49, 383-432.

LIPARDI, C., WEI, Q. & PATERSON, B. M. 2001. RNAi as random degradative PCR: siRNA primers convert mRNA into dsRNAs that are degraded to generate new siRNAs. *Cell,* 107, 297-307.

LIPPMAN, M. E., DICKSON, R. B., GELMANN, E. P., ROSEN, N., KNABBE, C., BATES, S., BRONZERT, D., HUFF, K. & KASID, A. 1987. Growth regulation of human breast carcinoma occurs through regulated growth factor secretion. *J Cell Biochem,* 35, 1-16.

LIU, C., XU, P., LAMOUILLE, S., XU, J. & DERYNCK, R. 2009. TACE-mediated ectodomain shedding of the type I TGF-beta receptor downregulates TGF-beta signaling. *Mol Cell,* 35, 26-36.

LIU, P. C., LIU, X., LI, Y., COVINGTON, M., WYNN, R., HUBER, R., HILLMAN, M., YANG, G., ELLIS, D., MARANDO, C., KATIYAR, K., BRADLEY, J., ABREMSKI, K., STOW, M., RUPAR, M., ZHUO, J., LI, Y. L., LIN, Q., BURNS, D., XU, M., ZHANG, C., QIAN, D. Q., HE, C., SHARIEF, V., WENG, L., AGRIOS, C., SHI, E., METCALF, B., NEWTON, R., FRIEDMAN, S., YAO, W., SCHERLE, P., HOLLIS, G. & BURN, T. C. 2006. Identification of ADAM10 as a major source of HER2 ectodomain sheddase activity in HER2 overexpressing breast cancer cells. *Cancer Biol Ther,* 5, 657-64.

LIU, W. H. & CHANG, L. S. 2011. Fas/FasL-dependent and -independent activation of caspase-8 in doxorubicin-treated human breast cancer MCF-7 cells: ADAM10 down-regulation activates Fas/FasL signaling pathway. *Int J Biochem Cell Biol,* 43, 1708-19.

LIVAK, K. J. & SCHMITTGEN, T. D. 2001. Analysis of relative gene expression data using real-time quantitative PCR and the 2(-Delta Delta C(T)) Method. *Methods,* 25, 402-8.

LOHI, J., WILSON, C. L., ROBY, J. D. & PARKS, W. C. 2001. Epilysin, a novel human matrix metalloproteinase (MMP-28) expressed in testis and keratinocytes and in response to injury. *J Biol Chem,* 276, 10134-44.

LOVELOCK, J. D., BAKER, A. H., GAO, F., DONG, J. F., BERGERON, A. L., MCPHEAT, W., SIVASUBRAMANIAN, N. & MANN, D. L. 2005. Heterogeneous effects of tissue inhibitors of matrix metalloproteinases on cardiac fibroblasts. *Am J Physiol Heart Circ Physiol,* 288, H461-8.

LU, G. L., WEN, J. M., XU, J. M., ZHANG, M., XU, R. B. & TIAN, B. L. 2003. [Relationship between TIMP-3 expression and promoter methylation of TIMP-3 gene in hepatocellular carcinoma]. *Zhonghua Bing Li Xue Za Zhi,* 32, 230-3.

MAATTA, M., SOINI, Y., LIAKKA, A. & AUTIO-HARMAINEN, H. 2000. Localization of MT1-MMP, TIMP-1, TIMP-2, and TIMP-3 messenger RNA in normal, hyperplastic, and neoplastic endometrium. Enhanced expression by endometrial adenocarcinomas is associated with low differentiation. *Am J Clin Pathol,* 114, 402-11.

MACOSKA, J. A. 2011. Chemokines and BPH/LUTS. *Differentiation,* 82, 253-60.

MARCELLI, M., HAIDACHER, S. J., PLYMATE, S. R. & BIRNBAUM, R. S. 1995. Altered growth and insulin-like growth factor-binding protein-3 production in PC3 prostate carcinoma cells stably transfected with a constitutively active androgen receptor complementary deoxyribonucleic acid. *Endocrinology,* 136, 1040-8.

MARCHENKO, G. N., RATNIKOV, B. I., ROZANOV, D. V., GODZIK, A., DERYUGINA, E. I. & STRONGIN, A. Y. 2001. Characterization of matrix

metalloproteinase-26, a novel metalloproteinase widely expressed in cancer cells of epithelial origin. *Biochem J,* 356, 705-18.

MAREEL, M. & LEROY, A. 2003. Clinical, cellular, and molecular aspects of cancer invasion. *Physiol Rev,* 83, 337-76.

MARETZKY, T., YANG, G., OUERFELLI, O., OVERALL, C. M., WORPENBERG, S., HASSIEPEN, U., EDER, J. & BLOBEL, C. P. 2009. Characterization of the catalytic activity of the membrane-anchored metalloproteinase ADAM15 in cell-based assays. *Biochem J,* 420, 105-13.

MARIC, M. A., TAYLOR, M. D. & BLUM, J. S. 1994. Endosomal aspartic proteinases are required for invariant-chain processing. *Proc Natl Acad Sci U S A,* 91, 2171-5.

MATTHEWS, R. T., GARY, S. C., ZERILLO, C., PRATTA, M., SOLOMON, K., ARNER, E. C. & HOCKFIELD, S. 2000. Brain-enriched hyaluronan binding (BEHAB)/brevican cleavage in a glioma cell line is mediated by a disintegrin and metalloproteinase with thrombospondin motifs (ADAMTS) family member. *J Biol Chem,* 275, 22695-703.

MCLAREN, I. D., JERDE, T. J. & BUSHMAN, W. 2011. Role of interleukins, IGF and stem cells in BPH. *Differentiation,* 82, 237-43.

MCNEAL, J. E. 1978. Origin and evolution of benign prostatic enlargement. *Invest Urol,* 15, 340-5.

MCNEAL, J. E. 1997. Prostate cancer volume. *Am J Surg Pathol,* 21, 1392-3.

MCVARY, K. T. 2006. BPH: epidemiology and comorbidities. *Am J Manag Care,* 12, S122-8.

METTLIN, C., LITTRUP, P. J., KANE, R. A., MURPHY, G. P., LEE, F., CHESLEY, A., BADALAMENT, R. & MOSTOFI, F. K. 1994. Relative sensitivity and specificity of serum prostate specific antigen (PSA) level compared with age-referenced PSA, PSA density, and PSA change. Data from the American Cancer Society National Prostate Cancer Detection Project. *Cancer,* 74, 1615-20.

MI, Z., BHATTACHARYA, S. D., KIM, V. M., GUO, H., TALBOT, L. J. & KUO, P. C. 2011. Osteopontin promotes CCL5-mesenchymal stromal cell-mediated breast cancer metastasis. *Carcinogenesis,* 32, 477-87.

MILLER, D. C., HAFEZ, K. S., STEWART, A., MONTIE, J. E. & WEI, J. T. 2003. Prostate carcinoma presentation, diagnosis, and staging: an update form the National Cancer Data Base. *Cancer,* 98, 1169-78.

MILLS, P. K., BEESON, W. L., PHILLIPS, R. L. & FRASER, G. E. 1989. Cohort study of diet, lifestyle, and prostate cancer in Adventist men. *Cancer,* 64, 598-604.

MINIATI, D. N., CHANG, Y., SHU, W. P., PEEHL, D. M. & LIU, B. C. 1996. Role of prostatic basal cells in the regulation and suppression of human prostate cancer cells. *Cancer Lett,* 104, 137-44.

MINO, N., TAKENAKA, K., SONOBE, M., MIYAHARA, R., YANAGIHARA, K., OTAKE, Y., WADA, H. & TANAKA, F. 2007. Expression of tissue inhibitor of metalloproteinase-3 (TIMP-3) and its prognostic significance in resected non-small cell lung cancer. *J Surg Oncol,* 95, 250-7.

MIYAZAKI, T., KATO, H., NAKAJIMA, M., FARIED, A., TAKITA, J., SOHDA, M., FUKAI, Y., YAMAGUCHI, S., MASUDA, N., MANDA, R., FUKUCHI, M., OJIMA, H., TSUKADA, K. & KUWANO, H. 2004. An immunohistochemical study of TIMP-3 expression in oesophageal squamous cell carcinoma. *Br J Cancer,* 91, 1556-60.

MOCHIZUKI, S., SHIMODA, M., SHIOMI, T., FUJII, Y. & OKADA, Y. 2004. ADAM28 is activated by MMP-7 (matrilysin-1) and cleaves insulin-like growth factor binding protein-3. *Biochem Biophys Res Commun,* 315, 79-84.

MOHAMMED, F. F., SMOOKLER, D. S., TAYLOR, S. E., FINGLETON, B., KASSIRI, Z., SANCHEZ, O. H., ENGLISH, J. L., MATRISIAN, L. M., AU, B., YEH, W. C. & KHOKHA, R. 2004. Abnormal TNF activity in Timp3-/- mice leads to chronic hepatic inflammation and failure of liver regeneration. *Nat Genet,* 36, 969-77.

MOLHOEK, K. R., ERDAG, G., RASAMNY, J., MURPHY, C., DEACON, D., PATTERSON, J. W., SLINGLUFF, C. L., JR. & BRAUTIGAN, D. L. 2011. VEGFR-2 expression in human melanoma: Revised assessment. *Int J Cancer.*

MOLOKWU, C. N., ADENIJI, O. O., CHANDRASEKHARAN, S., HAMDY, F. C. & BUTTLE, D. J. 2010. Androgen regulates ADAMTS15 gene expression in prostate cancer cells. *Cancer Invest,* 28, 698-710.

MONGE, A., JAGLA, M., LAPOUGE, G., SASORITH, S., CRUCHANT, M., WURTZ, J. M., JACQMIN, D., BERGERAT, J. P. & CERALINE, J. 2006. Unfaithfulness and promiscuity of a mutant androgen receptor in a hormone-refractory prostate cancer. *Cell Mol Life Sci,* 63, 487-97.

MONTGOMERY, B. T., YOUNG, C. Y., BILHARTZ, D. L., ANDREWS, P. E., PRESCOTT, J. L., THOMPSON, N. F. & TINDALL, D. J. 1992. Hormonal regulation of prostate-specific antigen (PSA) glycoprotein in the human prostatic adenocarcinoma cell line, LNCaP. *Prostate,* 21, 63-73.

MOROTE, J., RAVENTOS, C. X., LORENTE, J. A., LOPEZ-PACIOS, M. A., ENCABO, G., DE TORRES, I. & ANDREU, J. 1997. Measurement of free PSA in the diagnosis and staging of prostate cancer. *Int J Cancer,* 71, 756-9.

MOSS, M. L., JIN, S. L., BECHERER, J. D., BICKETT, D. M., BURKHART, W., CHEN, W. J., HASSLER, D., LEESNITZER, M. T., MCGEEHAN, G., MILLA, M., MOYER, M., ROCQUE, W., SEATON, T., SCHOENEN, F., WARNER, J. & WILLARD, D. 1997a. Structural features and biochemical properties of TNF-alpha converting enzyme (TACE). *J Neuroimmunol,* 72, 127-9.

MOSS, M. L., JIN, S. L., MILLA, M. E., BICKETT, D. M., BURKHART, W., CARTER, H. L., CHEN, W. J., CLAY, W. C., DIDSBURY, J. R., HASSLER, D., HOFFMAN, C. R., KOST, T. A., LAMBERT, M. H., LEESNITZER, M. A., MCCAULEY, P., MCGEEHAN, G., MITCHELL, J., MOYER, M., PAHEL, G., ROCQUE, W., OVERTON, L. K., SCHOENEN, F., SEATON, T., SU, J. L., BECHERER, J. D. & ET AL. 1997b. Cloning of a disintegrin metalloproteinase that processes precursor tumour-necrosis factor-alpha. *Nature,* 385, 733-6.

MOUSTAKAS, A., PARDALI, K., GAAL, A. & HELDIN, C. H. 2002. Mechanisms of TGF-beta signaling in regulation of cell growth and differentiation. *Immunol Lett,* 82, 85-91.

MULLER-ESTERL, W., FRITZ, H., KELLERMANN, J., LOTTSPEICH, F., MACHLEIDT, W. & TURK, V. 1985a. Genealogy of mammalian cysteine proteinase inhibitors. Common evolutionary origin of stefins, cystatins and kininogens. *FEBS Lett,* 191, 221-6.

MULLER-ESTERL, W., FRITZ, H., MACHLEIDT, W., RITONJA, A., BRZIN, J., KOTNIK, M., TURK, V., KELLERMANN, J. & LOTTSPEICH, F. 1985b. Human plasma kininogens are identical with alpha-cysteine proteinase inhibitors. Evidence from immunological, enzymological and sequence data. *FEBS Lett,* 182, 310-4.

MURAI, T., MIYAZAKI, Y., NISHINAKAMURA, H., SUGAHARA, K. N., MIYAUCHI, T., SAKO, Y., YANAGIDA, T. & MIYASAKA, M. 2004.

Engagement of CD44 promotes Rac activation and CD44 cleavage during tumor cell migration. *J Biol Chem,* 279, 4541-50.

MURDOCH, C., GIANNOUDIS, A. & LEWIS, C. E. 2004. Mechanisms regulating the recruitment of macrophages into hypoxic areas of tumors and other ischemic tissues. *Blood,* 104, 2224-34.

MURDOCH, C. & LEWIS, C. E. 2005. Macrophage migration and gene expression in response to tumor hypoxia. *Int J Cancer,* 117, 701-8.

MURPHY, G., HOUBRECHTS, A., COCKETT, M. I., WILLIAMSON, R. A., O'SHEA, M. & DOCHERTY, A. J. 1991. The N-terminal domain of tissue inhibitor of metalloproteinases retains metalloproteinase inhibitory activity. *Biochemistry,* 30, 8097-102.

MURPHY, G., MCALPINE, C. G., POLL, C. T. & REYNOLDS, J. J. 1985. Purification and characterization of a bone metalloproteinase that degrades gelatin and types IV and V collagen. *Biochim Biophys Acta,* 831, 49-58.

MURTHA, P., TINDALL, D. J. & YOUNG, C. Y. 1993. Androgen induction of a human prostate-specific kallikrein, hKLK2: characterization of an androgen response element in the 5' promoter region of the gene. *Biochemistry,* 32, 6459-64.

MYLONA, E., MAGKOU, C., GIANNOPOULOU, I., AGROGIANNIS, G., MARKAKI, S., KERAMOPOULOS, A. & NAKOPOULOU, L. 2006. Expression of tissue inhibitor of matrix metalloproteinases (TIMP)-3 protein in invasive breast carcinoma: relation to tumor phenotype and clinical outcome. *Breast Cancer Res,* 8, R57.

NAGAI, A., TERASHIMA, M., SHEIKH, A. M., NOTSU, Y., SHIMODE, K., YAMAGUCHI, S., KOBAYASHI, S., KIM, S. U. & MASUDA, J. 2008. Involvement of cystatin C in pathophysiology of CNS diseases. *Front Biosci,* 13, 3470-9.

NAGASE, H. & KASHIWAGI, M. 2003. Aggrecanases and cartilage matrix degradation. *Arthritis Res Ther,* 5, 94-103.

NAGASE, H. & WOESSNER, J. F. 1999a. Matrix metalloproteinases. *J Biol Chem,* 274, 21491-21494.

NAGASE, H. & WOESSNER, J. F., JR. 1999b. Matrix metalloproteinases. *J Biol Chem,* 274, 21491-4.

NAKAMURA, M., ISHIDA, E., SHIMADA, K., KISHI, M., NAKASE, H., SAKAKI, T. & KONISHI, N. 2005a. Frequent LOH on 22q12.3 and TIMP-3 inactivation occur in the progression to secondary glioblastomas. *Lab Invest,* 85, 165-75.

NAKAMURA, M., SONE, S., TAKAHASHI, I., MIZOGUCHI, I., ECHIGO, S. & SASANO, Y. 2005b. Expression of versican and ADAMTS1, 4, and 5 during bone development in the rat mandible and hind limb. *J Histochem Cytochem,* 53, 1553-62.

NAKASHIMA, J., TACHIBANA, M., UENO, M., MIYAJIMA, A., BABA, S. & MURAI, M. 1998. Association between tumor necrosis factor in serum and cachexia in patients with prostate cancer. *Clin Cancer Res,* 4, 1743-8.

NARIMOTO, K., MIZOKAMI, A., IZUMI, K., MIHARA, S., SAWADA, K., SUGATA, T., SHIMAMURA, M., MIYAZAKI, K., NISHINO, A. & NAMIKI, M. 2010. Adrenal androgen levels as predictors of outcome in castration-resistant prostate cancer patients treated with combined androgen blockade using flutamide as a second-line anti-androgen. *Int J Urol,* 17, 337-45.

NAZARETH, L. V. & WEIGEL, N. L. 1996. Activation of the human androgen receptor through a protein kinase A signaling pathway. *J Biol Chem,* 271, 19900-7.

NEGRO, A., ONISTO, M., GRASSATO, L., CAENAZZO, C. & GARBISA, S. 1997. Recombinant human TIMP-3 from Escherichia coli: synthesis, refolding, physico-chemical and functional insights. *Protein Eng,* 10, 593-9.

NEUMANN, E., SCHAEFER-RIDDER, M., WANG, Y. & HOFSCHNEIDER, P. H. 1982. Gene transfer into mouse lyoma cells by electroporation in high electric fields. *EMBO J,* 1, 841-5.

NGAN, S., STRONACH, E. A., PHOTIOU, A., WAXMAN, J., ALI, S. & BULUWELA, L. 2009. Microarray coupled to quantitative RT-PCR analysis of androgen-regulated genes in human LNCaP prostate cancer cells. *Oncogene,* 28, 2051-63.

NISHIHIRA, J. & TACHIKAWA, H. 1999. Theoretical evaluation of a model of the catalytic triads of serine and cysteine proteases by ab initio molecular orbital calculation. *J Theor Biol,* 196, 513-9.

NOE, V., FINGLETON, B., JACOBS, K., CRAWFORD, H. C., VERMEULEN, S., STEELANT, W., BRUYNEEL, E., MATRISIAN, L. M. & MAREEL, M. 2001. Release of an invasion promoter E-cadherin fragment by matrilysin and stromelysin-1. *J Cell Sci,* 114, 111-118.

NOEL, A., MUNAUT, C., NUSGENS, B., FOIDART, J. M. & LAPIERE, C. M. 1992. The stimulation of fibroblasts' collagen synthesis by neoplastic cells is modulated by the extracellular matrix. *Matrix,* 12, 213-20.

NOMURA, S., YOSHITOMI, H., TAKANO, S., SHIDA, T., KOBAYASHI, S., OHTSUKA, M., KIMURA, F., SHIMIZU, H., YOSHIDOME, H., KATO, A. & MIYAZAKI, M. 2008. FGF10/FGFR2 signal induces cell migration and invasion in pancreatic cancer. *Br J Cancer,* 99, 305-13.

OGATA, S., MOROKUMA, J., HAYATA, T., KOLLE, G., NIEHRS, C., UENO, N. & CHO, K. W. 2007. TGF-beta signaling-mediated morphogenesis: modulation of cell adhesion via cadherin endocytosis. *Genes Dev,* 21, 1817-31.

OGATA, Y., NIISATO, N., FURUYAMA, S., CHEIFETZ, S., KIM, R. H., SUGIYA, H. & SODEK, J. 1997. Transforming growth factor-beta 1 regulation of bone sialoprotein gene transcription: identification of a TGF-beta activation element in the rat BSP gene promoter. *J Cell Biochem,* 65, 501-12.

OH, J., TAKAHASHI, R., KONDO, S., MIZOGUCHI, A., ADACHI, E., SASAHARA, R. M., NISHIMURA, S., IMAMURA, Y., KITAYAMA, H., ALEXANDER, D. B., IDE, C., HORAN, T. P., ARAKAWA, T., YOSHIDA, H., NISHIKAWA, S., ITOH, Y., SEIKI, M., ITOHARA, S., TAKAHASHI, C. & NODA, M. 2001. The membrane-anchored MMP inhibitor RECK is a key regulator of extracellular matrix integrity and angiogenesis. *Cell,* 107, 789-800.

OKADA, A., GARNIER, J. M., VICAIRE, S. & BASSET, P. 1994. Cloning of the cDNA encoding rat tissue inhibitor of metalloproteinase 1 (TIMP-1), amino acid comparison with other TIMPs, and gene expression in rat tissues. *Gene,* 147, 301-2.

OLAPADE-OLAOPA, E. O., OBAMUYIDE, H. A. & YISA, G. T. 2008. Management of advanced prostate cancer in Africa. *Can J Urol,* 15, 3890-8.

OLUMI, A. F., GROSSFELD, G. D., HAYWARD, S. W., CARROLL, P. R., TLSTY, T. D. & CUNHA, G. R. 1999. Carcinoma-associated fibroblasts direct tumor progression of initiated human prostatic epithelium. *Cancer Res,* 59, 5002-11.

ONO, M., TORISU, H., FUKUSHI, J., NISHIE, A. & KUWANO, M. 1999. Biological implications of macrophage infiltration in human tumor angiogenesis. *Cancer Chemother Pharmacol,* 43 Suppl, S69-71.

ORIDATE, N., LOTAN, R. & LOTAN, D. 1996. Reconstituted basement membrane (Matrigel): a useful semisolid medium for growth of tumor cell colonies. *In Vitro Cell Dev Biol Anim,* 32, 192-3.

PALAND, N., KAMER, I., KOGAN-SAKIN, I., MADAR, S., GOLDFINGER, N. & ROTTER, V. 2009. Differential influence of normal and cancer-associated fibroblasts on the growth of human epithelial cells in an in vitro cocultivation model of prostate cancer. *Mol Cancer Res,* 7, 1212-23.

PARKER, P. M., RICE, K. R., STERBIS, J. R., CHEN, Y., CULLEN, J., MCLEOD, D. G. & BRASSELL, S. A. 2011. Prostate cancer in men less than the age of 50: a comparison of race and outcomes. *Urology,* 78, 110-5.

PARRY, G. C. & MACKMAN, N. 1994. A set of inducible genes expressed by activated human monocytic and endothelial cells contain kappa B-like sites that specifically bind c-Rel-p65 heterodimers. *J Biol Chem,* 269, 20823-5.

PATTERSON, M. L., ATKINSON, S. J., KNAUPER, V. & MURPHY, G. 2001. Specific collagenolysis by gelatinase A, MMP-2, is determined by the hemopexin domain and not the fibronectin-like domain. *FEBS Lett,* 503, 158-62.

PAVLOFF, N., STASKUS, P. W., KISHNANI, N. S. & HAWKES, S. P. 1992. A new inhibitor of metalloproteinases from chicken: ChIMP-3. A third member of the TIMP family. *J Biol Chem,* 267, 17321-6.

PEARL, L. H. 1987. The catalytic mechanism of aspartic proteinases. *FEBS Lett,* 214, 8-12.

PEETS, E. A., HENSON, M. F. & NERI, R. 1974. On the mechanism of the anti-androgenic action of flutamide (alpha-alpha-alpha-trifluoro-2-methyl-4'-nitro-m-propionotoluidide) in the rat. *Endocrinology,* 94, 532-40.

PEI, D. 1999. CA-MMP: a matrix metalloproteinase with a novel cysteine array, but without the classic cysteine switch. *FEBS Lett,* 457, 262-70.

PEI, D., KANG, T. & QI, H. 2000. Cysteine array matrix metalloproteinase (CA-MMP)/MMP-23 is a type II transmembrane matrix metalloproteinase regulated by a single cleavage for both secretion and activation. *J Biol Chem,* 275, 33988-97.

PHILLIPS, R. M. 1998. Prospects for bioreductive drug development. *Expert Opin Investig Drugs,* 7, 905-28.

PIETRUSZEWSKA, W., KOBOS, J., GRYCZYNSKI, M., DURKO, T. & BOJANOWSKA-POZNIAK, K. 2008. [Analysis of TIMP-1, TIMP-2 and TIMP-3 expression as a prognostic factor of laryngeal cancer progression]. *Otolaryngol Pol,* 62, 380-7.

PLANCKE, H. R., DELAERE, K. P. & THEUNISSEN, P. 1994. Secondary signet ring cell tumour of the prostate. *Urol Int,* 52, 223-4.

PLUMMER, T. H., JR., ELDER, J. H., ALEXANDER, S., PHELAN, A. W. & TARENTINO, A. L. 1984. Demonstration of peptide:N-glycosidase F activity in endo-beta-N-acetylglucosaminidase F preparations. *J Biol Chem,* 259, 10700-4.

PODVINEC, M., KAUFMANN, M. R., HANDSCHIN, C. & MEYER, U. A. 2002. NUBIScan, an in silico approach for prediction of nuclear receptor response elements. *Mol Endocrinol,* 16, 1269-79.

PORTER, S., CLARK, I. M., KEVORKIAN, L. & EDWARDS, D. R. 2005. The ADAMTS metalloproteinases. *Biochem J,* 386, 15-27.

PORTER, S., SCOTT, S. D., SASSOON, E. M., WILLIAMS, M. R., JONES, J. L., GIRLING, A. C., BALL, R. Y. & EDWARDS, D. R. 2004. Dysregulated expression of adamalysin-thrombospondin genes in human breast carcinoma. *Clin Cancer Res,* 10, 2429-40.

POWE, D. G., BROUGH, J. L., CARTER, G. I., BAILEY, E. M., STETLER-STEVENSON, W. G., TURNER, D. R. & HEWITT, R. E. 1997. TIMP-3 mRNA expression is regionally increased in moderately and poorly differentiated colorectal adenocarcinoma. *Br J Cancer,* 75, 1678-83.

QI, J. H., EBRAHEM, Q., MOORE, N., MURPHY, G., CLAESSON-WELSH, L., BOND, M., BAKER, A. & ANAND-APTE, B. 2003. A novel function for tissue inhibitor of metalloproteinases-3 (TIMP3): inhibition of angiogenesis by blockage of VEGF binding to VEGF receptor-2. *Nat Med,* 9, 407-15.

QUINTENS, H., CHEVALLIER, D., MICHELS, J. F., PADOVANI, B., VILLERS, A., AMIEL, J. & TOUBOL, J. 1990. [Can CT scanner and MRI predict capsular invasion of local cancer of the prostate? A study of 20 radical prostatectomies]. *Ann Urol (Paris),* 24, 335-9.

RADONIC, A., THULKE, S., MACKAY, I. M., LANDT, O., SIEGERT, W. & NITSCHE, A. 2004. Guideline to reference gene selection for quantitative real-time PCR. *Biochem Biophys Res Commun,* 313, 856-862.

RAGA, F., CASAN, E. M., WEN, Y., HUANG, H. Y., BONILLA-MUSOLES, F. & POLAN, M. L. 1999. Independent regulation of matrix metalloproteinase-9, tissue inhibitor of metalloproteinase-1 (TIMP-1), and TIMP-3 in human endometrial stromal cells by gonadotropin-releasing hormone: implications in early human implantation. *J Clin Endocrinol Metab,* 84, 636-42.

RAIVIO, T., TAPANAINEN, J. S., KUNELIUS, P. & JANNE, O. A. 2002. Serum androgen bioactivity during 5alpha-dihydrotestosterone treatment in elderly men. *J Androl,* 23, 919-21.

RAJENDER, S., POOJA, S., GUPTA, N. J., CHAKRABARTY, B., SINGH, L. & THANGARAJ, K. 2010. G708E Mutation in the Androgen Receptor Results in Complete Loss of Androgen Function. *J Androl.*

RAJENDER, S., SINGH, L. & THANGARAJ, K. 2007. L859F mutation in androgen receptor gene results in complete loss of androgen binding to the receptor. *J Androl,* 28, 772-6.

RAKESH, K. & AGRAWAL, D. K. 2005. Cytokines and growth factors involved in apoptosis and proliferation of vascular smooth muscle cells. *Int Immunopharmacol,* 5, 1487-506.

RAWLINGS, N. D. & BARRETT, A. J. 1990. Flusys - A Software Package for the Collection and Analysis of kinetic and Scanning Data from Perkin-Elmer Fluorimeters. *Comput Appl Biosci,* 6, 118-119.

RAWLINGS, N. D. & BARRETT, A. J. 1995. Evolutionary families of metallopeptidases. *Methods Enzymol,* 248, 183-228.

RAWLINGS, N. D., BARRETT, A. J. & BATEMAN, A. 2010. MEROPS: the peptidase database. *Nucleic Acids Res,* 38, D227-33.

REID, M. J., CROSS, A. K., HADDOCK, G., ALLAN, S. M., STOCK, C. J., WOODROOFE, M. N., BUTTLE, D. J. & BUNNING, R. A. 2009. ADAMTS-9 expression is up-regulated following transient middle cerebral artery occlusion (tMCAo) in the rat. *Neurosci Lett,* 452, 252-7.

REYNARD, J. & ABRAMS, P. 1994. Symptoms and symptom scores in BPH. *Scand J Urol Nephrol Suppl,* 157, 137-45.

RICCIO, A., PEDONE, P. V., LUND, L. R., OLESEN, T., OLSEN, H. S. & ANDREASEN, P. A. 1992. Transforming growth factor beta 1-responsive element: closely associated binding sites for USF and CCAAT-binding transcription factor-

nuclear factor I in the type 1 plasminogen activator inhibitor gene. *Mol Cell Biol,* 12, 1846-55.

RICE, P., LONGDEN, I. & BLEASBY, A. 2000. EMBOSS: the European Molecular Biology Open Software Suite. *Trends Genet,* 16, 276-7.

RIDDICK, A. C., SHUKLA, C. J., PENNINGTON, C. J., BASS, R., NUTTALL, R. K., HOGAN, A., SETHIA, K. K., ELLIS, V., COLLINS, A. T., MAITLAND, N. J., BALL, R. Y. & EDWARDS, D. R. 2005. Identification of degradome components associated with prostate cancer progression by expression analysis of human prostatic tissues. *Br J Cancer,* 92, 2171-80.

RISINGER, G. M., JR., UPDIKE, D. L., BULLEN, E. C., TOMASEK, J. J. & HOWARD, E. W. 2010. TGF-beta suppresses the upregulation of MMP-2 by vascular smooth muscle cells in response to PDGF-BB. *Am J Physiol Cell Physiol,* 298, C191-201.

ROBERTS, R. G. 1994. BPH: new guidelines based on symptoms and patient preference. The Agency for Health Care Policy and Research. *Geriatrics,* 49, 24-31.

ROCHE, P. J., HOARE, S. A. & PARKER, M. G. 1992. A consensus DNA-binding site for the androgen receptor. *Mol Endocrinol,* 6, 2229-35.

RODRIGUEZ-MANZANEQUE, J. C., WESTLING, J., THAI, S. N., LUQUE, A., KNAUPER, V., MURPHY, G., SANDY, J. D. & IRUELA-ARISPE, M. L. 2002. ADAMTS1 cleaves aggrecan at multiple sites and is differentially inhibited by metalloproteinase inhibitors. *Biochem Biophys Res Commun,* 293, 501-8.

ROITT I.M. & P.J., D. 2001. The Production of Effectors. *Essential Immunology.* Tenth ed. London: Blackwell Sciences Ltd.

RONNOV-JESSEN, L. & PETERSEN, O. W. 1993. Induction of alpha-smooth muscle actin by transforming growth factor-beta 1 in quiescent human breast gland fibroblasts. Implications for myofibroblast generation in breast neoplasia. *Lab Invest,* 68, 696-707.

RUSSELL, D. W. & WILSON, J. D. 1994. Steroid 5 alpha-reductase: two genes/two enzymes. *Annu Rev Biochem,* 63, 25-61.

RYO, A., UEMURA, H., ISHIGURO, H., SAITOH, T., YAMAGUCHI, A., PERREM, K., KUBOTA, Y., LU, K. P. & AOKI, I. 2005. Stable suppression of tumorigenicity by Pin1-targeted RNA interference in prostate cancer. *Clin Cancer Res,* 11, 7523-31.

SADLER, J. E. 1998. Biochemistry and genetics of von Willebrand factor. *Annu Rev Biochem,* 67, 395-424.

SAHIN, U. & BLOBEL, C. P. 2007. Ectodomain shedding of the EGF-receptor ligand epigen is mediated by ADAM17. *FEBS Lett,* 581, 41-4.

SALAH, Z., MAOZ, M., COHEN, I., PIZOV, G., PODE, D., RUNGE, M. S. & BAR-SHAVIT, R. 2005. Identification of a novel functional androgen response element within hPar1 promoter: implications to prostate cancer progression. *FASEB J,* 19, 62-72.

SALVESEN, G. S. 2002. Caspases and apoptosis. *Essays Biochem,* 38, 9-19.

SCHEFFERS, M. S., VAN DER BENT, P., PRINS, F., SPRUIT, L., BREUNING, M. H., LITVINOV, S. V., DE HEER, E. & PETERS, D. J. 2000. Polycystin-1, the product of the polycystic kidney disease 1 gene, co-localizes with desmosomes in MDCK cells. *Hum Mol Genet,* 9, 2743-50.

SCHELTER, F., GRANDL, M., SEUBERT, B., SCHATEN, S., HAUSER, S., GERG, M., BOCCACCIO, C., COMOGLIO, P. & KRUGER, A. 2011. Tumor cell-derived Timp-1 is necessary for maintaining metastasis-promoting Met-signaling via inhibition of Adam-10. *Clin Exp Metastasis,* 28, 793-802.

SCHNEIDER, F., SUKHOVA, G. K., AIKAWA, M., CANNER, J., GERDES, N., TANG, S. M., SHI, G. P., APTE, S. S. & LIBBY, P. 2008. Matrix-metalloproteinase-14 deficiency in bone-marrow-derived cells promotes collagen accumulation in mouse atherosclerotic plaques. *Circulation,* 117, 931-9.

SEALS, D. F. & COURTNEIDGE, S. A. 2003. The ADAMs family of metalloproteases: multidomain proteins with multiple functions. *Genes Dev,* 17, 7-30.

SEDLACEK, R., MAUCH, S., KOLB, B., SCHATZLEIN, C., EIBEL, H., PETER, H. H., SCHMITT, J. & KRAWINKEL, U. 1998. Matrix metalloproteinase MMP-19 (RASI-1) is expressed on the surface of activated peripheral blood mononuclear cells and is detected as an autoantigen in rheumatoid arthritis. *Immunobiology,* 198, 408-23.

SEE, W. A., MCLEOD, D., IVERSEN, P. & WIRTH, M. 2001. The Bicalutamide Early Prostate Cancer Program: Demography. *Urologic Oncology,* 6, 43-47.

SEEMULLER, E., LUPAS, A., STOCK, D., LOWE, J., HUBER, R. & BAUMEISTER, W. 1995. Proteasome from Thermoplasma acidophilum: a threonine protease. *Science,* 268, 579-82.

SEFTEL, A. 2005. Comparison of the Pharmacological Effects of a Novel Selective Androgen Receptor Modulator (SARM), the 5alpha-Reductase Inhibitor Finasteride, and the Antiandrogen Hydroxyflutamide in Intact Rats: New Approach for Benign Prostate Hyperplasia (BPH). *J Urol,* 173, 1279.

SELLS GALVIN, R. J., GATLIN, C. L., HORN, J. W. & FUSON, T. R. 1999. TGF-beta enhances osteoclast differentiation in hematopoietic cell cultures stimulated with RANKL and M-CSF. *Biochem Biophys Res Commun,* 265, 233-9.

SHAKIR, S., PEARCE, G. & MANN, R. D. 2001. Finasteride and tamsulosin used in benign prostatic hypertrophy: a review of the prescription-event monitoring data. *BJU Int,* 87, 789-96.

SHANKAR, S. L., MANI, S., O'GUIN, K. N., KANDIMALLA, E. R., AGRAWAL, S. & SHAFIT-ZAGARDO, B. 2001. Survivin inhibition induces human neural tumor cell death through caspase-independent and -dependent pathways. *J Neurochem,* 79, 426-36.

SHAPIRO, S. D., KOBAYASHI, D. K. & LEY, T. J. 1993. Cloning and characterization of a unique elastolytic metalloproteinase produced by human alveolar macrophages. *J Biol Chem,* 268, 23824-9.

SHIMAO, Y., NABESHIMA, K., INOUE, T. & KOONO, M. 1999. Role of fibroblasts in HGF/SF-induced cohort migration of human colorectal carcinoma cells: fibroblasts stimulate migration associated with increased fibronectin production via upregulated TGF-beta1. *Int J Cancer,* 82, 449-58.

SILVER, R. I., WILEY, E. L., DAVIS, D. L., THIGPEN, A. E., RUSSELL, D. W. & MCCONNELL, J. D. 1994. Expression and regulation of steroid 5 alpha-reductase 2 in prostate disease. *J Urol,* 152, 433-7.

SILVERMAN, G. A., BIRD, P. I., CARRELL, R. W., CHURCH, F. C., COUGHLIN, P. B., GETTINS, P. G., IRVING, J. A., LOMAS, D. A., LUKE, C. J., MOYER, R. W., PEMBERTON, P. A., REMOLD-O'DONNELL, E., SALVESEN, G. S., TRAVIS, J. & WHISSTOCK, J. C. 2001. The serpins are an expanding superfamily of structurally similar but functionally diverse proteins. Evolution, mechanism of inhibition, novel functions, and a revised nomenclature. *J Biol Chem,* 276, 33293-6.

SIMOSSIS, V. A. & HERINGA, J. 2005. PRALINE: a multiple sequence alignment toolbox that integrates homology-extended and secondary structure information. *Nucleic Acids Res,* 33, W289-94.

SIMPSON, R. J. 2007. Nomenclature on proteases, proteinases, and peptidases. *CSH Protoc,* 2007, pdb ip13.

SKOOG, T., AHOKAS, K., ORSMARK, C., JESKANEN, L., ISAKA, K. & SAARIALHO-KERE, U. 2006. MMP-21 is expressed by macrophages and fibroblasts in vivo and in culture. *Exp Dermatol,* 15, 775-83.

SOBEL, R. E. & SADAR, M. D. 2005a. Cell lines used in prostate cancer research: a compendium of old and new lines--part 1. *J Urol,* 173, 342-59.

SOBEL, R. E. & SADAR, M. D. 2005b. Cell lines used in prostate cancer research: a compendium of old and new lines--part 2. *J Urol,* 173, 360-72.

SOMERVILLE, R. P., LONGPRE, J. M., JUNGERS, K. A., ENGLE, J. M., ROSS, M., EVANKO, S., WIGHT, T. N., LEDUC, R. & APTE, S. S. 2003. Characterization of ADAMTS-9 and ADAMTS-20 as a distinct ADAMTS subfamily related to Caenorhabditis elegans GON-1. *J Biol Chem,* 278, 9503-13.

SONVILLA, G., ALLERSTORFER, S., STATTNER, S., KARNER, J., KLIMPFINGER, M., FISCHER, H., GRASL-KRAUPP, B., HOLZMANN, K., BERGER, W., WRBA, F., MARIAN, B. & GRUSCH, M. 2008. FGF18 in colorectal tumour cells: autocrine and paracrine effects. *Carcinogenesis,* 29, 15-24.

SPARANO, J. A., BERNARDO, P., STEPHENSON, P., GRADISHAR, W. J., INGLE, J. N., ZUCKER, S. & DAVIDSON, N. E. 2004. Randomized phase III trial of marimastat versus placebo in patients with metastatic breast cancer who have responding or stable disease after first-line chemotherapy: Eastern Cooperative Oncology Group trial E2196. *J Clin Oncol,* 22, 4683-90.

STOCKER, W. & BODE, W. 1995. Structural features of a superfamily of zinc-endopeptidases: the metzincins. *Curr Opin Struct Biol,* 5, 383-90.

STOCKER, W., GRAMS, F., BAUMANN, U., REINEMER, P., GOMIS-RUTH, F. X., MCKAY, D. B. & BODE, W. 1995. The metzincins--topological and sequential relations between the astacins, adamalysins, serralysins, and matrixins (collagenases) define a superfamily of zinc-peptidases. *Protein Sci,* 4, 823-40.

STRACKE, J. O., HUTTON, M., STEWART, M., PENDAS, A. M., SMITH, B., LOPEZ-OTIN, C., MURPHY, G. & KNAUPER, V. 2000. Biochemical characterization of the catalytic domain of human matrix metalloproteinase 19. Evidence for a role as a potent basement membrane degrading enzyme. *J Biol Chem,* 275, 14809-16.

STRUTZ, F., ZEISBERG, M., RENZIEHAUSEN, A., RASCHKE, B., BECKER, V., VAN KOOTEN, C. & MULLER, G. 2001. TGF-beta 1 induces proliferation in human renal fibroblasts via induction of basic fibroblast growth factor (FGF-2). *Kidney Int,* 59, 579-92.

STUELTEN, C. H., DACOSTA BYFIELD, S., ARANY, P. R., KARPOVA, T. S., STETLER-STEVENSON, W. G. & ROBERTS, A. B. 2005. Breast cancer cells induce stromal fibroblasts to express MMP-9 via secretion of TNF-alpha and TGF-beta. *J Cell Sci,* 118, 2143-53.

SU, A. I., WELSH, J. B., SAPINOSO, L. M., KERN, S. G., DIMITROV, P., LAPP, H., SCHULTZ, P. G., POWELL, S. M., MOSKALUK, C. A., FRIERSON, H. F., JR. & HAMPTON, G. M. 2001. Molecular classification of human carcinomas by use of gene expression signatures. *Cancer Res,* 61, 7388-93.

SU, S., DIBATTISTA, J. A., SUN, Y., LI, W. Q. & ZAFARULLAH, M. 1998. Up-regulation of tissue inhibitor of metalloproteinases-3 gene expression by TGF-beta in articular chondrocytes is mediated by serine/threonine and tyrosine kinases. *J Cell Biochem,* 70, 517-27.

SULKALA, M., LARMAS, M., SORSA, T., SALO, T. & TJADERHANE, L. 2002. The localization of matrix metalloproteinase-20 (MMP-20, enamelysin) in mature human teeth. *J Dent Res,* 81, 603-7.

SUZUKI, H., AKAKURA, K., KOMIYA, A., AIDA, S., AKIMOTO, S. & SHIMAZAKI, J. 1996. Codon 877 mutation in the androgen receptor gene in advanced prostate cancer: relation to antiandrogen withdrawal syndrome. *Prostate,* 29, 153-8.

SUZUKI, H., SATO, N., WATABE, Y., MASAI, M., SEINO, S. & SHIMAZAKI, J. 1993. Androgen receptor gene mutations in human prostate cancer. *J Steroid Biochem Mol Biol,* 46, 759-65.

SZLOSAREK, P., CHARLES, K. A. & BALKWILL, F. R. 2006. Tumour necrosis factor-alpha as a tumour promoter. *Eur J Cancer,* 42, 745-50.

TAKEDA, S., IGARASHI, T., MORI, H. & ARAKI, S. 2006. Crystal structures of VAP1 reveal ADAMs' MDC domain architecture and its unique C-shaped scaffold. *EMBO J,* 25, 2388-96.

TAKEUCHI, T., HISANAGA, M., NAGAO, M., IKEDA, N., FUJII, H., KOYAMA, F., MUKOGAWA, T., MATSUMOTO, H., KONDO, S., TAKAHASHI, C., NODA, M. & NAKAJIMA, Y. 2004. The membrane-anchored matrix metalloproteinase (MMP) regulator RECK in combination with MMP-9 serves as an informative prognostic indicator for colorectal cancer. *Clin Cancer Res,* 10, 5572-9.

TAM, E. M., MOORE, T. R., BUTLER, G. S. & OVERALL, C. M. 2004. Characterization of the distinct collagen binding, helicase and cleavage mechanisms of matrix metalloproteinase 2 and 14 (gelatinase A and MT1-MMP): the differential roles of the MMP hemopexin c domains and the MMP-2 fibronectin type II modules in collagen triple helicase activities. *J Biol Chem,* 279, 43336-44.

TANAKA, F., SONODA, H., OKAMOTO, M., MIMORI, K., UTSUNOMIYA, T., INOUE, H., HANAI, T. & MORI, M. 2007. TIMP-3 and Phosphatidylinositol 3-kinase genes were found to be related to the progression of colon cancer in a comparison of pneumoperitoneum and laparotomy in a murine model. *Surg Today,* 37, 220-5.

TANG, B. L. 2001. ADAMTS: a novel family of extracellular matrix proteases. *Int J Biochem Cell Biol,* 33, 33-44.

TAPLIN, M. E., RAJESHKUMAR, B., HALABI, S., WERNER, C. P., WODA, B. A., PICUS, J., STADLER, W., HAYES, D. F., KANTOFF, P. W., VOGELZANG, N. J. & SMALL, E. J. 2003. Androgen receptor mutations in androgen-independent prostate cancer: Cancer and Leukemia Group B Study 9663. *J Clin Oncol,* 21, 2673-8.

TARENTINO, A. L., GOMEZ, C. M. & PLUMMER, T. H., JR. 1985. Deglycosylation of asparagine-linked glycans by peptide:N-glycosidase F. *Biochemistry,* 24, 4665-71.

TCHETINA, E. V., SQUIRES, G. & POOLE, A. R. 2005. Increased type II collagen degradation and very early focal cartilage degeneration is associated with upregulation of chondrocyte differentiation related genes in early human articular cartilage lesions. *J Rheumatol,* 32, 876-86.

THANNICKAL, V. J., ALDWEIB, K. D., RAJAN, T. & FANBURG, B. L. 1998. Upregulated expression of fibroblast growth factor (FGF) receptors by transforming growth factor-beta1 (TGF-beta1) mediates enhanced mitogenic responses to FGFs in cultured human lung fibroblasts. *Biochem Biophys Res Commun,* 251, 437-41.

TODD, B., MOORE, D., DEIVANAYAGAM, C. C., LIN, G. D., CHATTOPADHYAY, D., MAKI, M., WANG, K. K. & NARAYANA, S. V. 2003. A structural model for the inhibition of calpain by calpastatin: crystal structures of the native domain VI of

calpain and its complexes with calpastatin peptide and a small molecule inhibitor. *J Mol Biol,* 328, 131-46.

TRAPMAN, J. & BRINKMANN, A. O. 1996. The androgen receptor in prostate cancer. *Pathol Res Pract,* 192, 752-60.

TRUE, L. D., HAWLEY, S., NORWOOD, T. H., BRAUN, K. R., EVANKO, S. P., CHAN, C. K., LEBARON, R. C. & WIGHT, T. N. 2009. The accumulation of versican in the nodules of benign prostatic hyperplasia. *Prostate,* 69, 149-58.

TSUGAYA, M., HARADA, N., TOZAWA, K., YAMADA, Y., HAYASHI, Y., TANAKA, S., MARUYAMA, K. & KOHRI, K. 1996. Aromatase mRNA levels in benign prostatic hyperplasia and prostate cancer. *Int J Urol,* 3, 292-6.

TUNUGUNTLA, R., RIPLEY, D., SANG, Q. X. & CHEGINI, N. 2003. Expression of matrix metalloproteinase-26 and tissue inhibitors of metalloproteinases TIMP-3 and -4 in benign endometrium and endometrial cancer. *Gynecol Oncol,* 89, 453-9.

TUXHORN, J. A., AYALA, G. E., SMITH, M. J., SMITH, V. C., DANG, T. D. & ROWLEY, D. R. 2002. Reactive stroma in human prostate cancer: induction of myofibroblast phenotype and extracellular matrix remodeling. *Clin Cancer Res,* 8, 2912-23.

TZIKAS, A., KARAISKOS, P., PAPANIKOLAOU, N., SANDILOS, P., KOUTSOUVELI, E., LAVDAS, E., SCARLEAS, C., DARDOUFAS, K., LIND, B. K. & MAVROIDIS, P. 2011. Investigating the clinical aspects of using CT vs. CT-MRI images during organ delineation and treatment planning in prostate cancer radiotherapy. *Technol Cancer Res Treat,* 10, 231-42.

UNO, H. 1995. [Clinical significance of PSA-density in differential diagnosis between BPH and early stages prostate cancer]. *Nihon Hinyokika Gakkai Zasshi,* 86, 1776-83.

UNOKI, H., FAN, J. & WATANABE, T. 1999. Low-density lipoproteins modulate endothelial cells to secrete endothelin-1 in a polarized pattern: a study using a culture model system simulating arterial intima. *Cell Tissue Res,* 295, 89-99.

URIA, J. A., FERRANDO, A. A., VELASCO, G., FREIJE, J. M. & LOPEZ-OTIN, C. 1994. Structure and expression in breast tumors of human TIMP-3, a new member of the metalloproteinase inhibitor family. *Cancer Res,* 54, 2091-4.

VANDE BROEK, I., VANDERKERKEN, K., VAN CAMP, B. & VAN RIET, I. 2008. Extravasation and homing mechanisms in multiple myeloma. *Clin Exp Metastasis,* 25, 325-34.

VAZQUEZ-ORTIZ, G., PINA-SANCHEZ, P., VAZQUEZ, K., DUENAS, A., TAJA, L., MENDOZA, P., GARCIA, J. A. & SALCEDO, M. 2005. Overexpression of cathepsin F, matrix metalloproteinases 11 and 12 in cervical cancer. *BMC Cancer,* 5, 68.

VELDSCHOLTE, J., RIS-STALPERS, C., KUIPER, G. G., JENSTER, G., BERREVOETS, C., CLAASSEN, E., VAN ROOIJ, H. C., TRAPMAN, J., BRINKMANN, A. O. & MULDER, E. 1990. A mutation in the ligand binding domain of the androgen receptor of human LNCaP cells affects steroid binding characteristics and response to anti-androgens. *Biochem Biophys Res Commun,* 173, 534-40.

VERMES, I., HAANEN, C., STEFFENS-NAKKEN, H. & REUTELINGSPERGER, C. 1995. A novel assay for apoptosis. Flow cytometric detection of phosphatidylserine expression on early apoptotic cells using fluorescein labelled Annexin V. *J Immunol Methods,* 184, 39-51.

VILLAR, J., TSAI-MORRIS, C. H., DAI, L. & DUFAU, M. L. 2012. Androgen-Induced Activation of Gonadotropin Regulated Testicular RNA Helicase (GRTH/Ddx25) Transcription: Essential Role of a Non-Classical Androgen Response Element Half-Site. *Mol Cell Biol.*

VISSE, R. & NAGASE, H. 2003. Matrix metalloproteinases and tissue inhibitors of metalloproteinases: structure, function, and biochemistry. *Circ Res,* 92, 827-39.

VIZOSO, F. J., GONZALEZ, L. O., CORTE, M. D., RODRIGUEZ, J. C., VAZQUEZ, J., LAMELAS, M. L., JUNQUERA, S., MERINO, A. M. & GARCIA-MUNIZ, J. L. 2007. Study of matrix metalloproteinases and their inhibitors in breast cancer. *Br J Cancer,* 96, 903-11.

WAHL, S. M. 1992. Transforming growth factor beta (TGF-beta) in inflammation: a cause and a cure. *J Clin Immunol,* 12, 61-74.

WALLACE, D. M., CHISHOLM, G. D. & HENDRY, W. F. 1975. T.N.M. classification for urological tumours (U.I.C.C.) - 1974. *Br J Urol,* 47, 1-12.

WANDEL, E., GRASSHOFF, A., MITTAG, M., HAUSTEIN, U. F. & SAALBACH, A. 2000. Fibroblasts surrounding melanoma express elevated levels of matrix metalloproteinase-1 (MMP-1) and intercellular adhesion molecule-1 (ICAM-1) in vitro. *Exp Dermatol,* 9, 34-41.

WANG, M. C., VALENZUELA, L. A., MURPHY, G. P. & CHU, T. M. 1979. Purification of a human prostate specific antigen. *Invest Urol,* 17, 159-63.

WANG, W. M., GE, G., LIM, N. H., NAGASE, H. & GREENSPAN, D. S. 2006. TIMP-3 inhibits the procollagen N-proteinase ADAMTS-2. *Biochem J,* 398, 515-9.

WANG, Y., DANG, J., WANG, H., ALLGAYER, H., MURRELL, G. A. & BOYD, D. 2000. Identification of a novel nuclear factor-kappaB sequence involved in expression of urokinase-type plasminogen activator receptor. *Eur J Biochem,* 267, 3248-54.

WEBBER, M. M., TRAKUL, N., THRAVES, P. S., BELLO-DEOCAMPO, D., CHU, W. W., STORTO, P. D., HUARD, T. K., RHIM, J. S. & WILLIAMS, D. E. 1999. A human prostatic stromal myofibroblast cell line WPMY-1: a model for stromal-epithelial interactions in prostatic neoplasia. *Carcinogenesis,* 20, 1185-92.

WELGUS, H. G., STRICKLIN, G. P., EISEN, A. Z., BAUER, E. A., COONEY, R. V. & JEFFREY, J. J. 1979. A specific inhibitor of vertebrate collagenase produced by human skin fibroblasts. *J Biol Chem,* 254, 1938-43.

WERNERT, N. 1997. The multiple roles of tumour stroma. *Virchows Arch,* 430, 433-43.

WETZEL, M., LI, L., HARMS, K. M., ROITBAK, T., VENTURA, P. B., ROSENBERG, G. A., KHOKHA, R. & CUNNINGHAM, L. A. 2008. Tissue inhibitor of metalloproteinases-3 facilitates Fas-mediated neuronal cell death following mild ischemia. *Cell Death Differ,* 15, 143-51.

WETZEL, M., ROSENBERG, G. A. & CUNNINGHAM, L. A. 2003. Tissue inhibitor of metalloproteinases-3 and matrix metalloproteinase-3 regulate neuronal sensitivity to doxorubicin-induced apoptosis. *Eur J Neurosci,* 18, 1050-60.

WIJFFELS, K. I., MARRES, H. A., PETERS, J. P., RIJKEN, P. F., VAN DER KOGEL, A. J. & KAANDERS, J. H. 2008. Tumour cell proliferation under hypoxic conditions in human head and neck squamous cell carcinomas. *Oral Oncol,* 44, 335-44.

WILSON, E. M. & FRENCH, F. S. 1976. Binding properties of androgen receptors. Evidence for identical receptors in rat testis, epididymis, and prostate. *J Biol Chem,* 251, 5620-9.

WINDSOR, L. J., STEELE, D. L., LEBLANC, S. B. & TAYLOR, K. B. 1997. Catalytic domain comparisons of human fibroblast-type collagenase, stromelysin-1, and matrilysin. *Biochim Biophys Acta,* 1334, 261-72.

WINGFIELD, P. T., SAX, J. K., STAHL, S. J., KAUFMAN, J., PALMER, I., CHUNG, V., CORCORAN, M. L., KLEINER, D. E. & STETLER-STEVENSON, W. G. 1999. Biophysical and functional characterization of full-length, recombinant human tissue inhibitor of metalloproteinases-2 (TIMP-2) produced in Escherichia coli. Comparison of wild type and amino-terminal alanine appended variant with implications for the mechanism of TIMP functions. *J Biol Chem,* 274, 21362-8.

WOESSNER, J. F., JR. 1996. Regulation of matrilysin in the rat uterus. *Biochem Cell Biol,* 74, 777-84.

WOLK, A. 2005. Diet, lifestyle and risk of prostate cancer. *Acta Oncol,* 44, 277-81.

WROBLEWSKI, L. E., PRITCHARD, D. M., CARTER, S. & VARRO, A. 2002. Gastrin-stimulated gastric epithelial cell invasion: the role and mechanism of increased matrix metalloproteinase 9 expression. *Biochem J,* 365, 873-9.

WU, C., OROZCO, C., BOYER, J., LEGLISE, M., GOODALE, J., BATALOV, S., HODGE, C. L., HAASE, J., JANES, J., HUSS, J. W., 3RD & SU, A. I. 2009a. BioGPS: an extensible and customizable portal for querying and organizing gene annotation resources. *Genome Biol,* 10, R130.

WU, C. T., ALTUWAIJRI, S., RICKE, W. A., HUANG, S. P., YEH, S., ZHANG, C., NIU, Y., TSAI, M. Y. & CHANG, C. 2007. Increased prostate cell proliferation and loss of cell differentiation in mice lacking prostate epithelial androgen receptor. *Proc Natl Acad Sci U S A,* 104, 12679-84.

WU, J., CHEN, D. & WU, Z. 2000. [Quantitative study on the expression of mRNA for TGF-beta and collagenase (MMP-1), tissue metalloproteinase inhibitor-1 (TIMP-1) in hypertrophic scar]. *Zhonghua Zheng Xing Wai Ke Za Zhi,* 16, 34-6.

WU, Y. J., LIANG, C. H., ZHOU, F. J., GAO, X., CHEN, L. W. & LIU, Q. 2009b. [A case-control study of environmental and genetic factors and prostate cancer in Guangdong]. *Zhonghua Yu Fang Yi Xue Za Zhi,* 43, 581-5.

XU, L. L., SU, Y. P., LABICHE, R., SEGAWA, T., SHANMUGAM, N., MCLEOD, D. G., MOUL, J. W. & SRIVASTAVA, S. 2001. Quantitative expression profile of androgen-regulated genes in prostate cancer cells and identification of prostate-specific genes. *Int J Cancer,* 92, 322-8.

YAMAZAKI, K., NAGAO, T., YAMAGUCHI, T., SAISHO, H. & KONDO, Y. 1997. Expression of basic fibroblast growth factor (FGF-2)-associated with tumour proliferation in human pancreatic carcinoma. *Virchows Arch,* 431, 95-101.

YANG, M. & KURKINEN, M. 1998. Cloning and characterization of a novel matrix metalloproteinase (MMP), CMMP, from chicken embryo fibroblasts. CMMP, Xenopus XMMP, and human MMP19 have a conserved unique cysteine in the catalytic domain. *J Biol Chem,* 273, 17893-900.

YANG, Q., FUNG, K. M., DAY, W. V., KROPP, B. P. & LIN, H. K. 2005. Androgen receptor signaling is required for androgen-sensitive human prostate cancer cell proliferation and survival. *Cancer Cell Int,* 5, 8.

YANG, T. T. & HAWKES, S. P. 1992. Role of the 21-kDa protein TIMP-3 in oncogenic transformation of cultured chicken embryo fibroblasts. *Proc Natl Acad Sci U S A,* 89, 10676-80.

YANG, W. I., CHOI, I. J., KIM, H. O. & LEE, K. S. 1991. Demonstration of estrogen receptor by immunohistochemical staining in paraffin sections of breast carcinoma. *Yonsei Med J,* 32, 117-25.

YEH, S., MIYAMOTO, H., SHIMA, H. & CHANG, C. 1998. From estrogen to androgen receptor: a new pathway for sex hormones in prostate. *Proc Natl Acad Sci U S A,* 95, 5527-32.

YOSHIDA, M., ABE, O., UCHINO, J., KIKUCHI, K., ABE, R., ENOMOTO, K., TOMINAGA, T., FUKAMI, A., SAKAI, K., KOYAMA, H., SUGIMACHI, K., NOMURA, Y., HATTORI, T. & OGAWA, N. 1997. Efficacy of postoperative adjuvant therapy for stage ilia breast cancer: Futraful vs futraful+tamoxifen for ER-positive patients and futraful vs futraful + adriamycin for ER-negative breast cancer. *Breast Cancer,* 4, 103-13.

YU, H. J. & LAI, M. K. 1998. The usefulness of prostate-specific antigen (PSA) density in patients with intermediate serum PSA level in a country with low incidence of prostate cancer. *Urology,* 51, 125-30.

YU, S. Q., HAN, B. M., SHAO, Y., WU, J. T., ZHAO, F. J., LIU, H. T., SUN, X. W., TANG, Y. Q. & XIA, S. J. 2009. Androgen receptor functioned as a suppressor in the prostate cancer cell line PC3 in vitro and in vivo. *Chin Med J (Engl),* 122, 2779-83.

ZANGERLE, P. F., DE GROOTE, D., LOPEZ, M., MEULEMAN, R. J., VRINDTS, Y., FAUCHET, F., DEHART, I., JADOUL, M., RADOUX, D. & FRANCHIMONT, P. 1992. Direct stimulation of cytokines (IL-1 beta, TNF-alpha, IL-6, IL-2, IFN-gamma and GM-CSF) in whole blood: II. Application to rheumatoid arthritis and osteoarthritis. *Cytokine,* 4, 568-75.

ZHANG, Y., JIANG, J., BLACK, R. A., BAUMANN, G. & FRANK, S. J. 2000. Tumor necrosis factor-alpha converting enzyme (TACE) is a growth hormone binding protein (GHBP) sheddase: the metalloprotease TACE/ADAM-17 is critical for (PMA-induced) GH receptor proteolysis and GHBP generation. *Endocrinology,* 141, 4342-8.

ZHANG, Y., TANG, H., CAI, J., ZHANG, T., GUO, J., FENG, D. & WANG, Z. 2011. Ovarian cancer-associated fibroblasts contribute to epithelial ovarian carcinoma metastasis by promoting angiogenesis, lymphangiogenesis and tumor cell invasion. *Cancer Lett,* 303, 47-55.

ZHAO, H., BERNARDO, M. M., OSENKOWSKI, P., SOHAIL, A., PEI, D., NAGASE, H., KASHIWAGI, M., SOLOWAY, P. D., DECLERCK, Y. A. & FRIDMAN, R. 2004. Differential inhibition of membrane type 3 (MT3)-matrix metalloproteinase (MMP) and MT1-MMP by tissue inhibitor of metalloproteinase (TIMP)-2 and TIMP-3 rgulates pro-MMP-2 activation. *J Biol Chem,* 279, 8592-601.

ZHAO, X. Y., BOYLE, B., KRISHNAN, A. V., NAVONE, N. M., PEEHL, D. M. & FELDMAN, D. 1999. Two mutations identified in the androgen receptor of the new human prostate cancer cell line MDA PCa 2a. *J Urol,* 162, 2192-9.

ZHU, Y. S., CAI, L. Q., YOU, X., CORDERO, J. J., HUANG, Y. & IMPERATO-MCGINLEY, J. 2003. Androgen-induced prostate-specific antigen gene expression is mediated via dihydrotestosterone in LNCaP cells. *J Androl,* 24, 681-7.

ZLOTTA, A. R. & SCHULMAN, C. C. 1999. Clinical evolution of prostatic intraepithelial neoplasia. *Eur Urol,* 35, 498-503.

ZUCKER, S., PEI, D., CAO, J. & LOPEZ-OTIN, C. 2003. Membrane type-matrix metalloproteinases (MT-MMP). *Curr Top Dev Biol,* 54, 1-74.

APPENDIX

FIGURE A1: IMAGES FROM TISSUE MICROARRAY ANALYSES WITHOUT DAPI NUCLEAR STAINING

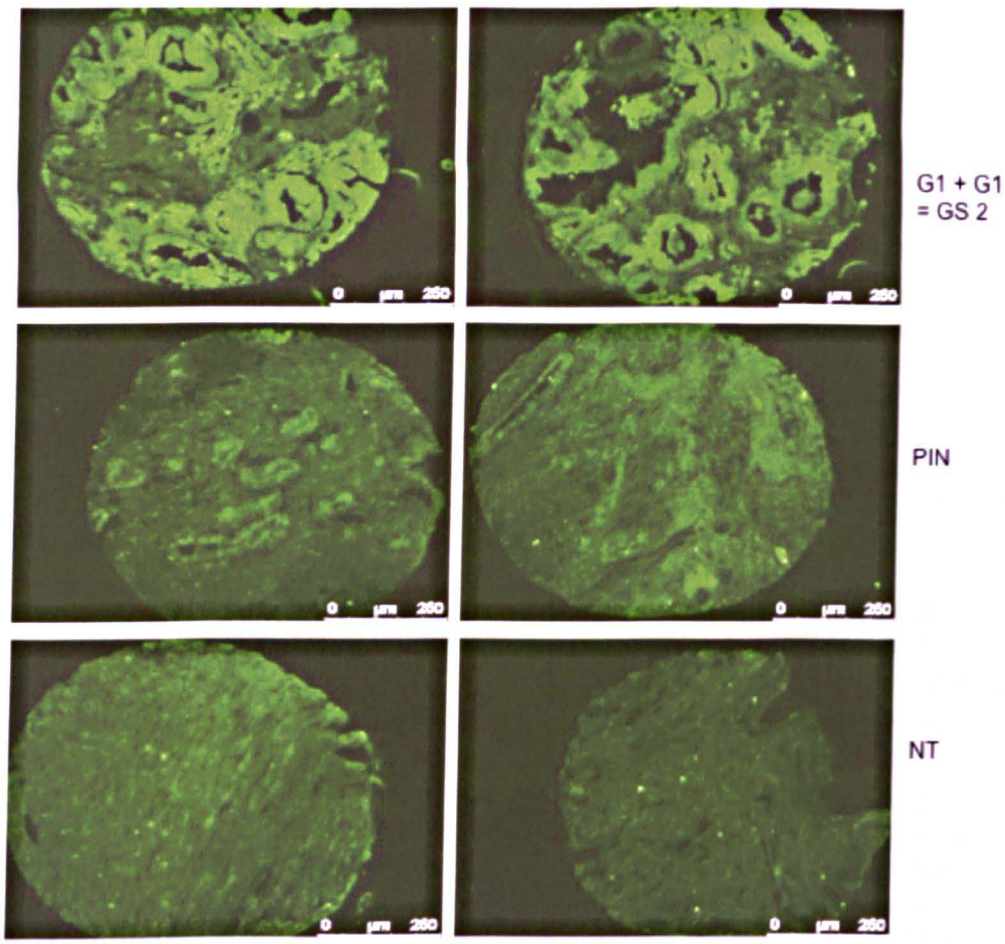

TIMP-3 Staining in Matched Prostate Cancer (GS 2), PIN and Normal Prostate (NT) Tissue Samples.

Note the higher intensity of TIMP-3 staining in the GS2 samples compared to the PIN and NT samples

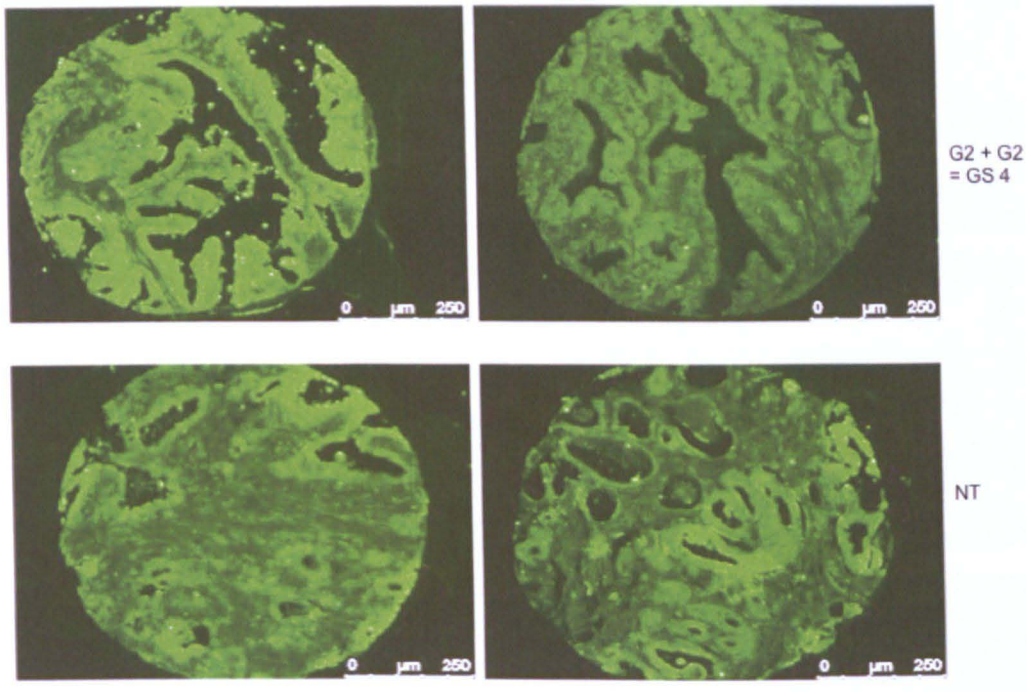

TIMP-3 Staining in Matched Prostate Cancer (GS 4) and Normal Prostate (NT) Tissue Samples.

Note the intensity of TIMP-3 staining is similar in all tissue samples. No matched PIN tissue for this sample set.

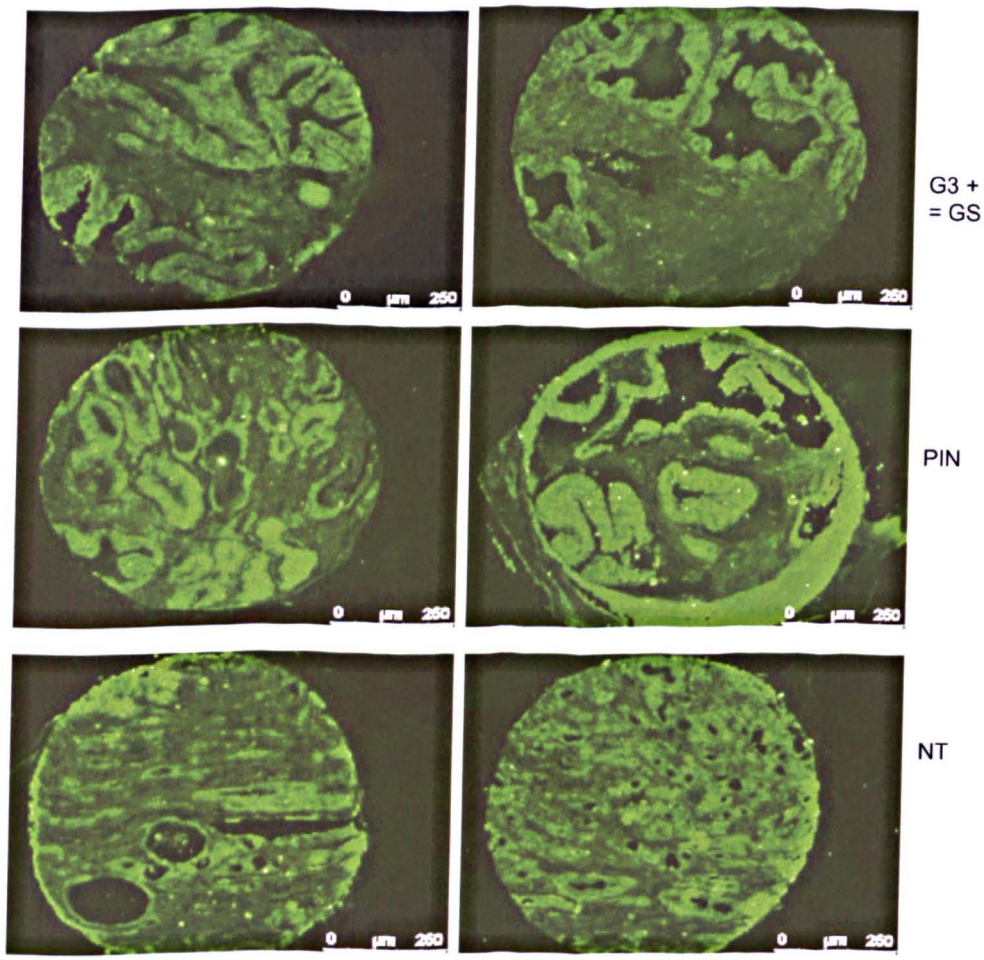

TIMP-3 Staining in Matched Prostate Cancer (GS 5), PIN and Normal Prostate (NT) Tissue Samples.

Note the higher intensity of staining in the PIN and NT samples compared to the GS 5 sample

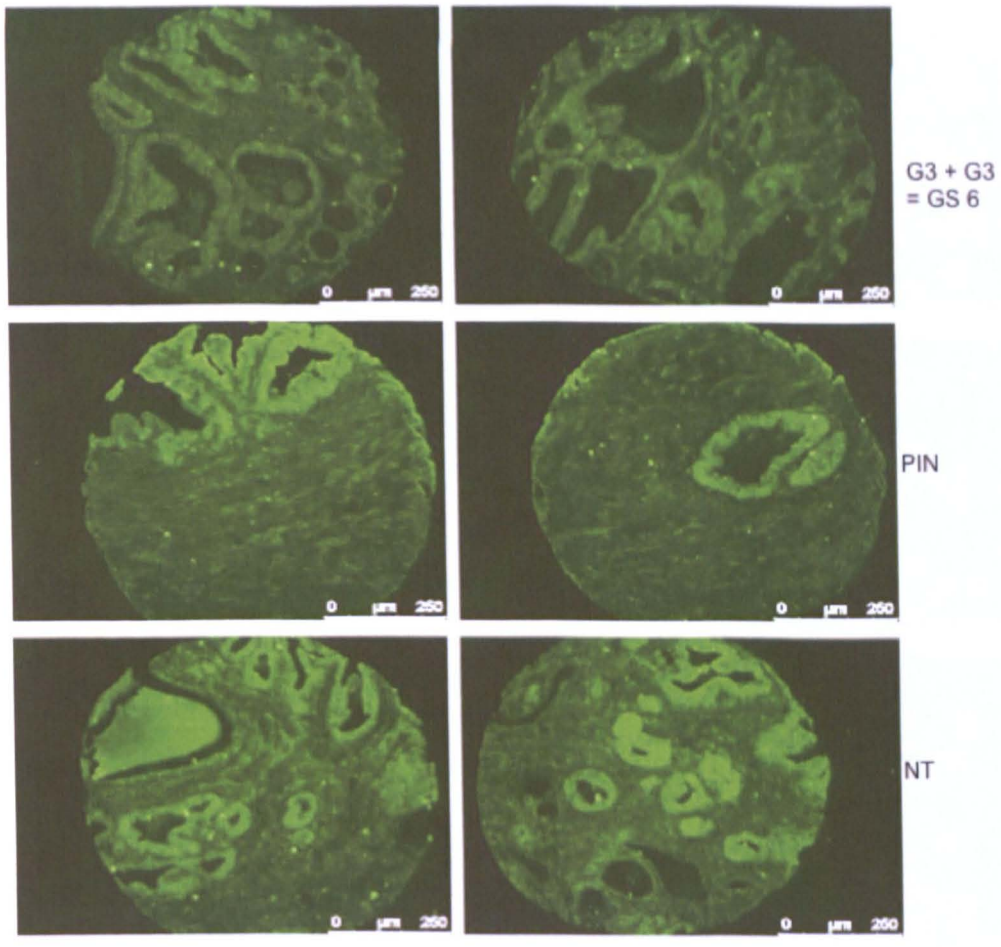

TIMP-3 Staining in Matched Prostate Cancer (GS 6), PIN and Normal Prostate (NT) Tissue Samples.

Note the higher intensity of staining in the NT samples compared to the GS 6 and PIN samples

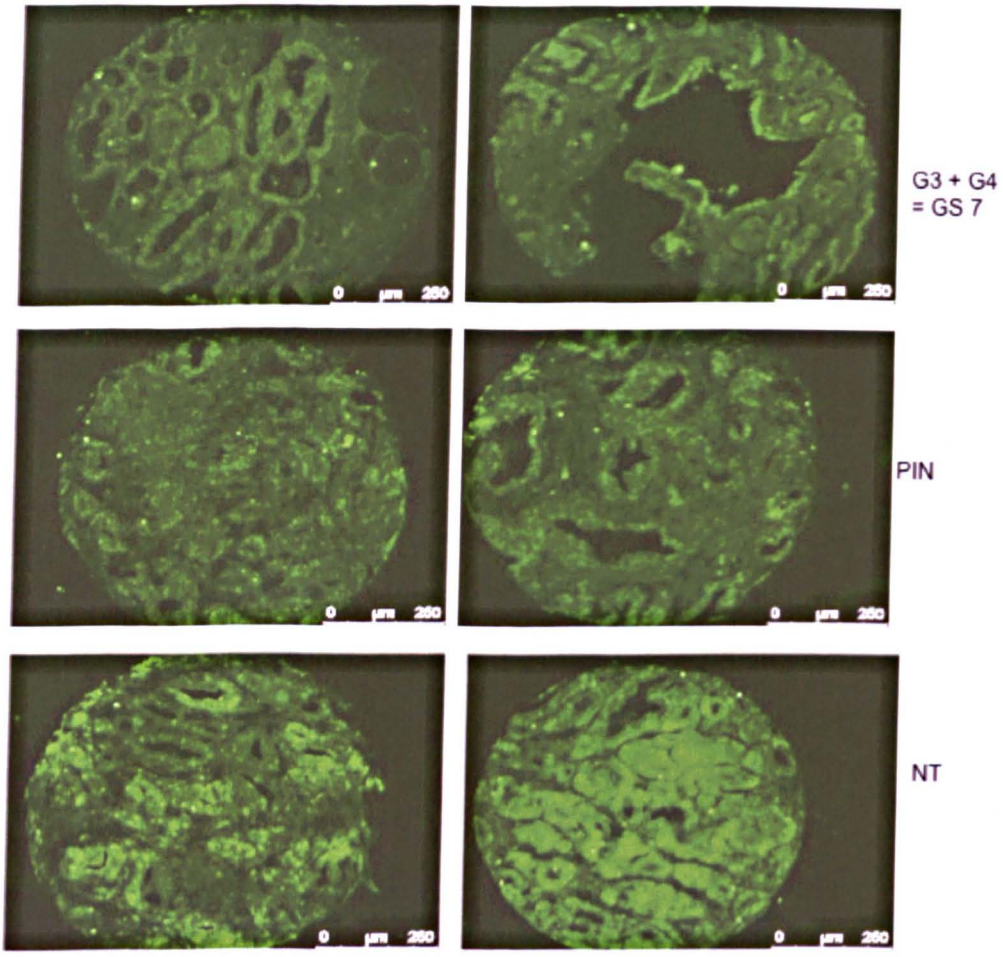

TIMP-3 Staining in Matched Prostate Cancer (GS 7), PIN and Normal Prostate (NT) Tissue Samples.

Note the higher intensity of staining in the NT samples compared to the GS 6 and PIN samples

FIGURE A2: PERMISSION FOR REPRODUCTION OF FIGURE 1.6:

ELSEVIER LICENSE
TERMS AND CONDITIONS

Feb 06, 2012

This is a License Agreement between Olajumoke O Popoola ("You") and Elsevier ("Elsevier") provided by Copyright Clearance Center ("CCC"). The license consists of your order details, the terms and conditions provided by Elsevier, and the payment terms and conditions.

All payments must be made in full to CCC. For payment instructions, please see information listed at the bottom of this form.

Supplier	Elsevier Limited The Boulevard,Langford Lane Kidlington,Oxford,OX5 1GB,UK
Registered Company Number	1982084
Customer name	Olajumoke O Popoola
Customer address	Unniversity of Sheffield Sheffield, S10 2RX
License number	2843071191883
License date	Feb 06, 2012
Licensed content publisher	Elsevier
Licensed content publication	Human Pathology
Licensed content title	Histologic grading of prostate cancer: A perspective
Licensed content author	Donald F. Gleason
Licensed content date	March 1992
Licensed content volume number	23
Licensed content issue number	3
Number of pages	7
Start Page	273
End Page	279
Type of Use	reuse in a thesis/dissertation
Portion	figures/tables/illustrations
Number of figures/tables/illustrations	1
Format	both print and electronic
Are you the author of this Elsevier article?	No
Will you be translating?	No
Order reference number	
Title of your thesis/dissertation	Evaluation of the functional role of TIMP-3 in prostate cancer progression
Expected completion date	Apr 2012

Estimated size (number of pages)	250
Elsevier VAT number	GB 494 6272 12
Permissions price	0.00 GBP
VAT/Local Sales Tax	0.0 USD / 0.0 GBP
Total	0.00 GBP
Terms and Conditions	

INTRODUCTION

1. The publisher for this copyrighted material is Elsevier. By clicking "accept" in connection with completing this licensing transaction, you agree that the following terms and conditions apply to this transaction (along with the Billing and Payment terms and conditions established by Copyright Clearance Center, Inc. ("CCC"), at the time that you opened your Rightslink account and that are available at any time at http://myaccount.copyright.com).

GENERAL TERMS

2. Elsevier hereby grants you permission to reproduce the aforementioned material subject to the terms and conditions indicated.

3. Acknowledgement: If any part of the material to be used (for example, figures) has appeared in our publication with credit or acknowledgement to another source, permission must also be sought from that source. If such permission is not obtained then that material may not be included in your publication/copies. Suitable acknowledgement to the source must be made, either as a footnote or in a reference list at the end of your publication, as follows:

"Reprinted from Publication title, Vol /edition number, Author(s), Title of article / title of chapter, Pages No., Copyright (Year), with permission from Elsevier [OR APPLICABLE SOCIETY COPYRIGHT OWNER]." Also Lancet special credit - "Reprinted from The Lancet, Vol. number, Author(s), Title of article, Pages No., Copyright (Year), with permission from Elsevier."

4. Reproduction of this material is confined to the purpose and/or media for which permission is hereby given.

5. Altering/Modifying Material: Not Permitted. However figures and illustrations may be altered/adapted minimally to serve your work. Any other abbreviations, additions, deletions and/or any other alterations shall be made only with prior written authorization of Elsevier Ltd. (Please contact Elsevier at permissions@elsevier.com)

6. If the permission fee for the requested use of our material is waived in this instance, please be advised that your future requests for Elsevier materials may attract a fee.

7. Reservation of Rights: Publisher reserves all rights not specifically granted in the combination of (i) the license details provided by you and accepted in the course of this licensing transaction, (ii) these terms and conditions and (iii) CCC's Billing and Payment terms and conditions.

8. License Contingent Upon Payment: While you may exercise the rights licensed immediately upon issuance of the license at the end of the licensing process for the

transaction, provided that you have disclosed complete and accurate details of your proposed use, no license is finally effective unless and until full payment is received from you (either by publisher or by CCC) as provided in CCC's Billing and Payment terms and conditions. If full payment is not received on a timely basis, then any license preliminarily granted shall be deemed automatically revoked and shall be void as if never granted. Further, in the event that you breach any of these terms and conditions or any of CCC's Billing and Payment terms and conditions, the license is automatically revoked and shall be void as if never granted. Use of materials as described in a revoked license, as well as any use of the materials beyond the scope of an unrevoked license, may constitute copyright infringement and publisher reserves the right to take any and all action to protect its copyright in the materials.

9. Warranties: Publisher makes no representations or warranties with respect to the licensed material.

10. Indemnity: You hereby indemnify and agree to hold harmless publisher and CCC, and their respective officers, directors, employees and agents, from and against any and all claims arising out of your use of the licensed material other than as specifically authorized pursuant to this license.

11. No Transfer of License: This license is personal to you and may not be sublicensed, assigned, or transferred by you to any other person without publisher's written permission.

12. No Amendment Except in Writing: This license may not be amended except in a writing signed by both parties (or, in the case of publisher, by CCC on publisher's behalf).

13. Objection to Contrary Terms: Publisher hereby objects to any terms contained in any purchase order, acknowledgment, check endorsement or other writing prepared by you, which terms are inconsistent with these terms and conditions or CCC's Billing and Payment terms and conditions. These terms and conditions, together with CCC's Billing and Payment terms and conditions (which are incorporated herein), comprise the entire agreement between you and publisher (and CCC) concerning this licensing transaction. In the event of any conflict between your obligations established by these terms and conditions and those established by CCC's Billing and Payment terms and conditions, these terms and conditions shall control.

14. Revocation: Elsevier or Copyright Clearance Center may deny the permissions described in this License at their sole discretion, for any reason or no reason, with a full refund payable to you. Notice of such denial will be made using the contact information provided by you. Failure to receive such notice will not alter or invalidate the denial. In no event will Elsevier or Copyright Clearance Center be responsible or liable for any costs, expenses or damage incurred by you as a result of a denial of your permission request, other than a refund of the amount(s) paid by you to Elsevier and/or Copyright Clearance Center for denied permissions.

LIMITED LICENSE

The following terms and conditions apply only to specific license types:

15. **Translation**: This permission is granted for non-exclusive world **English** rights only unless your license was granted for translation rights. If you licensed translation rights you may only translate this content into the languages you requested. A professional translator must perform all translations and reproduce the content word for word preserving the integrity of the article. If this license is to re-use 1 or 2 figures then permission is granted for

non-exclusive world rights in all languages.

16. **Website**: The following terms and conditions apply to electronic reserve and author websites:
Electronic reserve: If licensed material is to be posted to website, the web site is to be password-protected and made available only to bona fide students registered on a relevant course if:
This license was made in connection with a course,
This permission is granted for 1 year only. You may obtain a license for future website posting,
All content posted to the web site must maintain the copyright information line on the bottom of each image,
A hyper-text must be included to the Homepage of the journal from which you are licensing at http://www.sciencedirect.com/science/journal/xxxxx or the Elsevier homepage for books at http://www.elsevier.com , and
Central Storage: This license does not include permission for a scanned version of the material to be stored in a central repository such as that provided by Heron/XanEdu.

17. **Author website** for journals with the following additional clauses:

All content posted to the web site must maintain the copyright information line on the bottom of each image, and
he permission granted is limited to the personal version of your paper. You are not allowed to download and post the published electronic version of your article (whether PDF or HTML, proof or final version), nor may you scan the printed edition to create an electronic version,
A hyper-text must be included to the Homepage of the journal from which you are licensing at http://www.sciencedirect.com/science/journal/xxxxx , As part of our normal production process, you will receive an e-mail notice when your article appears on Elsevier's online service ScienceDirect (www.sciencedirect.com). That e-mail will include the article's Digital Object Identifier (DOI). This number provides the electronic link to the published article and should be included in the posting of your personal version. We ask that you wait until you receive this e-mail and have the DOI to do any posting.
Central Storage: This license does not include permission for a scanned version of the material to be stored in a central repository such as that provided by Heron/XanEdu.

18. **Author website** for books with the following additional clauses:
Authors are permitted to place a brief summary of their work online only.
A hyper-text must be included to the Elsevier homepage at http://www.elsevier.com

All content posted to the web site must maintain the copyright information line on the bottom of each image
You are not allowed to download and post the published electronic version of your chapter, nor may you scan the printed edition to create an electronic version.
Central Storage: This license does not include permission for a scanned version of the material to be stored in a central repository such as that provided by Heron/XanEdu.

19. **Website** (regular and for author): A hyper-text must be included to the Homepage of the journal from which you are licensing at
http://www.sciencedirect.com/science/journal/xxxxx. or for books to the Elsevier homepage at http://www.elsevier.com

20. **Thesis/Dissertation**: If your license is for use in a thesis/dissertation your thesis may be submitted to your institution in either print or electronic form. Should your thesis be published commercially, please reapply for permission. These requirements include permission for the Library and Archives of Canada to supply single copies, on demand, of the complete thesis and include permission for UMI to supply single copies, on demand, of the complete thesis. Should your thesis be published commercially, please reapply for permission.

21. **Other Conditions**:

v1.6

If you would like to pay for this license now, please remit this license along with your payment made payable to "COPYRIGHT CLEARANCE CENTER" otherwise you will be invoiced within 48 hours of the license date. Payment should be in the form of a check or money order referencing your account number and this invoice number RLNK500713378.
Once you receive your invoice for this order, you may pay your invoice by credit card. Please follow instructions provided at that time.

Make Payment To:
Copyright Clearance Center
Dept 001
P.O. Box 843006
Boston, MA 02284-3006

For suggestions or comments regarding this order, contact RightsLink Customer Support: customercare@copyright.com or +1-877-622-5543 (toll free in the US) or +1-978-646-2777.

Gratis licenses (referencing $0 in the Total field) are free. Please retain this printable license for your reference. No payment is required.

FIGURE A3: PERMISSION FOR REPRODUCTION OF FIGURE 1.5 AND 1.2 RESPECTIVELY:

nucleus

Statement of Charges

Statement Date: February 9, 2012
Nucleus Job #: 25970
Job Name: Thesis

Client #: 138881
Client Name: Mrs. Olajumoke Popoola
Firm Name: University of Sheffield
Client Address: Beech Hill Road
Medical School building
Sheffield, SH S10 2RX
United Kingdom

Page 1 of 1

Date	Description	Notes	#	Each	Subtotal
02/09/2012	Payment Made	- Order #N-25970-1328804749, 4547xxxxxxxx5136, 12/14, O O Popoola, Approval Code: 585570097357808Z:YNAX:	1.0	($50.00)	($50.00)
02/08/2012	Content License	BK00068 TNM Staging (Prostate Cancer) - Other Electronic Format - Literature review in PhD thesis	1.0	$25.00	$25.00
02/08/2012	Content License	si1208b Prostate Enlargement: Benign Prostatic Hyperplasia versus Normal Prostate Anatomy - Other Electronic Format - Literature review in PhD thesis	1.0	$25.00	$25.00

This document is your invoice. The amount shown at right is payable upon receipt. **Balance Due:** **$0.00**

You may pay the balance shown by MasterCard or Visa by calling (800) 333-0753,
or by mailing a check (payable to Nucleus Medical Media) with a copy of this document.

Toll Free: (800) 333-0753 - Fax (770) 805-0430
1275 Shiloh Road - Suite 3130 - Kennesaw - Georgia - 30144

FIGURE A4: PERMISSION FOR REPRODUCTION OF FIGURE 1.14:

ELSEVIER LICENSE
TERMS AND CONDITIONS

Aug 06, 2012

This is a License Agreement between Olajumoke O Popoola ("You") and Elsevier ("Elsevier") provided by Copyright Clearance Center ("CCC"). The license consists of your order details, the terms and conditions provided by Elsevier, and the payment terms and conditions.

All payments must be made in full to CCC. For payment instructions, please see information listed at the bottom of this form.

Supplier	Elsevier Limited The Boulevard,Langford Lane Kidlington,Oxford,OX5 1GB,UK
Registered Company Number	1982084
Customer name	Olajumoke O Popoola
Customer address	Unniversity of Sheffield Sheffield, S10 2RX
License number	2963040535914
License date	Aug 06, 2012
Licensed content publisher	Elsevier
Licensed content publication	Journal of Molecular Biology
Licensed content title	Structural Determinants of the ADAM Inhibition by TIMP-3: Crystal Structure of the TACE-N-TIMP-3 Complex
Licensed content author	Magdalena Wisniewska,Peter Goettig,Klaus Maskos,Edward Belouski,Dwight Winters,Randy Hecht,Roy Black,Wolfram Bode
Licensed content date	19 September 2008
Licensed content volume number	381
Licensed content issue number	5
Number of pages	13
Start Page	1307
End Page	1319
Type of Use	reuse in a thesis/dissertation
Portion	figures/tables/illustrations
Number of figures/tables /illustrations	1
Format	both print and electronic
Are you the author of this Elsevier article?	No
Will you be translating?	No
Order reference number	

Title of your thesis/dissertation	Evaluation of the Functional Role(s) of TIMP-3 in Prostate Cancer Progression
Expected completion date	Aug 2012
Estimated size (number of pages)	300
Elsevier VAT number	GB 494 6272 12
Permissions price	0.00 GBP
VAT/Local Sales Tax	0.0 USD / 0.0 GBP
Total	0.00 GBP
Terms and Conditions	

INTRODUCTION

1. The publisher for this copyrighted material is Elsevier. By clicking "accept" in connection with completing this licensing transaction, you agree that the following terms and conditions apply to this transaction (along with the Billing and Payment terms and conditions established by Copyright Clearance Center, Inc. ("CCC"), at the time that you opened your Rightslink account and that are available at any time at http://myaccount.copyright.com).

GENERAL TERMS

2. Elsevier hereby grants you permission to reproduce the aforementioned material subject to the terms and conditions indicated.

3. Acknowledgement: If any part of the material to be used (for example, figures) has appeared in our publication with credit or acknowledgement to another source, permission must also be sought from that source. If such permission is not obtained then that material may not be included in your publication/copies. Suitable acknowledgement to the source must be made, either as a footnote or in a reference list at the end of your publication, as follows:

"Reprinted from Publication title, Vol /edition number, Author(s), Title of article / title of chapter, Pages No., Copyright (Year), with permission from Elsevier [OR APPLICABLE SOCIETY COPYRIGHT OWNER]." Also Lancet special credit - "Reprinted from The Lancet, Vol. number, Author(s), Title of article, Pages No., Copyright (Year), with permission from Elsevier."

4. Reproduction of this material is confined to the purpose and/or media for which permission is hereby given.

5. Altering/Modifying Material: Not Permitted. However figures and illustrations may be altered/adapted minimally to serve your work. Any other abbreviations, additions, deletions and/or any other alterations shall be made only with prior written authorization of Elsevier Ltd. (Please contact Elsevier at permissions@elsevier.com)

6. If the permission fee for the requested use of our material is waived in this instance, please be advised that your future requests for Elsevier materials may attract a fee.

7. Reservation of Rights: Publisher reserves all rights not specifically granted in the combination of (i) the license details provided by you and accepted in the course of this licensing transaction, (ii) these terms and conditions and (iii) CCC's Billing and Payment

terms and conditions.

8. License Contingent Upon Payment: While you may exercise the rights licensed immediately upon issuance of the license at the end of the licensing process for the transaction, provided that you have disclosed complete and accurate details of your proposed use, no license is finally effective unless and until full payment is received from you (either by publisher or by CCC) as provided in CCC's Billing and Payment terms and conditions. If full payment is not received on a timely basis, then any license preliminarily granted shall be deemed automatically revoked and shall be void as if never granted. Further, in the event that you breach any of these terms and conditions or any of CCC's Billing and Payment terms and conditions, the license is automatically revoked and shall be void as if never granted. Use of materials as described in a revoked license, as well as any use of the materials beyond the scope of an unrevoked license, may constitute copyright infringement and publisher reserves the right to take any and all action to protect its copyright in the materials.

9. Warranties: Publisher makes no representations or warranties with respect to the licensed material.

10. Indemnity: You hereby indemnify and agree to hold harmless publisher and CCC, and their respective officers, directors, employees and agents, from and against any and all claims arising out of your use of the licensed material other than as specifically authorized pursuant to this license.

11. No Transfer of License: This license is personal to you and may not be sublicensed, assigned, or transferred by you to any other person without publisher's written permission.

12. No Amendment Except in Writing: This license may not be amended except in a writing signed by both parties (or, in the case of publisher, by CCC on publisher's behalf).

13. Objection to Contrary Terms: Publisher hereby objects to any terms contained in any purchase order, acknowledgment, check endorsement or other writing prepared by you, which terms are inconsistent with these terms and conditions or CCC's Billing and Payment terms and conditions. These terms and conditions, together with CCC's Billing and Payment terms and conditions (which are incorporated herein), comprise the entire agreement between you and publisher (and CCC) concerning this licensing transaction. In the event of any conflict between your obligations established by these terms and conditions and those established by CCC's Billing and Payment terms and conditions, these terms and conditions shall control.

14. Revocation: Elsevier or Copyright Clearance Center may deny the permissions described in this License at their sole discretion, for any reason or no reason, with a full refund payable to you. Notice of such denial will be made using the contact information provided by you. Failure to receive such notice will not alter or invalidate the denial. In no event will Elsevier or Copyright Clearance Center be responsible or liable for any costs, expenses or damage incurred by you as a result of a denial of your permission request, other than a refund of the amount(s) paid by you to Elsevier and/or Copyright Clearance Center for denied permissions.

LIMITED LICENSE

The following terms and conditions apply only to specific license types:

15. **Translation**: This permission is granted for non-exclusive world **English** rights only unless your license was granted for translation rights. If you licensed translation rights you may only translate this content into the languages you requested. A professional translator must perform all translations and reproduce the content word for word preserving the integrity of the article. If this license is to re-use 1 or 2 figures then permission is granted for non-exclusive world rights in all languages.

16. **Website**: The following terms and conditions apply to electronic reserve and author websites:
Electronic reserve: If licensed material is to be posted to website, the web site is to be password-protected and made available only to bona fide students registered on a relevant course if:
This license was made in connection with a course,
This permission is granted for 1 year only. You may obtain a license for future website posting,
All content posted to the web site must maintain the copyright information line on the bottom of each image,
A hyper-text must be included to the Homepage of the journal from which you are licensing at http://www.sciencedirect.com/science/journal/xxxxx or the Elsevier homepage for books at http://www.elsevier.com , and
Central Storage: This license does not include permission for a scanned version of the material to be stored in a central repository such as that provided by Heron/XanEdu.

17. **Author website** for journals with the following additional clauses:

All content posted to the web site must maintain the copyright information line on the bottom of each image, and the permission granted is limited to the personal version of your paper. You are not allowed to download and post the published electronic version of your article (whether PDF or HTML, proof or final version), nor may you scan the printed edition to create an electronic version. A hyper-text must be included to the Homepage of the journal from which you are licensing at http://www.sciencedirect.com/science/journal/xxxxx . As part of our normal production process, you will receive an e-mail notice when your article appears on Elsevier's online service ScienceDirect (www.sciencedirect.com). That e-mail will include the article's Digital Object Identifier (DOI). This number provides the electronic link to the published article and should be included in the posting of your personal version. We ask that you wait until you receive this e-mail and have the DOI to do any posting.

Central Storage: This license does not include permission for a scanned version of the material to be stored in a central repository such as that provided by Heron/XanEdu.

18. **Author website** for books with the following additional clauses:
Authors are permitted to place a brief summary of their work online only.
A hyper-text must be included to the Elsevier homepage at http://www.elsevier.com . All content posted to the web site must maintain the copyright information line on the bottom of each image. You are not allowed to download and post the published electronic version of your chapter, nor may you scan the printed edition to create an electronic version.

Central Storage: This license does not include permission for a scanned version of the material to be stored in a central repository such as that provided by Heron/XanEdu.

19. **Website** (regular and for author): A hyper-text must be included to the Homepage of the

journal from which you are licensing at http://www.sciencedirect.com/science/journal/xxxxx. or for books to the Elsevier homepage at http://www.elsevier.com

20. **Thesis/Dissertation**: If your license is for use in a thesis/dissertation your thesis may be submitted to your institution in either print or electronic form. Should your thesis be published commercially, please reapply for permission. These requirements include permission for the Library and Archives of Canada to supply single copies, on demand, of the complete thesis and include permission for UMI to supply single copies, on demand, of the complete thesis. Should your thesis be published commercially, please reapply for permission.

21. **Other Conditions**:

v1.6

If you would like to pay for this license now, please remit this license along with your payment made payable to "COPYRIGHT CLEARANCE CENTER" otherwise you will be invoiced within 48 hours of the license date. Payment should be in the form of a check or money order referencing your account number and this invoice number RLNK500832673.
Once you receive your invoice for this order, you may pay your invoice by credit card. Please follow instructions provided at that time.

Make Payment To:
Copyright Clearance Center
Dept 001
P.O. Box 843006
Boston, MA 02284-3006

For suggestions or comments regarding this order, contact RightsLink Customer Support: customercare@copyright.com or +1-877-622-5543 (toll free in the US) or +1-978-646-2777.

Gratis licenses (referencing $0 in the Total field) are free. Please retain this printable license for your reference. No payment is required.

FIGURE A5: PEER-REVIEWED PUBLICATION (SECOND AUTHOR):

Cancer Investigation, 28:698–710, 2010
ISSN: 0735-7907 print / 1532-4192 online

DOI: 10.3109/07357907.2010.489538

informa
healthcare

ORIGINAL ARTICLE
Cellular and Molecular Biology

Androgen Regulates *ADAMTS15* Gene Expression in Prostate Cancer Cells

Chidi N. Molokwu,[1,2] Olajumoke O. Adeniji,[2] Shankar Chandrasekharan,[1,2] Freddie C. Hamdy,[1,3] and David J. Buttle[2]

Academic Urology Unit, University of Sheffield Medical School, Sheffield, United Kingdom,[1] Academic Unit of Molecular Medicine and Rheumatology, University of Sheffield Medical School, Sheffield, United Kingdom,[2] Nuffield Department of Surgery, John Radcliffe Hospital, University of Oxford, Oxford, United Kingdom[3]

ABSTRACT

Prostate cancer is a major cause of mortality, largely as a consequence of metastases and transformation to androgen-independent growth. Metalloproteinases are implicated in cancer progression. A disintegrin and metalloproteinase with thrombospondin motifs (ADAMTS) are expressed in prostate cancer cells, with ADAMTS-1 and ADAMTS-15 being the most abundant. ADAMTS-15 but not ADAMTS-1 expression was downregulated by androgen in LNCaP prostate cancer cells, possibly through androgen response elements associated with the gene. ADAMTS-15 expression is predictive for survival in breast cancer, and the situation may be similar in prostate cancer, as androgen independence is usually due to aberrant signaling through its receptor.

INTRODUCTION

Prostate cancer is the most common cancer in men in the Western world and second only to lung cancer as a cause of cancer death in men (1, 2). Approximately 30% of men diagnosed with prostate cancer will die of the disease (3), usually as a result of metastases. The exact mechanisms by which cancer cells invade and metastasize are not clear, but some metalloproteinases are thought to play roles in the process of cancer progression (4, 5).

Prostate epithelial cells depend on androgens for proliferation (6). Testosterone from the circulation is converted in the prostate by 5-α-reductase to dihydrotestosterone (DHT), the androgen that is most active in prostate tissue (7, 8). Androgen deprivation therapy (ADT) in the form of surgical or medical castration is used in the management of locally advanced, metastatic, or relapsing disease. Androgen deprivation leads to reduction in the size of local tumors and the size and number of metastatic deposits (9). ADT reduces serum androgen concentration from about 2 nM to undetectable levels (10, 11), which has an adverse effect on hormone-sensitive prostate cancer cell survival and slows the development and progression of prostate cancer.

Androgen-regulated gene expression is mediated via the action of nuclear receptors. The activated androgen receptor translocates from the cytoplasm to the nucleus, where it binds to androgen response elements (AREs) located in proximity to androgen-regulated genes. AREs are 15-base-pair (15-bp) DNA sequences comprising two 6-bp half-sites separated by a 3-bp spacer. The sequence 5′-GGA/TACAnnnTGTTCT-3′ has been described as the consensus ARE (12), but there is considerable variation in the sequence and configuration of AREs located in association with androgen-responsive genes (13).

A disintegrin and metalloproteinase with thrombospondin motifs (ADAMTSs) are a group of proteolytic enzymes belonging to family M12 in protease clan MA of the MEROPS database (www.merops.sanger.ac.uk) (14) and thus are homologous to a disintegrin and metalloproteinase and matrix metalloproteinases (15). There are 19 ADAMTS enzymes in the human genome, which play diverse roles in the tissues in which they are expressed (16). ADAMTS-1 is essential for normal development of the urogenital tract in mice (17) and for ovulation (18), and ADAMTS-1 and ADAMTS-8 have antiangiogenic

Keywords: Bladder & prostate cancer, Gene expression, Growth factors & receptor, Tumor cell biology, Tumor suppressors
Correspondence to:
Dr. David J. Buttle
Academic Unit of Molecular Medicine and Rheumatology
University of Sheffield Medical School
Beech Hill Road, Sheffield S10 2RX, United Kingdom
email: d.j.buttle@sheffield.ac.uk

properties (19). ADAMTS-5 has been implicated in cartilage breakdown in arthritis (20, 21). ADAMTS-2, ADAMTS-3, and ADAMTS-14 are procollagen *N*-peptidases (22), and ADAMTS-13 has been identified as the von Willebrand factor cleaving protease that is an important part of the blood coagulation cascade (23). Expression levels of ADAMTS proteases in prostate cancer and stromal cells have been reported previously (24). ADAMTS-1 and ADAMTS-15 were the most abundantly expressed in each of the prostate cancer and stromal cell lines investigated, but their role in prostate cancer development and progression is not known.

Owing to homology with ADAMTS-1, ADAMTS-15 is predicted to have proteoglycanase properties (25). However the ADAMTSs undergo C-terminal proteolytic processing (26), which affects their localization and activities, and the multiple domains could be playing different roles, as is the case with ADAMTS-1, in which the proteolytic domain is responsible for aggrecanase activity, while the C-terminal domains are required for antiangiogenic activity (27).

Decreased ADAMTS-15 expression in malignant breast tumors correlates with poor patient prognosis (28), suggesting that ADAMTS-15 may be playing a protective role in breast cancer patients. As is the case with prostate cancer, breast cancer is a disease in which hormone deprivation plays a role in management, with the use of estrogen receptor antagonists in patients with estrogen-receptor-positive tumors (29).

In order to further understand the potential roles of ADAMTS-1 and ADAMTS-15 in prostate cancer progression, we set out to test the hypothesis that the expression of ADAMTS-1 and ADAMTS-15 is regulated by androgens in prostate cancer cells. Owing to their possible proteolytic and antiangiogenic effects, such a scenario might suggest that these proteases play important roles in prostate cancer progression.

MATERIALS AND METHODS

Cell culture

The androgen-sensitive LNCaP prostate cancer cell line (30) was used to test the effects of DHT on ADAMTS expression. The cells were plated into 24-well culture plates at a density of 1×10^4 cells/well for RNA extraction and in 6-well culture plates at 5×10^4 cells/well for protein extraction. Cells were grown to approximately 60% confluence in Dulbecco's modification of Eagle's medium supplemented with 10% fetal calf serum, 100 units/mL penicillin, 100 μg/mL streptomycin, and 0.25 μg/mL amphotericin B, at 37°C in a humidified atmosphere of 5% CO_2. Medium was changed to serum-free DCCM (Biological Industries, Kibbutz Beit HaEmek, Israel), supplemented with 2 mM L-glutamine, and cells were allowed to acclimatize to the new medium for 48 hr. The medium was then removed, and cells were treated in fresh DCCM medium for 24 hr with DHT (Sigma) or with flutamide (Sigma, Poole, UK), a nonsteroidal androgen receptor antagonist. LNCaP cell proliferation is maximally stimulated by DHT at concentrations between 1 and 10 nM (8, 30–32). To cover the range between castrate levels and maximal DHT stimulation, treatment doses of 0.1, 1.0, and 10 nM DHT were used. To determine whether an excess of flutamide would inhibit the effect of DHT, LNCaP cells were also treated with 1 μM flutamide or 10 nM DHT + 1 μM flutamide. DHT and flutamide were dissolved in 0.1% ethanol. The control arm was treated with 0.001% ethanol, as this was the final concentration of ethanol in the treatment arms.

RNA extraction and cDNA synthesis

For mRNA expression analysis, DHT treatment was carried out for 24 hr. This time point was used because previous experiments analyzing regulation of ADAMTS-15 had shown responsive changes in expression by this time point (24). The medium was removed, and TRI Reagent (Sigma) was applied to the wells to lyse the cells, using the supplier's protocol. The resulting cell lysate was stored at −80°C, awaiting RNA extraction. Total RNA was reverse-transcribed to cDNA with reverse transcriptase II (Invitrogen, Paisley, UK) using the supplier's protocol. Reactions for cDNA synthesis were run on a GeneAmp PCR System 9700 (Applied Biosystems). The thermal cycle was set at 25ooC for 2 min, 42°C for 50 min, and 70°C for 15 min and was then cooled to 4°C. Furthermore, cDNA was stored at −20°C until ready for use in real-time reverse-transcriptase polymerase chain reactions (RT-PCRs).

Real-time RT-PCR

Real-time RT-PCR was run in 10-μL reactions in duplicate, using 384-well plates on the ABI Prism 7900HT sequence detector with SDS 2.1 software (Applied Biosystems). TaqMan gene expression assays (Applied Biosystems) were used. Each assay contained a proprietary primer probe with a 6-carboxyfluorescein reporter and a quencher. Further, 5 μL of TaqMan master mix (Applied Biosystems, Warrington, UK), 0.5 μL of TaqMan gene expression assay, 2.5 μL of diethylpyrocarbonate-treated water, and 2 μL of cDNA were mixed in each well. The thermal cycle was set at 95°C for 5 min, and then 40 cycles were set at 95°C for 15 s and 60°C for 60 s. Independent cDNA samples were also analyzed using SYBR Green assays (Applied Biosystems). Each reaction consisted of 5 μL of 2× SYBR Green mastermix as supplied, 50–1,000 nM of each primer, and 1 μL of cDNA and made up to a final reaction volume of 10 μL with diethylpyrocarbonate-treated water.

Glyceraldehyde-3-phosphate dehydrogenase (GAPDH) or RNA polymerase II (RNAP) were used as the endogenous housekeeping genes to normalize between samples (33). Assay IDs of TaqMan assays were as follows: Hs00199608_mL for ADAMTS-1, Hs00373520_mL for ADAMTS-15, Hs00426859_gL for prostate-specific antigen (PSA), Hs99999905_mL for GAPDH, and Hs00992801_mL for RNAP. Primer sequences for SYBR Green experiments were as follows: for ADAMTS-1, forward 5′-GCACTGCAAGGCGTAGGAC and reverse 5′-AAGCATGGTTTCCACATAGCG; for ADAMTS-15, forward 5′-TCCTCTTCACCAGGCAGGAC and reverse 5′-GGTCACACATGGTACCCACATCA; and for

Table 1. Sequence Data for siGENOME SMARTpool siRNA From Dharmacon, Showing the Sequence ID and the Nucleotide Sequence for Each of the siRNA Duplexes

Gene	SMARTpool ID	Sense/Antisense	Sequence
ADAMTS15	D-006766-01	Sense	5′-GCGCGGACCUGGAACAUUAUU
		Antisense	5′-UAAUGUUCCAGGUCCGCGCUU
	D-006766-03	Sense	5′-CUGCGACGCUGCUUCUAUUUU
		Antisense	5′-AAUAGAAGCAGCGUCGCAGUU
	D-006766-04	Sense	5′-CCAAGCGUUUCGUGUCUAUUU
		Antisense	5′-AUAGACACGAAACGCUUGGUU
	D-006766-05	Sense	5′-GCAAGAAGGUGACUGGACUUU
		Antisense	5′-AGUCCAGUCACCUUCUUGCUU

GAPDH, forward 5′-GCTCCTCCTGTTCGACAGTCA and reverse 5′-AACTTCCCCATGGTGTCTGA. Expression levels of mRNA in the treated cells relative to the control cells were determined using the $2^{-\Delta\Delta C_T}$ method (34). This allowed the normalization of the expression levels of the gene of interest in individual experiments.

Protein extraction

For protein extraction, cells were treated with DHT and flutamide for 72 hr, after which medium was removed and cells were gently washed with phosphate-buffered saline. Tris-buffered saline was mixed with 0.01% Triton X-100 at 4°C in a volume ratio of 100:1 with protease inhibitor cocktail (Sigma) containing 4-(2-aminoethyl)benzenesulfonyl fluoride, pepstatin A, bestatin, leupeptin, aprotinin, and trans-epoxysuccinyl-L-leucylamido(4-guanido)-butane (E-64) according to the supplier's protocol. Each well was applied with 200 μL of the mixture for 1 hr at 4°C to lyse the cells. The lysate was centrifuged at 12,000 × *g* for 10 min at 4°C. The supernatant was removed and saved, while the pellet containing cell debris was discarded. The supernatant was stored at −40°C, awaiting protein quantification and Western blotting. Protein quantification was achieved using the MicroBCA assay (Pierce, Loughborough, UK) according to the manufacturer's protocol.

Characterization of an antibody to the propeptide of ADAMTS-15

We are unaware of any publications describing the specificity of an antibody to ADAMTS-15. It was therefore essential that we first characterized a commercial antibody before we could go on to use it in this study. This was achieved by siRNA knockdown of ADAMTS-15 expression and then analysis of changes in protein expression by Western blotting, using a rabbit antibody directed against the propeptide of ADAMTS-15 (Abcam, Cambridge, UK, ab45047). In addition, siGENOME SMARTpool siRNA against ADAMTS-15 was synthesized by Dharmacon (Epsom, UK). Each SMARTpool siRNA vial contained a pool of four different siRNA sequences directed against the gene of interest (Table 1). GAPDH was knocked down to serve as a positive control, and a nontargeting siRNA sequence (NTC) bearing no identity to any sequence in the human genome was transfected into cells in a separate set of wells as a negative control. The sequences of the positive and the negative control were proprietary. GAPDH and NTC experiments were carried out using siCONTROL GAPD (cat. no. D-001140-01-05) and siCONTROL nontargeting siRNA (cat. no. D-001206-13) respectively. The cells were transfected in DharmaFECT 2 Transfection Reagent (Dharmacon) according to the manufacturer's protocol. The androgen-independent, LNCaP-derived C4–2b4 cell line (35) was used for validating the anti-ADAMTS-15 antibody. The cells were detached using trypsin-EDTA, and a small amount of serum-containing medium was added to the cell suspension to inactivate the trypsin. The cells were centrifuged at 1,000 × *g* for 5 min, and the medium was removed from the cell pellet. The cells were resuspended in the medium containing 10% (v/v) fetal calf serum without antibiotics and counted. Wells of a 96-well polystyrene plate were used to prepare the reagents for the transfections. In one well, 2.5 μg of siRNA was added to 10 μL of serum-free medium, and in a separate well, 0.4 μL of DharmaFECT 2 was added to 19.6 μL of serum-free medium. The contents of the first well were added to the second, and the mixture was left at ambient temperature for 20 min, before being placed into the wells of a 48-well plate. A total of 3×10^4 cells were added to each of the wells containing the siRNA mixture, and the final volume of each well was made up to 200 μL with the medium containing no antibiotics. Knockdown of target siRNA was analyzed by real-time RT-PCR at 72 hr posttransfection, and protein knockdown was analyzed at 120 hr posttransfection by Western blotting as described below.

Protein samples were prepared by heating to 95°C for 5–10 min in reducing sample buffer [62.5 mM Tris-HCl; 25% (v/v) glycerol; 2% (w/v) sodium dodecyl sulfate; 0.01% bromophenol blue; 350 mM dithiothreitol, pH 6.8]. Sodium dodecyl sulfate–polyacrylamide gel electrophoresis was performed using 10% (w/v) polyacrylamide gels. Each well was loaded with 100 μg of protein, and the gels were electrophoresed for 1 hr at a constant voltage of 200 V. Protein from the gel was then transferred to a polyvinyledene fluoride membrane at a constant current of 400 A for 10 min at pH 11.0. The membrane was blocked for 1 hr in blocking buffer [6% (w/v) casein, 0.05% Tween-20 in TBS (TBST)]. After blocking, the membrane was probed for 6 hr using the rabbit anti-ADAMTS-15 antibody (Abcam, ab45047) raised against the propeptide of ADAMTS-15, at a dilution of 1:5,000 (200 ng/mL) in blocking buffer. After three washes in TBST, the membrane was probed for 1 hr with

a horseradish-peroxidase-conjugated (HRP-conjugated) swine antirabbit IgG antibody (Dako Cytomation, P0399, Ely, UK) at a dilution of 1:3,000 (113 ng/mL). HRP detection was done with ECL Plus Western blotting detection kit (Amersham, Little Chalfont, UK) according to the manufacturer's protocol. Hyperfilm ECL (Amersham) X-ray film was used to expose and develop the membranes.

For reprobing, the polyvinyledene fluoride membranes were washed three times in TBST and stripped of anti-ADAMTS-15 antibody by agitation at 4°C for 6 hr in TBST brought to pH 2.0 with HCl. GAPDH was probed with rabbit polyclonal anti-GAPDH IgG (Abcam, ab9485) at a dilution of 1:1,000 (1 μg/mL). Secondary antibody probing and HRP detection were done as described earlier.

Densitometry

Bands detected on X-ray films from Western blotting experiments were semiquantitatively analyzed by densitometry using a GS-710 Calibrated Imaging Densitometer (Bio-Rad, Hemel Hempstead, UK) running on Quantity One version 4.5.1 software (Bio-Rad). A boundary was drawn around each band for analysis. The adjusted area and density (volume) of the band from each treatment sample was compared with the band from the control sample, measured as optical density × mm^2, and was defined by the software as the sum of the intensities of the pixels (in optical density) within a volume boundary multiplied by the area of a single pixel (in mm^2) minus the background volume.

ADAMTS15 gene analysis

The genomic sequences of the *ADAMTS1* and *ADAMTS15* genes were obtained from the Ensembl genome database, Release 49 (www.ensembl.org) (36). The Ensembl online tool was used to determine the 5'-flanking sequence containing the gene regulatory region, the transcription start point (TSP), and the gene sequence with intron and exon information. Using an *in silico* approach with the online nuclear receptor binding site search tool NUBIScan version 2.0 (www.nubiscan.unibas.ch) (37), a matrix was created consisting of the following nine ARE half-sites: AGAACA, TGTACC, TGTACA, TGTTCT, GGTACA, AGTGCT, TGGTCA, AGTTCT, and AGTACG. Each half-site has previously been shown to be functional (13). A search strategy was designed to search for putative AREs composed of direct repeats (DRs), inverted repeats (IRs), and everted repeats (ERs) of these half-sites interposed by a nonspecific 3-bp sequence, forming a complete 15-bp ARE. A threshold score of 0.8 was set to minimize false-positive predictions. This threshold setting ensured that only putative AREs with sequences corresponding to 80–100% similarity with the half-sites in the matrix were detected. The frequency and position of AREs that met the search criteria were recorded. For comparison, the promoter regions and sequences of PSA (human kallikrein 3, *hKLK3*) and prostate-specific membrane antigen (folate hydrolase 1, *FOLH1*) genes were also analyzed using the same strategy. *hKLK3* gene expression is known to be upregulated by androgen, and the promoter region contains the functional ARE (AGAACAgcaAGTGCT) at −170 bp from the TSP (38). The expression of the *FOLH1* gene is downregulated by androgen (39).

Statistical analyses

The Kruskall-Wallis test was used to identify significant differences between the medians of each treatment group. Differences in expression levels were tested for significance with the Dunn's multiple-comparison test, which analyzes differences in rank sum between each treatment group and control. The Grubb's test was used to identify and remove outlying samples where appropriate. All tests were performed on GraphPad Prism 5.0 (GraphPad Software Inc.). Statistically significant differences were defined by $p \leq .05$.

RESULTS

Regulation of ADAMTS-1 and ADAMTS-15 mRNA expression by DHT

The effect of DHT and flutamide on expression of ADAMTS-1 and ADAMTS-15 mRNA was analyzed using real-time RT-PCR. DHT treatment did not significantly regulate expression of ADAMTS-1 mRNA at any of the concentrations used [Figure 1(a)]. In contrast to this, DHT treatment downregulated the expression of ADAMTS-15 mRNA. ADAMTS-15 mRNA was downregulated by 40% and 70% with treatments of 0.1 and 1 nM DHT respectively [Figure 1(b)]. The Kruskall–Wallis test demonstrated that the medians had a significantly different variance ($p = .0022$). Dunn's multiple-comparison test was used to analyze differences in rank sum between each treatment group and control. ADAMTS-15 mRNA expression was significantly downregulated with treatments of 0.1 nM DHT ($p < .05$), 1 nM DHT ($p < .001$), 1 μM flutamide ($p < .01$), and 10 nM DHT with 1 μM flutamide ($p < .05$). Comparing the 10 nM DHT treatment group with the 10 nM DHT plus 1 μM flutamide treatment group showed no significant difference in ADAMTS-15 expression. Grubb's test was applied to the 10 nM DHT treatment group to identify and remove an outlying sample, after which the difference in the median ADAMTS-15 mRNA expression between the control and the 10 nM DHT group was significant ($p < .05$). Independent cDNA samples ($n = 5$) from LNCaP cells treated with DHT and flutamide were analyzed using SYBR Green assays. Results from these experiments also showed downregulation of ADAMTS-15 mRNA by DHT that was not inhibited by flutamide (data not shown). As a positive control, regulation of PSA mRNA by DHT was also analyzed. As expected, PSA mRNA expression was upregulated by DHT in a dose-dependent manner. Compared with control, PSA mRNA was upregulated 4-fold by 0.1 nM DHT, 9-fold by 1 nM DHT, and 45-fold by 10 nM DHT (data not shown).

Antibody validation

As we failed to find characterization of ADAMTS-15 antibodies in the literature, we undertook an investigation of the utility of one such antibody, ab45047, raised against a region

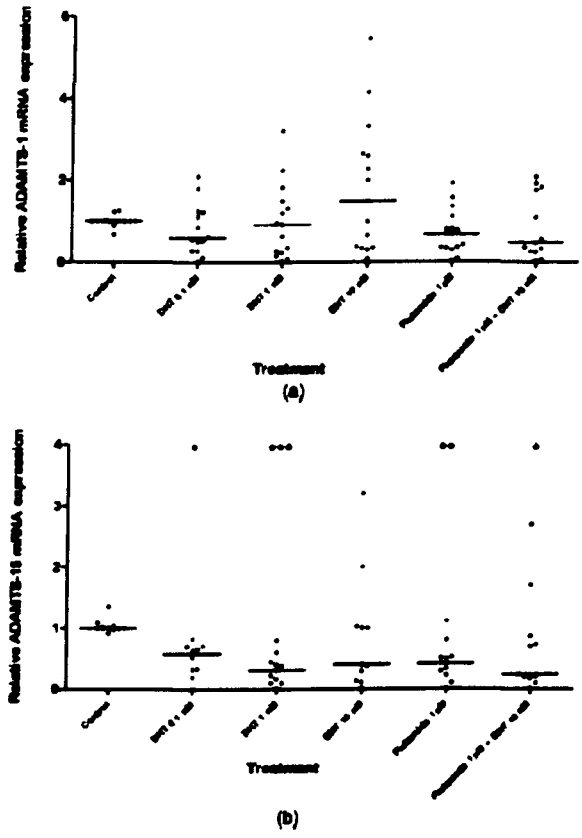

Figure 1. Expression of ADAMTS-1 and -15 mRNA in LNCaP cells treated with DHT and the nonsteroidal androgen antagonist flutamide. Cells were treated for 24 hr with the specified doses of DHT or flutamide and were lysed, and cDNA was synthesized for analysis by real-time RT-PCR. Each data point represents an individual sample of cDNA. The horizontal bars denote the median expression level for each treatment group. Expression levels in treated cells are shown as fold changes relative to controls. (a) Results ($n = 15$) collated from 15 separate experiments, showing the expression level of ADAMTS-1 mRNA in the treated cells relative to expression in untreated cells (control). (b) Results collated from 11 separate experiments ($n = 11$), showing the expression level of ADAMTS-15 mRNA in the treated cells relative to expression in untreated cells (control). The asterisks are used at the top to denote treatment groups in which difference in expression levels relative to control were statistically significant ($^{*}p < .05$, $^{**}p < .01$, $^{***}p < .001$).

of the propeptide of ADAMTS-15. C4–2b4 cells expressed more ADAMTS-15 than did LNCaP cells in preliminary experiments (Figure 2), making the effect of knockdown more readily detectable on a Western blot. We therefore utilized the former cell line in these characterization studies. ADAMTS-15 mRNA expression in C4–2b4 prostate cancer cells was inhibited by 80% (± 10%, $n = 3$) by siRNA specific for ADAMTS-15. Protein expression was analyzed by Western blotting. Bands of 50 kDa were detected in all the lanes, but the band was attenuated in the cells treated with ADAMTS-15 siRNA. Densitometric analysis of the 50-kDa band showed that its expression was knocked down by over 80% (Figure 3). To control for errors in sample loading, the membrane was stripped and then reprobed with anti-GAPDH antibody. Bands of 34 kDa were detected with equal intensity in the NTC and ADAMTS-15 knockdown lanes. The band was absent in the GAPDH knockdown lane (Figure 3). The detection of downregulated expression of the 50-kDa band by the antibody in the cells treated with siRNA to the *ADAMTS15* gene verified the specificity of the antibody and illustrated that the major product from these cells was a form of the enzyme of approximately 50 kDa.

Regulation of ADAMTS-15 protein expression by DHT

To analyze the effect of DHT stimulation on ADAMTS-15 protein expression, LNCaP cells were treated with DHT with and without flutamide for 72 hr. Western blotting with the

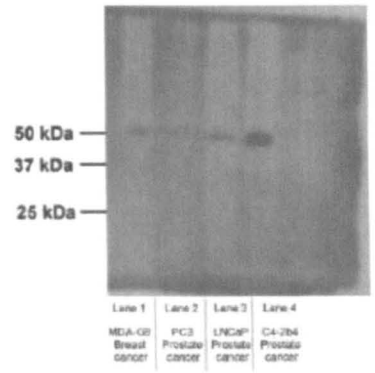

Figure 2. ADAMTS-15 expression in breast and prostate cancer cell lines probed with Abcam ab45047 anti-ADAMTS-15 antibody. Each lane was loaded with 100 μg of protein. Bands of 50 kDa were detected on Western blots.

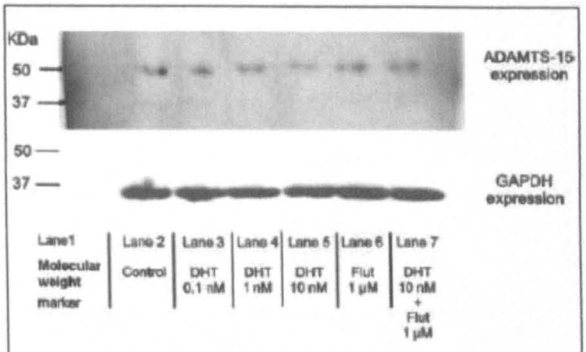

Figure 4. Effect of DHT on ADAMTS-15 protein expression. Western blotting was used to detect ADAMTS-15 expression in LNCaP cells treated for 72 hr with control, 0.1 nM DHT, 1 nM DHT, 10 nM DHT, 1 μM flutamide, and 10 nM DHT plus flutamide. Cell layers were lysed with Triton X-100 for protein extraction, and protein was quantified with the MicroBCA assay. Each lane was loaded with 100 μg of protein. Bands of 50 kDa were detected. The experiment is representative of two, with similar results.

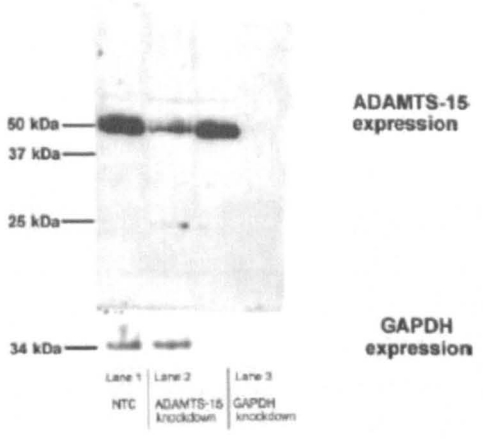

Figure 3. Validation of the specificity of the ADAMTS-15 antibody. ADAMTS-15 expression in C4–2b4 prostate cancer cells was transiently knocked down. Western blotting was performed with the cell lysates. Each lane was loaded with 100 μg of protein. Lane 1 was the lysate from mock-transfected cells (NTC); Lane 2 was from ADAMTS-15 knockdown cells; and Lane 3 was from GAPDH knockdown cells. The upper panel is an image of the blot after probing with the ADAMTS-15 antibody. A 50-kDa band was detected in each lane. The lower panel is an image of the same membrane after it had been stripped and reprobed with anti-GAPDH antibody. 34-kDa bands were detected in Lanes 1 and 2 of equal intensity, showing that the difference in intensity when the membrane was probed for ADAMTS-15 was not due to unequal sample loading. GAPDH knockdown led to complete absence of a band in Lane 3 on the lower panel. These results are representative of two experiments.

anti-ADAMTS-15 antibody revealed a 50-kDa band in all the lanes (Figure 4). These bands were analyzed by densitometry, and in keeping with the mRNA data, ADAMTS-15 protein was downregulated by DHT in a dose-dependent manner (Table 2). This effect was not inhibited by flutamide. In fact, as had been observed at the mRNA level, treatment with flutamide alone also caused downregulation of ADAMTS-15 protein.

Putative androgen response elements

The *ADAMTS15* gene has not been previously described as an androgen-regulated gene. Using the NUBIScan online nuclear receptor binding site search tool, the *ADAMTS15* gene promoter and gene sequence were screened to identify putative AREs. We identified 1 ARE in the *ADAMTS15* promoter and 12 AREs in the gene sequence. ADAMTS-1 mRNA expression was not regulated by DHT in our experiments. The *ADAMTS1* gene had no putative AREs in the promoter region but had two in the gene sequence. Table 3 gives the position, orientation, sequence, and score for the putative AREs identified. For comparison, we performed the same search on the *hKLK3* gene, which is upregulated by androgen, and on the *FOLH1* gene, which is downregulated by androgen (Table 4). Figure 5 shows a schematic representation of the AREs identified in the *ADAMTS1*, *ADAMTS15*, and *hKLK3* genes. The ARE detected at position 169 of the *hKLK3* promoter region is known to be the functional PSA ARE sequence AGAACAgcaAGTGCT (35). The *hKLK3* promoter had approximately double the ARE-to-bp ratio compared with the *ADAMTS15* and *FOLH1* promoters, and the *hKLK3* gene sequence had approximately 1.5 times the ratio found in the *ADAMTS15* and *FOLH1* gene sequences and approximately 3 times the ratio in the *ADAMTS1* gene sequence.

Table 2. Densitometric Analysis of Bands Detected on Western Blots Performed on Samples From Two Experiments, with Adjusted Volume of the Bands Quantified and Compared With Control

	Lane 1 Control	Lane 2 DHT 0.1 nM	Lane 3 DHT 1 nM	Lane 4 DHT 10 nM	Lane 5 Flutamide 1uM	Lane 6 DHT 10 nM + Flutamide 1 uM
Experiment 1						
Adjusted densitometric volume (OD mm^2)	0.2025	0.1238	0.0905	0.0483	0.0659	0.055
Adjusted volume relative to control	1	0.6	0.4	0.2	0.3	0.3
Experiment 2						
Adjusted densitometric volume (OD mm^2)	0.2036	0.2231	0.0217	0.0022	0.05	0.0093
Adjusted volume relative to control	1	1.1	0.1	0.01	0.2	0.05

Table 3. Position, Orientation, Sequence, and Similarity Score of the AREs Detected in the *ADAMTS1* and *ADAMTS15* Genes

	Position (Strand)	Repeat Orientation	ARE Sequence	Score
		ADAMTS1		
Promoter	–	–	–	–
Sequence	4933 (-)	DR	GGTGCTacaTGTGCT	0.82
	7676 (+)	DR	TGGTCAtcaTGTTCT	0.81
		ADAMTS15		
Promoter	-2319 (+)	ER	GGAACAtaaGGTGCG	0.81
Sequence	914 (+)	DR	AGCACCccgAGTACT	0.81
	914 (+)	ER	AGCACCccgAGTACT	0.88
	914 (+)	IR	AGCACCccgAGTACT	0.81
	926(-)	DR	AGTACTcggGGTGCT	0.88
	2357 (+)	ER	GGCACAgctAGTCCC	0.81
	6684 (-)	DR	AGTGCTctgAGTGCA	0.87
	6693 (-)	DR	AGTGCCgagAGTGCT	0.84
	7038 (+)	IR	TGTGCTgccTGGACT	0.86
	12880 (-)	DR	TGTCCCcacAGTGCC	0.81
	16123 (+)	DR	TGAACCgttAGTTCA	0.82
	16123 ( )	ER	TGAACCgttAGTTCA	0.89
	19163 (+)	IR	AGCACTctcTGAACT	0.81
	19177 (-)	DR	AGTTCAgagAGTGCT	0.90
	24790 (+)	IR	AGTGCAactTGCACC	0.84

Note: For the orientation, DR, ER, and IR denote direct repeat, everted repeat, and inverted repeat respectively.

Table 4. Summary of the ARE Data for *ADAMTS1*, *ADAMTS15*, *hKLK3*, and *FOLH1* Genes

	ADAMTS1	ADAMTS15	hKLK3	FOLH1
Gene location	21q21.3	11q24.3	19q13.33	11p11.2
Androgen regulation	Not regulated	Downregulated	Upregulated	Downregulated
Promoter				
Length (bp)	1,786	2,576	2,434	2,618
AREs	0	1	2	1
AREs per bp	0	0.00039	0.00082	0.00038
Sequence				
Length (bp)	9,121	24,846	5,850	62,033
AREs	2	12	4	25
AREs per bp	0.00022	0.00048	0.00068	0.0004

DISCUSSION

Hormone therapy for locally advanced and metastatic prostate cancer essentially consists of lowering circulating androgen concentration in order to silence androgen receptor signaling. In our experiments, we analyzed the expression of ADAMTS-1 and ADAMTS-15 under different concentrations of DHT in an androgen-responsive cell line, LNCaP. ADAMTS-1 mRNA expression was not significantly regulated by DHT. By contrast, DHT downregulated the expression of ADAMTS-15 mRNA and protein. The *ADAMTS15* gene has not previously been reported to be androgen regulated. It is known to be expressed in prostate cancer cell lines (24), and its expression in breast cancer is a good indicator of patient survival (28). This

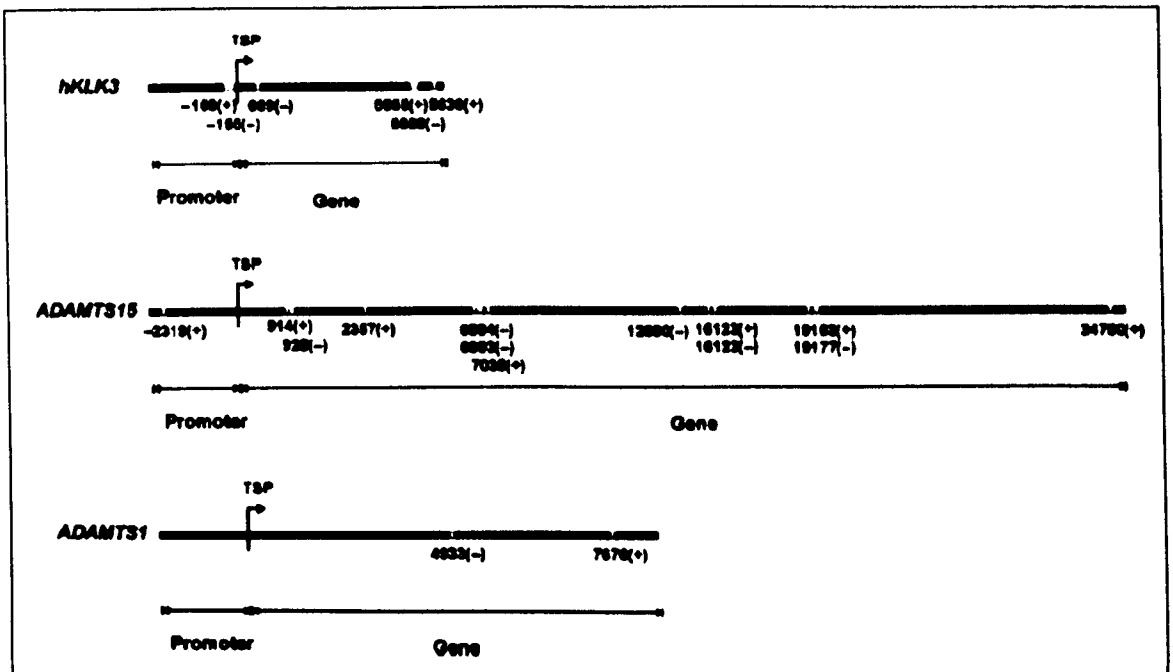

Figure 6. Putative AREs identified in the *ADAMTS1*, *ADAMTS15*, and *hKLK3* genes. The transcription start point (TSP) denotes the end of the promoter and the start of the gene sequence. The positions (bp) of the AREs relative to the TSP are indicated; (+) and (−) denote sense and antisense strands respectively.

raises the possibility that ADT could be upregulating ADAMTS-15 expression in prostate cancer cells and inhibiting tumor progression, at least until the cells become androgen independent. The relationship between tumor expression of ADAMTS-15 and survival has not yet been studied in prostate cancer patients.

Our experiments also showed that rather than inhibiting the action of DHT, flutamide actually had a similar effect as DHT in downregulating ADAMTS-15 expression. This supports previous findings that mutations in the androgen receptor of prostate cancer cells could lead to aberrant activation by adrenal steroids and nonsteroidal androgen receptor antagonists (40–42). LNCaP cells have a mutation in the androgen receptor ligand-binding domain in which threonine is changed to alanine at position 877 (T877A), leading to androgen receptor activation by flutamide (40). Other androgen receptor mutations have been identified in tumors of patients with prostate cancer (43). Up to 68% of prostate cancer patients with disease progression while on treatment with flutamide experience disease remission when flutamide is withdrawn (44–47). This phenomenon, known as the flutamide withdrawal syndrome, provides clinical evidence that mutations in the androgen receptor of prostate cancer cells could lead to aberrant activation by flutamide.

Activated androgen receptors bind to AREs in promoter regions of androgen-regulated genes, where transcription factors are recruited by the receptor–ligand complex (48). Transcription factors could be either coactivators or corepressors. Recruitment of coactivators by the receptor will lead to increased transcription of mRNA, while recruitment of corepressors leads to decreased transcription (48). Using an *in silico* approach we screened the *ADAMTS1* and *ADAMTS15* genes for putative AREs. One ARE was found in the promoter region of *ADAMTS15* but none in the promoter region of *ADAMTS1*. We also found several putative AREs downstream of the TSP of the *ADAMTS15* gene. This raises the possibility that one or more of these AREs could be acting as an enhancer. Unlike gene promoters, gene enhancers can be located many thousand bp upstream or downstream of the TSP (49). The *hKLK3* gene has such an enhancer containing an ARE that is located 4,200 bp upstream of the TSP (50), and several studies have found that proportionately more AREs are located in the gene sequence than in the promoter region of androgen-regulated genes (51), which is in keeping with our findings. The significance of the ARE to bp ratio with respect to androgen upregulation or downregulation is not known. Our analysis showed that the *hKLK3* promoter region had twice the density of putative AREs as the *FOLH1* and *ADAMTS15* promoters (Table 4). This may mean that more AREs are required to assemble coactivator complexes than are required for the assembly of corepressor complexes. A similar search for other transcription factor binding sites in the promoter regions of *ADAMTS1*,

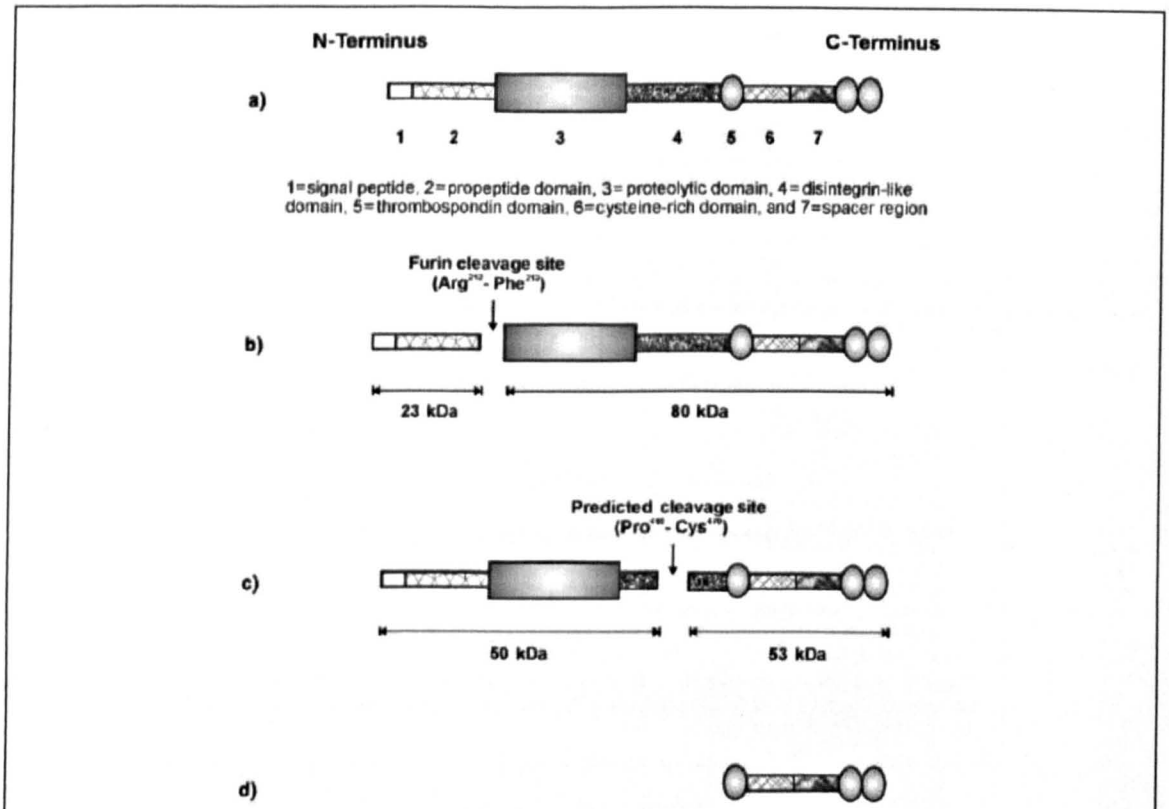

Figure 6. Domain structure of ADAMTS-15 and similarity of predicted cleavage products with ADAMTS-1. (a) A schematic diagram of the domains of full-length ADAMTS-15. (b) The furin cleavage site and the products that would result. Our Western blots did not detect a propeptide fragment of 23 kDa as would be expected from cleavage at this site. (c) The approximate position of the predicted cleavage site that would produce a 50-kDa propeptide fragment detected on Western blots, and the structure of the C-terminal region that would be released. (d) A schematic diagram of the C-terminal region that is responsible for the antiangiogenic activity of ADAMTS-1. The predicted C-terminal cleavage product from ADAMTS-15 (c) is similar in structure to the antiangiogenic region of ADAMTS-1.

ADAMTS15, *hKLK3*, and *FOLH1* did not identify differences between the androgen upregulated (*hKLK3*) and the androgen downregulated (*ADAMTS15* and *FOLH1*) genes. However the androgen-regulated genes (*ADAMTS15*, *hKLK3*, and *FOLH1*) had the myocyte enhancer factor 2 (MEF2) and the chorion factor 2 transcription factor binding sites in their promoter regions. The MEF2 and the chorion factor 2 transcription factors synergistically regulate gene expression (52). In addition to regulating myocyte differentiation, MEF2 maintains vascular integrity by promoting endothelial cell survival and proliferation (53). It is acknowledged that *in-silico*-based methods can identify the presence of transcription factors associated with genes but do not show functionality (54). Further studies are required to determine if the putative AREs identified in this study are functional.

The ADAMTS-15 antibody used in our experiments was described by the supplier as being directed against the propeptide domain of ADAMTS-15 and predicted a relative mass of 103 kDa on Western blotting. Our Western blot experiments (Figures 2–4) detected bands of 50 kDa from the cell and ECM lysate, which is about half the relative mass expected for the full length ADAMTS-15 protein and twice the relative mass of the propeptide domain, which is approximately 23 kDa. No bands were detected from the conditioned medium. The 50-kDa band was attenuated when ADAMTS-15 was knocked down with siRNA targeting ADAMTS-15 mRNA. This suggests that ADAMTS-15 was processed posttranslationally by proteolytic cleavage yielding an N-terminal fragment of 50 kDa, implying that the cleavage site lies within the disintegrin-like domain of ADAMTS-15 [Figure 6(c)]. Analysis of the X-ray crystal structure of the ADAMTS-1 disintegrin-like domain has shown that this domain is actually a cysteine-rich domain that fails to superimpose on the structures of the disintegrin domains of ADAM-10, VAP-1, and trimestatin (55). The sequence

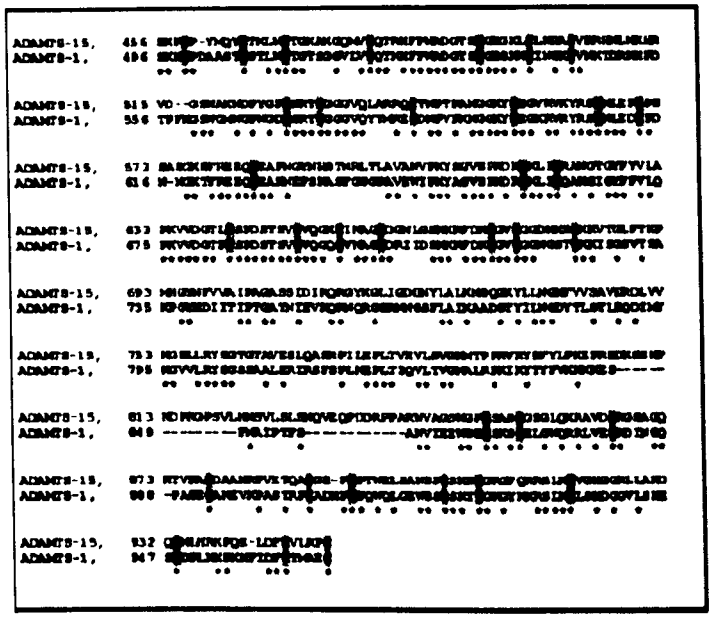

Figure 7. Protein sequence alignment of the predicted C-terminal cleavage product of ADAMTS-15 and the antiangiogenic C-terminal fragment of ADAMTS-1. The protein sequences were obtained from the Ensembl Web site (www.ensembl.org) and the sequences aligned using the online sequence alignment tool SIM (www.expasy.ch/tools/sim-prot.html). The conserved cysteine residues are highlighted in gray.

similarity of ADAMTS-15 and ADAMTS-1 (25) suggests that the ADAMTS-15 disintegrin-like domain, where we predict the cleavage site lies, is also a cysteine-rich domain with no disintegrin activity.

ADAMTS enzymes are known to be C-terminally processed (26, 56), and it is likely that the form of ADAMTS-15 we detected has lost its C-terminal ancillary domains but retains the propeptide and catalytic domains. The propeptide domain is thought to maintain the latency of the catalytic domain, and activation of the catalytic domain is mediated by cleavage by proprotein convertases such as furin (16). Retention of the propeptide implies that the catalytic domain of ADAMTS-15 remains inactive, and thus the proteolytic activity is muted. It is possible that a catalytically active form of ADAMTS-15, with the propeptide removed, is also expressed by LNCaP cells, as such a form would not have been detected by the antibody used in our study. Analogously, the full length ADAMTS-1 and the C-terminal region of ADAMTS-1 are reported to display prometastatic and antimetastatic properties respectively (27, 57). The C-terminal region containing three thrombospondin repeats and a spacer (Figure 6) is responsible for the antiangiogenic properties of ADAMTS-1 (57). This region of ADAMTS-1 is very similar to the C-terminal region that we predict is cleaved from ADAMTS-15 (Figures 6 and 7), leaving the propeptide and the catalytic domain of 50 kDa that we detected on our Western blots. It is conceivable that the potential proteolytic activity of the form of ADAMTS-15 that we have identified is muted because the propeptide remains bound to the catalytic domain, and the C-terminal half of the molecule is released to function as an inhibitor of angiogenesis in the tumor microenvironment. Somatic mutations of *ADAMTS15* have been identified in breast and colorectal cancer cells (58–60). Analysis of the *ADAMTS15* mutations in colorectal cancer cells predict that shortened, mutant forms of ADAMTS-15 are produced (60). No mutations of ADAMTS-15 have been reported in prostate cancer cells, but in addition to proteolytic processing, this could be another possible explanation for the detection of a 50-kDa ADAMTS-15 protein.

It is generally accepted that prostate and breast cancer angiogenesis correlates with disease severity (61–63), and as noted earlier, breast cancer patients with relatively higher tumor expression of ADAMTS-15 have better survival (28). Patients undergoing ADT eventually progress to hormone refractory prostate cancer (HRPC). In HRPC, by mechanisms which are not yet clearly understood, androgen receptor signaling resumes despite diminished levels of circulating androgen (64). On the basis of our findings, this is likely to result in downregulation of ADAMTS-15 in the tumor microenvironment, contributing to the poor prognosis of patients who develop HRPC.

In conclusion, we have shown that ADAMTS-15 expression is downregulated by androgen, suggesting that ADT leads to

increased expression of ADAMTS-15 in the tumor microenvironment, and mutations in the androgen receptor leading to an androgen-independent state may result in constitutive downregulation of ADAMTS-15. Its role in breast cancer suggests that ADAMTS-15 has a cancer-repressive role.

ACKNOWLEDGMENTS

The authors would like to thank Dr. Colby Eaton for providing the C4–2b4 prostate cancer cells and Dr. Ingunn Holen for providing the MDA-G8 breast cancer cells used in the experimental work.

Declaration of interest: The authors report no conflict of interest. The authors alone are responsible for the content and writing of this paper.

REFERENCES

1. Ferlay, J.; Autier, P.; Boniol, M.; Heanue, M.; Colombet, M.; Boyle, P. Estimates of the cancer incidence and mortality in Europe in 2006. O. Annncol 2007, *18*(3), 581–592.
2. Jemal, A.; Siegel, R.; Ward, E.; Hao, Y.; Xu, J.; Thun, M.J. Cancer statistics. Cancer, C.A. J Clin 2009, *59*(4), 225–249.
3. Aus, G.; Robinson, D.; Rosell, J.; Sandblom, G.; Varenhorst, E.; R. South-Easteglon C. Prostateancer Group. Survival in prostate carcinoma – outcomes from a prospective, population-based cohort of 8887 men with up to 15 years of follow-up: results from three countries in the population-based P. Nationalrostate R. Canceregistry of Sweden. Cancer 2008, *103*(5), 943–951.
4. Egeblad, M.; Werb, Z. New functions for the matrix metalloproteinases in cancer progression. R. Natev Cancer 2002, *2*(3), 161–174.
5. Rocks, N.; Paulissen, G.; El Hour, M.; Quesada, F.; Crahay, C.; Gueders, M.; Foidart, J.M.; Noel, A.; Cataldo, D. Emerging roles of ADAM and ADAMTS metalloproteinases in cancer. Biochimie 2008, *90*(2), 369–379.
6. Sandberg, A.A. Endocrine control and physiology of the prostate. Prostate 1980, *1*, 169–184.
7. Steers, W.D. 5α-Reductase activity in the prostate. Urology 2001, *58*(6 Suppl. 1), 17–24.
8. Zhu, Y.S.; Cai, L.Q.; You, X.; Cordero, J.J.; Huang, Y.; Imperato-McGinley, J. Androgen-induced prostate-specific antigen gene expression is mediated via dihydrotestosterone in LNCaP cells. J Androl 2008, *24*(5), 661–667.
9. Huggins, C. Effect of orchiectomy and irradiation on cancer of the prostate. S. Annurg 1942, *115*(6), 1192–1200.
10. de Jong, F.H.; Oloht, K.; Hayes, R.B.; Bogdanowicz, J.F.; Raatgever, J.W.; van der Maas, P.J.; Yoshida, O.; Schroeder, F.H. Peripheral hormone levels in controls and patients with prostatic cancer or benign prostatic hyperplasia: results from the Dutch-Japanese case-control study. R. Canceres 1981, *51*(13), 3445–3450.
11. Anderson, J.; Abrahamsson, P.A.; Crawford, D.; Miller, K.; Tombal, B. Management of advanced prostate cancer: can we improve on androgen deprivation therapy? Int, B.J.U 2008, *101*(12), 1497–1501.
12. Roche, P.J.; Hoare, S.A.; Parker, M.G. A consensus DNA-binding site for the androgen receptor. E. Molndocrinol 1992, *6*(12), 2229–2235.
13. Monge, A.; Jagla, M.; Lapouge, G.; Sasorith, S.; Cruchant, M.; Wurtz, J.M.; Jacqmin, D.; Bergerat, J.P.; Céraline, J. Untaithfulness and promiscuity of a mutant androgen receptor in a hormone-refractory prostate cancer. M. Cellol S. Lifeci 2008, *63*(4), 487–497.
14. Rawlings, N.D.; Morton, F.R.; Kok, C.Y.; Kong, J.; Barrett, A.J. MEROPS: the peptidase database. A. Nucleiccids Res 2008, *36*, D320–D325.
15. Nicholson, A.C.; Malik, S.B.; Logsdon, J.M.; Van Meir, E.; Functional, G. evolution of *ADAMTS* genes: evidence from analyses of phylogeny and gene organization. Evol, B.M.C Biol 2005, *5*(1), 11–23.
16. Porter, S.; Clark, I.M.; Kevorkian, L.; Edwards, D.R.; Clark, I.M.; Kevorkian, L.; Edwards, D.R. A. D. A. M. TheTS metalloproteinases. J. Biochem 2005, *389*(1), 15–27.
17. Shindo, T.; Kurihara, H.; Kuno, K.; Yokoyama, H.; Wada, T.; Kurihara, Y.; Imai, T.; Wang, Y.; Ogata, M.; Nishimatsu, H.; Moriyama, N.; Oh-hashi, Y.; Morita, H.; Ishikawa, T.; Nagai, R.; Yazaki, Y.; Matsushima, K. ADAMTS-1: a metalloproteinase-disintegrin essential for normal growth, fertility and organ morphology and function. J I. Clinnvest 2000, *105*(10), 1345–1352.
18. Russell, D.L.; Doyle, K.M.; Ochsner, S.A.; Sandy, J.D.; Richards, J.S. Processing and localization of ADAMTS-1 and proteolytic cleavage of versican during cumulus matrix expansion and ovulation. J C. Biolhem 2003, *278*(43), 42330–42339.
19. Vázquez, F.; Hastings, G.; Ortega, M.-A.; Lane, T.F.; Oikemus, S.; Lombardo, M.; Iruela-Arispe, M.L. METH-1, a human ortholog of ADAMTS-1, and METH-2 are members of a new family of proteins with angio-inhibitory activity. J C. Biolhem 1999, *274*(33), 23349–23357.
20. Stanton, H.; Rogerson, F.M.; East, C.J.; Golub, S.B.; Lawlor, K.E.; Meeker, C.T.; Little, C.B.; Last, K.; Farmer, P.J.; Campbell, I.K.; Fourie, A.M.; Fosang, A.J. ADAMTS5 is the major aggrecanase in mouse cartilage in vivo and in vitro. Nature 2005, *434*(7033), 648–652.
21. Glasson, S.S.; Askew, R.; Sheppard, B.; Carito, B.; Blanchet, T.; Ma, H.-L.; Flannery, C.R.; Peluso, D.; Kanki, K.; Yang, Z.; Majumdar, M.K.; Morris, E.A. Deletion of active ADAMTS-5 prevents cartilage degradation in a murine model of osteoarthritis. Nature 2005, *434*(7033), 644–648.
22. Colige, A.; Vandenberghe, I.; Thiry, M.; Lambert, C.A.; van Beeumen, J.; Li, S.W.; Proctop, D.J.; Lapière, C.M.; Nusgens, B.V. Cloning and characterization of ADAMTS-14, a novel ADAMTS displaying high homology with ADAMTS-2 and ADAMTS-3. J C. Biolhem 2002, *277*(6), 5756–5766.
23. Fujikawa, K.; Suzuki, H.; McMullen, B.; Chung, D. Purification of human von Willebrand factor-cleaving protease and its identification as a new member of the metalloproteinase family. Blood 2001, *98*(6), 1662–1666.
24. Cross, N.A.; Chandrasekharan, S.; Jokonya, N.; Fowles, A.; Hamdy, F.C.; Buttle, D.J.; Eaton, C.L. The expression and regulation of ADAMTS-1, ADAMTS-4, ADAMTS-5, ADAMTS-9, and ADAMTS-15, and TIMP-3 by TGFβ1 in prostate cells: relevance to the accumulation of versican. Prostate 2005, *63*(3), 269–275.
25. Cal, S.; Obaya, A.J.; Llamazares, M.; Garabaya, C.; Quesada, V.; López-Otin, C. Cloning, expression analysis, and structural characterization of seven novel human ADAMTSs, a family of metalloproteinases with disintegrin and thrombospondin-1 domains. Gene 2002, *283*(1–2), 49–62.
26. Jones, G.C.; Riley, G.P. ADAMTS proteinases: a multi-domain, multi-functional family with roles in extracellular matrix turnover and arthritis. R. Arthritiess Ther 2005, *7*(4), 160–169.
27. Liu, Y.J.; Xu, Y.; Yu, Q. A. D. A. M. Full-lengthTS-1 and the ADAMTS-1 fragments display pro- and antimetastatic activity, respectively. Oncogene 2006, *25*(17), 2452–2467.
28. Porter, S.; Span, P.N.; Sweep, F.C.; Tjan-Heijnan, V.C.G.; Pennington, C.J.; Pedersen, T.X.; Johnsen, M.; Lund, L.R.; Remer, J.; Edwards, D.R. ADAMTS8 and ADAMTS15 expression predicts

survival in human breast carcinoma. J. Int Cancer 2006, *118*(5), 1241–1247.
29. Pearson, O.H.; Manni, A.; Aralah, B.M. Antiestrogen treatment of breast cancer: an overview. R. Canceres 1992, *42*(6 Suppl.), 3424S–3429S.
30. Horoszewicz, J.S.; Leong, S.S.; Kawinski, E. LNCaP model of human prostatic carcinoma. R. Canceres 1983, *43*(4), 1809–1818.
31. Lin, M.F.; Meng, T.C.; Rao, P.S.; Chang, C.; Schonthal, A.H.; Lin, F.F. Expression of human prostatic acid phosphatase correlates with androgen-stimulated cell proliferation in prostate cancer cell lines. J C. Biothem 1998, *273*(10), 5939–5947.
32. Sherwood, E.R.; Van Dongen, J.L.; Wood, C.G.; Liao, S.; Kozlowski, J.M.; Lee, C. Epidermal growth factor receptor activation in androgen-independent but not androgen-stimulated growth of human prostatic carcinoma cells. J. Br Cancer 1998, *77*(6), 855–861.
33. Radonić, A.; Thulke, S.; Mackay, I.M.; Landt, O.; Siegert, W.; Nitsche, A. Guideline to reference gene selection for quantitative real-time PCBiochem, R. R. Biophyses Commun 2004, *313*(4), 856–862.
34. Livak, K.J.; Schmittgen, T.D. Analysis of relative gene expression data using real-time quantitative PCR and the 2(-D. Deltaelta C(T)) method. Methods 2001, *25*(4), 402–408.
35. Thalmann, G.N.; Sikes, R.A.; Wu, T.T.; Degeorges, A.; Chang, S.M.; Ozen, M.; Pathak, S.; Chung, L.W. LNCaP progression model of human prostate cancer: androgen-independence and osseous metastasis. Prostate 2000, *44*(2), 91–103.
36. Birney, E.; Andrews, T.D.; Bevan, P.; Caccamo, M.; Chen, Y.; Clarke, L.; Coates, G.; Cuff, J.; Curwen, V.; Cutts, T.; Down, T.; Eyras, E.; Fernandez-Suarez, X.M.; Gane, P.; Gibbins, B.; Gilbert, J.; Hammond, M.; Hotz, H.R.; Iyer, V.; Jekosch, K.; Kahari, A.; Kasprzyk, A.; Keefe, D.; Keenan, S.; Lehvaslaiho, H.; McVicker, G.; Melsopp, C.; Meidl, P.; Mongin, E.; Pettett, R.; Potter, S.; Proctor, G.; Rae, M.; Searle, S.; Slater, G.; Smedley, D.; Smith, J.; Spooner, W.; Stabenau, A.; Stalker, J.; Storey, R.; Ureta-Vidal, A.; Woodwark, K.C.; Cameron, G.; Durbin, R.; Cox, A.; Hubbard, T.; Clamp, M. An overview of Ensembl. R. Genomees 2004, *14*(5), 925–928.
37. Podvinec, M.; Kaufmann, M.; Handschin, C.; Meyer, U. NUBIScan, an in silico approach for prediction of nuclear receptor response elements. E. Molndocrinol 2002, *16*(6), 1269–1279.
38. Riegman, P.H.; Vlietstra, R.J.; van der Korput, J.A.; Brinkmann, A.O.; Trapman, J. The promoter of the prostate-specific antigen gene contains a functional androgen responsive element. E. Molndocrinol 1991, *5*(12), 1921–1930.
39. Israeli, R.S.; Powell, C.T.; Corr, J.G.; Fair, W.R.; Heston, W.D. Expression of the prostate-specific membrane antigen. R. Canceres 1994, *54*(7), 1807–1811.
40. Veldschotte, J.; Berrevoets, C.A.; Ris-Stalpers, C. The androgen receptor in LNCaP cells contains a mutation in the ligand binding domain which affects steroid binding characteristics and response to antiandrogens. J B. Steroldiochem B. Mollol 1992, *41*(3–8), 665–669.
41. Culig, Z.; Hobisch, A.; Cronauer, M.V.; Cato, A.C.; Hittmair, A.; Radmayr, C.; Eberle, J.; Bartsch, G.; Klocker, H. Mutant androgen receptor detected in an advanced-stage prostatic carcinoma is activated by adrenal androgens and progesterone. E. Molndocrinol 1993, *7*(12), 1541–1550.
42. Zhao, X.Y.; Malloy, P.J.; Krishnan, A.V.; Swami, S.; Navone, N.M.; Peehl, D.M.; Feldman, D. Glucocorticoids can promote androgen-independent growth of prostate cancer cells through a mutated androgen receptor. M. Nated 2000, *6*(6), 703–706.
43. Taplin, M.E.; Bubley, G.J.; Shuster, T.D.; Frantz, M.E.; Spooner, A.E.; Ogata, G.K.; Keer, H.N.; Balk, S.P. Mutation of the androgen-receptor gene in metastatic androgen-independent prostate cancer. N J. Engl Med 1995, *332*(21), 1393–1398.
44. Sartor, A.O.; Tangen, C.M.; Hussain, M.H.; Eisenberger, M.A.; Parab, M.; Fontana, J.A.; Chapman, R.A.; Mills, G.M.; Raghavan, D.; Crawford, E.D.; O. Southwestncology Group. Antiandrogen withdrawal in castrate-refractory prostate cancer: a O. Southwestncology Group trial (SWOG 9426). Cancer 2000, *112*(11), 2393–2400.
45. Scher, H.I.; Kelly, W.K. Flutamide withdrawal syndrome: its impact on clinical trials in hormone-refractory prostate cancer. J O. Clinncol 1993, *11*(8), 1566–1572.
46. Herrada, J.; Dieringer, P.; Logothetis, C.J. Characterization of patients with androgen-independent prostatic carcinoma whose serum prostate specific antigen decreased following flutamide withdrawal. J Urol 1996, *155*(2), 620–623.
47. Dupont, A.; Gomez, J.L.; Cusan, L.; Koutsilieris, M.; Labrie, F. Response to flutamide withdrawal in advanced prostate cancer in progression under combination therapy. J Urol 1993, *150*(3), 906–913.
48. Heinlein, C.A.; Chang, C. Androgen receptor (AR) coregulators: an overview. R. Endocrev 2002, *23*(2), 175–200.
49. Kleinjan, D.A.; van Heyningen, V. Long-range control of gene expression: emerging mechanisms and disruption in disease. J. Am G. Humenet 2005, *76*(1), 8–32.
50. Clautjens, K.B.; van der Korput, H.A.; van Eekelen, C.C.; van Rooij, H.C.; Faber, P.W.; Trapman, J. An androgen response element in a far upstream enhancer region is essential for high, androgen-regulated activity of the prostate-specific antigen promoter. E. Molndocrinol 1997, *11*(2), 148–161.
51. Horie-Inoue, K.; Bono, H.; Okazaki, Y.; Inoue, S. Identification and functional analysis of consensus androgen response elements in human prostate cancer cells. B. Biochemiophys C. Resommun 2004, *325*(4), 1312–1317.
52. Tanaka, K.K.; Bryantsev, A.L.; Cripps, R.M. Myocyte enhancer factor 2 and chorion factor 2 collaborate in activation of the myogenic program in Drosophila. C. Molell Biol 2008, *28*(5), 1616–1629.
53. Potthoff, M.J.; Olson, E.N. MEF2: a central regulator of diverse developmental programs. Development 2007, *134*(23), 4131–4140.
54. Wasserman, W.W.; Sandelin, A. Applied bioinformatics for the identification of regulatory elements. R. Natev Genet 2004, *5*(4), 276–287.
55. Gerhardt, S.; Hassall, G.; Hawtin, P.; McCall, E.; Flavell, L.; Minshull, C.; Hargreaves, D.; Ting, A.; Pauptit, R.A.; Parker, A.E.; Abbott, W.M. Crystal structures of human ADAMTS-1 reveal a conserved catalytic domain and a disintegrin-like domain with a fold homologous to cysteine-rich domains. J B. Mollol 2007, *373*(4), 891–902.
56. Kashiwagi, M.; Enghild, J.J.; Gendron, C.; Hughes, C.; Caterson, B.; Itoh, Y.; Nagase, H. Altered proteolytic activities of ADAMTS-4 expressed by C-terminal processing. J C. Biothem 2004, *279*(11), 10109–10119.
57. Kuno, K.; Bannai, K.; Hakozaki, M.; Matsushima, K.; Hirose, K. The carboxyl-terminal half region of ADAMTS-1 suppresses both tumorigenicity and experimental tumor metastatic potential. B. Biochemiophys C. Resommun 2004, *319*(4), 1327–1333.
58. Sjöblom, T.; Jones, S.; Wood, L.D.; Parsons, D.W.; Lin, J.; Barber, T.D.; Mandelker, D.; Leary, R.J.; Ptak, J.; Silliman, N.; Szabo, S.; Buckhaults, P.; Farrell, C.; Meeh, P.; Markowitz, S.D.; Willis, J.; Dawson, D.; Wilson, J.K.; Gazdar, A.F.; Hartigan, J.; Wu, L.; Liu, C.; Parmigiani, G.; Park, B.H.; Bachman, K.E.; Papadopoulos, N.; Vogelstein, B.; Kinzler, K.W.; Velculescu, V.E. The consensus coding sequences of human breast and colorectal cancers. Science 2006, *314*(5797), 268–274.
59. Wood, L.D.; Parsons, D.W.; Jones, S.; Lin, J.; Sjöblom, T.; Leary, R.J.; Shen, D.; Boca, S.M.; Barber, T.; Ptak, J.; Silliman, N.; Szabo, S.; Dezso, Z.; Ustyanksky, V.; Nikolskaya, T.; Nikolsky, Y.; Karchin, R.; Wilson, P.A.; Kaminker, J.S.; Zhang, Z.; Croshaw, R.; Willis, J.; Dawson, D.; Shipitsin, M.; Willson, J.K.; Sukumar, S.; Polyak, K.; Park, B.H.; Pethiyagoda, C.L.; Pant, P.V.; Ballinger, D.G.; Sparks, A.B.; Hartigan, J.; Smith, D.R.; Suh, E.; Papadopoulos, N.;

Buckhaults, P.; Markowitz, S.D.; Parmigiani, G.; Kinzler, K.W.; Velculescu, V.E.; Vogelstein, B. The genomic landscapes of human breast and colorectal cancers. Science **2007**, *318*(5853), 1108–1113.

60. Viloria, C.G.; Obaya, A.J.; Moncada-Pazos, A.; Llamazares, M.; Astudillo, A.; Capellá, G.; Cal, S.; López-Otín, C. Genetic inactivation of ADAMTS15 metalloprotease in human colorectal cancer. R. Canceres **2009**, *69*(11), 4926–4934.
61. Weidner, N.; Carroll, P.R.; Flax, J.; Blumenfeld, W.; Folkman, J. Tumor angiogenesis correlates with metastasis in invasive prostate carcinoma. J. Am Pathol **1993**, *143*(2), 401–409.
62. Revelos, K.; Petraki, C.; Scorilas, A.; Stefanakis, S.; Malovrouvas, D.; Alevizopoulos, N.; Kanellis, G.; Halapas, A.; Koutsilieris, M. Correlation of androgen receptor status, neuroendocrine differentiation and angiogenesis with time-to-biochemical failure after radical prostatectomy in clinically localized prostate cancer. R. Anticanceres **2007**, *27*(5B), 3651–3660.
63. van 't Veer, L.J.; Dai, H.; van de Vijver, M.J.; He, Y.D.; Hart, A.A.M.; Mao, M.; Peterse, H.L.; van der Kooy, K.; Marton, M.J.; Witteveen, A.T.; Schreiber, G.J.; Kerkhoven, R.M.; Roberts, C.; Linsley, P.S.; Bernards, R.; Friend, S.H. Gene expression profiling predicts clinical outcome of breast cancer. Nature **2002**, *415*(6871), 530–536.
64. Yuan, X.; Balk, S.P. Mechanisms mediating androgen receptor reactivation after castration. O. Uroincol **2009**, *27*(1), 36–41.